# PERFORMANCE-BASED STANDARDS FOR SOUTH AFRICAN CAR-CARRIERS

Christopher Charles de Saxe

A dissertation submitted to the Faculty of Engineering and the Built Environment, University of the Witwatersrand, Johannesburg, in fulfilment of the requirements for the degree of Master of Science in Engineering.

Johannesburg, 2012

I declare that this dissertation is my own unaided work. It is being submitted to the degree of Master of Science in Engineering to the University of the Witwatersrand, Johannesburg. It has not been submitted before for any degree or examination to any other University.

_____

Signature of Candidate

_____ day of _____, year _____

# Abstract

Until recently, car-carriers in South Africa operated under abnormal load permits allowing a finite relaxation of legal height and length limits. This practice is being phased out, and exemption will only be granted if a car-carrier complies with the Australian Performance-Based Standards (PBS) scheme. A low-speed turning model was developed in Matlab®, and used to benchmark the tail swing performance of the existing South African car-carrier fleet. About 80 per cent of the fleet were shown to not comply with the 0.30 m tail swing limit, due to South Africa's inadequate rear overhang legislation which permits tail swing of up to 1.25 m. TruckSim® was used to conduct detailed PBS assessments of two car-carrier designs. Critical performance areas were identified; most notably yaw damping and tail swing for the truck and tag-trailer combination, and maximum of difference and difference of maxima for the tractor and semitrailer combination. These were remedied through appropriate design modifications. The Matlab® model was shown to be versatile, accurate and efficient, with potential for future application. The TruckSim® assessments highlighted complexities unique to car-carriers in a PBS context and showed how these may be addressed. This research has shown the benefit of PBS for heavy vehicles, and has guided car-carrier design to improve safety.

*To Rachel and Mom,*
*for your patience and support.*

# Acknowledgements

I would like to thank Dr. Frank Kienhöfer for supervising this work, for bringing the CSIR Studentship opportunity to my attention, and for making my attendance at the UMTRI Mechanics of Heavy Duty Truck Systems (MHDT) course possible.

I would like to thank Mr. Paul Nordengen for involving me in interesting and challenging work at the CSIR. I would also like to thank the CSIR and the Transport Systems and Operations competency area in particular for funding this work through the Studentship programme, and for allowing me to gain valuable experience within the organisation.

I am indebted to Mr. Thomas Dessein (previously of the University of the Witwatersrand) for helping me and working with me in interpreting the PBS assessment rules and discussing how best to assess PBS performance using TruckSim®.

Much of this work relied upon the support of various OEMs in providing technical data and permitting the publication thereof. Without this cooperation this work would not be possible. I would like to thank: Unipower (Natal) and Mr. Andrew Colepeper; Volvo Trucks South Africa and Mr. Malcolm Gush; Renault Trucks South Africa and Messrs. Wouter Kotze and Patrick Bourin; BPW axles and Mr. Günther Heyman; Kässbohrer Transport Technik; Lohr; and Vehicle Delivery Services (VDS). Mr. Andrew Colepeper is emphasized in this acknowledgement for his participation and patience with respect to the PBS assessments of Chapter 3.

I would like to thank Messrs. Chris Stretch and Shane Millward (KwaZulu-Natal Department of Transport) and Prof. Peter Lyne (University of KwaZulu-Natal) as well as the other members of the Smart Truck Review Panel and Smart Truck Steering Committee for their guidance and reception.

I am grateful for the knowledge imparted to me by Mr. Chris Winkler, Dr. Thomas Gillespie and Mr. Steve Karamihas of the University of Michigan Transportation Research Institute through the MHDT course and through subsequent correspondence.

The following individuals are acknowledged for their contributions in the form of responding to queries and parting with valuable experience: Mr. Anthony Germanchev (ARRB Group), Prof. David Cebon (University of Cambridge), Mr. Rob Di Cristoforo (Advancia Transport Consulting), Messrs. Jose Arredondo and Marcus Coleman (Australian National Transport Commission), Mr. Bob Woodward (Barkwood Consulting), Mr. Phil Mather (TruckSim® technical support) and Prof. Schalk Els (University of Pretoria).

Thanks are extended to Mr. David Reinecke of the Defence, Peace, Safety and Security business unit of the CSIR for the use of the TruckSim® licence.

This research was partially supported by the National Research Foundation (NRF) using the Technology and Human Resources for Industry Programme (THRIP) and by Eskom through the Tertiary Education Support Program (TESP).

# Table of Contents

# List of Figures

# List of Tables

# List of Symbols

| Symbol | Description | Units |
|---|---|---|
| $A$ | Amplitude | - |
| $\overline{A}$ | Amplitude ratio | - |
| $AY$ | Lateral acceleration | $m/s^2$ |
| $c$ | Y axis intercept in the global reference frame | m |
| $C_{\alpha,f/r}$ | Sum of tyre cornering stiffnesses, front/rear | N/° |
| $d$ | Spacing between adjacent axles within a non-steering axle group | m |
| $D$ | Damping ratio | - |
| $Diff$ | Difference between the frontal swing-out of adjacent vehicle units at a given $x$ coordinate | m |
| $Dolly$ | Binary identifier for a dolly unit ($Dolly$ = 0,1) | - |
| $e$ | Lateral offset between outer steer-tyre wall and prescribed path | m |
| $E$ | Young's modulus of elasticity | GPa |
| $f$ | Frequency | Hz |
| $F$ | General applied force | kN |
| $F_{x/y/z}$ | Longitudinal/Lateral/Vertical tyre force | N |
| $FC_{long}$ | Longitudinal position of front corner (positive forward of the steer axle or hitch point). | m |
| $FC_{wid}$ | Vehicle width at front corner (= $2 \cdot FC_{lat}$) | m |
| $g$ | Acceleration due to gravity, 9.81 $m/s^2$ | $m/s^2$ |
| $G$ | Shear modulus of elasticity | GPa |
| $h$ | Centre of gravity height above ground | m |
| $H$ | Hitch point location (positive rearward of the steer axle or hitch point) | m |
| $i$ | Incremental solution step ($1 \leq i \leq \eta$) | - |
| $I$ | Moment of area | $mm^4$ |

| | | |
|---|---|---|
| $I_{xx/yy/zz}$ | Roll/Pitch/Yaw mass moment of inertia | $kg \cdot m^2$ |
| $IE_{wid}$ | Vehicle width at inner edge (= $2 \cdot IE_{lat}$) | m |
| $j$ | Respective vehicle units within a vehicle combination ($1 \leq j \leq N$) | - |
| $J$ | Polar moment of area | $mm^4$ |
| $K_r$ | Anti-roll bar roll stiffness | Nm/rad |
| $l$ | Beam segment length | mm |
| $m$ | Mass | kg |
| $M$ | Axle load | kg |
| $n$ | Number of non-steering axles within an axle group | - |
| $N$ | Number of vehicle units in a vehicle combination (including dollies) | - |
| $q$ | Alternative incremental solution step ($1 \leq q \leq \eta$) | - |
| $r_{i/o}$ | Inner/outer radius of anti-roll bar cross-section | mm |
| $R_{car}$ | Corner radius of passenger vehicle load projection | mm |
| $rc_{L/UL}$ | Roll centre height above axle centre (laden/unladen) | mm |
| $RC_{long}$ | Longitudinal position of rear corner (positive rearward of the steer axle or hitch point) | m |
| $RC_{wid}$ | Vehicle width at rear corner (= $2 \cdot RC_{lat}$) | m |
| $Res$ | Residual | m |
| $s$ | Beam deflection per kN applied force | mm |
| $\Delta s_A$ | Linear step size of steer axle or hitch point | m |
| $\Delta s_B$ | Linear step size of rear axle | m |
| $SPW$ | Swept path width | m |
| $T$ | Steer-tyre track width (between outer steer-tyre walls) | m |
| $TF$ | Tandem factor | $m^2$ |
| $v$ | Velocity | m/s |
| $WB$ | Geometric wheelbase | m |
| $WB_{Eq}$ | Equivalent wheelbase | m |
| $x,y,z$ | Coordinates in the global reference frame ($z$ vertically upwards) | m |
| $\bar{x}$ | Longitudinal coordinate in the vehicle reference frame (behind steer axle/hitch) | m |
| X,Y,Z | The global reference frame (Z vertically upwards) | - |
| $\bar{z}$ | Vertical coordinate in the vehicle reference frame (above ground) | m |

| | | |
|---|---|---|
| $\alpha$ | Orientation of the displacement vector generated by an incremental step of the steer axle/hitch point (relative to the global X axis) | ° |
| $\beta$ | Characteristic deflection (spring hysteresis) | mm |
| $\gamma$ | Gradient of a straight line in the global reference frame | - |
| $\delta$ | Roll-induced steer angle (positive steer to the left) | ° |
| $\Delta$ | Distance between an axle within a non-steering axle group and the geometric centre of that group | m |
| $\zeta$ | Tyre slip angle | ° |
| $\eta$ | Total number of solution steps | - |
| $\theta$ | Yaw angle relative to global X axis | ° |
| $\lambda$ | Inclination of equivalent axle locating link (positive angled down towards the rear) | ° |
| $\mu_{peak}$ | Peak road-tyre friction coefficient | - |
| $\rho$ | Radius of gyration | m |
| $\sigma$ | Number of tyres on the steer axle/s | - |
| $\tau$ | Beam angular deflection | rad |
| $\varphi$ | Number of amplitudes before the 5% cut-off is reached (yaw damping) | - |
| $\psi$ | Turn angle ($0 \leq \psi \leq \pi/2$) | ° |
| $\omega$ | Sprung mass roll angle relative to unsprung mass (positive clockwise when viewed from the rear) | ° |

**Additional subscripts:**

| | |
|---|---|
| *FC* | Front outer corner reference point |
| *IE* | Inner edge reference point |
| *P* | Prescribed path |
| *RC* | Rear outer corner reference point |
| *s* | Sprung mass |
| *tot* | Total mass |
| *us* | Unsprung mass |

# Nomenclature

| | |
|---|---|
| **ABS** | Anti-lock Braking System |
| **ALTC** | (South African) Abnormal Loads Technical Committee |
| **ARRB** | Australian Road Research Board (ARRB Group) |
| **CAD** | Computer-Aided Design |
| **CoG** | Centre of Gravity |
| **CSIR** | Council for Scientific and Industrial Research |
| **DoM** | Difference of Maxima |
| **DoT** | Department of Transport |
| **EBS** | Electronic Braking System |
| **FS** | Frontal Swing |
| **GCM** | Gross Combination Mass |
| **GVM** | Gross Vehicle Mass |
| **HSTO** | High-Speed Transient Offtracking |
| **LAP** | Load Accreditation Programme |
| **LSSP** | Low-Speed Swept Path |
| **MoD** | Maximum of Difference |
| **NHVAS** | National Heavy Vehicle Accreditation Scheme |
| **NRTA** | (South African) National Road Traffic Act |
| **NRTC** | (Australian) National Road Transport Commission (later to become NTC) |
| **NRTR** | (South African) National Road Traffic Regulations |
| **NTC** | (Australian) National Transport Commission (previously NTRC) |
| **OEM** | Original Equipment Manufacturer |
| **PBS** | Performance-Based Standards |
| **RA** | Rearward Amplification |
| **rcu/rrcu** | Roll-coupled unit/Rearmost roll-coupled unit |
| **ROH** | Rear Overhang |
| **RTMS** | Road Transport Management System |
| **SMART** | Safer Management of Australian Road Transport |
| **SRT** | Static Rollover Threshold |

| | |
|---|---|
| **STFD** | Steer-Tyre Friction Demand |
| **SUV** | Sports Utility Vehicle |
| **TASP** | Tracking Ability on a Straight Path |
| **TRH** | Technical Recommendations for Highways |
| **TS** | Tail Swing |
| **UMTRI** | University of Michigan Transportation Research Institute |
| **YDC** | Yaw Damping Coefficient |

# Glossary

**A-double** A vehicle combination consisting of a truck-tractor drawing a semitrailer, to which a full-trailer (or dolly and semitrailer) is coupled via an A-type coupling.

**A-type coupling** A coupling that provides little or no resistance to relative roll motion between coupled vehicles, e.g. a pintle hitch.

**acceleration capability** The time taken for a vehicle to cover a given distance, from rest.

**anti-roll bar** A U-shaped bar affixed between an axle and the chassis, the purpose of which is to provide auxiliary roll stiffness.

**auxiliary roll stiffness** Resistance to relative roll motion between sprung and unsprung masses in excess of that provided by the springs.

**B-double** A vehicle combination consisting of a truck-tractor drawing a "leader" semitrailer to which a "follower" semitrailer is coupled, where both couplings are B-type couplings.

**B-type coupling** A coupling that provides significant resistance to relative roll motion between coupled vehicles, e.g. a fifth wheel.

**BAB-quad** A long road-train combination consisting of a B-double drawing a dolly and two semitrailers.

**bump** See "jounce".

**cornering stiffness** The constant of proportionality between a tyre's slip angle and the resultant lateral force developed (in a linearized tyre model).

**difference of maxima** The difference between the maximum frontal swing of adjacent vehicle units (at least one of which is a semitrailer, e.g. a tractor and semitrailer) during the exit section of a low-speed ninety-degree turn.

**directional stability under braking** The ability of a vehicle to maintain stability and control under heavy braking.

**dolly** A small trailer pulled via a drawbar and fitted with a fifth wheel to which a semitrailer may be coupled, forming a self-supporting trailer with front and rear axles. The term is used here to include the non-detachable front axle assembly of a full-trailer. (See

Figure B.1 – the second vehicle unit is a dolly).

**fifth wheel** A vehicle coupling device that provides significant restraint to relative roll motion between vehicles. A B-type coupling.

**frontal swing** The maximum swing-out of the outer front corner of a vehicle during the exit section of a low-speed ninety-degree turn, measured perpendicularly to the exit tangent.

**gradeability** A vehicle's ability to maintain forward motion or attain a specific speed on a given incline.

**high-speed transient offtracking** The maximum lateral deviation of the rearmost unit of a vehicle combination during a high-speed lane-change manoeuvre, measured at centre of the rearmost axle.

**jounce** The vertical, upward displacement of an axle or wheel assembly, relative to the sprung mass (also known as "bump").

**lash** (Suspension) The gap between the spring leaf and its retaining pin, through which the spring travels unimpeded when spring load is reduced to zero. (See Figure C.3).

(Fifth wheel) The angular displacement range through which a fifth wheel will allow relative roll motion without significant resistance (due to mechanical clearances).

**low-speed swept path** The maximum road space utilised by a vehicle during a low-speed ninety-degree turn as its rear axles, and those of trailing units, "cut in" to the inside of the turn, measured between the innermost and outermost paths transcribed by the vehicle during the turn.

**maximum of difference** The maximum difference between the trajectories of the front outer corners of adjacent vehicle units (at least one of which is a semitrailer, e.g. a tractor and semitrailer) during the exit section of a low-speed ninety-degree turn and measured perpendicularly to the exit tangent.

**rearward amplification** The "whipping" effect in which a lateral acceleration input at the leading vehicle is amplified in trailing vehicles units, which can lead to rollover of the rearmost vehicle unit.

**rebound** The vertical, downward displacement of an axle or wheel assembly, relative to the sprung mass.

**roll centre** The imaginary point about which relative roll motion between the sprung and unsprung masses occurs. Also defined as the point through which the resultant of all lateral forces (or lateral constraints) between sprung and unsprung masses acts.

**roll-couple** A B-type coupling. E.g. a truck-tractor and semitrailer coupled via a fifth wheel are said to be "roll-coupled".

| | |
|---|---|
| **semitrailer** | A type of trailer with no front axles that couples to a leading vehicle through a fifth wheel which supports a large portion of the semitrailer's mass. |
| **slip angle** | The angle between a tyre's direction of heading (the direction in which it is pointed) and its direction of travel (its velocity vector). This gives rise to lateral tyre forces. |
| **sprung mass** | The portion of a vehicle's total mass that is supported by the suspension. This will typically include the chassis, payload and suspension sub-frame, but will exclude the axles, wheel assemblies and most suspension components. |
| **startability** | A vehicle's ability to start from rest on a given incline. |
| **static rollover threshold** | The maximum steady-state lateral acceleration a vehicle can withstand without rolling over. |
| **steer-tyre friction demand** | The maximum frictional force required by the steering tyres of the hauling vehicle during a low-speed ninety-degree turn, as a percentage of the maximum available friction. |
| **tag-trailer** | A trailer with no front axles which is coupled to a leading vehicle via an A-type coupling. |
| **tail swing** | The maximum swing-out of the outer rear corner of a vehicle during the entry section of a low-speed ninety-degree turn, measured perpendicularly to the entry tangent. |
| **tandem factor** | A measure used to quantify the effect of multiple non-steering axles (i.e. in a tandem or tridem axle group) on vehicle turning. |
| **track bar** | A usually V-shaped bar affixed between the chassis and the top of an axle (usually to the top of the differential housing of a drive axle), which provides the primary means of lateral constraint for the axle. |
| **tracking ability on a straight path** | The ability of the trailers in a vehicle combination to track the same path as the hauling vehicle when subjected to a cross-sloping and uneven road profile. |
| **tyre scrub** | The deformation of tyres (causing lateral force generation) within a multiple-axle non-steering axle set as slip angles are incurred during low-speed turning. |
| **unsprung mass** | The portion of a vehicle's mass not supported by the suspension. This will typically include axles, wheel assemblies, and most suspension components. |
| **yaw damping** | The tendency of yaw oscillations to decay in a vehicle combination after being subjected a steering pulse input. |

# Chapter 1

# Introduction

## 1.1 Background

Until recently, it has been standard practice for South African car-carriers to operate under abnormal load permits, issued under Section 81 of the South African National Road Traffic Act (NRTA) [1]. These permits allow the vehicles to exceed legislated height and length limits by 300 mm and 500 mm respectively. Generally speaking, abnormal load permits are granted for indivisible loads (e.g. large machinery components), and so the granting of these permits to car-carrier operators has been under a special concession of the TRH11 (Technical Recommendations for Highways: Dimensional and Mass Limitations and Other Requirements for Abnormal Load Vehicles) [2]. This concession was granted in response to requests from the car-carrier industry so as to improve productivity and remain economically competitive.

In 2006, at a meeting of the South African Abnormal Loads Technical Committee (ALTC), it was decided that this practice would be phased out due to concerns of vehicle safety (due to increased height) and the definition of "indivisible load". This decision is currently enforced by the omission of any reference to car-carriers in the latest edition of the TRH11 [3]. The granting of limited-period abnormal load permits will continue until 31 March 2013 for existing car-carriers registered before 1st April 2010; any car-carriers registered after this date will not be granted permits (including new vehicles of the same design as existing vehicles).

To maintain levels of productivity to which the industry is accustomed, the Committee has proposed a replacement framework for over-length and over-height car carriers. The

proposal suggests that if an operator wishes to operate a car-carrier that exceeds prescribed height and length limits, two requirements must be met, namely:

1. the transport operator must be accredited with the Road Transport Management System (RTMS), and
2. the vehicle design must comply with the Australian Performance-Based Standards or "PBS" scheme, which is currently the basis for a PBS demonstration project in South Africa [4].

As a result, a number of transport operators, in collaboration with associated car-carrier body and trailer manufacturers, are pursuing PBS car-carrier projects. This work aims to show the benefits of such a framework, and how it can be used to improve car-carrier design and safety whilst maximising productivity. Compliance with the PBS scheme is assessed through detailed computer simulation, the capacity for which exists locally at the University of the Witwatersrand, Johannesburg (Wits University) and at the Council for Scientific and Industrial Research (CSIR).

## 1.2 Literature Review

The review of the literature begins with a look at the prevailing issues of South African road freight transport. The concept of performance-based standards for heavy vehicles as an alternative to prescriptive standards is introduced, with a focus on the established Australian PBS scheme. The initiative to introduce a PBS framework to South Africa is subsequently discussed, and pertinent local research conducted thus far is summarised. Lastly, the specific context of car-carriers and the matters of tail swing and low-speed turn modelling are discussed.

### 1.2.1 The state of South African road freight transport

South Africa's economy, and that of most countries, relies heavily on freight transport and on the ability of the road infrastructure to support it. Inland freight transport in South Africa is achieved via rail or road and, due to an ageing rail infrastructure and lack of investment in rail transport, an estimated 70 per cent of freight is transported by road [5]. Since 1970, the growth of goods vehicle traffic on South African roads has been three times the growth of the road network [6]. This increase in heavy vehicles per kilometre of road has led to accelerated road infrastructure deterioration and a higher risk of heavy vehicle-related accidents.

Furthermore, despite notable efforts by the provinces, overloading has for many years been a significant problem in South Africa due to a number of factors, including insufficient policing and deliberate overloading by operators [7]. The 20 to 25 per cent of heavy vehicles that are overloaded (2000 study) contribute an estimated 60 per cent of the annual road wear [8]. This is a disproportionately large figure and overloading has hence been a topic of extensive study in South Africa, most notably at the CSIR. Not only does overloading have a negative impact on the roads, but overloaded vehicles are less stable and pose a higher safety risk.

In 2002, fatalities associated with heavy vehicle accidents in South Africa were disproportionately higher than other countries at around thirteen fatalities per 100 million kilometres compared to around two per 100 million kilometres for developed countries [9]. Increased heavy vehicle traffic and overloading have been highlighted as contributing factors to this statistic, but equally important factors include driver training, vehicle maintenance, speeding, and vehicle design – the last contributor being pivotal to this work.

### 1.2.2 Prescriptive vs. performance standards for heavy vehicles

The purpose of heavy vehicle regulation is to address two primary issues: vehicle safety and road infrastructure protection. In many countries including South Africa, this is accomplished using prescriptive mass and dimension limits (for example, in South Africa, the overall length of a vehicle combination may not exceed 22 m [1]). Prescriptive standards make for straight-forward policing methods and universal application. In South Africa, vehicle mass and dimensions are governed by the National Road Traffic Regulations (NRTR), enforced under Section 75 of the NRTA [1].

Within the envelope of typical prescriptive constraints, one vehicle design could be intrinsically safe in operation and cause minimal wear on the infrastructure, whereas another (perfectly legal) vehicle design could be intrinsically unsafe and/or may cause accelerated damage to the infrastructure. Furthermore, prescriptive requirements impose constraints on productivity [10] (i.e. by limiting maximum vehicle mass and dimensions, and hence payload) and innovation in design [11]. Design innovation might include the use of actively-steered rear axles, which can allow longer vehicles to utilise the same road space as a shorter vehicle during a turn. A prescriptive framework does not recognise this, and the actively-steered vehicle will be illegal if it is over-length, regardless of its turning capabilities. Productivity and innovation are important factors in improving the efficiency, economy and safety of road freight transport. An alternative legislative

framework, performance-based standards or "PBS", proposes to address these shortcomings of prescriptive standards.

The PBS approach serves to directly rather than indirectly regulate the desired outcomes of vehicle safety and performance. It achieves this by specifying how the vehicle should perform in operation rather than by specifying the means by which this might be achieved. The safety benefit of a PBS approach is not exclusive and there are significant spin-offs. By not constraining vehicle parameters and rather evaluating the resultant safety and road wear performance, opportunity for innovation is created. PBS designed vehicles might be longer and taller than prescriptively designed vehicles at no expense of, or with improvement in, safety and/or road wear. Further benefits include increased productivity, reduced fuel consumption per ton of freight per kilometre (with reductions in associated costs and emissions), reduction in fleet size (and hence fewer vehicles on the road) and an increase in awareness and understanding of vehicle safety.

In Australia, the National Transport Commission (NTC) has developed a well-established PBS scheme. Vehicles operating within the scheme are known as "SMART" trucks (Safer Management of Australian Road Transport). The most up-to-date Australian PBS framework is contained in the document, "Performance Based Standards Scheme: The Standards and Vehicle Assessment Rules," (10 November 2008) [4]. The current scheme is offered as an alternative to prescriptive regulations but not as a replacement – involvement in the scheme is voluntary [10]. The scheme consists of a set of twenty standards: sixteen safety standards and four infrastructure standards. If a vehicle is shown to comply with all of these standards, it may be exempted from certain Australian vehicle regulations pertaining to length, width, overhangs, drawbar length, gross combination mass *etc.* Compliance of a vehicle with these standards is assessed either via physical testing or computer simulation. This assessment process required to prove a vehicle's compliance with the various performance standards presents one disadvantage of a performance-based approach. The process of design optimisation, testing or computer simulation, and approval can be significantly more costly and time-consuming than for a legal vehicle. However, depending on the application, tonnage and lead distances, the improvements in productivity, safety, fuel savings, and emissions often outweigh these disadvantages in the long term.

Thirteen of the sixteen safety standards are summarised in Table 1.1 with a description of each standard and a description of the associated test or manoeuvre. The three remaining standards – overtaking provision, ride quality and handling quality – are under review and awaiting the results of further research before they are enforced as part of the scheme. The four infrastructure standards are: pavement horizontal loading, pavement

vertical loading, tyre contact pressure distribution and bridge loading. These standards are predominantly prescriptive due to the nature of the vehicle-infrastructure interaction, though research towards appropriate performance measures is underway. Standards 1 to 7 in Table 1.1 may be referred to as the "low-speed" standards and standards 8 to 13 may be referred to as the "high-speed" or "dynamic" standards.

**Table 1.1: The safety standards of the Australian PBS scheme** [4]

| Manoeuvre | Safety Standard | Description |
|---|---|---|
| Accelerate from rest on an incline | 1. Startability (St) | Self-explanatory. |
| Maintain speed on an incline | 2. Gradeability (Gr) | Self-explanatory. |
| Cover 100 m from rest | 3. Acceleration capability (AC) | Intersection/rail crossing clearance times. |
| Low-speed 90° turn | 4. Low-speed swept path (LSSP) | "Corner cutting" of long vehicles. |
| | 5. Frontal swing (FS) | Swing-out of the vehicle's front corner. |
| | 5a. Maximum of Difference (MoD) | The difference in frontal swing-out of adjacent vehicle units where one of the units is a semitrailer. |
| | 5b. Difference of Maxima (DoM) | |
| | 6. Tail swing (TS) | Swing-out of the vehicle's rear corner. |
| | 7. Steer-tyre friction demand (STFD) | The maximum friction utilised by the steer-tyres. |
| Straight road of specified roughness and cross-slope | 8. Tracking ability on a straight path (TASP) | Total road width utilised by the vehicle as it responds to the uneven road at speed. |
| Constant radius turn (increasing speed) or tilt-table testing | 9. Static rollover threshold (SRT) | The maximum steady lateral acceleration a vehicle can withstand before rolling. |
| Single lane-change | 10. Rearward amplification (RA) | "Whipping" effect as lateral accelerations are amplified in trailing units. |
| | 11. High-speed transient offtracking (HSTO) | "Overshoot" of the rearmost trailing unit. |
| Pulse steer input | 12. Yaw damping coefficient (YDC) | The rate at which yaw oscillations settle. |
| Brake from 60 km/h to rest | 13. Directional stability under braking (DSB) | Directional stability and controllability of the vehicle under heavy braking. |

For each of the standards there are quantitative criteria against which the vehicle must be assessed. For example, to comply with the static rollover threshold (SRT) standard, the vehicle must exhibit an SRT of at least $0.35 \cdot g$, where $g$ is the acceleration due to gravity. In some of the standards, the criterion is not universal and its value depends on the type of road access the vehicle will utilise. For this purpose, the PBS scheme has four defined road access levels: Levels 1, 2, 3 and 4. Level 1 represents unrestricted access to the Australian road network, with the most stringent performance criteria, and is restricted to vehicles not greater than 20 m in length [12]. Levels 2, 3 and 4 represent subsets of the road network, in increasing order of route restriction, that have been deemed fit for the

operation of longer vehicle combinations that meet less stringent performance criteria. Level 4 vehicles are typically "triple road trains" up to 60 m in length that operate on remote cross-country routes. A summary of the road access levels and their descriptions is given in Table 1.2.

**Table 1.2: Road classification levels for the Australian PBS scheme** [12]

| Road Access Level | Permitted Vehicle Length | Permitted Routes | Performance Criteria |
|---|---|---|---|
| Level 1 | ≤ 20 m | Unrestricted road access | Most stringent |
| Level 2 | ≤ 30 m | Significant freight routes | ↑↓ |
| Level 3 | ≤ 42 m | Major freight routes | |
| Level 4 | ≤ 60 m | Remote areas | Most lenient |

Subject to minor adjustments, the Australian standards have been adopted for use in the South African PBS demonstration project. The details of this are covered in the following section.

### 1.2.3 Performance-based standards development in South Africa

Published in 2004, the South African National Overload Strategy [13] sought to address the problem of overloading facing South Africa. The report identified the primary causes and assessed the possible solutions to overloading. One of the proposed solutions was self-regulation: a scheme by which initiatives are implemented by industry to establish sound vehicle management practices. Such a scheme has materialised and is known as the Road Transport Management Scheme (RTMS) (previously the Load Accreditation Programme – LAP). The scheme is industry-led and accreditation is voluntary. It aims to promote sound vehicle management systems that address issues of road infrastructure protection, vehicle safety and logistics efficiency [9].

Because RTMS accreditation is voluntary, incentives are required to promote industry participation. Currently, two such incentives exist, the first being the "weigh-less" principle whereby accredited operators are subjected to fewer spot checks and weigh-ins at weigh-bridges. The second incentive is that RTMS accredited operators will have the opportunity to take advantage of the South African PBS demonstration project [14]. Compliance with PBS criteria is not as simple to assess in operation as prescriptive criteria, and hence assurance is required that operators load and operate their vehicles professionally so as to maintain PBS compliance. RTMS accreditation aids in providing such assurance.

For the implementation of the RTMS and PBS initiatives in South Africa, the Australian National Heavy Vehicle Accreditation Scheme (NHVAS) and PBS scheme respectively were chosen as the foundations upon which to develop the South African equivalents [14] [15]. The Australian PBS scheme is being closely followed with a few exceptions:

1. All PBS vehicles require an Anti-lock Braking System (ABS) and Electronic Braking System (EBS) in lieu of the directional stability under braking standard [15].
2. In lieu of the four infrastructure standards, the South African abnormal load bridge formula requirements must be met [15], and a road wear analysis is encouraged to support the application for approval indicating, at the very least, improvement over the baseline vehicle.
3. A speed limit of 80 km/h applies to all PBS vehicles, though lower limits may be enforced for larger vehicles [15].
4. The length requirements of the road classification levels (Table 1.2) are altered so as to be compatible with the South African prescriptive legislation. The allowable vehicle length will be subject to the route and application in question as well as the jurisdiction of the authorities. Level 2 vehicles and higher will require detailed route assessments accompanying their applications for approval [15]. Level 1 vehicles will not typically be restrained to less than 22 m.

A South African Smart Truck Review Panel was formed which meets approximately every three months to assess PBS applications and to regulate the implementation of PBS in South Africa. A Smart Truck Steering Committee was also formed which comprises of representatives from the industry, transport authorities and research entities.

Some relevant PBS research conducted in South Africa thus far includes the development of an A-double for transporting steel pipes for Hall Longmore [16], the development of a BAB-quad road train for Unitrans Freight and Logistics [17] and a PBS analysis of current South African semitrailer combinations [18].

The Hall Longmore project involved the development of an innovative optimisation model by Dessein *et al.* that optimises vehicle parameters (including payload) within the envelope of the PBS requirements by making use of simple analytical/empirical estimates. A number of performance standards were excluded from the optimisation process, including yaw damping coefficient, frontal swing and tail swing. (These excluded standards were not critical to the particular vehicle in question, and so were

simply assessed post-optimisation to verify that their criteria were satisfied by the optimised design.)

It should be noted that fundamental differences and conflicts exist between South African and Australian heavy vehicle regulations: between certain features of the Australian PBS scheme and South Africa's NRTR, and also between Australia's existing prescriptive regulations (i.e. the Australian Design Rules) and South Africa's NRTR. Further, it is important to bear in mind that the selection of many of the pass/fail criteria for the Australian performance standards has been a result of the characteristic performance of the existing, non-PBS, Australian heavy vehicle fleet (see [19]), which would have been designed within the confines of prescriptive Australian regulations.

An example of one such conflict is the fact that Level 1 PBS vehicles are limited to a maximum length of 20 m in Australia, whereas the NRTR allow vehicles of up to 22 m to operate unrestricted on South African roads. In addition, vehicles are limited to a maximum width of 2.5 m in Australia [20], whereas widths of up to 2.6 m are permitted within the NRTR. The result is that certain performance standards may prove more restrictive for typical South African vehicle designs, presenting resistance to the adoption of the scheme in its current guise. (For example, an operator may question the benefits of a 20 m Level 1 PBS vehicle when a 22 m vehicle combination may be operated under existing South African regulations.) These will be important factors to consider in this work and in the future implementation of PBS in South Africa.

Car-carriers present a new and unique opportunity for the application of PBS, the details of which are discussed in the next section.

### 1.2.4 Car-carriers

Car-carriers in South Africa typically exist in the form of one of two vehicle combinations: tractor and semitrailer combinations and truck and tag-trailer combinations. The term "tag-trailer" is adopted from Australian terminology and denotes a trailer with no front axles and connected to the preceding vehicle through an A-type coupling (as opposed to a B-type coupling or fifth wheel). The tag-trailer is predominantly of the centre-axle type in which the trailer axle group is located approximately beneath the trailer load centre. Illustrations of the two vehicle types are shown in Figure 1.1. The vehicles are shown with the dimensions permitted by the outgoing abnormal load concession. A characteristic feature of existing car-carrier designs is their large rear overhangs which are commonly of the order of four to six metres.

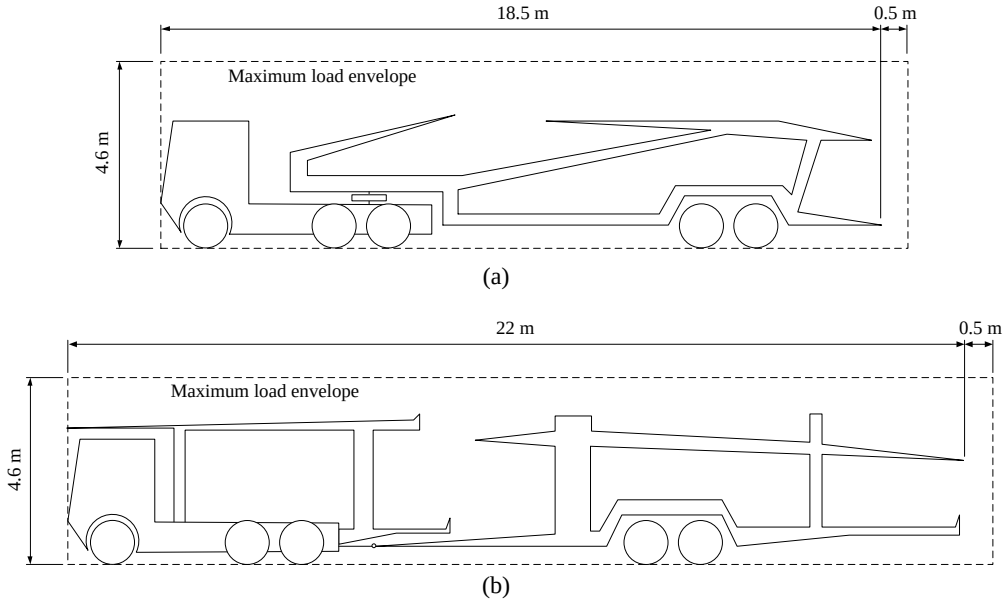


**Figure 1.1: Typical South African car-carriers: (a) tractor and semitrailer, (b) truck and centre-axle tag-trailer**

The additional 300 mm allowance in height (from 4.3 to 4.6 m) is crucial for increased productivity. Without the allowance, the number of vehicles that may be carried is reduced and the possibility of an upper deck of vehicles is unlikely except when transporting low-profile vehicles. A similar point may be argued for the additional length (from 18.5 to 19 m for semitrailer configurations and from 22 to 22.5 m for truck-trailer configurations). Loading optimisation for car-carriers is complex and plays a critical role in the operation of such a business (see for example [21]).

Of the two options presented to the South African car-carrier industry by the ALTC (see Section 1.1), the option of adhering to the requirements of the NRTR was considered uneconomical. Within the PBS framework, car-carriers up to 23 m in length (22 m excluding load projections) and 4.6 m in height (4.3 m unladen) would be considered for Level 1 applications.

In Australia, certain states such as South Australia, New South Wales and Northern Territory have car-carrier-specific regulations (see [22–24]). In some cases the vehicles operate under special permits and, depending on the routes used and vehicle configuration, can be up to 23 m or 25 m in length. Rear overhangs are limited to 3.7 m and, because the width of the load is significantly less than that of the vehicle body, the load projection may exceed this up to a total rear overhang of 4.9 m. South Australia limits the unladen length of car-carriers to 19 m and enforces that no multi-deck car-carriers may operate at a height exceeding 4.3 m (up to 4.6 m) with vehicles on the upper

deck unless the lower deck has been filled. South Australia limits car-carrier speed to 100 km/h.

A review of the literature could find no documented research on the use of PBS to evaluate car-carrier safety or to use a PBS framework to design car-carriers. In such a context, the large rear overhangs of the typical car-carrier designs are a cause for concern for tail swing. This is discussed in detail in the following section.

### 1.2.5 Tail swing

The current Australian Level 1 tail swing limit of 0.30 m originates from an extensive analysis of the PBS performance of the existing Australian heavy vehicle fleet, conducted by the National Road Transport Commission (the NRTC – later to become the NTC) [19]. At the time of the study, the tail swing limit was 0.50 m. In the study, the highest level of tail swing observed was 0.333 m (this was a car-carrier) and hence a reduction in the tail swing limit to 0.35 m was recommended. In 2003, the limit was further reduced to 0.30 m in response to a proposal from the New South Wales Roads and Traffic Authority [25].

In Australia, heavy vehicle configurations and dimensions are governed by Australian Design Rule (ADR) 43/04 [20], which governs vehicle rear overhang to a maximum of 3.7 m as measured from the centre of the rearmost axle unit. This limit is retained in the car-carrier-specific regulations of South Australia and New South Wales. In contrast, South African Regulations do not stipulate an overriding rear overhang limit, but only govern it to a percentage of vehicle wheelbase or vehicle length. The result is that rear overhangs of up to 7 m are possible (for an 11.3 m tridem-axle tag-trailer). Furthermore, the Regulations allow for vehicle widths of up to 2.6 m whereas in Australia the limit is 2.5 m [20], and this also has an aggravating effect on tail swing performance. A tail swing limit of 0.30 m, based on the performance of Australian vehicles with strictly limited rear overhangs, is critical for South African vehicles which were designed within the comparatively lenient confines of the NRTR.

As tail swing is a critical factor for the PBS compliance of car-carriers, it is desirable to have a simplified model (i.e. not one developed in a complex multibody dynamics software package) that can quickly and easily predict the tail swing performance of a given vehicle or group of vehicles. The optimisation model developed by Dessein *et al.* [16] did not evaluate tail swing performance and, in applications with large rear overhangs, such an inclusion would be valuable. The following section reviews the literature on low-speed turning models and the application thereof for calculating tail swing.

### 1.2.6 Low-speed turn modelling

The NTC's low-speed turn manoeuvre used to assess tail swing is a ninety-degree constant-radius turn, with straight entry and exit tangents. It is required that the path be followed with respect to the outer tyre wall of the outer steer-tyre. The swing-out of the rearmost outer corner of the vehicle is tracked and measured relative to the entry tangent to determine tail swing. Other reference points on the vehicle are tracked during the manoeuvre to determine LSSP, FS, DoM and MoD.

The "WHI formula" (developed by the Western Highway Institute in 1970) is a simple geometric relationship for determining the low-speed swept path of an articulated vehicle (see [19]). Although the formula has proven very useful, it has no means for predicting tail swing behaviour, and relies on predetermined coefficients based on the prescribed path in question. Furthermore, it does not take into account the effect of tandem and tridem axle groups on turning behaviour (i.e. due to tyre scrub – see for example [26]).

Wang and Linnett [27] developed a kinematic model based on a rigid, four-wheeled vehicle. The model is capable of determining the paths of any point on a vehicle or vehicle combination as it follows a path with respect to any vehicle reference point. It is hence possible to determine tail swing with this model. The model requires that the path be mathematically described. Two such cases were analysed in the work, namely straight and circular paths. Analytical solutions to these cases were derived and the solution obtained via successive numerical solution of a first order differential equation. The model simplifies multiple non-steering axles to a single axle located at the geometric centre of the group, thereby neglecting the effects of tyre scrub.

Erkert *et al.* [28] used a bicycle model and the "tractrix" concept to determine vehicle motion. As with Wang and Linnett, analytical relationships were determined for a mathematically-defined path, requiring the solution of a differential equation for each motion increment. The formulation was restricted to problems in which the centre of the steer axle follows the required path. The model shares Wang and Linnett's simplification method for multiple non-steering axles. Vehicle overhangs were considered in developing the model and hence it may be used to determine tail swing.

In 2003, McGovern [29] developed a spreadsheet for the calculation of required articulated vehicle motion to turn within the constraints of a given entry gate and confining walls (of a repair yard for example). The model calculates vehicle motion based on meeting certain clearance requirements between vehicle extremities and confining walls. The approach is similar to the tractrix approach of Erkert *et al.* [28] but solves the problem using a step-wise geometric method. The model is limited in its application to

turning within the restraints of a given geometry, and cannot (without modification) be applied to problems in which a prescribed path is followed. As the model was developed as a spreadsheet, the number of solution steps and hence step size is limited, thereby restricting the accuracy of the model. Again, the model simplifies tandem and tridem axle units to single axles located at the geometric centres of the respective axle groups.

All of the above models simplify multiple non-steering rear axle groups to a single axle located at the geometric centre of each group – effectively neglecting tyre scrub. In 1972, Morrison [30] developed a low-speed turning model which included non-linear tyre mechanics to incorporate tyre scrub. The model uses an "instantaneous centre" method which advances the vehicle an incremental distance, and assumes rigid rotation about a calculated instantaneous centre to determine the subsequent yaw angle.

The model uses a calculated "effective length" which equates to the location of an effective single non-steering rear axle emulating the effects of tyre scrub or – it is important to note – the effects of lateral hitch forces. Tyre scrub effects (due to slip angles generated) need not be a result of multiple non-steering rear axles: the lateral component of an applied hitch force will also result in slip angles being generated to balance moments, even for a single rear axle. Morrison noted that the effect of towing forces on offtracking are small, yielding an error of up to 2%. The model calculates effective length via an iterative procedure at each incremental step. The model incorporates steer-tyre path-following.

Morrison's model is extensive and the validation results show it to be reasonably accurate. However, the iterative solution method required for yaw angle and effective length calculation necessary at *each incremental step* means that the model is computationally demanding. Furthermore, the incorporation of tyre mechanics modelling necessitates the availability of tyre cornering stiffness properties.

In a 1998 study [31], Winkler and Aurell presented an "equivalent wheelbase" principle, similar in concept to Morrison's effective length, for the analysis of rigid truck steady-state handling (i.e. not restricted to low-speed turning). The equivalent wheelbase represents the wheelbase of an equivalent two-axle vehicle that would yield the same steady-state handling behaviour as a vehicle with multiple rear axles. Whereas Morrison's effective length must be recalculated for each incremental step due to non-linear tyre properties, Winkler and Aurell's equivalent wheelbase is constant for a given vehicle owing to the assumption of linear tyre stiffness properties.

### 1.2.7 Significance of this research

In the light of the published literature, the significance of this research lies in the following areas:

1. A research gap exists to develop a low-speed turning model – which incorporates the benefits of certain existing models (such as the versatility of McGovern's geometric approach to the tractrix problem) but omits the shortcomings of others (such as the computational demands of Morrison's model, and the lack of tyre scrub modelling in others) – which can assess the tail swing performance of South African car-carriers.
2. There is no published evidence of PBS assessments of car-carriers in South Africa or elsewhere, and as a result the low- and high-speed safety performance of these vehicles is unknown. Such assessments would further the application of PBS, especially in South Africa where the initiative is still in its infancy, and address concerns of the South African road transport authorities.

## 1.3 Objectives

The objectives of this work are to:

1. develop a mathematical model capable of assessing the low-speed turning performance of car-carriers, which should
    a. be accurate for a range of vehicle configurations,
    b. be able to track the motion paths of any point of any vehicle unit and hence determine LSSP, TS, FS, MoD and DoM,
    c. be compatible with the steer-tyre path-following requirement of the Australian PBS scheme, and
    d. take into account the tyre scrub effect of multiple non-steering rear axles;
2. use the model to quantify and benchmark the tail swing performance of the existing South African car-carrier fleet;
3. assess two proposed car-carrier designs (one tractor and semitrailer combination and one truck and tag-trailer combination) against the requirements of the Australian PBS scheme; and,
4. if necessary, address any shortcomings of the proposed designs.

## 1.4 Methodology and Resources

Matlab® was used to develop the low-speed turning model and TruckSim® was used as the detailed multibody vehicle simulation package for the full PBS assessments. Matlab® was also used for the post-processing of TruckSim® data. The versions of the software packages used were as follows:

- Matlab® (© The MathWorks Inc.) R2007a (V7.4)
- TruckSim® (© Mechanical Simulation Corporation) V8.01

The South African car-carrier tail swing study was split into two components. The first component quantitatively assessed the tail swing performance of the existing South African car-carrier fleet. Basic dimensions of a representative sample of existing car-carriers were obtained, and the car-carriers were assessed using the low-speed turning model. The second component of the study was to compare this performance to what is legally possible within the prescriptive framework of South African legislation. For this purpose, the South African Regulations were consulted to establish a number of vehicles with worst-case legal dimensions to determine the allowable tail swing.

The detailed PBS assessments included two vehicle designs – one tractor and semitrailer and one truck and tag-trailer as required – as proposed by local car-carrier body-builder, Unipower (Natal). Using TruckSim®, detailed models of these two vehicles were developed and assessed in each of the five required manoeuvres: a low-speed turn, a longitudinal tracking test, a rollover test, a single lane-change and a pulse steer (see Table 1.1). The input data required for the vehicle models were sourced from the relevant Original Equipment Manufacturers (OEMs). Where unavailable, suitable representative data were sourced from the literature or suitable estimation techniques were used.

The vehicles were initially assessed as per the proposed designs. These are termed the "baseline vehicles". Through the baseline vehicle assessments, the shortcomings of the vehicle designs in respect of meeting the PBS criteria were determined. Suitable design modifications were made and the revised vehicles were assessed to confirm compliance.

The low-speed turning model and detailed PBS assessments are presented in the two central chapters of this dissertation, Chapter 2 and Chapter 3 respectively. Each chapter contains the development, application and chapter-specific conclusions of the respective studies. Chapter 4 serves to present the all-encompassing observations, conclusions and recommendations of the work as applicable to the broader context of the PBS initiative in South Africa.

# Chapter 2

# Low-Speed Turning Model

This chapter covers the development of a mathematical model which can predict the low-speed manoeuvrability of a vehicle or vehicle combination given only its basic dimensions. The term manoeuvrability is used here to mean the directional behaviour of a vehicle as it follows a prescribed path at low speed. In the context of performance-based standards, the model can predict LSSP, TS, FS, DoM and MoD. The chapter develops as follows:

1. Preliminary concepts are formulated and discussed.
2. The mathematical foundations of the model are developed, including the incorporation of steer-tyre path-following and the modelling of tyre scrub.
3. The model is validated against equivalent TruckSim® models for a number of representative scenarios.
4. The validated model is used to quantify and benchmark the tail swing performance of the existing South African car-carrier fleet.

## 2.1 Preliminaries

This section covers details of the low-speed turn manoeuvre and associated performance standards, and summarises the concept development phase of the model.

### 2.1.1 Low-speed turn manoeuvre and associated standards

This section expands on the brief description of the low-speed turn manoeuvre given in Chapter 1, giving the details required for the remainder of the current chapter.

The manoeuvre required for the assessment of LSSP, TS, FS, DoM, MoD and STFD is a ninety-degree turn of radius 12.5 m. This path is represented graphically in Figure 2.1 with entry and exit tangents aligned with the negative Y and positive X axes respectively. X, Y and Z represent the global earth-fixed coordinate system (with Z defined as positive upwards). This particular choice of axis orientation is recommended as any deviations from the entry and exit tangents can be inferred directly from the global *x* and *y* coordinates. This is useful when determining tail swing and frontal swing.

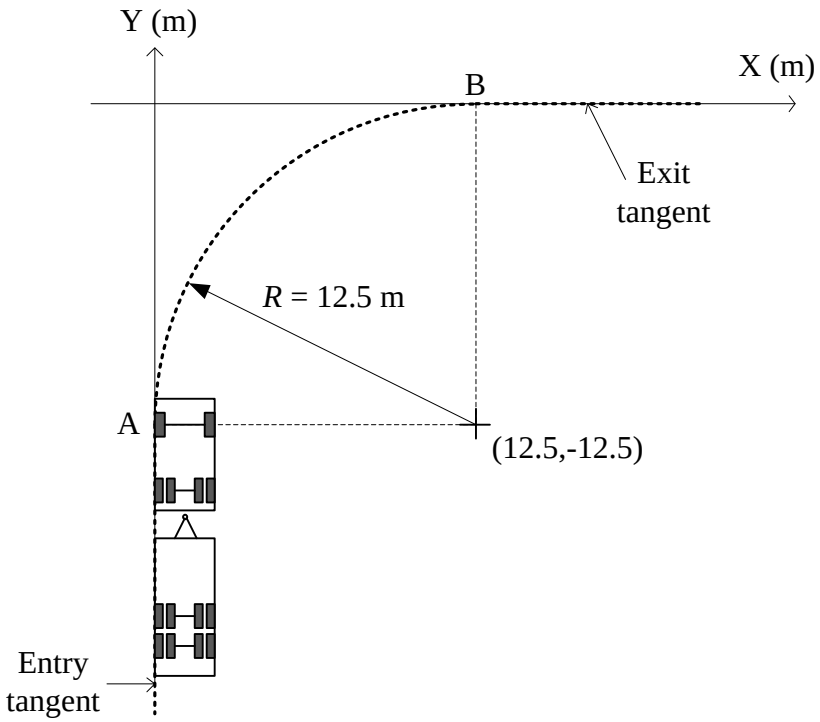


**Figure 2.1: Ninety-degree low-speed turn as prescribed by the NTC**

The path must be followed with respect to the vertical projection of the outermost point on the left steer-tyre wall (see Figure 2.2). In this work, this is denoted "steer-tyre path-following". The NTC requires that a lateral offset of no more than 50 mm be maintained between the steer-tyre wall and the path for the duration of the manoeuvre. With reference to Figure 2.1, the vehicle begins the manoeuvre with the leftmost tyre wall of the left steer-tyre aligned with the Y axis at point A and facing the positive Y direction. The entire vehicle combination must be straight at this point. The vehicle follows the path towards point B and continues along the exit tangent of the path until the point of maximum offtracking has been reached (to be described shortly). The test is conducted at a speed of no more than 5 km/h and the vehicle must be tested both laden and unladen.

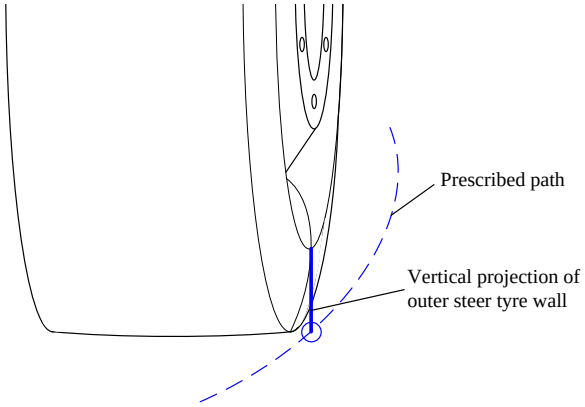


**Figure 2.2: Steer-tyre path-following**

Figure 2.3 shows an example tractor and semitrailer combination performing the prescribed manoeuvre. The trajectories of various vehicle reference points are shown. A discussion of the significance of these trajectories, and how they relate to the various low-speed performance standards follows.

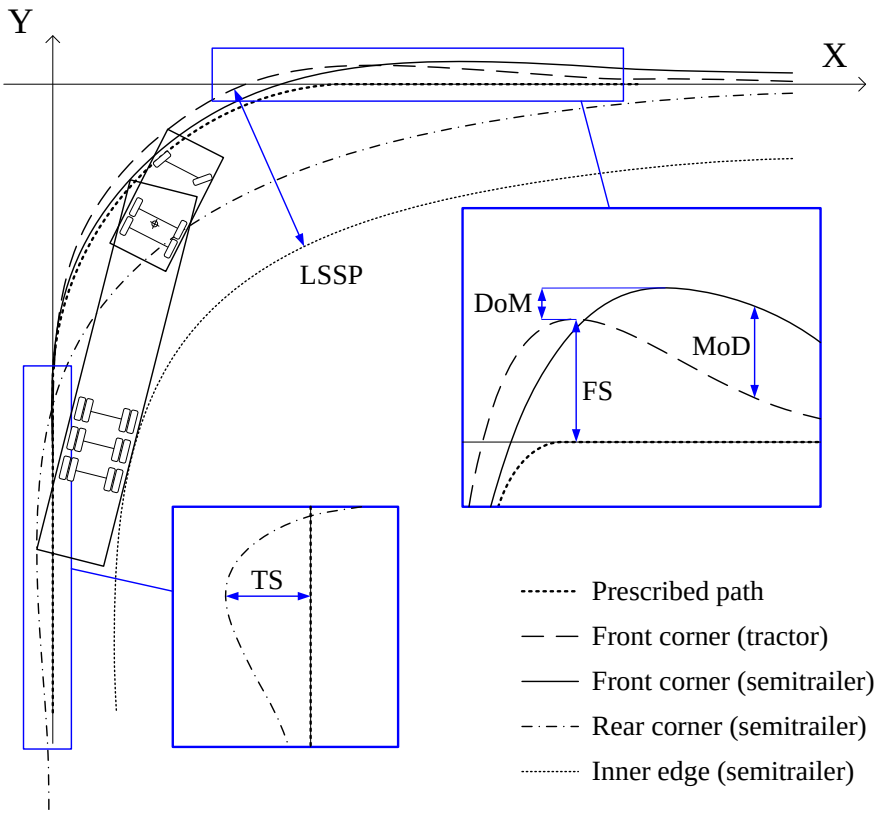


**Figure 2.3: Illustration of the low-speed manoeuvrability standards (example shown for a tractor and semitrailer combination)**

During the turn, the non-steering rear axles of a vehicle, or of any of the vehicles within a combination, will always track inside of the path of the steer axle (or hitch point for trailers) [32]. The longer the wheelbase of a particular vehicle, the more pronounced this offtracking will be. In a ninety-degree turn, the offtracking increases to a maximum and eventually reduces to zero as the vehicle straightens out along the exit tangent. This is unlike a steady-state turn sometimes used in manoeuvrability tests, in which the vehicle will settle into a constant slip angle relative to the prescribed path (usually circular), resulting in constant steady-state offtracking.

The maximum offtracking is termed low-speed swept path or "LSSP". It is defined as the maximum perpendicular distance between the innermost and outermost trajectories of the vehicle. Its magnitude is also affected by the amount of front corner swing-out and not only the rear axle offtracking. Excessive offtracking or road width usage increases the risk of collision with other vehicles, roadside furniture or pedestrians.

During the initial stage of the turn, the rear outer corner of the vehicle will typically swing outwards as the yaw angle of the vehicle increases relative to the Y axis. This is more pronounced on vehicles with large rear overhangs and is known as tail swing (TS). The implications of tail swing are similar to those of LSSP: the tail can swing out into adjacent lanes or into the vicinity of sidewalks and emergency lanes, posing a threat to other vehicles, and to pedestrians and cyclists. For vehicles possessing actively-steered trailers, tail swing may also occur during the exit of the turn. Tail swing is measured relative to the entry tangent of the prescribed path (and to the exit tangent if there is swing-out during exit). Figure 2.3 shows an enlarged view of the trajectory of the rear outer corner of the semitrailer in the entry region of the turn, which describes how tail swing is measured. Note that tail swing may occur in each of the vehicle units in a combination.

In the region in which the steer-tyre approaches the exit tangent, the front corner of the leading vehicle (truck or truck-tractor) will reach a point of maximum swing-out in the Y direction. This maximum swing-out is known as frontal swing or "FS" and is measured relative to the exit tangent of the prescribed path.

For vehicle combinations consisting of one or more semitrailers, the semitrailers will also exhibit front corner swing-out in the exit region of the turn. It is important that a semitrailer does not swing out significantly more than the preceding vehicle. A driver is typically able to visually judge the swing-out of the front corner of the leading vehicle and navigate a turn accordingly, whilst avoiding roadside obstacles or other vehicles. It is more difficult however to judge or observe the swing-out of trailing units. If one of the

trailing units were to swing out significantly more than the leading vehicle, collision with one of the afore-mentioned obstacles may result. To address this risk, the NTC has defined two standards, namely difference of maxima (DoM) and maximum of difference (MoD). DoM is a measure of the difference in *maximum* frontal swing-out of adjacent vehicle units (i.e. a truck and coupled semitrailer, or a leading semitrailer and coupled following semitrailer), and MoD is a measure of the *maximum difference* between the frontal swing-out trajectories of adjacent vehicle units *at any point* along the exit tangent. Figure 2.3 shows an enlarged view of the front corner trajectories of the tractor and semitrailer in the exit region of the turn which assists in the description of FS, DoM and MoD.

### 2.1.2 Motivation to develop a new low-speed turning model

A summary of existing low-speed turning models and their shortcomings follows:

1. The WHI formula [19] can only predict low-speed swept-path, requires predetermined coefficients unique to the path geometry, does not include tyre scrub effects and cannot incorporate steer-tyre path-following.
2. Wang and Linnet's model [27] requires the path to be mathematically defined, requires tyre cornering stiffness to be specified and does not model tyre scrub.
3. Erkert *et al.*'s method [28] uses a tractrix method, the path must be mathematically defined, and steer-tyre path-following and tyre scrub are not accounted for.
4. McGovern's spreadsheet implementation of the tractrix method [29] solves the problem geometrically which negates the need for mathematically-defined paths and the solution of differential equations. However, the spreadsheet environment limits the accuracy of the model, and tyre scrub effects and steer-tyre path-following are not accounted for.
5. Morrison's model [30] incorporates tyre scrub effects by deriving an "effective length" parameter, is computationally inefficient and requires the availability of tyre stiffness properties.
6. Winkler and Aurell's [31] equivalent wheelbase concept is a useful and simpler alternative to Morrison's effective length.

Considering the above points and recalling the objectives in Section 1.3, the geometric tractrix method was redeveloped in Matlab® in this research, incorporating steer-tyre path-following, tyre scrub and the ability to calculate LSSP, TS, FS, DoM and MoD.

## 2.2 Development of a New Low-Speed Turning Model

This section outlines the mathematical development of the model, beginning with the geometric tractrix method, followed by the incorporation of steer-tyre path-following, tyre scrub modelling, and reference point tracking.

### 2.2.1 Tractrix method

Predicting the motion of the rear axle of a vehicle as the front axle follows a set path, can be formulated as a problem in which the leading edge of a rigid link is made to transcribe a certain path while the trailing edge of the link follows passively (restrained to motion in the direction of the link axis). The curve transcribed by the trailing point on the link, or the rear axle of the vehicle, is called a "tractrix" curve [28]. The tractrix concept can be used to build a low-speed vehicle turning model.

Figure 2.4 shows a bicycle model of a rigid vehicle following a prescribed path with respect to the centre of the steering axle. The model assumes pure rolling motion of the wheels (no tyre stiffness effects) and possesses only three degrees of freedom (yaw and in-plane translation). The steering axle is represented by point A and the rear axle by point B. The vehicle has wheelbase $WB$ and the yaw angle of the vehicle relative to the global X axis is denoted by $\theta$. Individual solution steps are recognised by the counter $i$ where $1 \leq i \leq \eta$. The vehicle advances a distance $\Delta s_A$ along the path from point A($i$–1) to point A($i$) and the rear axle advances $\Delta s_B$ in the direction of A($i$–1) from point B($i$–1) to point B($i$). This movement of the rear axle is an approximation that approaches theoretically exact behaviour as $\Delta s_A$ tends towards zero.

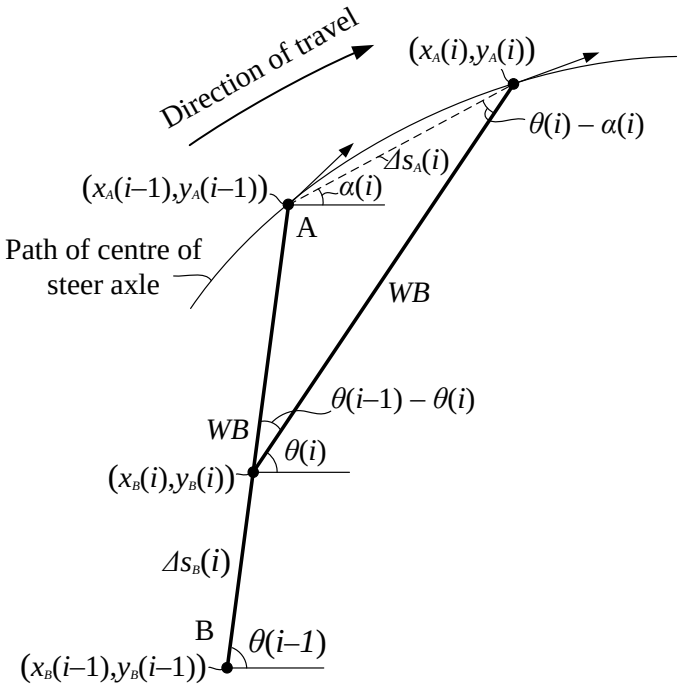


**Figure 2.4: Geometric estimation of the tractrix method**

The prescribed path is taken to be a given input, in discretised form, with $\eta$ denoting the total number of straight-line segments into which the path is broken (i.e. the total number of incremental steps, $i$). If $(x_P(i),y_P(i))$ represents a general point on the discretised path, the requirement that point A follows the path can be described mathematically as

$$\begin{aligned} x_A(i) &= x_P(i) \\ y_A(i) &= y_P(i) \end{aligned} \quad (1 \le i \le \eta). \tag{2.1}$$

For the ninety-degree turn, assuming the entry tangent to be aligned with the Y axis,

$$\theta(1) = \frac{\pi}{2}. \tag{2.2}$$

The advancement from point A($i$–1) to A($i$) can be characterised by a displacement, $\Delta s_A$, and direction, $\alpha$, as

$$\Delta s_A(i) = \sqrt{\left(\Delta x_A(i)\right)^2 + \left(\Delta y_A(i)\right)^2} \quad (2 \le i \le \eta), \tag{2.3}$$

$$\alpha(i) = \arctan\left(\frac{\Delta y_A(i)}{\Delta x_A(i)}\right) \quad (2 \le i \le \eta), \tag{2.4}$$

where

$$\begin{aligned}\Delta x_A(i) &= x_A(i) - x_A(i-1)\\ \Delta y_A(i) &= y_A(i) - y_A(i-1)\end{aligned} \quad (2 \le i \le \eta). \tag{2.5}$$

Geometry gives the yaw angle, $\theta$, and rear axle coordinates, $(x_B(i),y_B(i))$, at step $i$ to be

$$\theta(i) = \theta(i-1) - \arcsin\left(\frac{\Delta s_A(i) \cdot \sin\big(\theta(i-1) - \alpha(i)\big)}{WB}\right) \quad (2 \le i \le \eta), \tag{2.6}$$

$$\begin{aligned}x_B(i) &= x_A(i) - WB \cdot \cos\big(\theta(i)\big)\\ y_B(i) &= y_A(i) - WB \cdot \sin\big(\theta(i)\big)\end{aligned} \quad (1 \le i \le \eta). \tag{2.7}$$

In the case of a vehicle combination consisting of two or more vehicles (or "vehicle units"), the same equations apply for each individual vehicle, except that for trailer units the hitch point takes the place of the steer axle. Let $j$ denote the individual vehicle unit, and let $N$ denote the total number of vehicle units in the combination (including dollies). Assuming the hitch point to be aligned with the longitudinal axis of the preceding vehicle, and denoting its location rearward of the steer axle (or preceding hitch point) as $H$, the global coordinates of the hitch point $A_j$ are described as

$$\begin{aligned}x_{A,j}(i) &= x_{A,j-1}(i) - H_{j-1} \cdot \cos_{j-1}\big(\theta(i)\big)\\ y_{A,j}(i) &= y_{A,j-1}(i) - H_{j-1} \cdot \sin_{j-1}\big(\theta(i)\big)\end{aligned} \quad \begin{pmatrix}1 \le i \le \eta\\ 2 \le j \le N\end{pmatrix}. \tag{2.8}$$

Thereafter, Equations (2.2) to (2.8) apply as before with the simple addition of the vehicle subscript, $j$. Equations (2.9) to (2.16) represent the generalised solution of the basic geometric model for a vehicle combination consisting of any number of vehicle units.[1]

$$\begin{aligned}x_{A,1}(i) &= x_P(i)\\ y_{A,1}(i) &= y_P(i)\end{aligned} \quad (1 \le i \le \eta) \tag{2.9}$$

$$\theta_j(1) = \frac{\pi}{2} \quad (1 \le j \le N) \tag{2.10}$$

$$\begin{aligned}\Delta x_{A,j}(i) &= x_{A,j}(i) - x_{A,j}(i-1)\\ \Delta y_{A,j}(i) &= y_{A,j}(i) - y_{A,j}(i-1)\end{aligned} \quad \begin{pmatrix}2 \le i \le \eta\\ 1 \le j \le N\end{pmatrix} \tag{2.11}$$

$$\Delta s_{A,j}(i) = \sqrt{\big(\Delta x_{A,j}(i)\big)^2 + \big(\Delta y_{A,j}(i)\big)^2} \quad \begin{pmatrix}2 \le i \le \eta\\ 1 \le j \le N\end{pmatrix} \tag{2.12}$$

[1] Using these basic model equations, axle trajectories were found to converge to within 1 mm using a constant step size of 5 mm to discretise the input path.

$$\alpha_j(i) = \arctan\left(\frac{\Delta y_{A,j}(i)}{\Delta x_{A,j}(i)}\right) \quad \begin{pmatrix} 2 \le i \le \eta \\ 1 \le j \le N \end{pmatrix} \tag{2.13}$$

$$\theta_j(i) = \theta_j(i-1) - \arcsin\left(\frac{\Delta s_{A,j}(i) \cdot \sin\left(\theta_j(i-1) - \alpha_j(i)\right)}{WB_j}\right) \quad \begin{pmatrix} 2 \le i \le \eta \\ 1 \le j \le N \end{pmatrix} \tag{2.14}$$

$$\begin{aligned} x_{A,j}(i) &= x_{A,j-1}(i) - H_{j-1} \cdot \cos\left(\theta_{j-1}(i)\right) \\ y_{A,j}(i) &= y_{A,j-1}(i) - H_{j-1} \cdot \sin\left(\theta_{j-1}(i)\right) \end{aligned} \quad \begin{pmatrix} 1 \le i \le \eta \\ 2 \le j \le N \end{pmatrix} \tag{2.15}$$

$$\begin{aligned} x_{B,j}(i) &= x_{A,j}(i) - WB_j \cdot \cos\left(\theta_j(i)\right) \\ y_{B,j}(i) &= y_{A,j}(i) - WB_j \cdot \sin\left(\theta_j(i)\right) \end{aligned} \quad \begin{pmatrix} 1 \le i \le \eta \\ 1 \le j \le N \end{pmatrix} \tag{2.16}$$

### 2.2.2 Steer-tyre path-following

The preceding derivation of the tractrix method was based on the leading vehicle following the path with respect to the centre of the steer axle. To achieve steer-tyre path-following, some adjustments to the model must be made.

Whereas Morrison's instantaneous centre method allows a choice of path-following reference point, the tractrix method does not. An alternative method of obtaining steer-tyre path-following was hence required. With reference to Figure 2.5, at the commencement of the turn (location 1), by laterally offsetting the steer axle from the prescribed path, A, by a distance *T*/2 (half the "steer-tyre track width" – defined here as the distance between extreme tyre walls), the outer steer-tyre wall will be aligned with the prescribed path as desired. As the vehicle follows path B into the turn however (general location 2), the steer axle is no longer perpendicular to the prescribed path, and so the steer-tyre wall will no longer be aligned with path A as intended. The lateral offset of *T*/2 is only applicable at the commencement of the turn. At all subsequent points, a non-constant offset, *e*, between the outer steer-tyre wall and the prescribed path must be accounted for as illustrated in the figure. This offset easily exceeds the NTC allowance of 50 mm.

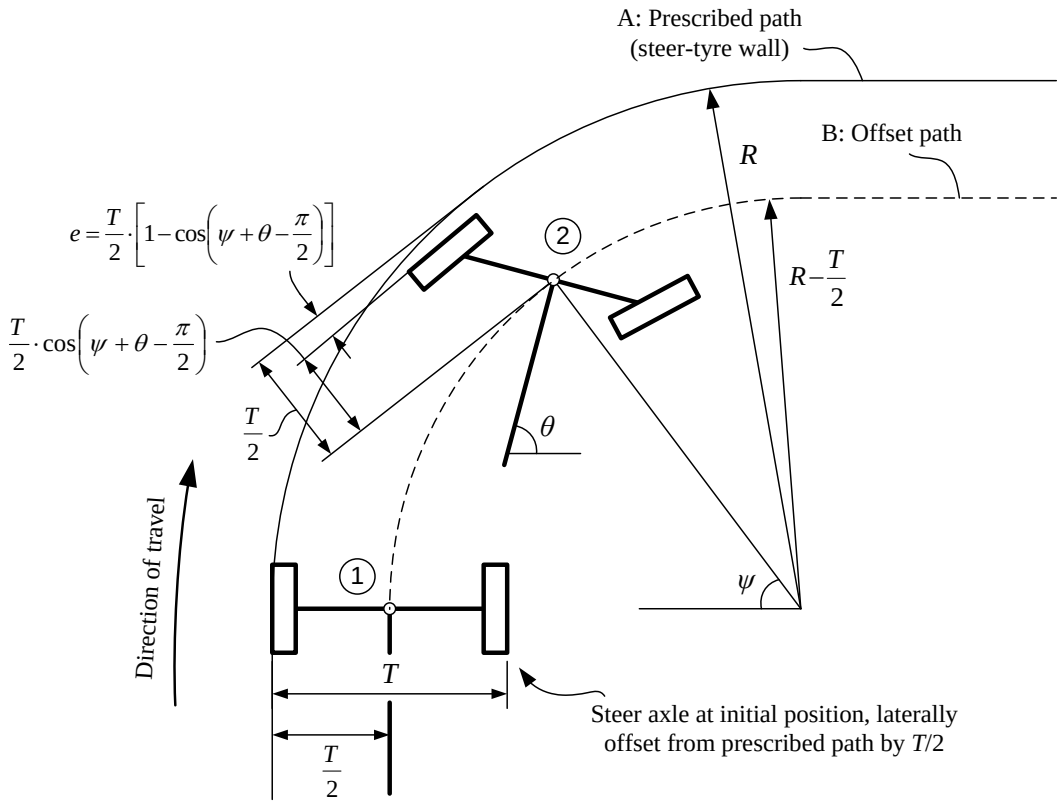


**Figure 2.5: The effect of offsetting the prescribed path by half the steer-tyre track width ($T/2$) in a first attempt at achieving steer-tyre path-following**

The methodology employed to achieve steer-tyre path-following was as follows:

1. The prescribed path, A, is redefined as perpendicularly offset by half the steer-tyre track width ($T/2$) towards the centre of the turn to give a new offset path, B.

2. A preliminary solution is found solving Equations (2.1) to (2.7) considering only the leading vehicle following path B. (Solving for trailing vehicles at this stage is irrelevant and would only increase computation time.)

3. Using this preliminary solution, the lateral offset, $e$, between the path of the steer-tyre wall and the prescribed path is calculated using

$$e(i) = \frac{T}{2} \cdot \left[1 - \cos\left(\psi(i) + \theta(i) - \frac{\pi}{2}\right)\right] \quad (1 \le i \le \eta) \tag{2.17}$$

   where $\psi$ is the turn angle (see Figure 2.5) and ranges from 0° to 90° during the turn and remains constant at 90° during the exit tangent.

4. Path B is then redefined, subtracting $e(i)$ from the original $T/2$ offset, to give path C (see Figure 2.6).

5. The final solution is found solving Equations (2.9) to (2.16) as the leading vehicle follows path C, with the steer-tyre wall following path A as required.

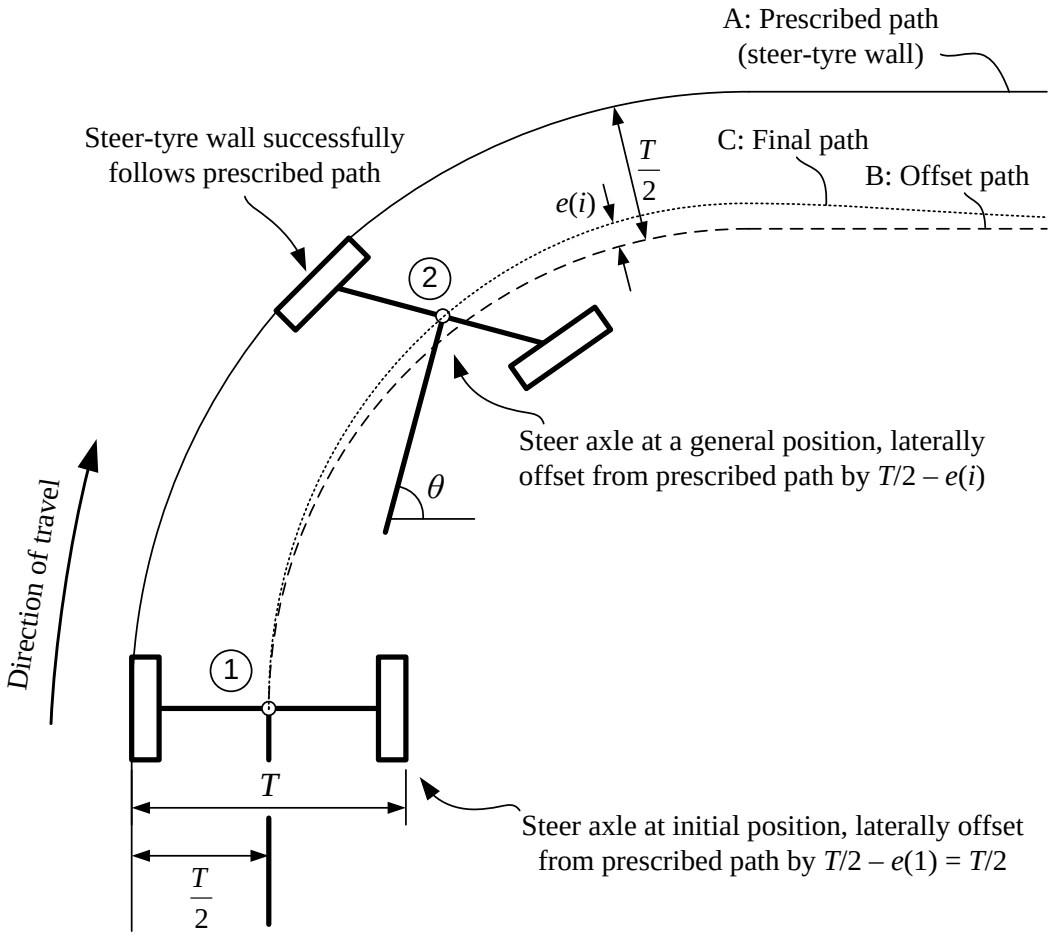


**Figure 2.6: Second path offset of *e*(*i*) to successfully achieve steer-tyre path-following**

The above method does not take into account the fact that the steer angle would cause the outermost point of the tyre to lie off the axle centreline. Furthermore, the method assumes the kingpin is located a lateral distance $T/2$ from the axle centre when in reality the kingpin is located inside of this point. For the NTC 12.5 m radius ninety-degree turn, these effects were negligible.

### 2.2.3 Tyre scrub

Due to large payloads, trucks and trailers commonly utilise axle groups consisting of two or more axles. Such axle groups are predominantly non-steering and result in slip angles being generated which effect the vehicle's turning behaviour.

Figure 2.7 (a) shows a bicycle model of a two-axle rigid truck in a low-speed turning manoeuvre. The arrows indicate the direction of travel of the tyres. The perpendiculars to

the tyre directions of travel intersect at the centre of the turn and no slip angles or lateral tyre forces are generated. The tyres experience pure rolling motion and this scenario is denoted "Ackerman turning" [32]. Figure 2.7 (b) shows an identical vehicle but with two non-steering rear axles. Because the two rear axles are parallel to each other, perpendicular lines projected along their axes can never meet at the centre of the turn. Slip angles $\zeta_2$ and $\zeta_3$ and lateral forces $F_{y,2}$ and $F_{y,3}$ are generated. The two lateral forces act in opposing directions and generate a yaw moment. To counter this moment, a slip angle $\zeta_1$ and lateral force $F_{y,1}$ are developed at the steer axle.

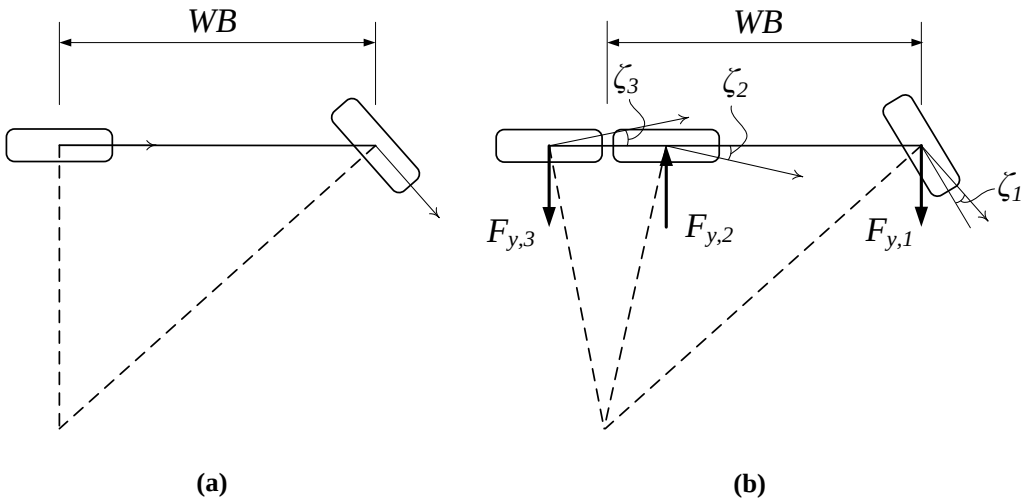


**Figure 2.7: Effect of multiple non-steering rear axles on the low-speed turning behaviour of a rigid truck: (a) single rear axle, and (b) dual non-steering rear axles**

To model these effects, Winkler and Aurell proposed the "equivalent wheelbase" principle [31]. This is based upon the premise that a vehicle with multiple non-steering axles with wheelbase *WB* may be reduced to an equivalent two-axle vehicle with equivalent wheelbase $WB_{Eq}$, producing the same steady-state turning behaviour. The principle is illustrated in Figure 2.8 (adapted from [31] for the specific case of low-speed turning). The broken lines represent a bicycle model of a rigid truck with two non-steering rear axles. The equivalent two-axle vehicle is depicted by the continuous lines. The vehicle has geometric wheelbase *WB* and the distance to each non-steering axle from the geometric centre of the axle group is denoted by $\Delta$.

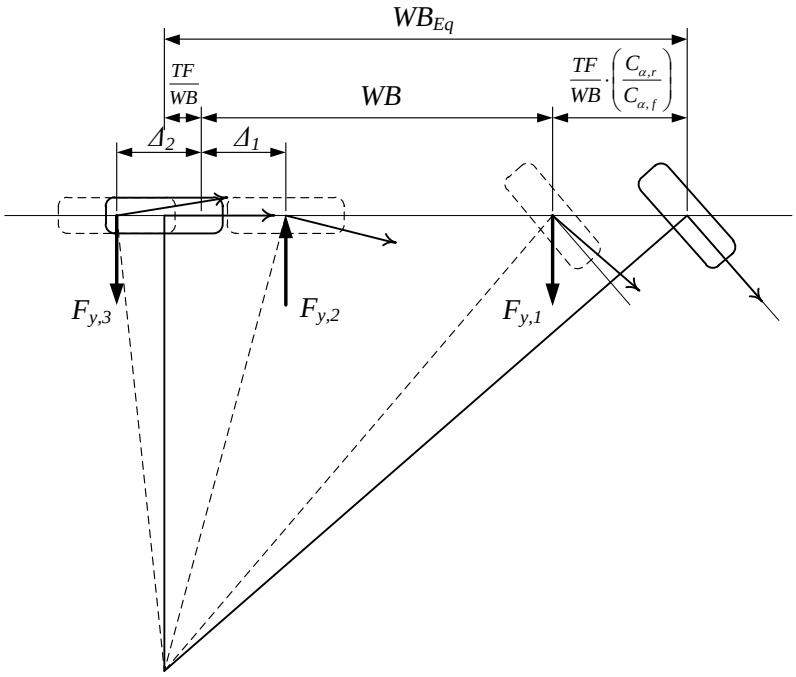


**Figure 2.8: Equivalent wheelbase principle illustrated for a three-axle rigid truck (adapted from** [31] **for the specific case of low-speed turning)**

The wheelbase of the equivalent two axle vehicle may be defined as

$$WB_{Eq} = WB + \frac{TF}{WB} + \frac{TF}{WB}\cdot\left(\frac{C_{\alpha,r}}{C_{\alpha,f}}\right) \tag{2.18}$$

where $TF$ is denoted the "tandem factor" in $m^2$, and $C_{\alpha,f/r}$ is the sum of the cornering stiffnesses of the front/rear tyres in N/° (where cornering stiffness is, in a linearized tyre model, the constant of proportionality between a tyre's slip angle and the resultant lateral force developed, i.e. $F_y = C_\alpha \cdot \zeta$). Equation (2.18) assumes the effects of dual tyres to be negligible relative to the effect of multiple non-steering axles, and that each of the rear axles is subjected to equal vertical loads and fitted with identical linear tyres. For a vehicle with $n$ non-steering rear axles, the tandem factor, $TF$, is defined as

$$TF = \frac{\sum_{p=1}^{n} \Delta_p^{\,2}}{n}. \tag{2.19}$$

The second term in Equation (2.18) may be interpreted as the position of the equivalent rear axle rearward of the geometric centre of the original rear axle group, and the third term may be interpreted as the position of the equivalent steer axle forward of its original position. In the specific case of low-speed turning, this equivalent vehicle model develops no slip angles or lateral forces and satisfies the Ackerman turning condition.

Winkler and Aurell showed that Equation (2.18) addresses the effect of tyre scrub in steady-state vehicle handling analyses of a rigid truck with multiple non-steering rear axles. The study was concerned with the steady-state relationships between lateral acceleration, steer angle, turn radius, velocity and wheelbase. No consideration was given to the tracking of vehicle reference points. In the context of a low-speed geometric model, it is necessary to disregard the third term in Equation (2.18) in increasing the trailing distance of the rear axle from $WB$ to $WB_{Eq}$. The second term addresses the effect of the multiple non-steering axles on the trailing behaviour of the rear axle group, a necessary requirement for the low-speed turning model. The third term addresses the change in steer angle that the equivalent vehicle model incurs to achieve the same behaviour as the actual vehicle when considering variables such as are associated with handing diagrams. This is of no relevance here and can be ignored. A positive implication of this is that the geometric model is insensitive to tyre cornering stiffness – although the model assumes that all tyres exhibit identical and linear cornering stiffness properties.

The low-speed turn in question is a *transient* manoeuvre, in that the vehicle does not stabilise to a fixed level of steady-state offtracking as it would do in a sustained circular turn (see Section 2.1.1). It may seem, therefore, that Winkler and Aurell's equivalent wheelbase principle, derived using the assumption of *steady-state* turning, has been used beyond its scope. In the context of Winkler and Aurell's study however, steady-state is taken to mean constant acceleration (e.g. constant lateral acceleration and constant forward velocity). For example, steady-state "handling diagrams" are typically generated by driving a vehicle along a circular path and incrementally increasing the vehicle's speed at a low rate of around $0.1 \cdot g$ [32]. Although the speed is increasing (and so therefore is lateral acceleration), the rate at which it does so is small enough such that a pseudo-steady-state is achieved and suitable steady-state data may be inferred at each of the speed increments. In the context of the low-speed turn, the speed has been assumed low enough such that acceleration is zero, i.e. constant. Furthermore, due to the low speed during the turn, the rate at which changes in vehicle parameters such as slip angles occur is low. The turn is therefore a pseudo-steady-state turn in the context of Winkler and Aurell's study, and the equivalent wheelbase principle may be used.

Although Winkler and Aurell's argument was presented for the case of a rigid truck, the same may be applied to trailers. The primary difference is that the hitch point of the trailer effectively becomes the steer axle. However, another difference lies in the fact that lateral hitch forces are not present in the case of a rigid truck. Adding trailers introduces this complexity to each of the vehicle units in the combination – a complexity that is not incorporated into the derivation of the equivalent wheelbase concept. The effects of hitch

forces on the equivalent wheelbase were assumed negligible in line with the findings of Morrison [30]. For larger turn radii (and hence smaller articulation angles) the effects of this assumption would decrease. With the above considerations, Equation (2.18) becomes

$$WB_{j,Eq} = WB_j + \frac{TF_j}{WB_j}. \tag{2.20}$$

Denoting the axle spacing (the distance between adjacent axles within an axle group) as *d*, Equation (2.19) may be substituted into Equation (2.20) to yield the three common cases of a single rear axle, tandem rear axle group and tridem rear axle group as shown in Equations (2.21), (2.22) and (2.23) respectively.

$$\begin{gathered} n_j = 1 \\ WB_{j,Eq} = WB_j \end{gathered} \tag{2.21}$$

$$\begin{gathered} n_j = 2 \\ \Delta_{j,1} = d_j/2, \Delta_{j,2} = d_j/2 \\ WB_{j,Eq} = WB_j + \frac{1}{2}\cdot\left(\frac{\left(d_j/2\right)^2 + \left(d_j/2\right)^2}{WB_j}\right) \end{gathered} \tag{2.22}$$

$$\begin{gathered} n_j = 3 \\ \Delta_{j,1} = d_j, \Delta_{j,2} = 0, \Delta_{j,3} = d_j \\ WB_{j,Eq} = WB_j + \frac{1}{3}\cdot\left(\frac{{d_j}^2 + {d_j}^2}{WB_j}\right) \end{gathered} \tag{2.23}$$

For the general case of *n* non-steering rear axles, the values for $\Delta_{j,i}$ to $\Delta_{j,n}$ may be calculated according to whether the number of axles is odd or even. For example, if *n* is an odd number, $\Delta_{j,1} = 0$, $\Delta_{j,2} = \Delta_{j,3} = d$, $\Delta_{j,4} = \Delta_{j,5} = 2\cdot d$, $\Delta_{j,6} = \Delta_{j,7} = 3\cdot d$ *etc.* according to a basic numerical pattern. If *n* is an even number, $\Delta_{j,1} = \Delta_{j,2} = (1/2)\cdot d$, $\Delta_{j,3} = \Delta_{j,4} = (3/2)\cdot d$, $\Delta_{j,5} = \Delta_{j,6} = (5/2)\cdot d$ *etc*. These types of patterns are easily implementable in Matlab®. The model therefore theoretically caters for any number of non-steering rear axles. $WB_{j,Eq}$ may be substituted for $WB_j$ in Equations (2.9) to (2.16) to incorporate the effects of multiple non-steering rear axles.

### 2.2.4 Reference point tracking

Having derived the motion paths of the front and rear axle centres for all vehicles, inferring the motions of any reference point on any vehicle reduces to a simple geometric problem. For the purposes of calculating LSSP, TS, FS, DoM and MoD, three vehicle reference points are required: a front outer corner, a rear outer corner, and the innermost edge of the vehicle (the trajectory of which is used to deduce LSSP). The three points may be described in the $j^{th}$ vehicle's reference frame by the following parameters:

- $FC_{long,j}$: Front outer corner, longitudinal location forward of the steer axle/hitch.
- $FC_{lat,j}$: Front outer corner, lateral location to the left of the vehicle axis.
- $RC_{long,j}$: Rear outer corner, longitudinal location rearward of the steer axle/hitch.
- $RC_{lat,j}$: Rear outer corner, lateral location to the left of the vehicle axis.
- $IE_{lat,j}$: Inner edge used for LSSP tracking, lateral location to the right of the vehicle axis. The longitudinal location if this point rearward of the steer axle/hitch is taken to be $WB_{j,Eq}$.

Hereafter, unless otherwise stated, the terms "front corner", "rear corner" and "inner edge" will be taken to mean the "front outer corner giving rise to the maximum frontal swing-out," "rear outer corner giving rise to the maximum tail swing-out," and "the innermost edge relative to the curvature of the prescribed path giving rise to the maximum swept path." The *global* coordinates $(x_{FC,j}(i),y_{FC,j}(i))$, $(x_{RC,j}(i),y_{RC,j}(i))$ and $(x_{IE,j}(i),y_{IE,j}(i))$, representing the trajectories of the front corner, rear corner and inner edge respectively, are described by (for all $1 \le i \le \eta$ and $1 \le j \le N$)

$$\begin{aligned} x_{FC,j}(i) &= x_{A,j}(i) + FC_{long,j} \cdot \cos\left(\theta_j(i)\right) - FC_{lat,j} \cdot \cos\left(\frac{\pi}{2} - \theta_j(i)\right), \\ y_{FC,j}(i) &= y_{A,j}(i) + FC_{long,j} \cdot \sin\left(\theta_j(i)\right) + FC_{lat,j} \cdot \sin\left(\frac{\pi}{2} - \theta_j(i)\right), \end{aligned} \tag{2.24}$$

$$\begin{aligned} x_{RC,j}(i) &= x_{A,j}(i) - RC_{long,j} \cdot \cos\left(\theta_j(i)\right) - RC_{lat,j} \cdot \cos\left(\frac{\pi}{2} - \theta_j(i)\right), \\ y_{RC,j}(i) &= y_{A,j}(i) - RC_{long,j} \cdot \sin\left(\theta_j(i)\right) + RC_{lat,j} \cdot \sin\left(\frac{\pi}{2} - \theta_j(i)\right), \end{aligned} \tag{2.25}$$

$$x_{IE,j}(i) = x_{A,j}(i) - WB_j \cdot \cos\left(\theta_j(i)\right) + IE_{lat,j} \cdot \cos\left(\frac{\pi}{2} - \theta_j(i)\right),$$
$$y_{IE,j}(i) = y_{A,j}(i) - WB_j \cdot \sin\left(\theta_j(i)\right) - IE_{lat,j} \cdot \sin\left(\frac{\pi}{2} - \theta_j(i)\right). \quad (2.26)$$

Figure 2.9 illustrates the three vehicle reference points (in the vehicle's frame of reference) and their associated coordinates (in the global frame of reference). Figure 2.3 illustrates the trajectories formed by the motion of these reference points (for the example case of a tractor and semitrailer) and the associated measurement of LSSP, TS, FS, DoM and MoD. The two figures should be used for reference in the following discussion.

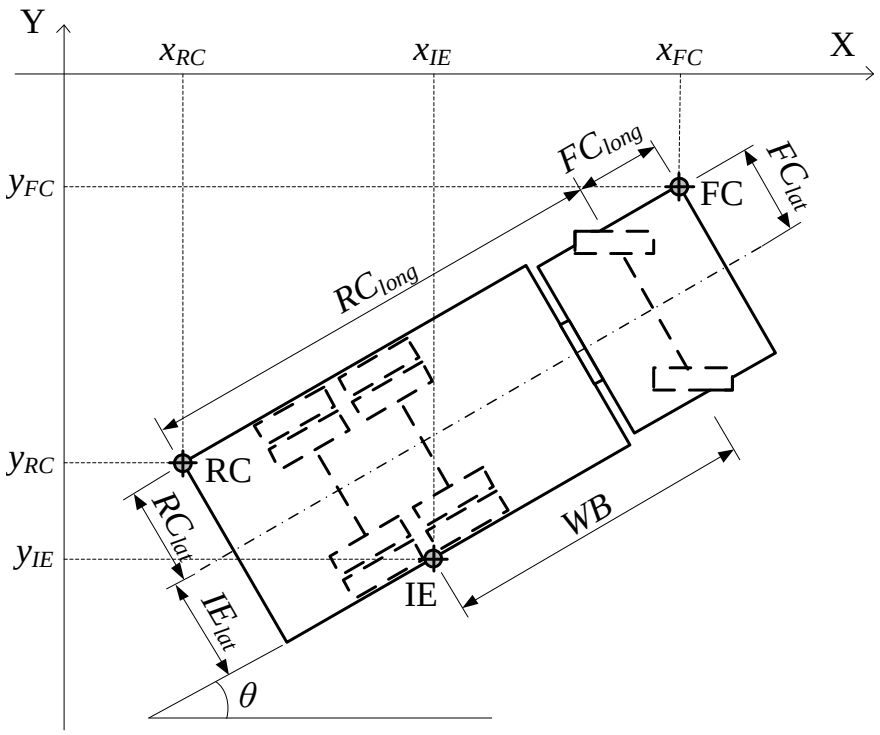


**Figure 2.9: Vehicle reference points and associated global coordinates**

Due to the manner in which the prescribed path was described in the global reference frame – with the entry and exit tangents aligned with the negative Y and positive X axes respectively – tail swing and frontal swing may be deduced from minimum *x* and maximum *y* values respectively over the extent of the manoeuvre. The tail swing for individual vehicle units, $TS_j$, is calculated using

$$TS_j = \left| \min\left(x_{RC,j}(i)\right) \right| \quad \begin{pmatrix} 1 \le i \le \eta \\ 1 \le j \le N \end{pmatrix}. \quad (2.27)$$

The overall maximum tail swing, TS, is hence

$$\mathrm{TS} = \max\left(\mathrm{TS}_j\right) \quad (1 \le j \le N). \tag{2.28}$$

Frontal swing is defined as the maximum swing-out of the front corner of the first vehicle unit and may be found using

$$\mathrm{FS} = \max\left(y_{FC,1}(i)\right) \quad (1 \le i \le \eta). \tag{2.29}$$

Difference of maxima is simply the difference in frontal swing-out of adjacent vehicles units where one of the vehicles is a semitrailer. Due to the manner in which vehicle units were defined to include dollies, care must be taken to note when an adjacent vehicle unit, i.e. vehicle unit ($j$+1), is a dolly. In such a case, the algorithm is made aware of the fact and utilises the subsequent vehicle, ($j$+2), in the calculation instead. The subsequent DoM calculation will start with vehicle unit ($j$+2) and not ($j$+1), and the value of DoM for vehicle $j$ (in front of the dolly) is simply set to zero. $N$–1 values of DoM will be calculated. So, for the case of adjacent vehicles not incorporating a dolly (such as a tractor and semitrailer), $\mathrm{DoM}_j$ may be calculated according to

$$\mathrm{DoM}_j = \max\left(y_{FC,j}(i)\right) - \max\left(y_{FC,j+1}(i)\right) \quad (1 \le i \le \eta). \tag{2.30}$$

If the vehicle at position ($j$+1) is a dolly, as would be the case for a truck and full-trailer combination, the equation becomes

$$\mathrm{DoM}_j = \max\left(y_{FC,j}(i)\right) - \max\left(y_{FC,j+2}(i)\right) \quad (1 \le i \le \eta). \tag{2.31}$$

The overall reportable result for $\mathrm{DoM}_j$ is

$$\mathrm{DoM} = \max\left(\mathrm{DoM}_j\right) \quad (1 \le j \le N-1). \tag{2.32}$$

MoD and LSSP are not as straight forward to calculate as TS, FS and DoM, and require additional data manipulation. The calculation of MoD will be described first.

The trajectory of the front corner of the leading vehicle in question, $j$, was arbitrarily selected as the baseline trajectory from which to calculate $\mathrm{MoD}_j$. To save computation time, it is unnecessary to consider values of $y_{FC,j}$ less than zero (see Figure 2.10 where X and Y represent the global, "earth-fixed" coordinate system). Thereafter, for each coordinate point ($x_{FC,j}(i)$,$y_{FC,j}(i)$), the difference between the swing-out of the $j^{\text{th}}$ vehicle unit and the vehicle unit in position ($j$+1) or ($j$+2) (as applicable) may be calculated. Because the $i^{\text{th}}$ coordinate of $y_{FC,j}$ and the $i^{\text{th}}$ coordinate of $y_{FC,j+1}$ (or $y_{FC,j+2}$) will not, in general, share the same $x$ coordinate, $\mathrm{MoD}_j$ cannot be calculated as the difference between $y_{FC,j}(i)$ and $y_{FC,j+1}(i)$ (or $y_{FC,j}(i)$ and $y_{FC,j+2}(i)$). As an approximation, it can be calculated by interpolating $y_{FC,j+1}(i)$ or $y_{FC,j+2}(i)$ at an $x$ value of $x_{FC,j}(i)$.

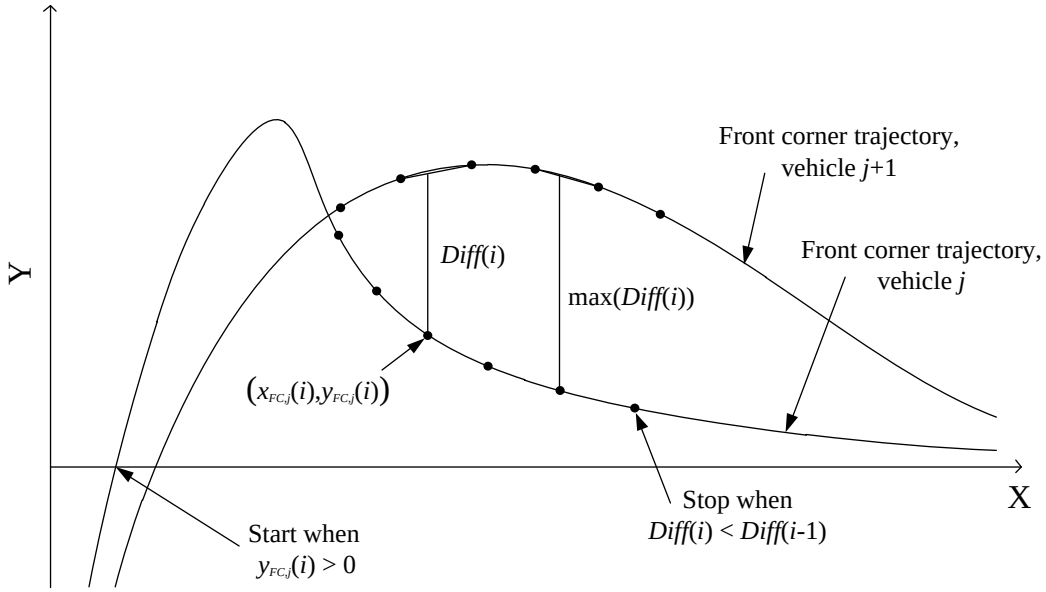


**Figure 2.10: MoD calculation method**

The variable $Diff_j$, as described in Figure 2.10, is defined as

$$Diff_j(i) = y_{FC,j}(i) - y_{FC,j+1}\big|_{x_{FC,j}(i)} \quad \begin{pmatrix} 1 \le i \le \eta \\ y_{FC,j}(i) > 0 \end{pmatrix}, \tag{2.33}$$

or, if vehicle unit ($j$+1) is a dolly,

$$Diff_j(i) = y_{FC,j}(i) - y_{FC,j+2}\big|_{x_{FC,j}(i)}. \tag{2.34}$$

In the interest of further reducing computation time, the steps after which $Diff_j(i)$ starts to decline in magnitude may be disregarded as only one maximum will exist. $MoD_j$ may be calculated using

$$\mathrm{MoD}_j = \max\left(\left|Diff_j(i)\right|\right) \quad \begin{pmatrix} 1 \le i \le \eta \\ 1 \le j \le N-1 \end{pmatrix}, \tag{2.35}$$

and the overall reportable value of MoD will be

$$\mathrm{MoD} = \max\left(\mathrm{MoD}_j\right) \quad (1 \le j \le N-1). \tag{2.36}$$

LSSP is defined as the maximum swept path width between the trajectory of the front corner of the leading vehicle unit and that of the inner edge of the rearmost vehicle unit. The swept path width is a maximum at the point where the width is perpendicular to both the inner and outer path trajectories. Therefore, if for each step a line was projected perpendicularly from the first trajectory until it intersected the second, and the length of this line was measured, the point at which this line reached its maximum length would be the point that it was perpendicular to the second trajectory, and this length would be the

maximum swept path width. The details of this approach are now discussed with the aid of Figure 2.11.

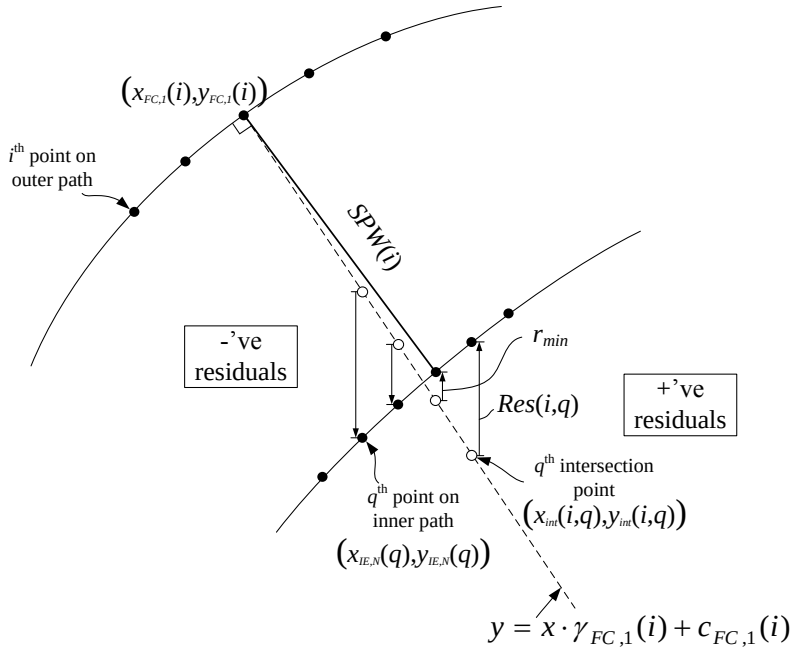


**Figure 2.11: LSSP solution method**

Taking ($x_{FC,1}$,$y_{FC,1}$) to be the outer trajectory, the gradient, $\gamma_{FC,1}(i)$, of a line passing through each point perpendicular to the path's tangent at that point may be determined. Matlab® contains built-in functions that were used for this purpose. The Y intercept of this line, $c_{FC,1}(i)$, may be determined by substituting $x_{FC,1}(i)$, $y_{FC,1}(i)$ and $\gamma_{FC,1}(i)$ into

$$c_{FC,1}(i) = y_{FC,1}(i) - \gamma_{FC,1}(i) \cdot x_{FC,1}(i) \quad (1 \le i \le \eta). \tag{2.37}$$

The intercept of this line with the inner trajectory, ($x_{IE,N}$,$y_{IE,N}$) may be determined via various means. An example is the "intersections.mat" m-file developed by Douglas M. Schwarz, Copyright (c) 2008, which is freely available for public use and can calculate the intersections of any two curves characterised by two sets of ($x$,$y$) coordinates. However, such a method is computationally very expensive, especially for the size of data arrays anticipated in the geometric model. A simplified method was derived in order to reduce the computation time.

For each step, $i$, the perpendicular line $y = \gamma_{FC,1}(i) \cdot x + c_{FC,1}(i)$ is constructed as discussed above. For each of these steps in turn, for every $q^{th}$ point on the inner path, the "residual", *Res*, representing the ordinate distance from the line to the point ($x_{IE,N}(q)$, $y_{IE,N}(q)$), may be calculated. This is done by first substituting $x_{IE,N}(q)$ into

$$y_{\text{int}}(i,q) = \gamma_{FC,1}(i) \cdot x_{IE,N}(q) + c_{FC,1}(i) \quad \begin{pmatrix} 1 \le i \le \eta \\ 1 \le q \le \eta \end{pmatrix} \tag{2.38}$$

and then calculating the residual according to

$$Res\ (i,q) = y_{IE}(q) - y_{\text{int}}(i,q) \quad \begin{pmatrix} 1 \le i \le \eta \\ 1 \le q \le \eta \end{pmatrix} \tag{2.39}$$

to give an $\eta$-by-$\eta$ *Res* matrix.

For each point $i$, the $q^{\text{th}}$ point at which $Res(i,q)$ is a minimum, $q_{\text{minRes}}(i)$, represents the point at which the perpendicular line projected from the first curve approximately intersects the second. The length of this line segment is denoted $SPW(i)$ and may be determined according to

$$SPW(i) = \sqrt{\left[x_{FC,1}(i) - x_{IE,N}(q_{\text{minRes}}(i))\right]^2 + \left[y_{FC,1}(i) - y_{IE,N}(q_{\text{minRes}}(i))\right]^2} \tag{2.40}$$

for all $1 \le i \le \eta$, from which LSSP can be calculated according to

$$\text{LSSP} = \max\left(SPW(i)\right). \tag{2.41}$$

In order to further reduce computation time, because the magnitude of $SPW(i)$ is typically three orders of magnitude larger than the incremental step size, negligible accuracy is lost by using a step size notably larger than that used in the original calculations. A step size of 0.1 m proved suitable for the calculation of LSSP.

The mathematical foundations of the geometric model have been presented, and the implementation of the model in Matlab® is covered in Appendix B.

## 2.3 Validation

The geometric model was validated using TruckSim®, a commercially available vehicle dynamics software package. TruckSim® is a product of many years of heavy vehicle research and experimental validation at the University of Michigan Transportation Research Institute (UMTRI), and is deemed to be a suitably accurate simulation tool against which to validate the geometric model. Two representative car-carrier configurations were selected for model validation: a truck and tag-trailer combination or "Vehicle 1", and a tractor and semitrailer combination or "Vehicle 2". Details of the two vehicles are given in Table 2.1.

**Table 2.1: Vehicle parameters for model validation**

| Parameter | Vehicle 1 | | Vehicle 2 | |
|---|---|---|---|---|
| | **Truck** | **Trailer** | **Tractor** | **Semitrailer** |
| Steer-tyre track width (m) | 2.494 | - | 2.277 | - |
| Wheelbase (m) | 4.083 | 9.000 | 3.800 | 9.600 |
| No. of rear axles | 2 | 3 | 1 | 2 |
| Axle spacing (m) | 1.365 | 1.360 | - | 1.350 |
| Single/Dual tyres | Dual | Single | Dual | Single |
| Suspension | Steel | Steel | Steel | Air |
| Hitch location (m) | 5.745 | - | 3.400 | - |
| $FC_{long}$ (m) | 1.300 | - | 1.200 | 1.700 |
| $FC_{lat}$ (m) | 1.300 | - | 1.200 | 1.300 |
| $RC_{long}$ (m) | 7.000 | 14.500 | - | 13.700 |
| $RC_{lat}$ (m) | 1.300 | 1.300 | - | 1.300 |
| $IE_{lat}$ (m) | 1.300 | 1.300 | 1.300 | 1.300 |

Additional vehicle configurations were introduced by increasing and decreasing each trailer wheelbase by 1 m; increasing the number of validation cases to six. Furthermore, single, tandem and tridem trailer axle groups were assessed for each trailer. To identify the error introduced by variations in parameters to which the geometric model is not sensitive, dual tyre and unladen trailer scenarios were also investigated. The effect of the number of trailer axles was investigated using an unladen vehicle so as to reduce the skewing of the results due to unrealistic load scenarios – i.e. it is unrealistic to support a load designed to be supported by three axles with only one axle. A summary of the scenarios considered for the two vehicles is shown in Table 2.2. Fourteen scenarios were considered in total – one original and six variations of each vehicle configuration.

**Table 2.2: Validation scenario matrix**

| Scenario | Trailer axles | | Trailer tyres | Trailer load | Trailer wheelbase |
|---|---|---|---|---|---|
| | **Veh. 1** | **Veh. 2** | | | |
| **1** | 3 | 2 | Single | Laden | Original |
| **2** | 3 | 2 | ***Dual*** | Laden | Original |
| **3** | 3 | 2 | Single | Laden | ***Original + 1 m*** |
| **4** | 3 | 2 | Single | Laden | ***Original – 1 m*** |
| **5** | 3 | 2 | Single | ***Unladen*** | Original |
| **6** | ***2*** | ***1*** | Single | ***Unladen*** | Original |
| **7** | ***1*** | ***3*** | Single | ***Unladen*** | Original |

Validation results for LSSP, TS and FS are shown in Figure 2.12, Figure 2.13 and Figure 2.14 respectively. DoM and MoD results for Vehicle 2 are shown in Figure 2.15. The broken diagonal line in each figure represents equality between the geometric model results and TruckSim® results – the nearer the data are to this line, the smaller the discrepancy between models. The overall agreement of results between geometric and TruckSim® models was good. Results for Vehicle 1 corroborated less well than those of for Vehicle 2. For the cases considered, the geometric model marginally over-predicted LSSP but under-predicted TS, DoM and MoD. Results for FS were mostly under-predicted by the geometric model. An under-prediction is preferred as this yields conservative estimates of vehicle performance.

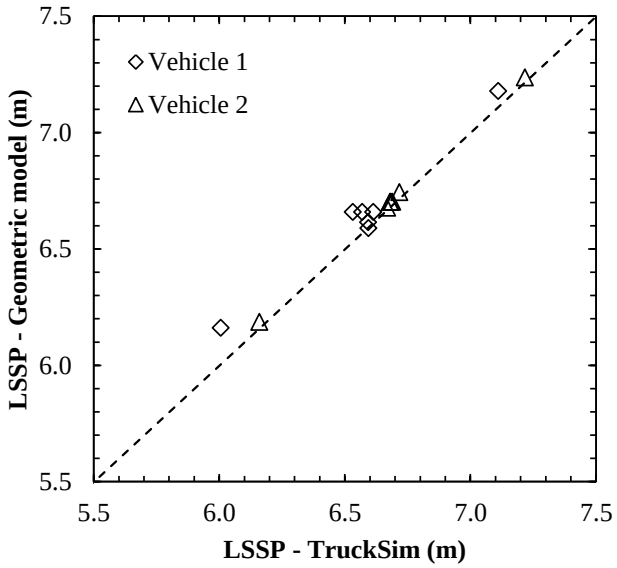


**Figure 2.12: Validation results, low-speed swept path**

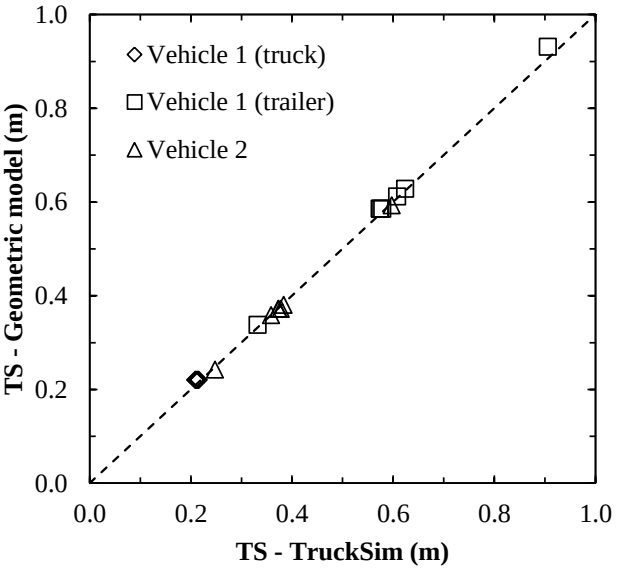


**Figure 2.13: Validation results, tail swing**

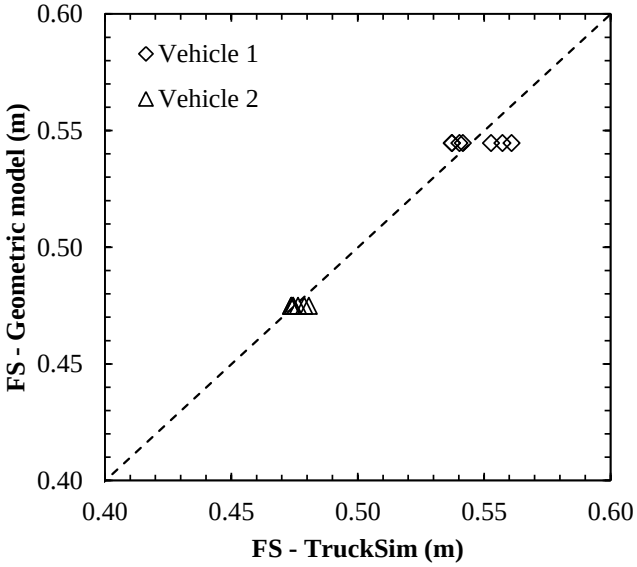


**Figure 2.14: Validation results, frontal swing**

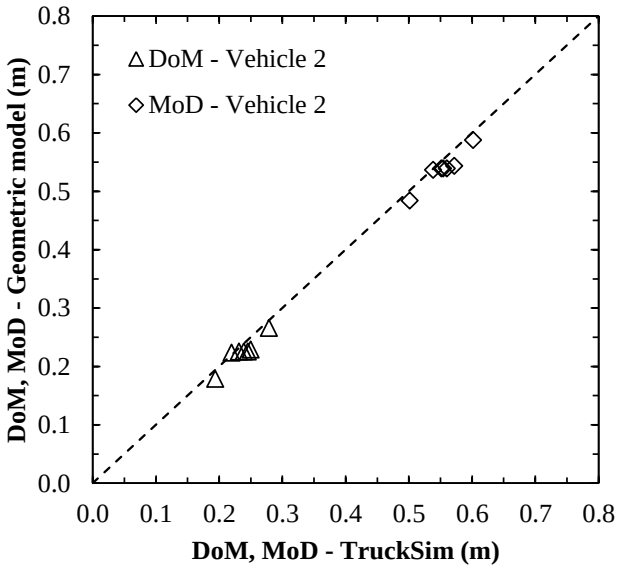


**Figure 2.15: Validation results, difference of maxima and maximum of difference**

Table 2.3 and Table 2.4 contain the actual validation differences for Vehicles 1 and 2 respectively. Included in each table is the maximum lateral offset between the prescribed path and the trajectory of the outer steer-tyre wall achieved by the TruckSim® simulation. This offset is primarily a function of the driver controller settings, is largely unpredictable, and varies with vehicle configuration and parameters such as tyre properties. Obtaining an offset less than 15 mm is not often achievable, and some vehicles can result in offsets much higher. The values achieved here are within the prescribed 50 mm offset allowance [4], but comparable in magnitude to many of the differences observed between the results of the model and those of TruckSim®. This

suggests that a portion of the calculated differences is attributable to TruckSim® and not the geometric model.

**Table 2.3: Vehicle 1 validation differences**

| | | Original | Dual tyres | WB + 1 m | WB – 1 m | Unladen | | |
|---|---|---|---|---|---|---|---|---|
| | | | | | | 3 axles | 2 axles | 1 alxe |
| **Scenario:** | | **1** | **2** | **3** | **4** | **5** | **6** | **7** |
| **Difference (mm):** | **LSSP** | 91 | 128 | 68 | 156 | 47 | 22 | –5 |
| | **TS (truck)** | 7 | 6 | 8 | 5 | 10 | 11 | 11 |
| | **TS (trailer)** | 12 | 11 | 5 | 25 | 7 | 4 | 4 |
| | **FS** | 3 | 7 | 7 | 4 | –8 | –13 | –16 |
| **Difference (%):** | **LSSP** | 1.4% | 2.0% | 1.0% | 2.6% | 0.7% | 0.3% | –0.1% |
| | **TS (truck)** | 3.3% | 2.8% | 3.9% | 2.1% | 4.7% | 5.3% | 5.5% |
| | **TS (trailer)** | 2.1% | 1.9% | 1.6% | 2.8% | 1.2% | 0.6% | 0.7% |
| | **FS** | 0.5% | 1.3% | 1.4% | 0.8% | –1.5% | –2.3% | –2.9% |
| **TruckSim® offset (mm):** | | 14 | –12 | 11 | 18 | 24 | 29 | 32 |

**Table 2.4: Vehicle 2 validation differences**

| | | Original | Dual tyres | WB + 1 m | WB – 1 m | Unladen | | |
|---|---|---|---|---|---|---|---|---|
| | | | | | | 2 axles | 1 axle | 3 alxes |
| **Scenario:** | | **1** | **2** | **3** | **4** | **5** | **6** | **7** |
| **Difference (mm):** | **LSSP** | 22 | 19 | 19 | 27 | 13 | 9 | 27 |
| | **TS** | –6 | –2 | –6 | –5 | –1 | –3 | 0 |
| | **FS** | 0 | 1 | 0 | 1 | –4 | –6 | –2 |
| | **DoM** | –14 | –20 | –13 | –15 | –6 | 4 | –21 |
| | **MoD** | –15 | –21 | –14 | –18 | –13 | –2 | –29 |
| **Difference (%):** | **LSSP** | 0.3% | 0.3% | 0.3% | 0.4% | 0.2% | 0.1% | 0.4% |
| | **TS** | –1.6% | –0.4% | –2.3% | –0.8% | –0.2% | –0.9% | –0.1% |
| | **FS** | 0.1% | 0.2% | 0.1% | 0.2% | –0.9% | –1.2% | –0.3% |
| | **DoM** | –5.6% | –8.0% | –4.6% | –7.8% | –2.5% | 1.9% | –8.3% |
| | **MoD** | –2.8% | –3.7% | –2.3% | –3.5% | –2.3% | –0.4% | –5.1% |
| **TruckSim® offset (mm):** | | 8 | –9 | –9 | 10 | 10 | 12 | –11 |

The model provides accurate predictions of low-speed turning behaviour with an average absolute relative error of 2.0% over the full range of validation results. Actual performance results are given in Table A.1 and Table A.2 in Appendix A.

Lastly, an important aspect of a computational model is the time required to obtain results, particularly when conducting parametric studies. Solution speed improvements of between 261% and 546% were observed when using the model, compared to equivalent TruckSim® simulations.

The geometric model was shown to be accurate for a representative spread of scenarios including various vehicle configurations, vehicle dimensions and loading cases; and computationally efficient. In the next section, the geometric model is applied to assess the tail swing performance of the South African car-carrier fleet.

## 2.4 Application: Tail Swing Performance of the South African Car-Carrier Fleet

Chapter 1 highlighted that due to the leniency of South African legislation with respect to rear overhang when compared with Australia, typical South African car-carrier designs would perform poorly in the tail swing standard. In this section, the geometric low-speed turning model is used to validate and quantify this. Two areas of interest exist: firstly, to quantify the tail swing performance of the existing (non-PBS) car-carrier fleet, and secondly, to evaluate the theoretical tail swing performance possible within the confines of South African legislation. The tail swing limits imposed by the NTC are road access level-specific and range from 0.30 m for Level 1 road access to 0.50 m for Level 4 road access. Level 2 and Level 3 share a common limit of 0.35 m.

### 2.4.1 Existing South African fleet

The South African car-carrier fleet make-up was obtained from the Chairman of the South African Car Transporters Association, Mr. Andrew Colepeper [33]. Dimensions of individual vehicle designs were obtained directly from the applicable manufacturers. The estimated South African car-carrier fleet make-up is outlined in Table 2.5. Vehicle dimensions were obtained for the six most abundant designs on South African roads amounting to 510 vehicles or 65% of the estimated total South African car-carrier fleet. Five of these six are Unipower (Natal) vehicles representing an estimated 55% of the total fleet. The sample consists of three truck and tag-trailer combinations and three tractor and semitrailer combinations. It was assumed that the relative proportions of configurations and dimensions of the remaining vehicles are similar to those of the sample group. Vehicle dimensions are given in Table A.3 and Table A.4, Appendix A.

**Table 2.5: Current South African car-carrier fleet make-up** [33]

| Vehicle | Configuration | Number of vehicles | Percentage of sample |
|---|---|---|---|
| "A" | Tractor-semitrailer | 90 | 17.6% |
| "B" | Tractor-semitrailer | 110 | 21.6% |
| "C" | Tractor-semitrailer | 30 | 5.9% |
| "X" | Truck and tag-trailer | 105 | 20.6% |
| "Y" | Truck and tag-trailer | 80 | 15.7% |
| "Z" | Truck and tag-trailer | 95 | 18.6% |

The tail swing performance of the fleet is shown in Figure 2.16 as a function of vehicle rear overhang (excluding load projection). The Level 1, Level 2/3 and Level 4 Australian tail swing limits are indicated by the broken horizontal lines. In the case of the truck and tag-trailer combinations, the tail swing of the truck and trailer have been shown separately. A high correlation between tail swing and rear overhang is clear. Only one design (21.6% of the fleet) meets the Level 1 PBS requirement of 0.30 m and only two designs (39.2% of the fleet) meet the common Level 2/3 requirement of 0.35 m. The maximum tail swing obtained was 0.71 m for vehicle "Z".

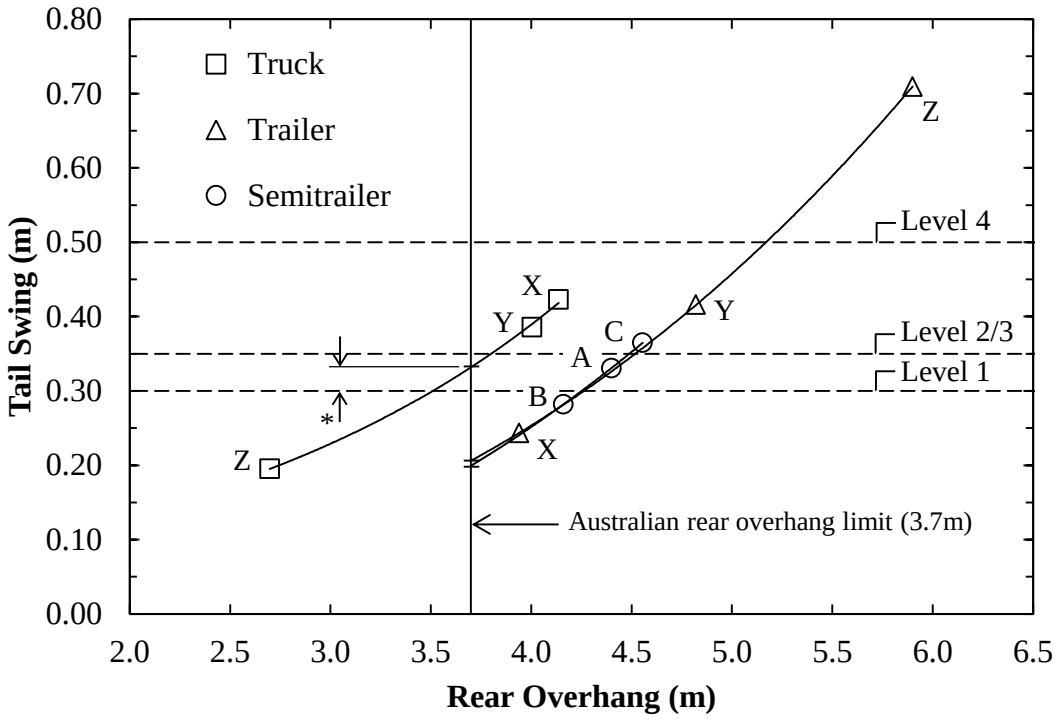


**Figure 2.16: Tail swing performance of the South African car-carrier fleet**

The Australian Design Rule 43/04 rear overhang limit of 3.7 m is indicated in the figure, and the South African fleet results were inter-/extrapolated to this value. At this

rear overhang, trailer and semitrailer results are shown to be safely within the 0.30 m limit, but the truck results are approximately 30 mm in excess thereof (labelled "*" in the figure). In Section 1.2.5, it was suggested that the 0.30 m tail swing limit is a direct result of the 3.7 m rear overhang limit enforced on Australian vehicles, but the truck results shown here (and hence truck-trailer results) seem to imply this may not be the case. However, South African vehicles may have widths up to 2.6 m versus 2.5 m in Australia, which equates to an additional 50 mm either side of the vehicle. With all other vehicle parameters equal, and assuming maximum tail swing to occur at a yaw angle of about 45°, this translates into an additional $50 \cdot \cos(45°) = 35$ mm of tail swing. Subtract this from the truck results and the relationship between a maximum rear overhang of 3.7 m and a maximum tail swing of 0.30 m becomes clear.

The percentages of the current fleet that would not comply with a range of enforced tail swing limits are presented in Figure 2.17. At the Level 1 criterion of 0.30 m, nearly 80% of the fleet would not comply. Strictly enforcing such a limit on the existing fleet (and hence only allowing around 20% of the fleet to operate at full capacity) would have a negative impact on the industry. The majority of the fleet (over 80%) would be included at a limit of 0.45 m whilst at least one particularly unsafe design would be excluded.

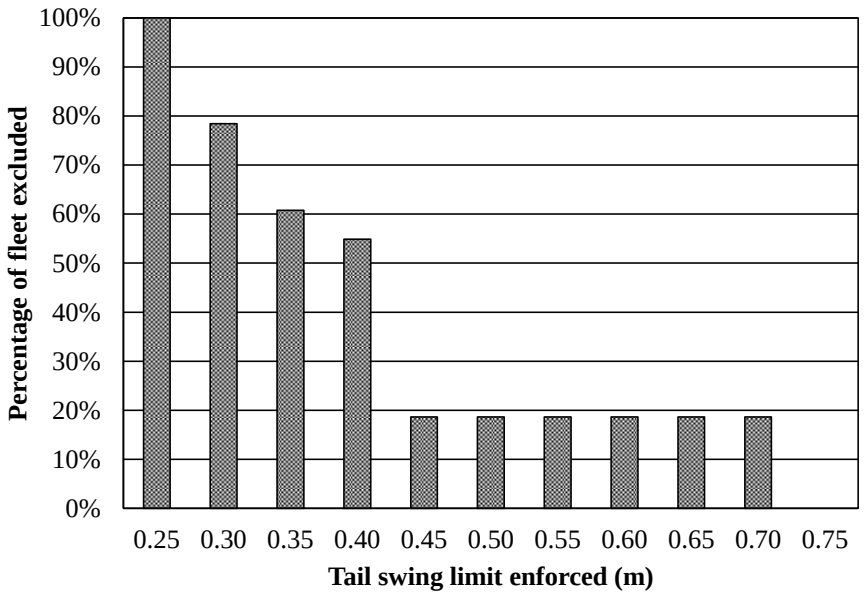


**Figure 2.17: Current fleet percentages excluded by various tail swing limits enforced**

Given these results, it is unlikely that car-carriers based on existing designs would comply with the requirements of the PBS scheme. The operators of existing vehicles registered after the cut-off date for abnormal load permits, are therefore obliged to operate them within legal dimensional constraints of the NRTR, limiting their height to

4.3 m and their length to 18.5 m and 22 m for tractor-semitrailer and truck-trailer combinations respectively. Such limitations will have an impact on the number and size of vehicles able to be transported, with a direct impact on the productivity of such an operator and on the industry at large.

The following section explores the extent of South Africa's rear overhang legislation and the implications for tail swing.

### 2.4.2 South African legislation

"Part III: Vehicle Dimensions" of the NRTR [1] governs the restrictions on vehicles such as combination length, wheelbase, and front and rear overhangs. Within the envelope of these restrictions, potentially worst-case scenario vehicles (in terms of tail swing performance) were conceptualised and assessed using the geometric model.

The Regulations govern rear overhang to 50% of trailer length in the case of a tag-trailer and 60% of the wheelbase in the case of a conventional rigid truck, semitrailer or drawbar-trailer [1]. As tail swing performance is predominantly a function of rear overhang, maximising this parameter yields maximum tail swing. NRTR rear overhang is measured from the rearmost *axle*, and not from the geometric centre of the rearmost *axle group* (as in ADR 43/04). The effective rear overhang, as defined in ADR 43/04, can therefore be increased by increasing the number of axles within that axle group. This is illustrated in Figure 2.18 for a tridem-axle semitrailer with 1.35 m axle spacing.

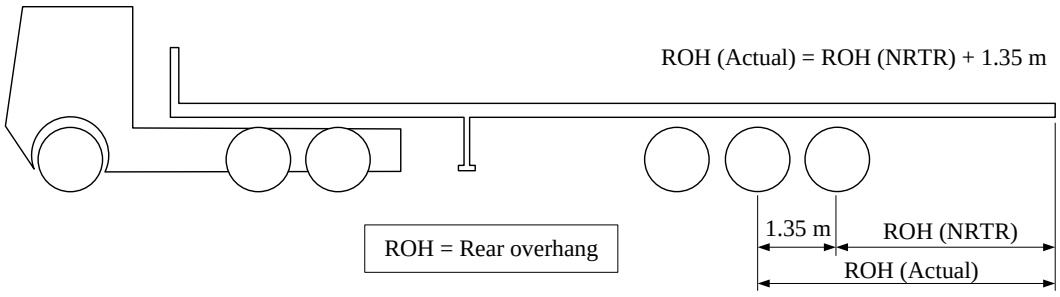


**Figure 2.18: Comparing NRTR-defined rear overhang to actual rear overhang**

Three cases were considered, namely a rigid truck (no trailer hitched), a tractor and semitrailer combination, and a truck and tag-trailer combination (assessing trailer tail swing in isolation). Drawbar-trailers were not considered. The rigid truck and both trailers were assumed to have tridem axle groups. The truck in the truck-trailer combination and the tractor in the tractor-semitrailer combination were specified with single rear axles in order for the maximum dimensions of the trailer and semitrailer to be realised. Some typical vehicle dimensions were assumed, namely:

1. a steer-tyre track width of 2.480 m,
2. a vehicle width of 2.6 m,
3. tractor/rigid truck front overhang of 1.4 m,
4. a minimum rigid truck/prime mover wheelbase of 3.5 m,
5. an axle spacing of 1.35 m where applicable, and
6. a hitch offset of 1 m behind/ahead of the rear axle of the prime mover (trailer/semitrailer).

The dimensions of the vehicles are given in Table A.5, Appendix A.

In addition to the afore-mentioned restrictions on rear overhang as a function of wheelbase or trailer length, these wheelbases and lengths as well as the overall vehicle length are subject to their own constraints under the NRTR. The relevant constraints affecting rear overhang are summarised in Table 2.6.

**Table 2.6: Dimensional constraints governing rear overhang (NRTR** [1]**)**

| **Vehicle type** | **Maximum dimensions** | | |
|---|---|---|---|
| | **Rear overhang**† | **Wheelbase/length** | **Combination length** |
| Rigid truck | 60%·WB | WB ≤ 8.5 m | 12.5 m |
| Semitrailer | 60%·WB | WB ≤ 10 m | 18.5 m |
| Tag-trailer | 50%·Trailer length | Trailer length ≤ 11.3 m | 22.0 m |

† Using the NRTR definition of rear overhang as measured relative to the rearmost axle

To determine the maximum allowable rear overhang dimensions, all three of the above constraints were considered for each vehicle type. Maximum rear overhang as a function of only wheelbase/trailer length may not be practically achievable due to the overall length constraint. In the case of the tag-trailer, the maximum combination length of 22 m does not constrain the achievable maximum rear overhang, and so the maximum is simply 50%·11.3 + 1.35 = 7 m (50% of the maximum trailer length of 11.3 m, with a further 1.35 m as per Figure 2.18). For the rigid truck and for the semitrailer, maximum rear overhang was calculated using linear optimisation.

The results of the optimisation exercise are shown in Figure 2.19 and Figure 2.20 for the rigid truck and semitrailer respectively. Adding 1.35 m to the points of maximum rear overhang (to account for the tridem axle spacing) yields maximum practical rear overhangs of 5.01 m for the rigid truck and 6.32 m for the semitrailer.

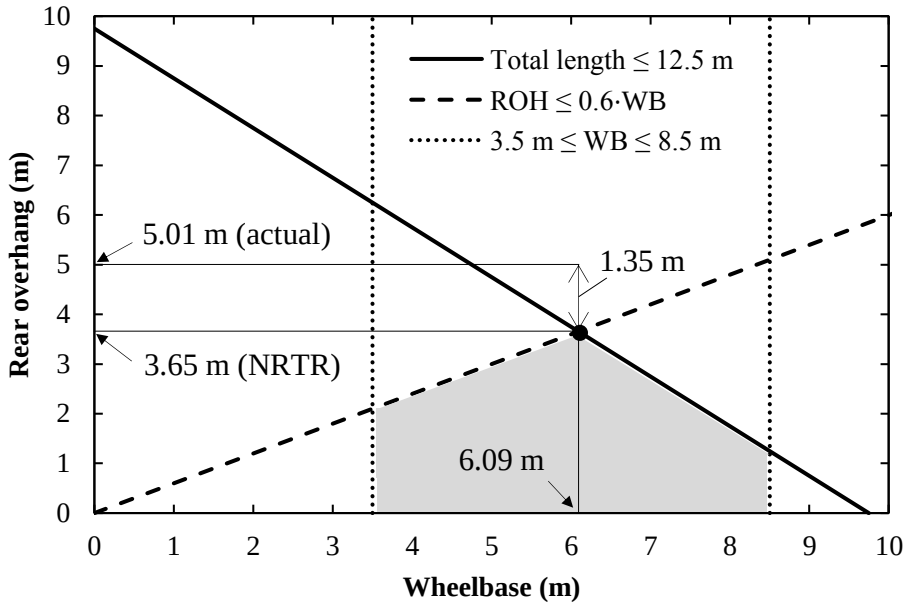


**Figure 2.19: Maximum practical rear overhang for a rigid truck within the NRTR**

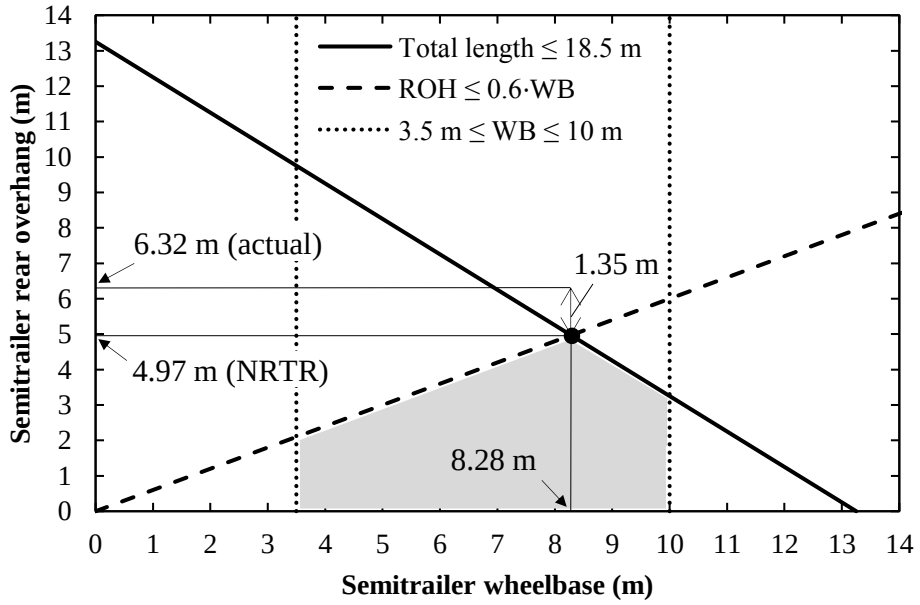


**Figure 2.20: Maximum practical rear overhang for a semitrailer within the NRTR**

The results are summarised in Table 2.7 shown in comparison to the Australian rear overhang limit. “Theoretical” maximum rear overhang pertains to the value obtained by only considering the first two constraints of Table 2.6. The “practical” rear overhang pertains to the value limited by overall length.

**Table 2.7: Comparison of rear overhang legislation between Australia and South Africa**

| Vehicle type | Maximum rear overhang | | |
|---|---|---|---|
| | Australia (ADR 43/04) | South Africa (NRTR) | |
| | | Theoretical | Practical |
| Rigid truck | 3.7 m | 6.45 m | 5.01 m |
| Semitrailer | 3.7 m | 7.35 m | 6.32 m |
| Trailer | 3.7 m | 7.00 m | 7.00 m |

Having shown that rear overhangs well in excess of 3.7 m are possible, the implications for tail swing were investigated. The geometric model was used to model a range of vehicles up to the point of theoretically maximum tail swing. Figure 2.21 shows the tail swing performance of the rigid truck. The three broken horizontal lines represent the tail swing limits for Levels 1, 2/3 and 4. For every value of wheelbase, the associated maximum rear overhang is used (= 60%·WB + 1.35 m). The maximum tail swing obtained was 0.60 m at a wheelbase of 6.09 m and associated rear overhang of 5.01 m as per the optimisation exercise. Even near the lower end of the wheelbase spectrum, if the maximum allowable rear overhang is utilised, tail swing in excess of the Level 1 limit will result.

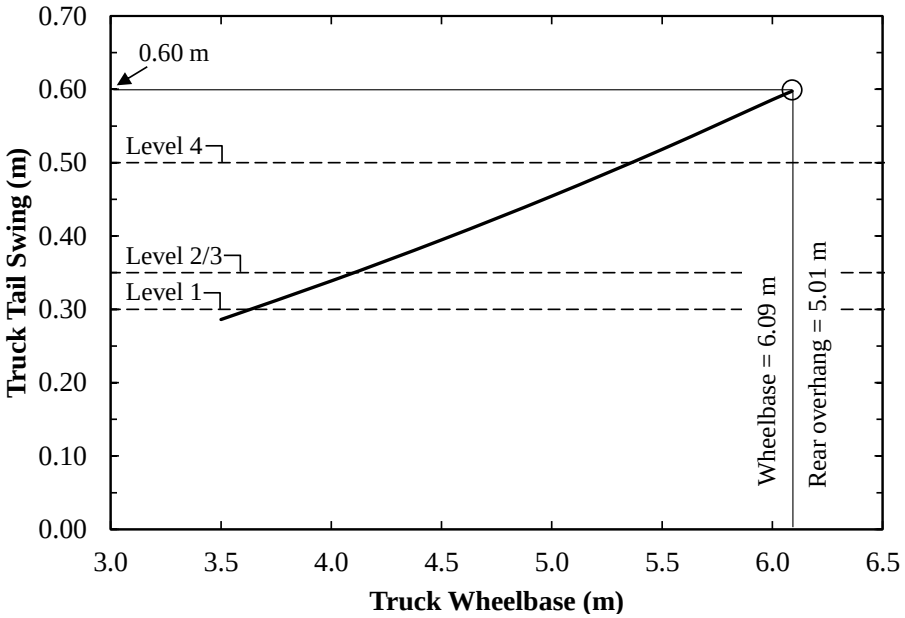


**Figure 2.21: Theoretical tail swing allowed by the NRTR, rigid truck**

The results for the tractor and semitrailer combination are shown in Figure 2.22 for a range of semitrailer and tractor (or prime mover) wheelbases. A maximum tail swing of 0.87 m was calculated for a minimum prime mover wheelbase and a semitrailer wheelbase of 8.28 m with an associated rear overhang of 6.32 m.

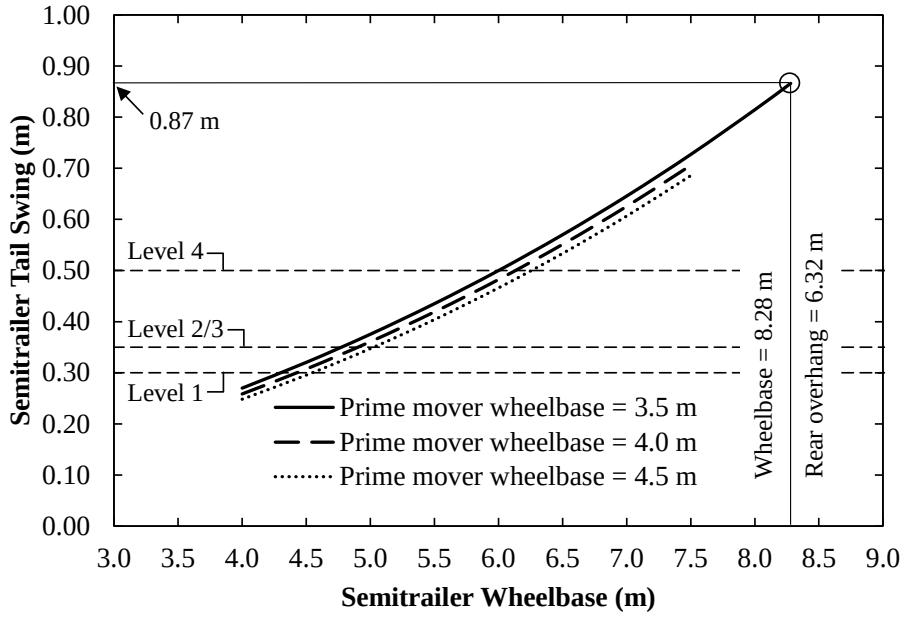


**Figure 2.22: Theoretical tail swing allowed by the NRTR, tractor and semitrailer**

Tail swing performance of the truck and tag-trailer combination as a function of truck wheelbase and trailer drawbar length is shown in Figure 2.23. Trailer length and rear overhang are constant at the maximum 11.3 m and 7 m respectively. A maximum tail swing of 1.25 m was calculated at the minimum truck wheelbase and minimum drawbar length. In the NRTR, the "drawbar" of a tag-trailer refers to the portion of the trailer ahead of the loading area and is excluded from the "length" of the trailer. Maximum tail swing was observed for a drawbar length of 0 m as this gave the highest rear overhang-to-wheelbase ratio.

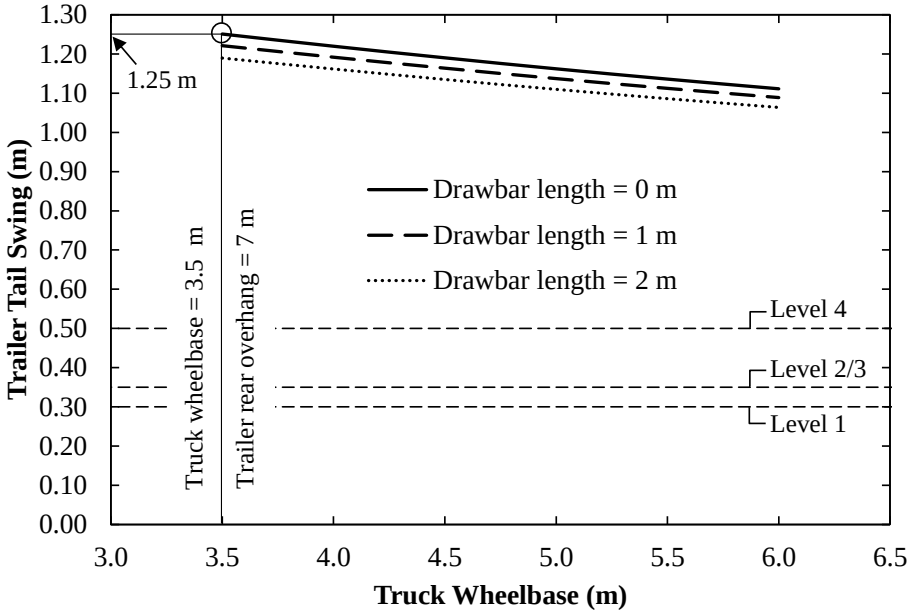


**Figure 2.23: Theoretical tail swing allowed by the NRTR, truck and tag-trailer**

A summary of the results is given in Table 2.8. The Level 4 tail swing limit is exceeded in all three cases. The tag-trailer allows for the highest theoretical tail swing of 1.25 m, 417% of the Level 1 limit.

**Table 2.8: Theoretical tail swing performance allowable within the NRTR**

| Vehicle type | Australian PBS | South African NRTR | |
|---|---|---|---|
| | Level 1 limit | Maximum | % of L1 |
| Rigid truck | 0.30 m | 0.60 m | 200% |
| Semitrailer | 0.30 m | 0.87 m | 290% |
| Trailer | 0.30 m | 1.25 m | 417% |

The results indicate the ineffectiveness of the existing South African legislation to adequately govern tail swing. This stems from a lack of a finite rear overhang limit and from the definition of rear overhang used in the NRTR. Existing legislation allows for vehicles exhibiting a tail swing of up to 1.25 m. In comparison, the worst tail swing from the preceding study of the existing car-carrier fleet was 0.71 m.

### 2.4.3 Conclusions

Based on these findings, a proposal to relax the tail swing limit to 0.45 m was tabled at a meeting of the Smart Truck Review Panel (26 September 2011, Kwazulu-Natal Department of Transport, Pietermaritzburg). Although not as strict as the Australian limit, it would still represent a significant improvement over the current legislation and would eradicate one particularly poor-performing existing design. Such a relaxation would be applicable during an "implementation phase" of the revised regulatory framework for car-carriers, giving sufficient time for manufacturers to design a new generation of PBS-compliant vehicles. To enforce a tail swing limit of 0.30 m on a fleet of vehicles designed within a framework that allows up to 1.25 m of tail swing could negatively impact on the success of the PBS car-carrier initiative.

The Panel rejected the proposal citing concerns over modifying the Australian standards too early in the implementation of PBS in South Africa. The Panel suggested that such calls for relaxation would compromise the support of the project from South African transport authorities, which is crucial for the project's success. As a result, a number of vehicle combinations are currently operating without abnormal load permits and at NRTR-confined dimensions with subsequent productivity losses.

Conclusions that are drawn from the tail swing study are as follows:

1. The existing South African car-carrier fleet exhibits poor tail swing performance. Nearly 80% of the fleet does not comply with the 0.30 m Level 1 PBS limit, and one individual vehicle design was calculated to have a tail swing of 0.71 m.
2. The 0.30 m tail swing criterion is shown to be representative of the Australian Design Rule 43/04 rear overhang limit of 3.7 m. In comparison, South African legislation allows rear overhangs of up to 7 m, and tail swing of up to 1.25 m. This is shown to be due to the lack of a finite rear overhang limit and a misguided definition of rear overhang.
3. It was proposed that a temporary relaxation of the tail swing limit from 0.30 m to 0.45 m be considered, which was turned down by the Smart Truck Review Panel.

## 2.5 Chapter Summary and Conclusions

This chapter outlined the development, validation and application of a geometric low-speed turning model, implemented in Matlab®. The ninety-degree, 12.5 m radius turn prescribed by the NTC was incorporated as the default path within the model, but the model is compatible with any arbitrarily complex path defined by vectors of $x$ and $y$ coordinates. The model incorporates the steer-tyre path-following method required by the NTC and incorporates the tyre scrub effects of multiple non-steering rear axles. It is able to calculate LSSP, TS, FS, DoM and MoD.

The model was validated against equivalent TruckSim® models for LSSP, TS, FS, DoM and MoD and showed good agreement. The model offers the following advantages over TruckSim®:

1. The model solves significantly quicker than TruckSim® and is hence better suited to parametric studies of low-speed manoeuvrability.
2. The model can analyse any vehicle combination consisting of any number of vehicle units and any number of axles, whereas TruckSim® is limited to vehicles combinations not exceeding three vehicle units (except for one A-double combination with single rear axles throughout) or three rear axles per vehicle unit.
3. The model exhibits repeatable and predictable path-following behaviour whereas TruckSim® incurs non-repeatable and unpredictable lateral offset errors.

The model is able to analyse vehicle combinations possessing passively steered rear axles as well as dual steer axles but cannot incorporate any active-steering characteristics.

This may be possible if the model is developed further. The model can easily be incorporated into a larger optimisation algorithm such as that of Dessein *et al.* [16].

The model was used to show that nearly 80% of the existing car-carriers in South Africa do not meet the 0.30 m Level 1 tail swing requirement of the NTC. Within the confines of the NRTR, legal vehicles with rear overhangs up to 7 m and exhibiting tail swing of up to 1.25 m are allowable. This was shown to be a result of the leniency of existing South African legislation with respect to rear overhang. The Australian Level 1 tail swing limit was shown to be a result of the 3.7 m rear overhang constraint enforced by Australian Design Rule 43/03.

# Chapter 3

# PBS Vehicle Assessments

In this chapter, detailed models of two PBS car-carrier proposals are developed and assessed in accordance with the Australian Performance-Based Standards scheme. The car-carriers consist of one truck and tag-trailer combination and one tractor and semitrailer combination, both of which are Unipower (Natal) designs. These assessments are the first of their kind for car-carriers and the results are intended to offer insight into the feasibility of implementing PBS as a requirement for over-size car-carriers. These results form a mandatory component of the documentation required for the PBS approval of the vehicles. This work is confined to the study of vehicle manoeuvrability and stability; the driveability standards (i.e. startability, gradeability, and acceleration capability) were not considered.

The chapter proceeds as follows:

1. The proposed baseline vehicles are described, highlighting significant features.
2. An overview of the vehicle modelling process is presented with a specific discussion on payload modelling.
3. Pertinent aspects of the various manoeuvres and their modelling are discussed.
4. Results of the baseline vehicle assessments are presented, and used to identify and address design shortcomings.
5. The revised vehicles are reassessed, and the results are presented and discussed.

## 3.1 Vehicle Descriptions

Two Unipower (Natal) car-carriers were assessed: the Maxiporter™ truck and tag-trailer combination and Flexiporter™ tractor and semitrailer combination. The two models fall within the Uniporter™ series of designs and are based on existing designs. Under the outgoing abnormal load permit scheme, the Flexiporter is 18.5 m and the Maxiporter is 22.0 m in length. Both have a maximum rear load projection of 0.5 m and a maximum loaded height of 4.6 m. These designs are referred to as the "baseline" vehicles. The vehicles are intended for general distribution vehicle transport and were assessed for Level 1 PBS approval (unrestricted road access).

The baseline Maxiporter is shown in Figure 3.1 (a). It consists of a Volvo FM400 6x2 truck chassis with a three-car superstructure and a tridem-axle tag-trailer. The truck has a single drive axle and a tag axle (both with dual tyres), mechanical suspension on all axles and a Gross Vehicle Mass (GVM) of 27 000 kg. The trailer has single-fitment tyres and mechanical suspension. The Gross Combination Mass (GCM) is 45 000 kg. The baseline Flexiporter is shown in Figure 3.1 (b). It consists of a Renault Midlum 280.18 DXi Sleeper Cab truck-tractor and a semitrailer. The truck-tractor has a single drive axle with dual tyres, mechanical suspension on all axles and a GVM of 18 000 kg. The trailer has tandem axles with single tyres and air suspension. The GCM is 24 000 kg.

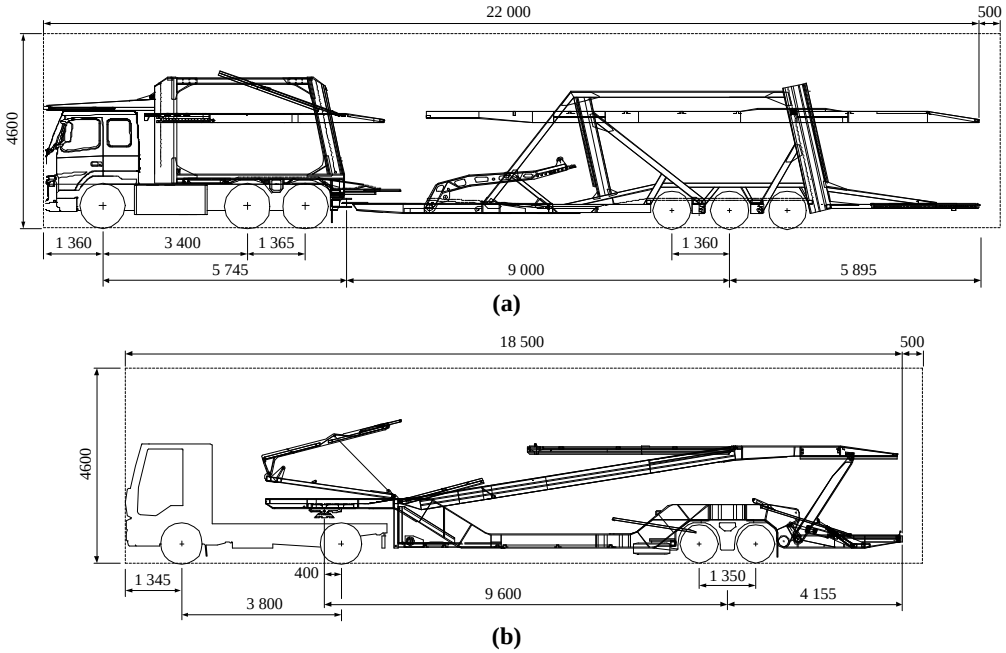


**Figure 3.1: Baseline vehicles: (a) Maxiporter and (b) Flexiporter (courtesy of Unipower)**

A number of design features are evident which give insight into the performance of the vehicles in a PBS context. Common to both vehicles is an elevated payload height and hence sprung mass centre of gravity, critical for standards such as static rollover threshold and rearward amplification. However, the bulk density of the payload is relatively low and so the overall implications are difficult to predict. The detailed assessments will quantify this. Also common to both vehicles, though substantially more so on the Maxiporter, is a large trailer rear overhang, which has a negative implication for tail swing performance. With a rear overhang of nearly 6 m excluding load projection, it is unlikely that the Maxiporter satisfies the tail swing requirement (see Section 2.4.1).

A characteristic design feature of the Maxiporter is the centre-axle configuration of the trailer. This is a common feature of this type of car-carrier and aims to reduce the low-speed offtracking of the vehicle, to maximise geometric loading capacity, and to minimise the amount of trailer load supported by the hitch. Dynamically however, a short trailer wheelbase has a significant negative effect on yaw damping, rearward amplification and high-speed transient offtracking [19]. In comparison, the Flexiporter should perform well dynamically owing to the stabilising effects of roll-coupling (through the roll stiffness of the fifth wheel) and the high roll-stiffness characteristics of the air suspension. However, the Flexiporter features a notable semitrailer front overhang, with load projections in excess of this overhang. This typically results in poor performance in the difference of maxima and maximum of difference performance standards.

The above assessment is qualitative, and a quantitative understanding of how the vehicles perform requires detailed computer simulation, taking into account vehicle parameters such as tyre properties, spring stiffness and inertial properties. The following two sections outline aspects of the vehicle models as they were developed in TruckSim®.

## 3.2 Vehicle Modelling

TruckSim® is a multibody dynamics software package that focuses on heavy vehicle combinations. Wits University previously conducted PBS assessments of (non-car-carrier) vehicles using TruckSim® which were corroborated by ARRB Group in Australia, showing good agreement. This supports the use of the software here. The current section outlines some of the vehicle parameters required for the models and the sources of these parameters.

Primary considerations for a vehicle model are the vehicle's sprung mass, associated centre of gravity location (height above ground and longitudinal location) and moments

of inertia; as well as the unsprung masses and their associated centres of gravity and moments of inertia. In the case of the Maxiporter trailer and Flexiporter semitrailer, detailed CAD (Computer-Aided Design) models were provided by Unipower from which all sprung mass inertial data were calculated. In the case of the prime movers, the relevant Original Equipment Manufacturers (OEMs) made data available in the form of axle loads, total mass (lumped sprung and unsprung masses), total centre of gravity height and, in Volvo's case, unsprung masses. Sprung mass and sprung mass centre of gravity were calculated from total mass and unsprung mass data (see Section C.1.1, Appendix C). Prime mover sprung mass moments of inertia were estimated using the work of Fancher *et al.* at UMTRI [34]. Driver and fuel were modelled as additional sprung mass components where necessary.

Unknown unsprung masses were estimated using generic UMTRI data [34], scaled according to axle load rating. Other unsprung mass properties, such as the spin inertia of wheel assemblies, were estimated according to the experimental measurements of Winkler *et al.* [35], [36]. Details of unsprung mass modelling are given in Section C.1.2. The sprung and unsprung mass inertial properties of the Maxiporter and Flexiporter are summarised in Table 3.1 and Table 3.2 respectively.

**Table 3.1: Summarised inertial data, Maxiporter (unladen)**

| Vehicle Parameter | Units | Truck | Trailer |
|---|---|---|---|
| Sprung mass | kg | 8 882[†] | 7 355 |
| Sprung mass centre of gravity height | m | 1 259[†] | 1 311 |
| Unsprung mass (all axles) | kg | 2 950 | 1 950 |

[†] Truck chassis and superstructure. Excludes driver and fuel.

**Table 3.2: Summarised inertial data, Flexiporter (unladen)**

| Vehicle Parameter | Units | Tractor | Semitrailer |
|---|---|---|---|
| Sprung mass | kg | 3 743[†] | 7 367 |
| Sprung mass centre of gravity height | m | 1 067[†] | 1 334 |
| Unsprung mass (all axles) | kg | 1 920 | 1 500 |

[†] Includes driver and fifth wheel. Excludes fuel.

Suspension characteristics such as spring stiffness, roll centre height and auxiliary roll stiffness are important considerations for manoeuvres involving rollover or lateral load transfer. Vertical spring stiffness characteristics were provided by the respective OEMs. For the air suspension on the Flexiporter semitrailer, detailed loading curves were provided by BPW. Roll centre heights were either provided by the relevant OEM or deduced via the estimation techniques suggested by UMTRI [37]. Suspension lash was

measured from detailed suspension drawings provided by the OEMs and modelled accordingly. Details of suspension modelling are given in Sections C.2.1 and C.2.2.

For axles fitted with an anti-roll bar, auxiliary roll stiffness was calculated from first principles (see Section C.2.3). For the air suspension, the work of Fu and Cebon [38] was used to source a representative auxiliary roll stiffness value.

Damping originates from the viscous damping of dampers (or "shock absorbers") or from the Coulomb friction in leaf spring stacks. In the case of leaf spring Coulomb friction, it also introduces hysteresis to the loading and unloading characteristics of the springs. Where dampers were present, loading curves (force as a function of compression/extension rate) were sourced from the relevant OEMs, and the damper was assumed to be the only source of damping (excluding hysteresis effects). Where no damper was present, a representative amount of Coulomb friction was modelled according to the type of suspension. In all cases of mechanical suspension, hysteresis was introduced to the loading and unloading curves of the springs according to the amount of assumed Coulomb friction present. All representative Coulomb friction data were sourced from Fancher *et al.* [34]. Damper modelling is discussed further in Section C.2.4.

Tyre compliance properties play a crucial role in determining the dynamic response characteristics of a vehicle. The most critical tyre properties in the context of this work are lateral and vertical stiffnesses. Vertical stiffnesses were obtained from Michelin® (as these were readily available) and lateral stiffnesses, for which OEM data are not readily available, were sourced from an extensive study conducted by UMTRI in the 1980s [39]. The study experimentally determined various compliance properties for a number of truck and bus tyres of various sizes and manufacturers. Although the UMTRI study is dated, it was assumed that any tyre technology advances giving rise to changes in general stiffness properties of tyres since the 1980s, if any, would yield improved and not deteriorated stiffness properties. The use of the UMTRI data was hence conservative.

Longitudinal tyre stiffness properties are only critical to acceleration or braking manoeuvres. As none of the manoeuvres assessed in this work include any braking or significant longitudinal acceleration, and because the UMTRI study did not provide longitudinal stiffness data for all the tyre sizes considered in this work, it was deemed suitable to use default TruckSim® data according to the load rating of the tyres. Detailed tyre properties used in this work are given in Section C.3.

Summarised axle and suspension properties are given in Table 3.3 and Table 3.4 for the Maxiporter and Flexiporter respectively.

**Table 3.3: Summarised axle and suspension data, Maxiporter**

| Vehicle Parameter | Units | Steer axle | Drive axle | Tag axle | Trailer axles |
|---|---|---|---|---|---|
| Designation | | Volvo FAL 8.0 | Volvo RADT-AR | | BPW NHSFVBT 6410 Eco Maxx |
| Steel/air springs | | Steel | Steel | | Steel |
| Load rating | kg | 8 000 | 19 000 | | 6 400 (per axle) |
| Axle track | mm | 2 109 | 1 854 | 1 854 | 2 310 |
| Roll centre (above axle) | mm | 85 | –38 | 0 | –80 |
| Vertical spring stiffness | N/mm | 311 | 746 | 746 | 650 |
| Auxiliary roll stiffness | N·m/° | 6 299 | 0 | | 0 |
| Dampers | | Yes | No | | No |
| Tyres | | 385/65 R22.5 | 315/80 R22.5 (dual fitment) | | 285/70 R19.5 |

**Table 3.4: Summarised axle and suspension data, Flexiporter**

| Vehicle Parameter | Units | Steer axle | Drive axle | Semitrailer axles |
|---|---|---|---|---|
| Designation | | Renault M500 | Volvo RAD-L80 | BPW NHSFSLU 6410 Eco Maxx |
| Steel/air springs | | Steel | Steel | Air |
| Load rating | kg | 7 100 | 11 500 | 6 400 (per axle) |
| Axle track | mm | 1 982 | 1 834 | 2 310 |
| Roll centre (above axle) | mm | 118 | 244 | –99 |
| Vertical spring stiffness | N/mm | 227 | 426/840 (2-stage) | (Non-linear) |
| Auxiliary roll stiffness | N·m/° | 6 326 | 2 677 | 6 080 |
| Dampers | | Yes | Yes | Yes |
| Tyres | | 295/80 R22.5 | 295/80 R22.5 (dual fitment) | 285/70 R19.5 |

The hitch of the Maxiporter was modelled as a simple three degree-of-freedom constraint in the translational directions. The hitch was assumed to have no roll, yaw or pitch constraints. In the case of the Flexiporter's fifth wheel, in addition to the three translational constraints, roll stiffness was modelled to provide roll-coupling between the two vehicle units. A representative roll stiffness was sourced from an NTC study [40]. Fifth wheel lash was excluded from the model.

Aerodynamics, tyre rolling resistance, suspension compliance effects (i.e. due to the compliance of suspension members other than the spring itself) and axle dive, longitudinal and lateral movement due to axle jounce were neglected.

In-depth descriptions, derivations and sources of vehicle parameter data are given in Appendix C. Detailed vehicle-specific data for the Maxiporter and Flexiporter are given in Appendix D and Appendix E respectively.

For bulk material transport, payloads are of relatively repeatable density, shape and volume, and hence have predictable and repeatable mass, centre of gravity location and moment of inertia properties. The payloads for car-carrier vehicles are highly variable and the next section is dedicated to this important aspect of the modelling process.

## 3.3 Payload Modelling

The type and size of the vehicles transported by car-carriers can range from large, heavy Sport Utility Vehicles (SUVs) to small, light compact hatchbacks; and a typical payload is often a combination of both. This presents a challenge in the modelling of the payload for PBS assessments. Which loading scenario is least ideal for each of the performance standards? What properties should be used to model the individual vehicles making up the payload?

In a general sense, the NTC prescribes which load scenarios must be considered for each manoeuvre. In the case of the low-speed turn, it is explicitly required that the test be conducted with the vehicle fully laden and with the vehicle unladen. For the remaining manoeuvres, it is required that the tests be conducted with the vehicle laden as well as with the vehicle in its "least favourable load condition". This condition could be a result of load asymmetries or partial loading and cannot be universally prescribed as vehicles may differ widely in this respect.

Increasing the centre of gravity height and/or increasing the mass of a payload has been shown to have a negative influence on SRT, RA, HSTO, TASP and YDC (the "dynamic" standards) [19]. But consider the common car-carrier scenario in which only the upper loading platform is loaded but the lower is not. The sprung mass centre of gravity is higher than when both platforms are loaded which would have a destabilising effect, but its mass is reduced which has a stabilising effect. Which effect is dominant?

The answer will be a function of many parameters such as suspension properties, relative heights of loading platforms to that of the car-carrier centre of gravity, the relative numbers of vehicles which can be loaded onto each of the loading platforms and the inertial properties of the unladen car-carrier. For this reason, a number of generic load scenarios were conceptualised and the most appropriate subset for each manoeuvre was chosen [19]. The loading scenario matrix is shown in Table 3.5. The laden, unladen and "top laden" scenarios pertain to a loading condition of the entire vehicle. Where the scenario name is preceded by "truck" or "trailer", it pertains to the loading condition of that unit, with the other unit unladen. "Laden" has the same meaning as "fully laden".

**Table 3.5: Loading scenarios considered**

| Loading Scenario | Low-speed turn | Rollover | Single lane-change | Pulse steer | Longitudinal tracking |
|---|---|---|---|---|---|
| Laden | ✓ | ✓ | ✓ | ✓ | ✓ |
| Unladen | ✓ | | | | |
| Top laden | | ✓ | ✓ | ✓ | ✓ |
| Truck laden | | | | ✓ | |
| Trailer laden | | ✓† | ✓ | ✓ | |
| Truck top laden | | | | ✓ | |
| Trailer top laden | | ✓† | ✓ | ✓ | |

† Required for determining the lower limit criterion for RA if the rearmost vehicle is not first to roll.

Recall from Chapter 1 that South Australian car-carrier legislation requires that no multi-deck car-carrier should operate at a height exceeding 4.3 m with vehicles on the upper deck unless the lower deck has been filled. This is an indication of "least favourable load scenario" considerations. This scenario is considered for all the manoeuvres except the low-speed turn.

For a given loading configuration, with passenger vehicles located in exactly the same positions on the truck and trailer or semitrailer, individual vehicles with a high mass and high centre of gravity height will give rise to a more adverse loading condition than vehicles with a lower mass and centre of gravity height. Assuming the vehicles to be rigidly fixed to the car-carrier structure, the combined effect may be considered as the product of the two variables, representing the inertial overturning moment generated by the load as the car-carrier experiences lateral acceleration.

To identify the passenger vehicle with the least favourable combination of mass and centre of gravity height, the database compiled by Heydinger *et al.* [41] was investigated. The database contains inertial and dimensional data for a number of American vehicles spanning the years 1971 to 1998, covering a vast span of vehicle types including SUVs, compact hatches, four-door sedans and cabriolets. The data were ranked by the product of mass and centre of gravity height, whilst removing any contributions of ballasts, drivers and/or passengers used in the measurement of each datum. The vehicle that ranked highest was a 1998 Ford Expedition SUV with a mass of 2 562 kg and a centre of gravity 777 mm above ground. A schematic of the vehicle is shown in Figure 3.2 indicating overall dimensions and the location of the centre of gravity [41–43]. The Expedition's inertial properties are summarised in Table 3.6.

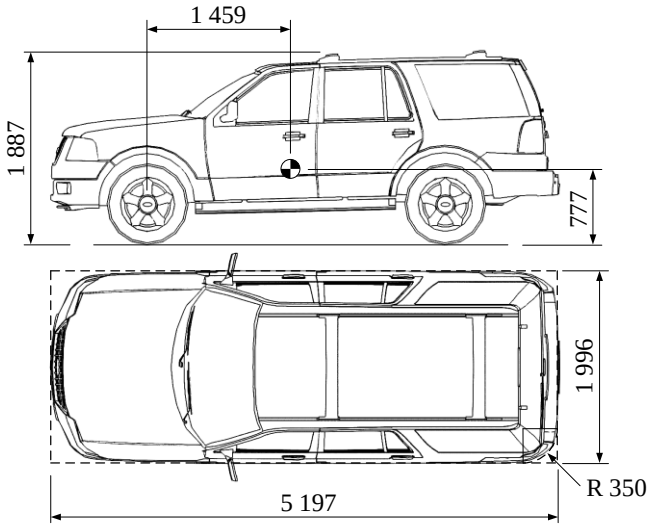


**Figure 3.2: 1998 Ford Expedition dimensions and location of centre of gravity (**[41–43]**)**

**Table 3.6: 1998 Ford Expedition inertial properties** [41]

| Mass (kg) | CoG location (m) | | Moments of inertia (kg.m$^2$) | | |
|---|---|---|---|---|---|
| | Behind steer axle | Above ground | Roll | Pitch | Yaw |
| 2 562 | 1.459 | 0.777 | 1 210 | 5 398 | 5 639 |

The passenger vehicles were arranged on the car-carriers by superimposing scaled silhouettes of the Expedition on each car-carrier using AutoCAD®. Although there is no prescriptive limit imposed on load projections within a PBS framework, the Smart Truck Review Panel restricted projections to one metre at either the front or rear of the vehicle (subject to a maximum total length of 23 m). Conservatively therefore, the vehicles were arranged within a load envelope projecting one metre at the front and rear of the car-carriers, and 4.6 m in height. The loading arrangements are shown in Figure 3.3.

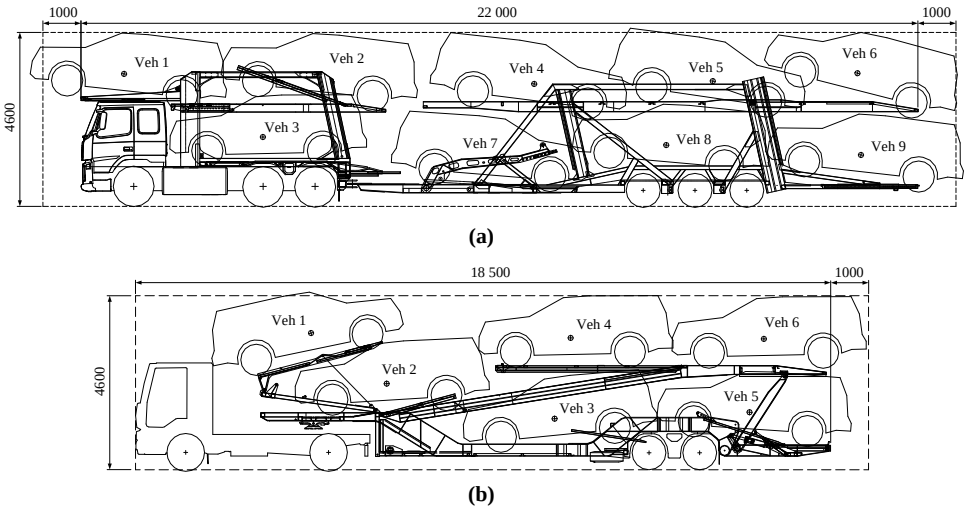


**Figure 3.3: Load placement: (a) Maxiporter, (b) Flexiporter**

Some overlapping/interference of the Expeditions is suggested in Figure 3.3(a), and this seems to imply that such a loading case is not realistic. It should be noted however that the purpose of this payload model is to model a worst-case anticipated payload that is suitably distributed on the vehicle (in terms of overall centre of gravity location and moments of inertia). Although it is unlikely that six actual 1998 Ford Expeditions may be loaded on the trailer, certain existing (or future) vehicle models may be of such shape and dimensions (but similar mass), such that they *can* be loaded, and this eventuality must be accounted for. The coordinates of each Expedition's centre of gravity are shown in Table 3.7. Longitudinal locations are given relative to the steer axle or respective hitch, whichever is applicable (positive rearwards). Vertical locations are given positive above the ground. The vehicles are assumed to be aligned with the longitudinal axis of the car-carrier.

**Table 3.7: Passenger vehicle centre of gravity locations**

| Vehicle | Maxiporter | | Flexiporter | |
|---|---|---|---|---|
| | Behind steer axle/hitch (m) | Above ground (m) | Behind steer axle/hitch (m) | Above ground (m) |
| 1 | –0.253 | 3.510 | –0.066 | 3.614 |
| 2 | 4.760 | 3.495 | 1.947 | 2.276 |
| 3 | 3.393 | 1.840 | 6.414 | 1.350 |
| 4 | 4.772 | 3.231 | 6.841 | 3.485 |
| 5 | 9.463 | 3.313 | 11.600 | 1.521 |
| 6 | 13.261 | 3.522 | 11.982 | 3.459 |
| 7 | 3.754 | 1.258 | - | - |
| 8 | 8.240 | 1.621 | - | - |
| 9 | 13.354 | 1.360 | - | - |

The overall inertial properties of the payload for the truck and trailer of the Maxiporter are shown in Table 3.8. The cases of laden and "top laden" are included for each. Equivalent data for the Flexiporter are given in Table 3.9.

**Table 3.8: Maxiporter payload inertial properties**

| Load Scenario | Mass (kg) | Centre of gravity | | Moments of inertia (kg·m$^2$) | | |
|---|---|---|---|---|---|---|
| | | Behind steer axle/hitch (m) | Above ground (m) | Roll | Pitch | Yaw |
| Truck | | | | | | |
| Laden (Veh 1-3) | 7 686 | 2.633 | 2.948 | 9 783 | 55 322 | 51 541 |
| Top laden (Veh 1-2) | 5 124 | 2.254 | 3.503 | 5 426 | 45 298 | 44 424 |
| Trailer | | | | | | |
| Laden (Veh 4-9) | 15 372 | 8.807 | 2.384 | 26 532 | 260 030 | 247 281 |
| Top laden (Veh 4-6) | 7 686 | 9.165 | 3.355 | 13 775 | 117 197 | 110 879 |

**Table 3.9: Flexiporter payload inertial properties**

| Load Scenario | Mass (kg) | Centre of gravity | | Moments of inertia (kg·m$^2$) | | |
|---|---|---|---|---|---|---|
| | | Behind steer axle/hitch (m) | Above ground (m) | Roll | Pitch | Yaw |
| Laden (Veh 1-6) | 15 372 | 6.453 | 2.618 | 23 401 | 353 648 | 341 643 |
| Top laden (Veh 1,4,6) | 7 686 | 6.251 | 3.519 | 11 145 | 210 064 | 204 629 |

Considering the geometric implications of projecting loads at the front and rear of the car-carriers, the context of car-carriers is again unique and variable. A suitable worst case scenario was once again used. The wider a projecting vehicle, the sharper its corner radii and the further it is projected, the more likely it is that it will be a cause for concern in the manoeuvrability standards such as frontal swing and tail swing. The dimensions of the Expedition itself, with its maximum width of 1 996 mm and minimum corner radius of 350 mm (see Figure 3.2), were found to be appropriate. A maximum 1 m load projection was used in accordance with the requirements of the Smart Truck Review Panel (and in line with the findings of De Pont [44]).

To model the rounded corner of the projecting load, the apex of the corner (i.e. assuming a radius of zero) was tracked in TruckSim® as a reference point. During post-processing in Matlab®, this point was used to project ten points representing the rounded corner using basic geometry and the vehicle's position and yaw angle. This method is illustrated in Figure 3.4, where $R_{car}$ refers to the corner radius of the Expedition. Further details of the payload modelling process are given in Section C.1.1, Appendix C.

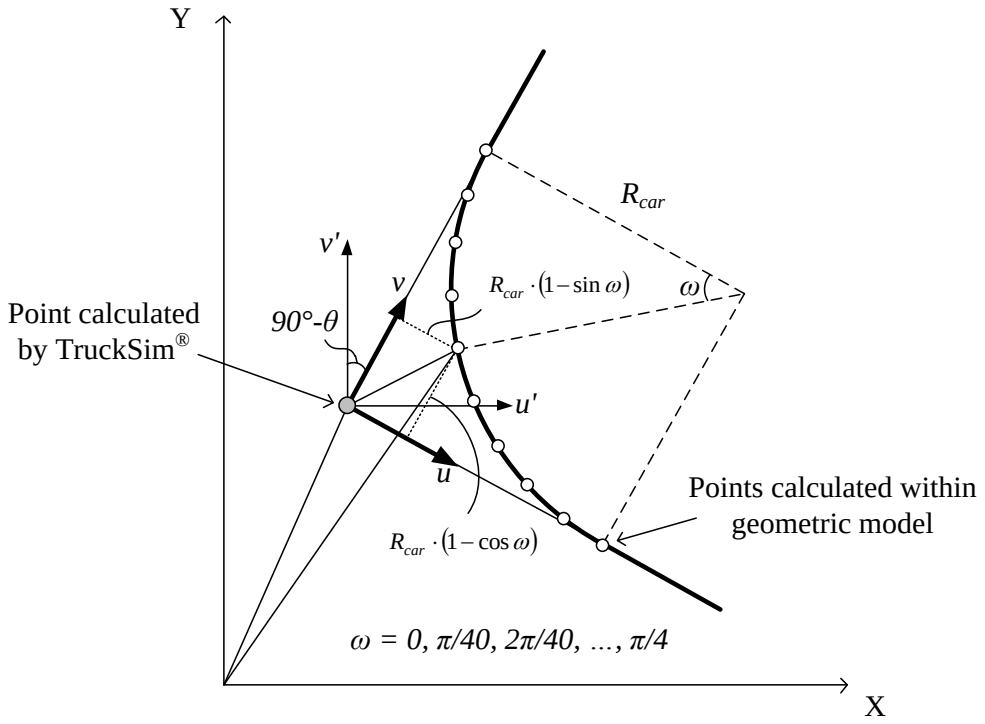


**Figure 3.4: Post-processing to incorporate the corner radii of load projections**

## 3.4 Manoeuvre Descriptions and Modelling

In this section, the various manoeuvres required for the assessment of the safety standards will be described. Detailed descriptions of the manoeuvres are given in the NTC's "Performance Based Standards Scheme – The Standards and Vehicle Assessment Rules," [4] and only certain aspects of the manoeuvres are summarised here, outlining where applicable: the standards associated with each manoeuvre and the purpose and safety implications of each, the path description, the path-following criteria, the speed at which the vehicle must complete the manoeuvre, and the load scenarios that must be considered.

A summary of the manoeuvres, associated standards, rounding conventions and criteria for compliance is given in Table 3.10. The rounding convention prescribes the nearest decimal up or down to which the result must be rounded. The rounding conventions prescribe the levels of tolerance for each of the standards, and are always rounded toward a less favourable result. This leads to conservative reporting (e.g. an FS result of 0.51 m would be reported as 0.6 m and not to 0.5 m).

**Table 3.10: Rounding conventions and criteria for compliance** [4]

| Manoeuvre | Standard | Rounding convention | PBS criteria | | | |
|---|---|---|---|---|---|---|
| | | | Level 1 | Level 2 | Level 3 | Level 4 |
| Low-speed turn | LSSP | ↑ 0.1 m | ≤ 7.4 m | ≤ 8.7 m | ≤ 10.6 m | ≤ 13.7 m |
| | TS | ↑ 0.01 m | ≤ 0.30 m | ≤ 0.35 m | | ≤ 0.50 m |
| | FS | ↑ 0.1 m | ≤ 0.7 m (rigid trucks, prime movers)<br>≤ 1.5 m (buses and coaches) | | | |
| | DoM | ↑ 0.01 m | ≤ 0.20 m | | | |
| | MoD | ↑ 0.01 m | ≤ 0.40 m | | | |
| | STFD | ↑ 1% | ≤ 80% | | | |
| Rollover | SRT | ↓ 0.01·$g$ | ≥ 0.35·$g$<br>≥ 0.40·$g$ (dangerous goods, buses and coaches) | | | |
| Single lane-change | RA | ↑ 0.01 | ≤ 5.7·$SRT_{rrcu}$ | | | |
| | HSTO | ↑ 0.1 m | ≤ 0.6 m | ≤ 0.8 m | ≤ 1.0 m | ≤ 1.2 m |
| Pulse steer | YDC | ↓ 0.01 | ≤ 0.15 | | | |
| Longitudinal tracking | TASP | ↑ 0.1 m | ≤ 2.9 m | ≤ 3.0 m | ≤ 3.1 m | ≤ 3.3 m |

### 3.4.1 Low-speed turn

The low-speed turn manoeuvre was covered in depth in Section 2.1.1. From the paths tracked by the respective reference points on the vehicle during the turn, LSSP, TS, FS, DoM and MoD can be calculated. The NTC requires that rear-view mirrors and signalling devices are ignored in these measurements. These standards address the road space required for a low-speed turn and the associated risks to pedestrians, other road users and roadside furniture.

The sixth standard assessed in the low-speed turn manoeuvre is steer-tyre friction demand or "STFD". This is quantified by the ratio of the friction level demanded by the steer-tyres to that which is available, and addresses the risk of the steer-tyres losing traction when steer axle loads are low and/or when surface friction is limited. This is typically a concern for vehicles with a "tri-drive" truck or truck-tractor (which has three drive axles at the rear, which support an additional portion of what would otherwise be vertical load on the steer axle, reducing steer-tyre vertical forces and hence increasing the chances of their losing friction and "ploughing ahead"). STFD is calculated as a percentage according to

$$\mathrm{STFD} = \frac{100}{\mu_{peak}} \cdot \left| \frac{\sum_{p=1}^{\sigma} \sqrt{{F_{x,p}}^2 + {F_{y,p}}^2}}{\sum_{p=1}^{\sigma} F_{z,p}} \right| \tag{3.1}$$

where $F_x$, $F_y$ and $F_z$ are the longitudinal, lateral and vertical steer-tyre forces respectively in N, $\mu_{peak}$ is the coefficient of friction between the tyre and road, and $\sigma$ is the number of tyres on the steer axle or steer axle group. The NTC prescribes that $\mu_{peak}$ must not be more than 0.80. (For simulation purposes $\mu_{peak}$ is set to 0.80.)

For all of the low-speed standards, the manoeuvre must be conducted with the vehicle fully laden and unladen. For the laden scenario, load projections were set to 1 m where applicable and are based on the dimensions of the 1998 Ford Expedition.

The TruckSim® driver model is only able to follow a path with respect to the vehicle datum, and as a result, in order to achieve steer-tyre path-following, an offset-adjustment technique similar to that described in Section 2.2.2 was necessary. A preview time (which is transformed into a preview *distance* using the vehicle's speed) is used to determine how far ahead the driver model must "look" to compare current and desired vehicle motion paths. The objective of the driver model is to minimise this error. It was found that for low preview times and realistic values of steer-tyre relaxation length (for lateral force development) the driver model would become unstable with large and rapid steering variations. A driver preview time of 0.2 s was found to give an acceptable compromise between path-following accuracy and driver model stability.

In the measurement of frontal and tail swing, when reference is given to the entry and exit tangents of the path, it is taken to mean the path actually transcribed by the outer steer-tyre wall and not the prescribed path it is *supposed* to follow. This is to take account of the offset incurred by TruckSim®. To illustrate, if the front corner swings out to a maximum of $y$ = 0.60 m at a certain $x$ coordinate, and the offset between the steer-tyre path and prescribed path at that $x$ coordinate is +0.01 m (to the inside of the turn), the resultant frontal swing will be 0.61 m.

### 3.4.2 Rollover

The maximum steady-state lateral acceleration a vehicle can withstand before rolling over is known as the static rollover threshold and gives a good indication of the vehicle's rollover stability. A higher static rollover threshold indicates a more stable vehicle. This standard directly addresses one of the concerns cited by the transport authorities regarding the stability of car-carriers at the 4.6 m loaded height.

The NTC requires that the rollover test must be conducted either by means of a tilt-table test or a constant radius quasi-steady turn at incrementally increasing speed. The more representative constant radius turn was selected for simulation purposes and

consists of a circular road of radius 100 m along which the vehicle is driven at increasing speed. The initial speed was set at 50 km/h. After 15 s the speed was incrementally increased at a rate of 0.5 km/h/s until the vehicle – or one of the vehicle units – rolled over. The rate of 0.5 km/h/s is the maximum allowable speed increment prescribed by the NTC such that the quasi-steady-state condition is satisfied. The lateral acceleration of the sprung mass centre of gravity of the first vehicle unit – or roll-coupled unit – at rollover was taken to be the static rollover threshold of the vehicle combination in units of $g$ where $g$ = 9.81 m/s$^2$. The test was conducted with the vehicle both fully laden and in its least favourable load condition. Rollover is taken to occur when all vertical tyre forces on one side of the vehicle have reduced to zero (excluding the steer-tyre on that side of the vehicle, due to the steer axle's softer springs which offer relatively little resistance to roll motion).

The term "roll-coupled unit" is included in the definition to incorporate the stabilising effect of roll-coupling between adjacent vehicle units. In the context of roll motion, when two adjacent vehicle units are roll-coupled, they behave almost as a single unit. The NTC provides detailed requirements for calculating the combined lateral acceleration of a roll-coupled unit, $AY_{rcu}$, which may be summarised as

$$AY_{rcu} = \frac{\sum m_s h_s AY_s}{\sum m_s h_s} \tag{3.2}$$

where $m_s$ is the sprung mass in kg, $h_s$ is the sprung mass centre of gravity height in m, and $AY_s$ is the lateral acceleration of the sprung mass centre of gravity in m/s$^2$.

### 3.4.3 Single lane-change

For the single lane-change manoeuvre, the NTC prescribes the use of the "Single sine-wave lateral acceleration input" test method as described in ISO 14791:2000(E) [45]. The path is described by

$$y = \frac{AY_{\max}}{(2\pi f)^2}\left[2\pi f \frac{x}{v} - \sin\left(2\pi f \frac{x}{v}\right)\right] \tag{3.3}$$

where $v$ is the velocity in m/s, $f$ is the frequency of the manoeuvre in Hz, and $AY_{max}$ is the maximum lateral acceleration in m/s$^2$. The manoeuvre is illustrated in Figure 3.5. Maximum lateral acceleration and steer frequency must be $0.15 \cdot g$ and 0.40 Hz respectively.

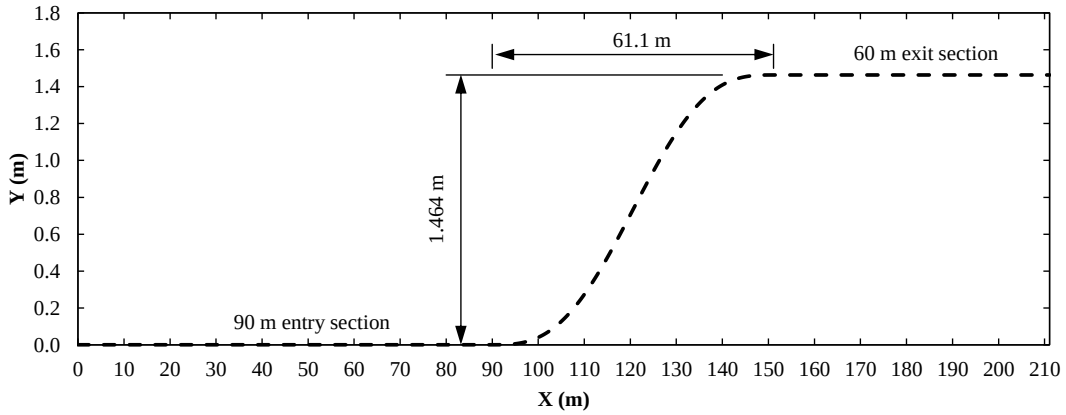


**Figure 3.5: Prescribed path for the single lane-change manoeuvre**

The path must be followed with respect to the centre of the steer axle with a maximum lateral offset of 30 mm, or such that the afore-mentioned lateral acceleration and steer frequency requirements are met. Vehicle speed must be 88 km/h throughout the manoeuvre. The test must be conducted with the vehicle fully laden and at the least favourable load condition.

The manoeuvre is used to assess two safety standards: rearward amplification and high-speed transient offtracking. Rearward amplification pertains to the tendency of articulated vehicles to experience an amplified lateral acceleration response in trailing vehicle units when subjected to a lateral acceleration input at the leading vehicle unit. As a result, the rearmost unit or units may experience a lateral acceleration in excess of their rollover threshold and roll over. Quantitatively, rearward amplification is defined as the ratio of the maximum absolute lateral acceleration experienced by the sprung mass centre of gravity of the rearmost roll-coupled unit, $|AY_{rrcu}|_{\max}$, to that of the centre of the steer axle, $|AY_{steer\ axle}|_{\max}$, during the manoeuvre. This is expressed as

$$\mathrm{RA} = \frac{\left|AY_{rrcu}\right|_{\max}}{\left|AY_{steer\ axle}\right|_{\max}}. \tag{3.4}$$

TruckSim® does not track a variable associated with $AY_{steer\ axle}$. The nearest available variables are the lateral acceleration of the total prime mover centre of gravity or that of the sprung mass centre of gravity. To obtain the lateral acceleration of the steer axle, the lateral acceleration of the total prime mover centre of gravity was combined with the yaw rate, yaw acceleration and relative locations of centre of gravity and steer axle centre according to the principles of planar rigid-body kinetics. Although the difference between the lateral acceleration of the prime mover centre of gravity and that of the steer axle was small, the calculated steer axle lateral acceleration was used in calculations.

During the manoeuvre, the rearmost vehicle will swing laterally outwards relative to the path followed by the steer axle. Depending on the extent of this "overshoot", the vehicle may encroach on other lanes or roadsides presenting a safety risk to other road users or pedestrians. The NTC limits the amount by which the rearmost vehicle unit may deviate from the prescribed path. This lateral displacement is measured at the centre of the rearmost axle and is denoted "high-speed transient offtracking".

### 3.4.4 Pulse steer

The pulse steer manoeuvre is intended to assess the yaw damping characteristics of a vehicle or vehicle combination. Yaw damping refers to the rate at which yaw oscillations decay after a severe steer input. The NTC requires a minimum rate of decay of the oscillations when the vehicle is subjected to a prescribed steer input.

The required steering input is as per the "Steering pulse" of ISO 14791:2000(E) [45]. The standard requires that the amplitude of the steering input shall be such that it generates a maximum lateral acceleration of at least 2 m/s$^2$ and that the duration of the pulse be no greater than 0.6 s. For numerical modelling purposes, the NTC prescribes the equation governing the form of the steering pulse as one period of a haversine function. The steering pulse with amplitude and duration used here is shown in Figure 3.6. The steering amplitude is 300° which, with a steering ratio of 25-to-1, yields a steer input of 12° at the front wheels. The steer input duration is 0.1 s.

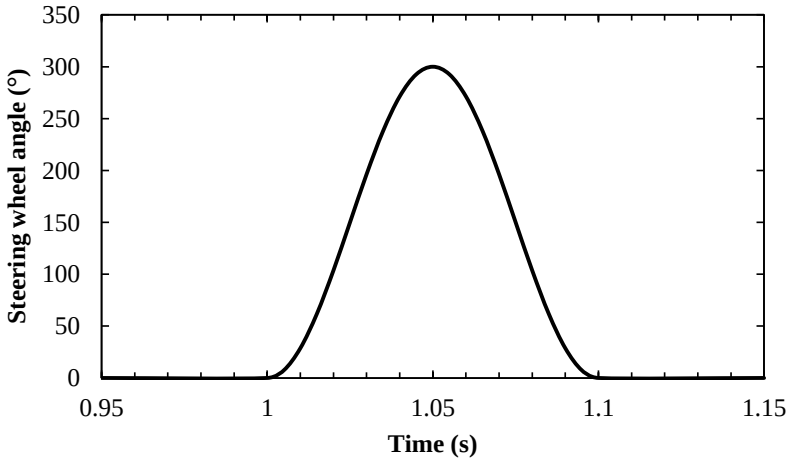


**Figure 3.6: Pulse steer input**

Once subjected to the steering pulse, the vehicle variables that must be recorded are the articulation angle between adjacent vehicle units (°), the articulation rate between adjacent vehicle units (°/s), and the yaw rate of each individual vehicle unit (°/s). The

yaw damping ratio must be calculated using each of these variables and the lowest ratio must be reported. The yaw damping ratio is calculated according to

$$\overline{A} = \frac{1}{\varphi - 2}\left(\frac{A_1}{A_3} + \frac{A_2}{A_4} + \frac{A_3}{A_5} + \ldots + \frac{A_{\varphi-2}}{A_\varphi}\right), \tag{3.5}$$

$$D = \frac{\ln\left(\overline{A}\right)}{\sqrt{(2\pi)^2 + \left[\ln\left(\overline{A}\right)\right]^2}}, \tag{3.6}$$

where $\overline{A}$ and $D$ are the amplitude ratio and damping ratio respectively. $A_1$ to $A_\varphi$ represent the sequential amplitudes of the variable as illustrated in Figure 3.7. $A_\varphi$ must be at least 5% of $A_1$ and at least six amplitudes must be used in the calculation. $\varphi$ represents the number of amplitudes used in the calculation. If the 5% criterion is met before the sixth amplitude, the following equations must be used instead:

$$\overline{A} = \frac{1}{\varphi - 1}\left(\frac{A_1}{A_2} + \frac{A_2}{A_3} + \frac{A_3}{A_4} + \ldots + \frac{A_{\varphi-1}}{A_\varphi}\right), \tag{3.7}$$

$$D = \frac{\ln\left(\overline{A}\right)}{\sqrt{(\pi)^2 + \left[\ln\left(\overline{A}\right)\right]^2}}. \tag{3.8}$$

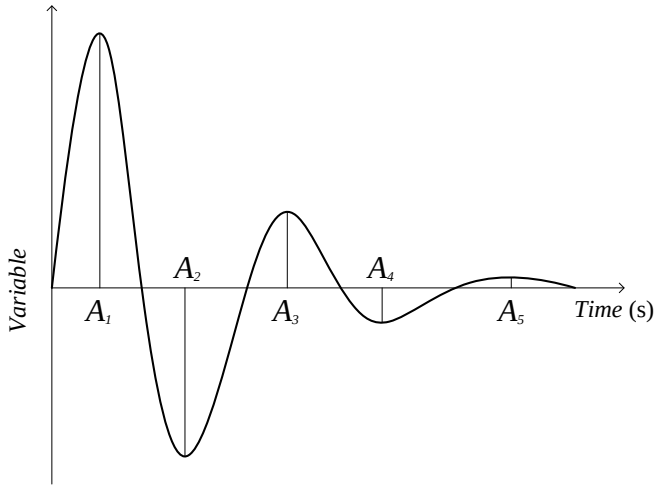


**Figure 3.7: Typical yaw damping response**

The speed at which the manoeuvre must be conducted is not explicitly provided by the NTC. For PBS compliance, the yaw damping ratio must be, "not less than 0.15 at the certified vehicle speed." In the context of the South African PBS scheme, maximum vehicle speed is limited to 80 km/h [15]. Further, the NRTR imposes an 80 km/h speed limit on vehicles with a gross combination mass exceeding 9 000 kg [1]. However, as the

South African scheme is still in its infancy, and because car-carriers are unique in a South African PBS context, a conservative speed of 100 km/h was used for simulation purposes. The NTC requires that the test be conducted with the vehicle fully laden and at the least favourable load condition.

### 3.4.5 Longitudinal tracking

The ability of a vehicle to remain within its lane when travelling at high speed on an uneven road surface is important; and deviation from the lane can present a significant safety risk to other road users. The NTC manages this risk by prescribing a maximum swept path utilisation of a vehicle when travelling along a straight road of defined cross-slope and surface roughness. This is termed tracking ability on a straight path or "TASP".

The specifications of the prescribed road are made available by the NTC for numerical simulation purposes. The road is specified by the vertical displacement of the paths tracked by the left and right wheels. TruckSim® requires a road profile to be specified relative to a global reference frame and not the vehicle. Even if the wheel path profiles are specified at a lateral offset from the road centre line equal to half the steer axle track width, the prescribed road profile will not be followed by other axles due to the deviation of the vehicle from the prescribed path. It is hence important to establish a suitable interpolation between the known road profiles.

Assuming a linear cross-slope between left and right wheel paths for each incremental distance travelled, a centreline road-profile can be established as the average of the left and right elevation profiles provided by the NTC. Assuming that the left and right wheel paths are separated laterally by 2.5 m, the NTC's road profiles may be specified at lateral coordinates of –1.25 m and +1.25 m relative to the centre line. TruckSim® interpolates and extrapolates these data to establish a three-dimensional profile of the road. An unavoidable implication of this method is that the further the vehicle deviates outward of the 2.5 m path width, the more amplified road roughness variations become. This is conservative and deemed suitable for application here. Figure 3.8, Figure 3.9 and Figure 3.10 depict the centreline elevation, "wheel-path elevations" and three-dimensional visualisation of the path used in TruckSim® respectively. 200 m feed-in and feed-out sections were included. The average cross-slope is 1.85° (sloping down to the right).

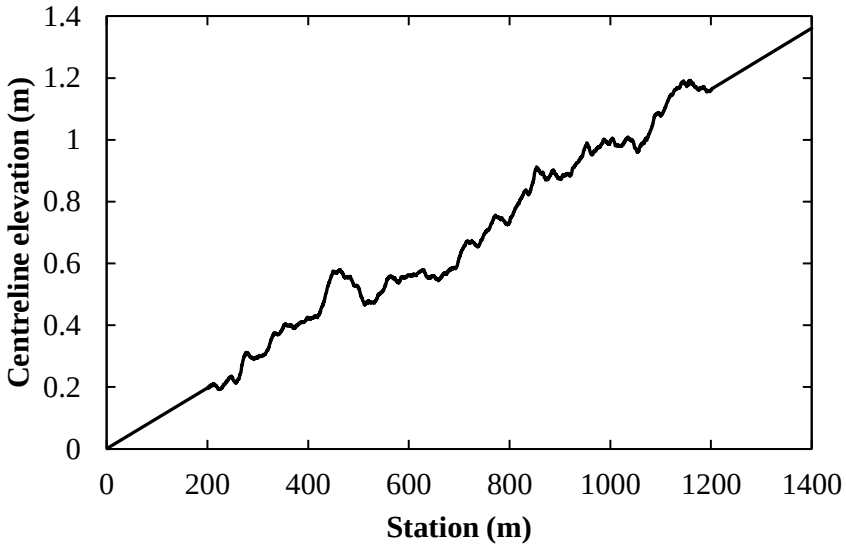


**Figure 3.8: Centreline elevation profile for longitudinal tracking**

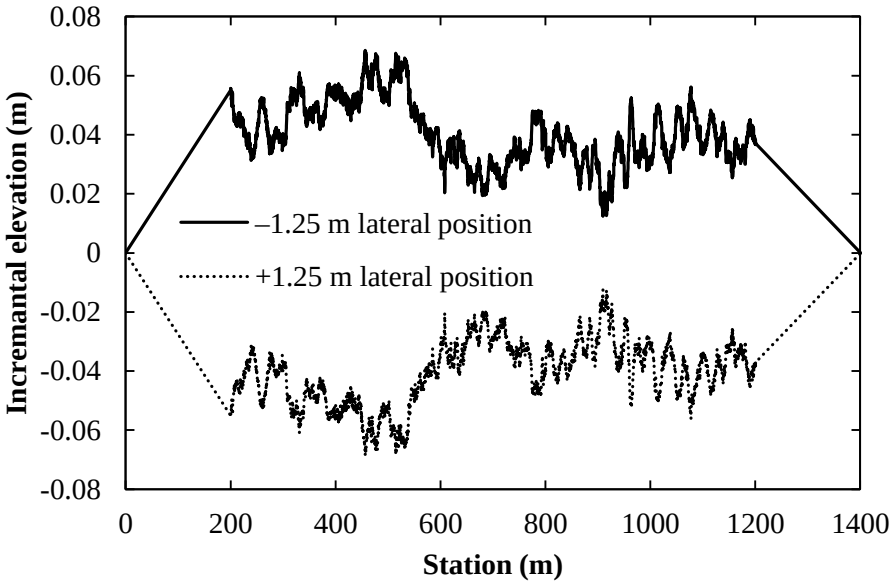


**Figure 3.9: Elevation profiles for the left and right wheel paths for longitudinal tracking**

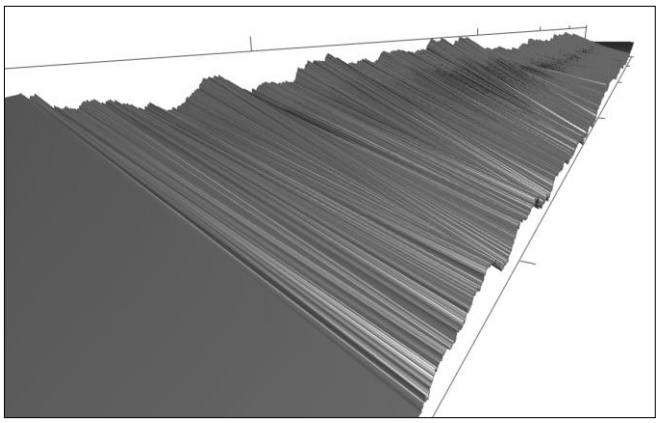

**Figure 3.10: Three-dimensional road profile used for longitudinal tracking (not to scale)**

A number of reference points representing the outermost extremities of the vehicle must be tracked to determine the maximum swept width utilised during the manoeuvre. Where more than one choice of reference point exists in a given vertical plane, the NTC requires that the point nearest the ground be chosen. This is an important definition for car-carriers. If a vehicle has outermost points in the same vertical plane that exist at both the top of the vehicle and near the bottom, the choice of the lower reference point means that roll motion will not significantly contribute to the swept width exhibited by the vehicle. As the test road has an inherent cross slope, roll motion can contribute a significant lateral displacement of reference points at or near the top of the vehicle. In the cases of the Maxiporter and Flexiporter, the side profiles of the vehicle structures are "flat" and so the reference points are typically situated near to the ground, aligned with the lower loading platform.

The test must be conducted at 90 km/h and the vehicle must be tested under both laden and least favourable loading conditions. In the case of numerical modelling, the NTC deems the 99$^{th}$ percentile of the swept width acceptable to cater for differences between computer models.

## 3.5 Baseline Vehicle Assessments

This section presents the assessment results for the baseline Maxiporter and baseline Flexiporter as they were described in Section 3.1. These are the vehicles as they were initially proposed with maximum one metre load projections. For each vehicle, the results are presented followed by a section briefly summarising significant observations and proposing design modifications required to address any non-compliances. A "Tail swing reinterpretation" section discusses an important aspect of tail swing highlighted during the assessments. Unless otherwise stated, results are quoted according to the rounding convention required by the NTC.

### 3.5.1 Maxiporter

Figure 3.11 shows the LSSP for the Maxiporter which was calculated to be 6.7 m (rounded from 6.629 m). This value is low for a 22 m-long vehicle and is mainly due to the short trailer wheelbase. The Level 1 limit for this standard is 7.4 m. The figure depicts the laden scenario as this exhibited the largest value of LSSP due to the additional swing-out of the front corner as a result of the projecting load.

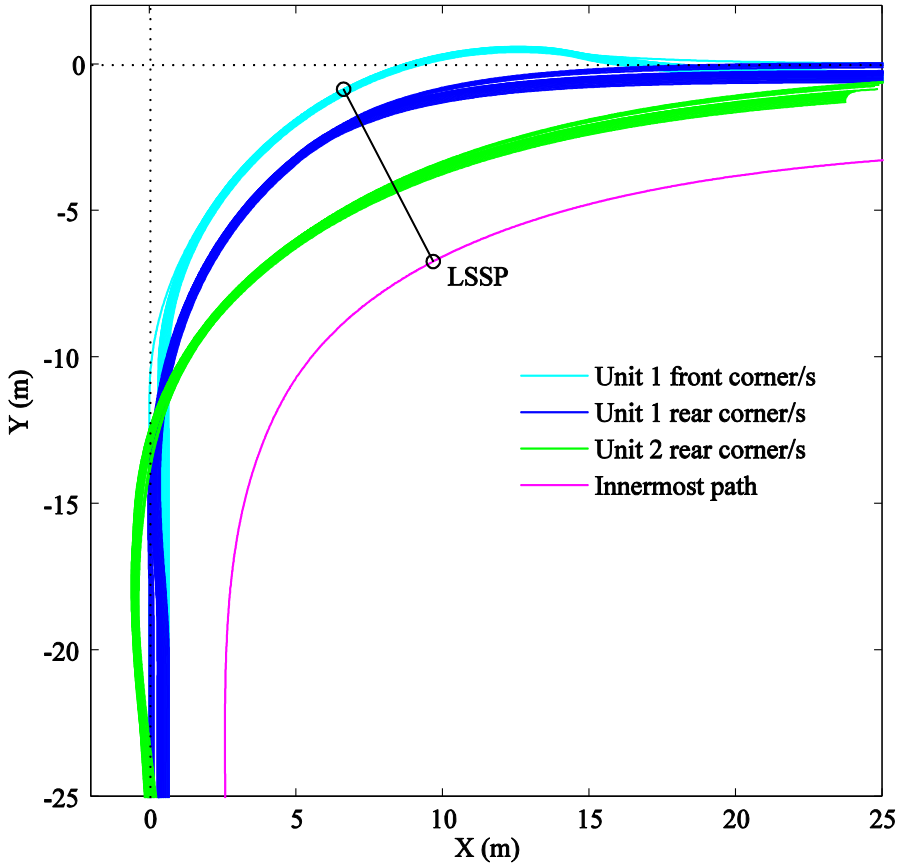


**Figure 3.11: Baseline Maxiporter, LSSP, laden**

Figure 3.12 and Figure 3.13 show isolated regions of Figure 3.11 highlighting tail swing and frontal swing respectively. Both cases are shown as laden as this yielded the maximum values of tail and frontal swing due to load projections. The multiple trajectories represent selected reference points on the car-carrier as well as the reference points representing the rounded corners of the load projections. The tail swing was calculated to 0.66 m (rounded from 0.655 m) – well in excess of the Level 1 limit of 0.30 m. The limiting factor in this case was the projecting load of the trailer (Unit 2), though it is noted that the trailer rear corner swung out in excess of 0.5 m – a simple reduction in the rear load projection could therefore not address this issue. The truck (Unit 1) exhibited very little tail swing due to its relatively short rear overhang. Frontal swing was calculated to be 0.7 m (rounded from 0.636 m) – also dominated by the projecting load but within the allowable limit.

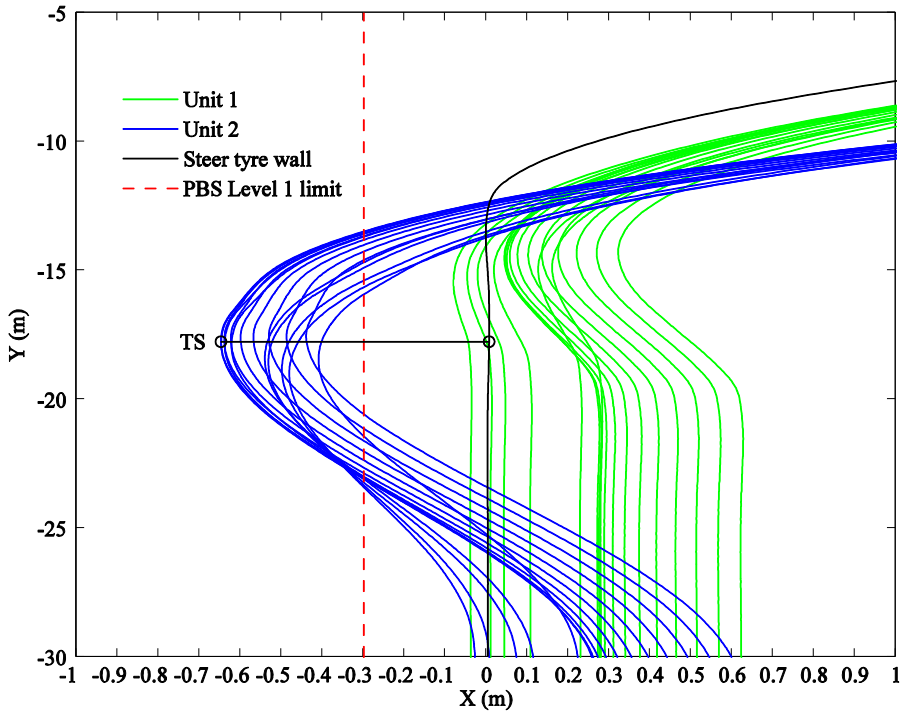


**Figure 3.12: Baseline Maxiporter, TS, laden**

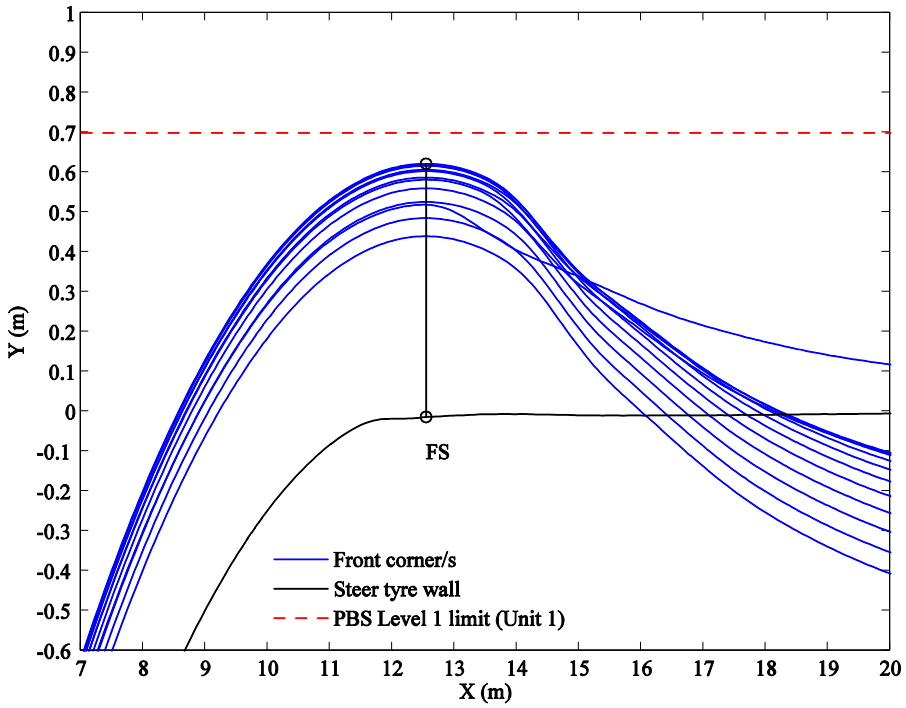


**Figure 3.13: Baseline Maxiporter, FS, laden**

Steer-tyre friction demand performance is shown in Figure 3.14. STFD was calculated to be 34% – well below the Level 1 maximum of 80%. This result represents the unladen scenario as this was shown to be the worst case due to reduced vertical steer-tyre forces, $F_z$, in the denominator of Equation (3.1).

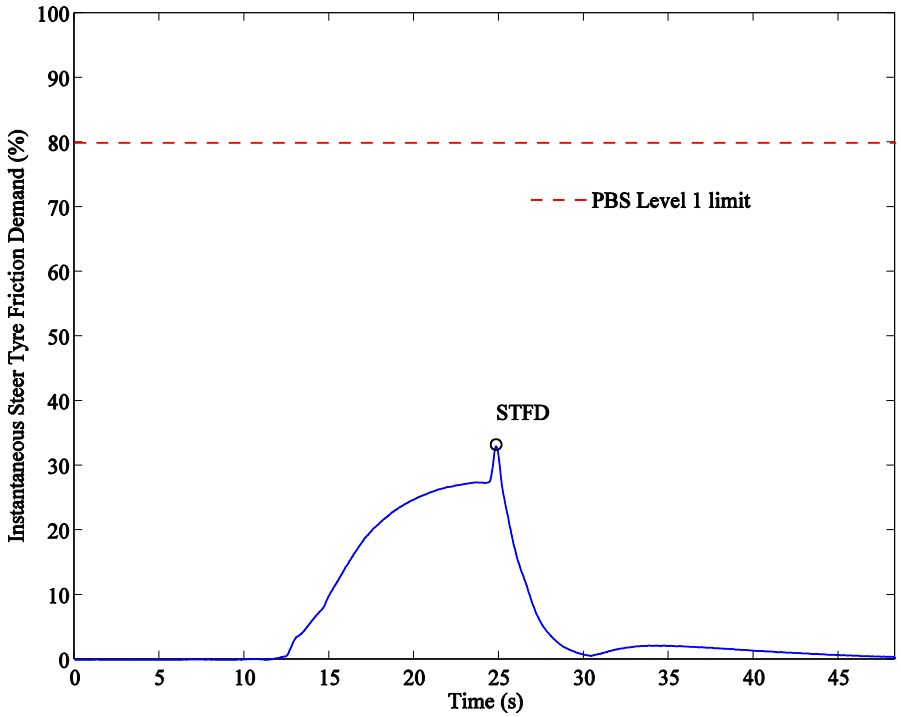


**Figure 3.14: Baseline Maxiporter, STFD, unladen**

A notable feature of Figure 3.14 is an isolated peak at around 25 seconds. This point coincides with the transition from the curved section of the path to the straight exit tangent. This peak is a result of the characteristics of the driver model and not truly representative of vehicle performance. It was found that at the point of curve transition, the steering rate of the driver model increased from a mean near zero just before the transition to about 600 °/s, resulting in a sharp rise in lateral and vertical tyre forces, and the sharp rise in calculated steer-tyre friction demand.

Figure 3.15 depicts the rollover results. The figure shows the increasing lateral accelerations experienced by the truck and trailer sprung mass centres of gravity as the speed of the vehicle is increased to the point of rollover. The truck was calculated to be the critical vehicle unit in this respect as it rolled first with an SRT of $0.35 \cdot g$ (rounded from $0.351 \cdot g$). This is at the lower limit allowed for all road access levels. This result was achieved with the "top laden" loading scenario. Oscillations in lateral acceleration occurred after 38 seconds as a result of the truck suspension rolling through the region of lash. Rollover occurs before the trailer enters its suspension lash region.

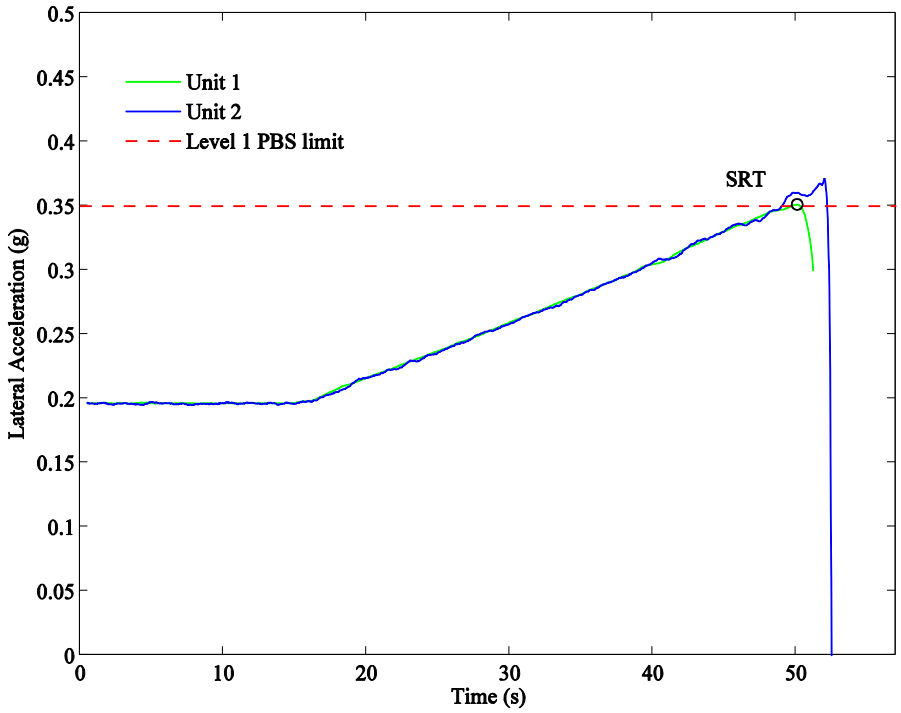


**Figure 3.15: Baseline Maxiporter, SRT, top laden**

The results for the single lane-change manoeuvre are shown in Figure 3.16 and Figure 3.17. Figure 3.16 depicts the lateral acceleration of the steer axle and of the sprung mass centre of gravity of the trailer. The rearward amplification was calculated to be 1.82 (rounded from 1.814). The worst case scenario for rearward amplification was determined to occur when the vehicle had a fully laden trailer but no load on the truck.

The maximum allowable value for RA is $5.7 \cdot SRT_{rrcu}$ where $SRT_{rrcu}$ is the static rollover threshold of the rearmost roll-coupled unit which, in this case, is the trailer. As the truck was the limiting vehicle in the SRT simulation, the SRT of the trailer was determined by conducting the SRT manoeuvre with the truck unladen such that the trailer could be taken to its maximum sustainable lateral acceleration. $SRT_{rrcu}$ was calculated to be $0.44 \cdot g$ and so the upper limit for RA in this case is $5.7 \cdot 0.44 \cdot g = 2.508 \cdot g$ which is rounded down to $2.5 \cdot g$. The vehicle meets the RA requirement. The favourable SRT of the trailer, and hence acceptable RA performance, may be attributed to its three single-fitment axles, each with large track width, large lateral spring separation and high spring stiffness.

Figure 3.17 depicts the motion of the rearmost trailer axle in the global coordinate system during the lane-change. The high-speed transient offtracking of the vehicle was calculated to be 0.7 m (rounded from 0.633 m) which is in excess of the 0.6 m Level 1 limit. The least favourable load condition was the same as that for rearward amplification.

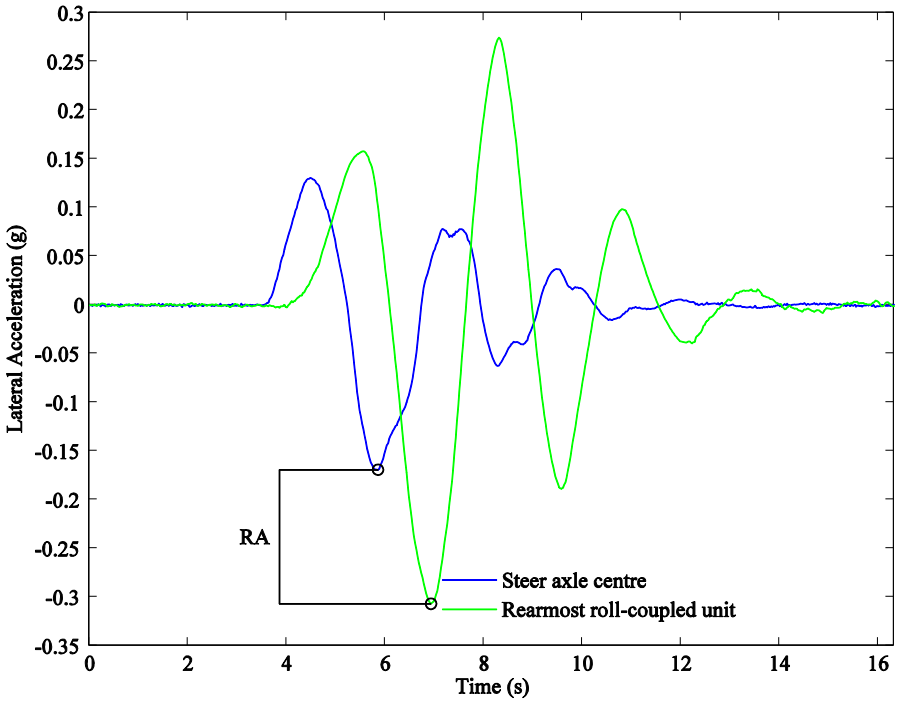


**Figure 3.16: Baseline Maxiporter, RA, trailer laden**

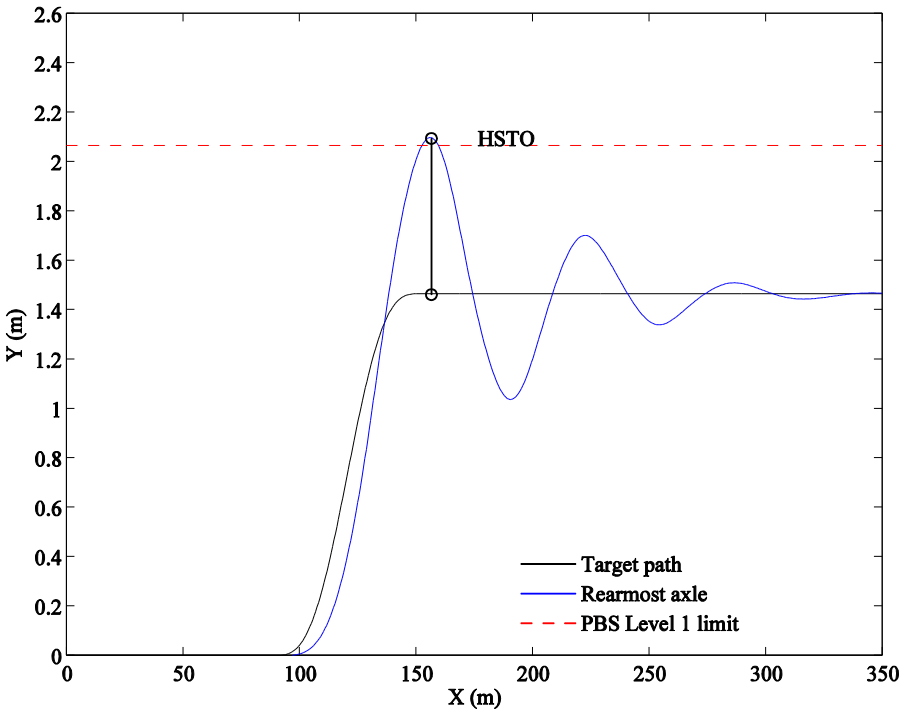


**Figure 3.17: Baseline Maxiporter, HSTO, trailer laden**

The yaw response of the Maxiporter to the pulse steer input is given in Figure 3.18. The variable shown is the hitch articulation rate. Due to the roll-steer properties of the steer axle, the vehicle maintained a steady steer response after the pulse input. Although not a concern for the test itself, this resulted in unfavourable response data for articulation angle and vehicle yaw rate response (values did not return to zero but rather to a finite steady-state value). The only variable in this case to converge to zero was the hitch articulation rate and hence it was used for the calculation of YDC.

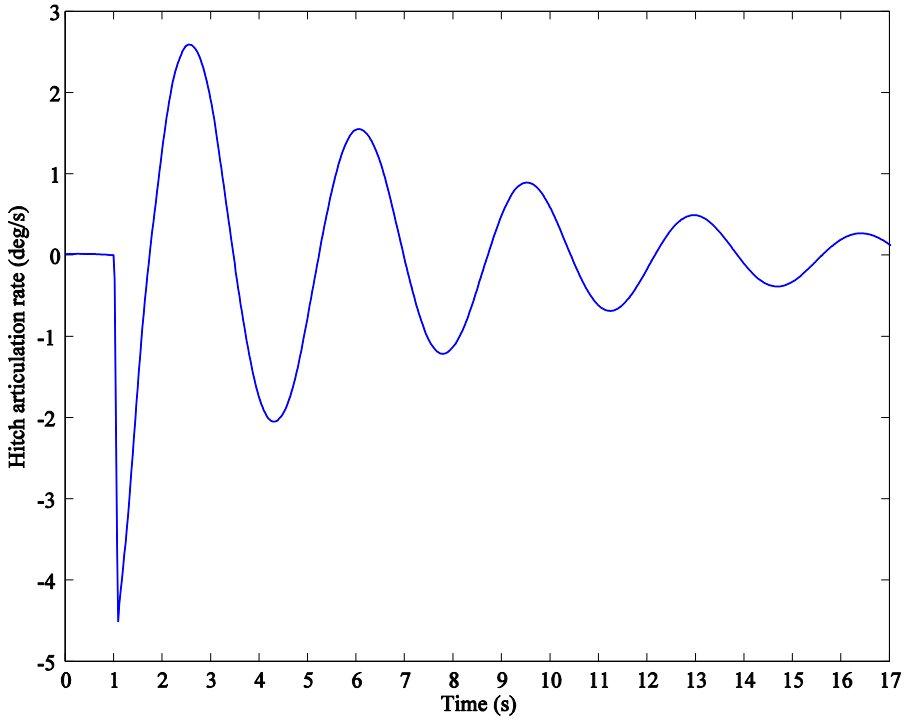


**Figure 3.18: Baseline Maxiporter, YDC, trailer top laden**

The yaw damping coefficient was calculated to be 0.09 (rounded from 0.095) – significantly below the lower limit of 0.15. This is a poor result, with large oscillations continuing after the initial input of the steering pulse. The worst-case scenario was an unladen truck with a "top laden" trailer. A centre-axle trailer results in the lateral tyre forces, which act to restore equilibrium, having a short moment arm and being less effective as compared to a trailer with the axle or axle group placed further back.

The results for tracking ability on a straight path are depicted in Figure 3.19. The trajectories of a number of critical reference points are shown in the figure and the maximum lateral displacement between any two trajectories over the course of the 1 000 m road is indicated. The value calculated was 3.0 m (rounded from 2.928 m) for the laden scenario, which fails to meet the 2.9 m requirement for Level 1 road access. The 99$^{th}$ percentile result was 2.906 m which rounds to the same figure of 3 m. During the feed-

out section the vehicle became unstable as is evident in the erratic trajectories after about 1 200 m. The calculation of TASP was restricted to the 1 000 m test section, however the instability of the vehicle was noted. The road profile used for this test is demanding and inherent vehicle instabilities are likely to be identified in such a test.

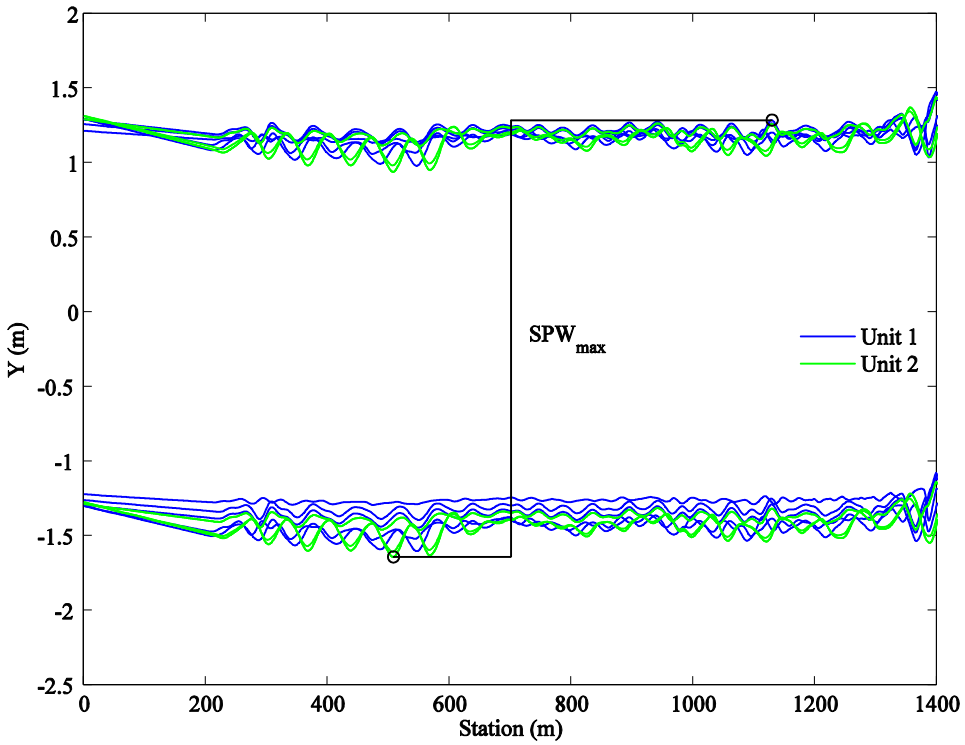


**Figure 3.19: Baseline Maxiporter, TASP, laden**

Results for the baseline Maxiporter are summarised in Table 3.11 for all simulated loading scenarios. The least favourable load condition for each standard is emphasised. Results as rounded according to the requirements of the NTC for all worst-case loading scenarios are shown in Table 3.12. The TASP results shown in Table 3.11 represent the actual and not 99$^{th}$ percentile results. The final figure given in Table 3.12 is based on the 99$^{th}$ percentile value of the worst-case scenario. The vehicle combination failed to meet the Level 1 road access criteria for tail swing, high-speed transient offtracking, tracking ability on a straight path and yaw damping. This is mostly attributable to the centre-axle configuration of the trailer.

**Table 3.11: Baseline Maxiporter results, not rounded, all loading scenarios**

| Standard | Unladen | Laden | Top laden | Truck laden | Truck top laden | Trailer laden | Trailer top laden |
|---|---|---|---|---|---|---|---|
| **LSSP** (m) | 6.543 | **6.629** | - | - | - | - | - |
| **TS** (m) | 0.544 | **0.655** | - | - | - | - | - |
| **FS** (m) | 0.525 | **0.636** | - | - | - | - | - |
| **STFD** (%) | **33** | 31 | - | - | - | - | - |
| **SRT** (*g*) | - | 0.353 | **0.351** | - | - | 0.440 | 0.451 |
| **RA** | - | 1.459 | 1.468 | - | - | **1.814** | 1.640 |
| **HSTO** (m) | - | 0.631 | 0.561 | - | - | **0.633** | 0.523 |
| **YDC** | - | 0.208 | 0.216 | 0.390 | 0.342 | 0.108 | **0.095** |
| **TASP** (m) | - | **2.928** | 2.910 | - | - | - | - |

**Table 3.12: Baseline Maxiporter results, rounded, worst-case loading scenarios**

| Standard | Level 1 criterion | Result | PBS level achieved | Critical scenario |
|---|---|---|---|---|
| **LSSP** (m) | ≤ 7.4 | 6.7 | All | Laden |
| **TS** (m) | ≤ 0.3 | 0.66 | **None** | Laden |
| **FS** (m) | ≤ 0.7 | 0.7 | All | Laden |
| **STFD** (%) | ≤ 80 | 34 | All | Unladen |
| **SRT** (*g*) | ≥ 0.35 | 0.35 | All | Top laden |
| **RA** | ≤ 2.5 | 1.82 | All | Trailer laden |
| **HSTO** (m) | ≤ 0.6 | 0.7 | **Level 2** | Trailer laden |
| **YDC** | ≥ 0.15 | 0.09 | **None** | Trailer top laden |
| **TASP** (m) | ≤ 2.9 | 3.0 | **Level 2** | Laden |

### 3.5.2 Maxiporter observations and design considerations

The failure of the Maxiporter to comply with the TS, HSTO, TASP and YDC performance standards was determined to be due to the short trailer wheelbase. A parametric study of the effects of increasing the trailer wheelbase was therefore conducted. Without changing any other vehicle parameters, an increase in the trailer wheelbase of one metre improved the Maxiporter's performance in the TS, HSTO, TASP and YDC standards, but increased LSSP. However, the increase in LSSP was small enough such that the upper limit of 7.4 m was not exceeded.

The increase trailer wheelbase was not sufficient to reduce the tail swing to below the 0.30 m Level 1 limit. However, it was found that the rearmost outer corner of the trailer served no mechanical purpose, and could be tapered to meet the 0.30 m limit. A further parametric study determined the dimensions to which this corner should be tapered. This

design modification was a relatively simple addition to the manufacturing of the trailer and was hence deemed a suitable means of attaining compliance. The dimensions of the required tapering are shown in Figure 3.20.

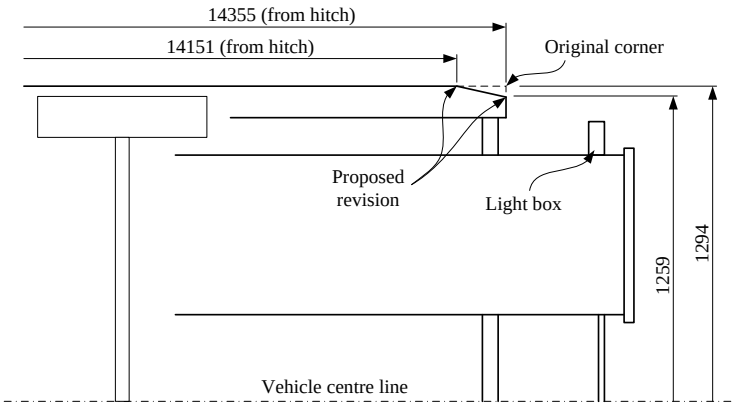


**Figure 3.20: Maxiporter trailer rear corner tapering to satisfy Level 1 tail swing criterion**

Although SRT was shown to meet the PBS criteria of 0.35·*g*, it did so by the smallest of margins. The increased trailer wheelbase was shown to improve the SRT of the vehicle. Factors that directly influence SRT are sprung mass, sprung mass centre of gravity height, suspension and tyre stiffness and auxiliary roll stiffness – none of which were altered. The reason for improvement in SRT lies in the vertical load redistribution caused by the change in trailer wheelbase. As rollover is approached, lateral load transfer occurs from one side of the vehicle to the other. Rollover occurs when all vertical load has been transferred from one side of the vehicle to the other (the vertical tyre loads on one side of the vehicle reduce to zero). If the standing vertical load can be increased *without* increasing the actual sprung mass of the vehicle, the amount of load transfer required for rollover, and hence the rollover threshold, is increased. In the case of the Maxiporter, the increased trailer wheelbase shifted a portion of the original trailer load from the trailer axle group to the hitch and hence to the truck. This resulted in the observed improvement in the rollover threshold of the truck and hence of the vehicle combination overall (because the truck is the limiting vehicle unit).

### 3.5.3 Flexiporter

Figure 3.21 depicts the LSSP of the Flexiporter. A calculated maximum LSSP of 6.6 m (rounded from 6.539 m) was achieved for the unladen scenario. Unlike the case of the Maxiporter where the laden scenario introduced a frontal load projection which increased frontal swing-out and hence LSSP, the Flexiporter experienced the greatest LSSP in the

unladen scenario. This is dictated solely by the effect of axle loads (decreased axle loads increase swept path except in rare exceptions [30]).

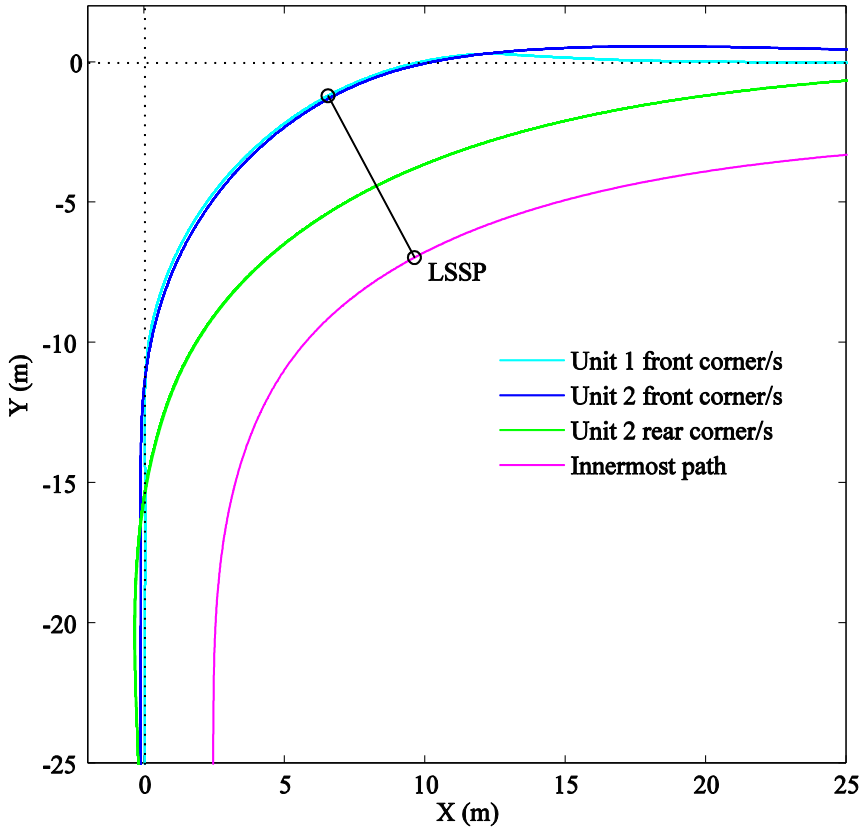


**Figure 3.21: Baseline Flexiporter, LSSP, unladen**

Swing-out of the semitrailer extremities exceeded the Level 1 tail swing limit with a magnitude of 0.38 m (rounded from 0.377 m). This is shown in Figure 3.22. A large portion of this result was due to the "lateral overhang" of the rearmost outer corner of the trailer relative to the outer steer-tyre wall. This concept is discussed in Section 3.5.5. The worst-case scenario was the laden condition: the vehicle tracks less to the inside of the path due to the increased axle loads, causing the tail to swing out further.

The worst-case (unladen) frontal swing scenario is shown in Figure 3.23. The calculated frontal swing was 0.4 m (rounded from 0.337 m) which is well under the upper limit of 0.7 m. As the axle loads are reduced, the offtracking increases which yields an increased yaw angle relative to the path tangent. This results in increased frontal swing as a larger portion of the front overhang dimension is projected in the positive Y direction.

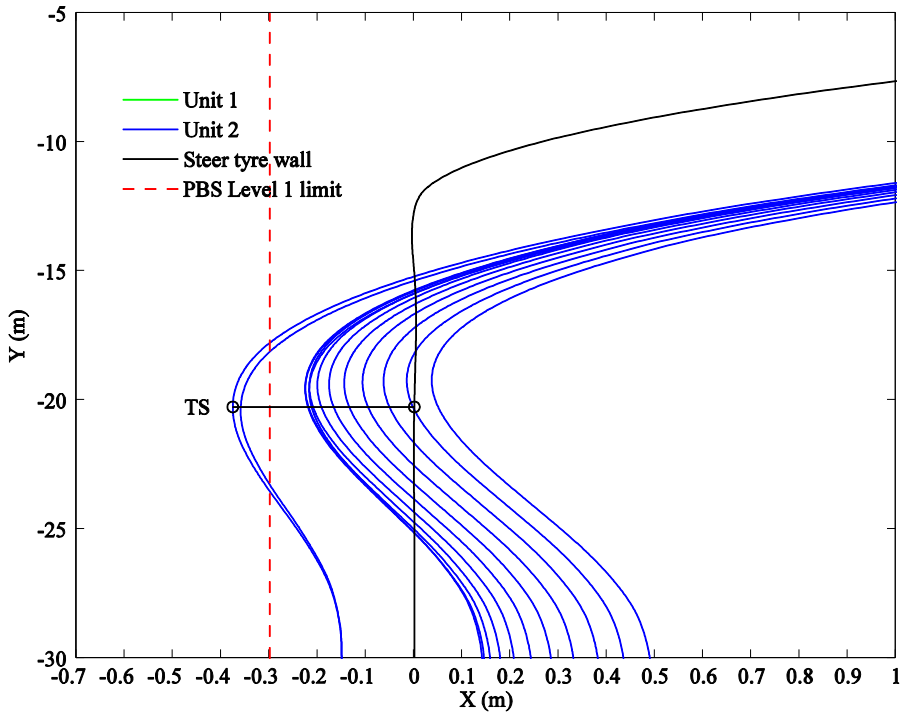


**Figure 3.22: Baseline Flexiporter, TS, laden**

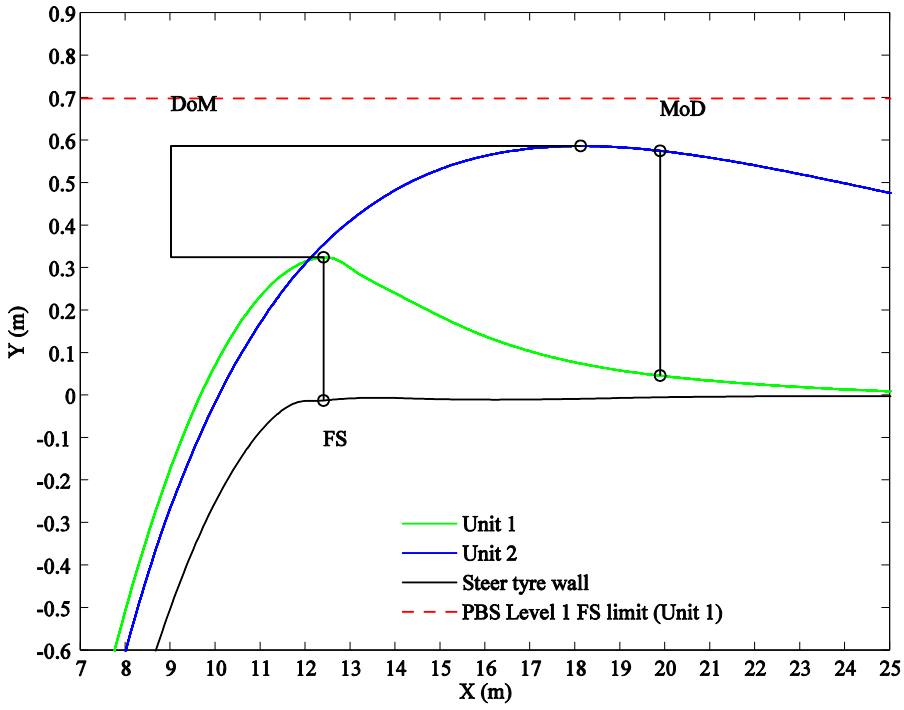


**Figure 3.23: Baseline Flexiporter, FS, unladen**

Although difference of maxima and maximum of difference are indicated in Figure 3.23, these do not represent the worst case scenarios. Due to the semitrailer front load projection introduced, the laden scenario yields the highest DoM and MoD values as

depicted in Figure 3.24. DoM was calculated to be 0.44 m (rounded from 0.440) and MoD was calculated to be 0.65 m (rounded from 0.644 m), both of which fail to meet the Level 1 upper limit criteria of 0.2 m and 0.4 m respectively. STFD is depicted in Figure 3.25 and was calculated to be 33% (unladen).

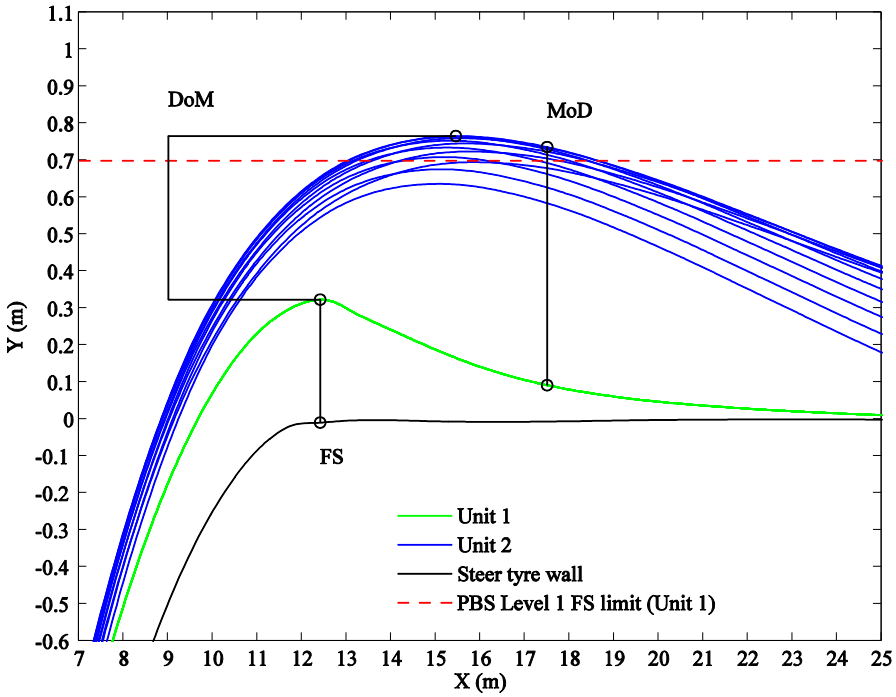


**Figure 3.24: Baseline Flexiporter, DoM and MoD, laden**

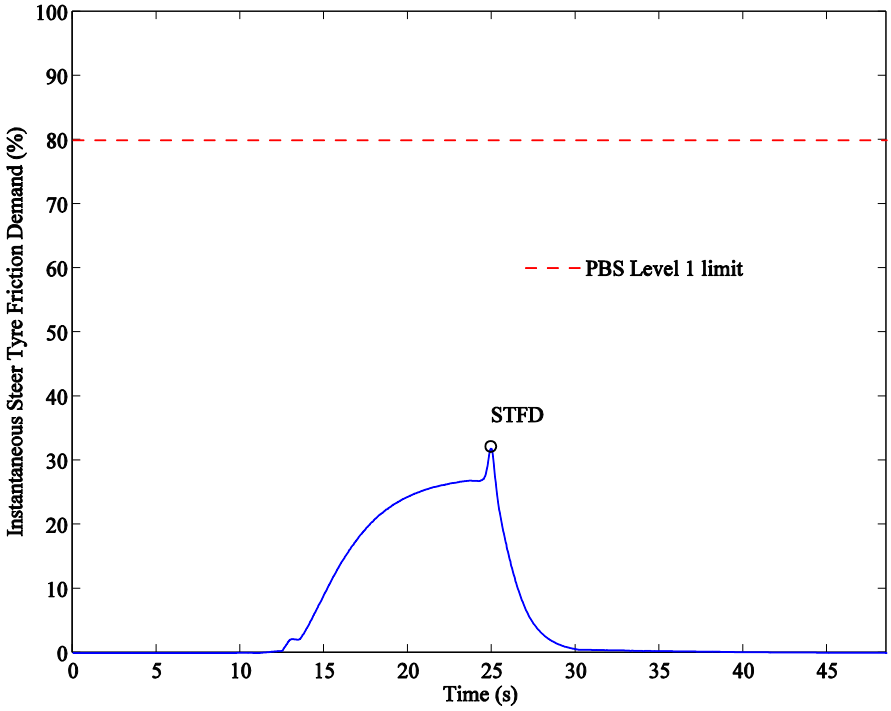


**Figure 3.25: Baseline Flexiporter, STFD, unladen**

Rollover simulation results are shown in Figure 3.26. The calculated SRT was 0.42·$g$ (rounded from 0.422·$g$) for the laden scenario. The air suspension and roll-coupling of the fifth wheel both contribute to the favourable performance in this standard.

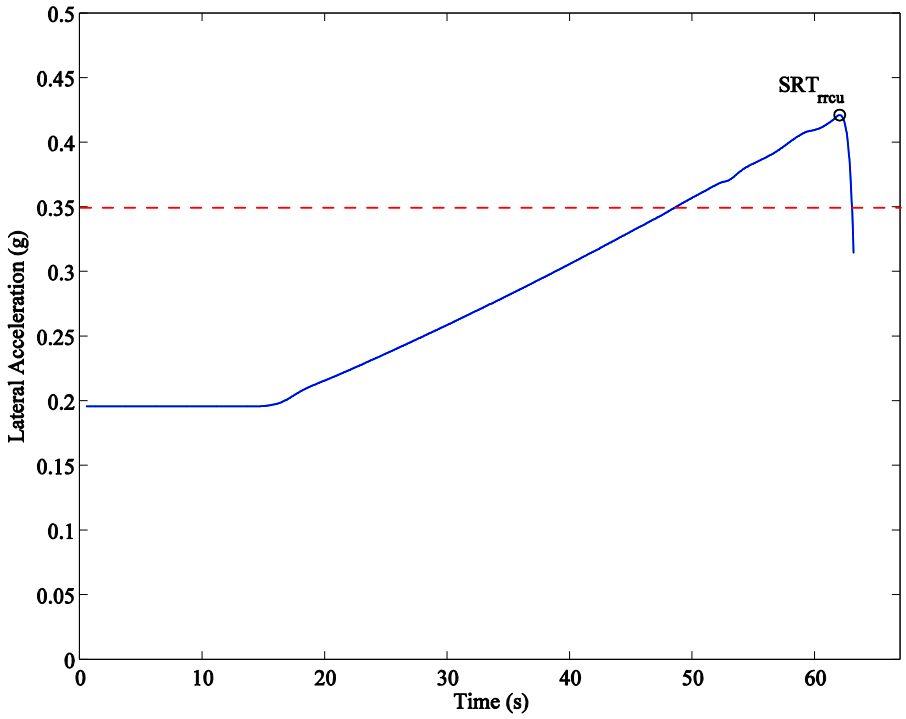


**Figure 3.26: Baseline Flexiporter, SRT, laden**

The RA results from the single lane-change manoeuvre are shown in Figure 3.27. A RA of 1.06 was calculated (rounded from 1.055) for the "top laden" condition, well under the limit of 2.39. Values near 1.00 are typical for tractor and semitrailer combinations and values below 1.00 are possible [19]. The fully laden HSTO results are shown in Figure 3.28. The calculated HSTO result was 0.4 m (rounded from 0.304 m) which is safely within the upper limit of 0.6 m.

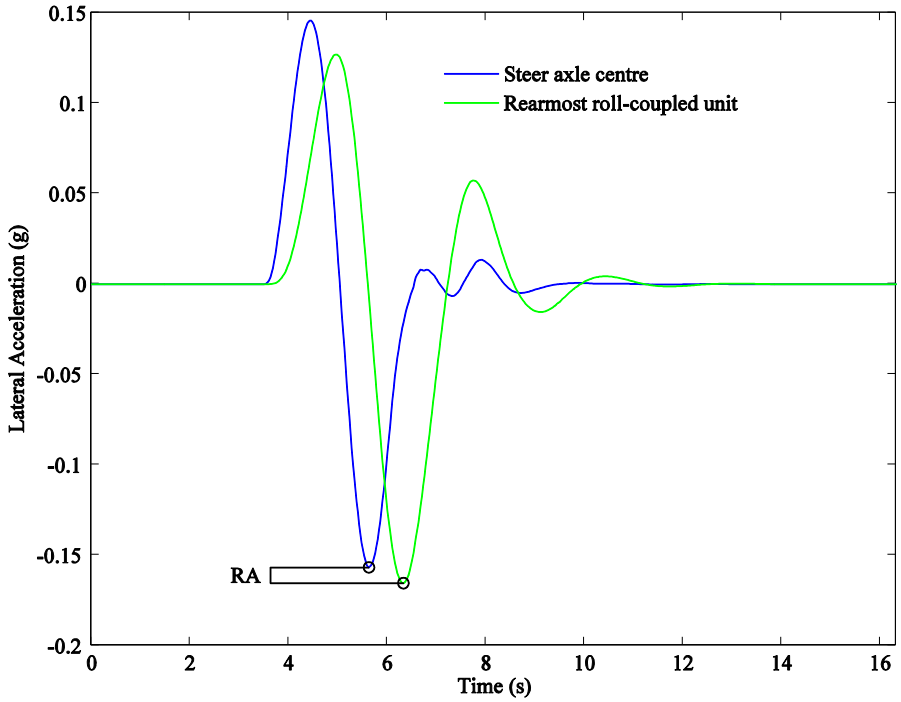


**Figure 3.27: Baseline Flexiporter, RA, top laden**

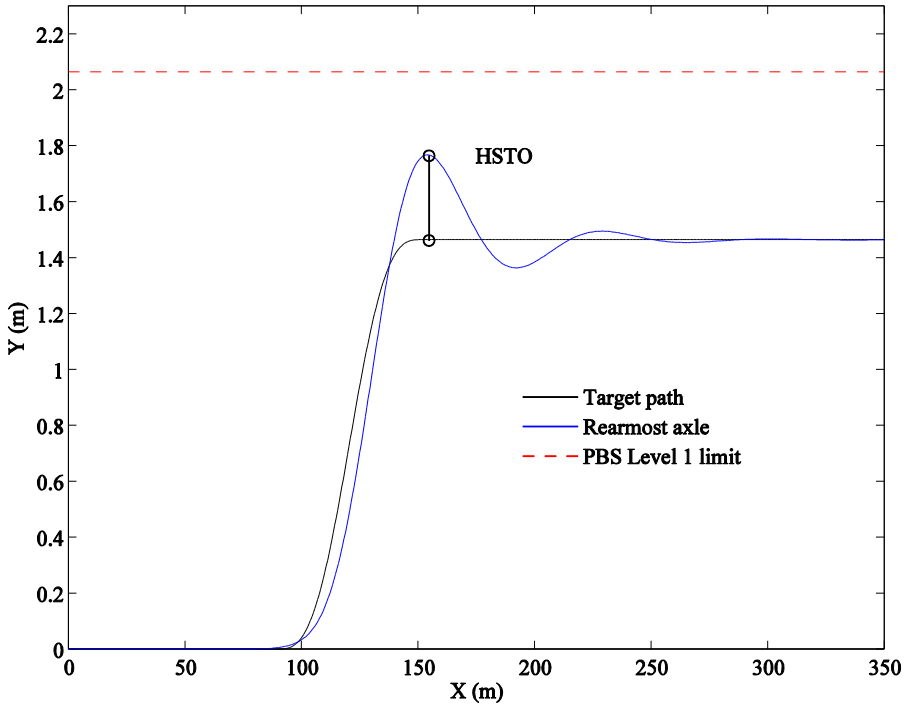


**Figure 3.28: Baseline Flexiporter, HSTO, laden**

The hitch articulation rate response to the pulse steer input is shown in Figure 3.29. Hitch articulation rate was chosen for the same reason given for the Maxiporter. The calculated yaw damping ratio was 0.32 (rounded from 0.328). This favourable yaw-damping behaviour is typical of tractor-semitrailer combinations [19].

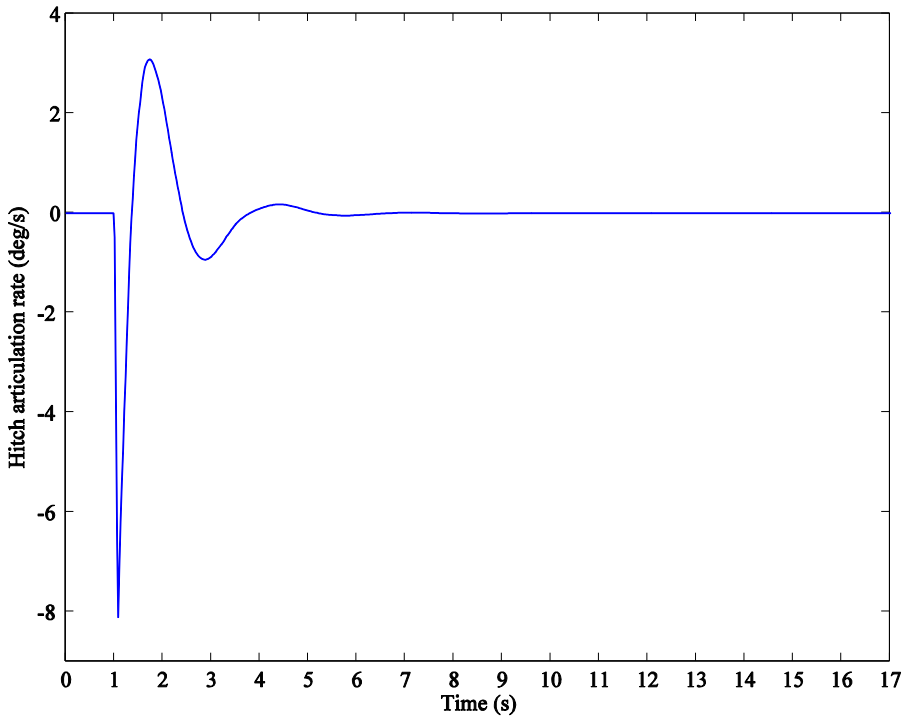


**Figure 3.29: Baseline Flexiporter, YDC, top laden**

The trajectories of pertinent reference points on the Flexiporter during the tracking ability manoeuvre are shown in Figure 3.30. The maximum swept path exhibited was 2.9 m (rounded from 2.846 m) for the laden scenario. The 99$^{th}$ percentile value was 2.835 m which is also rounded to 2.9 m. Very little deviation of the truck-tractor was calculated and the maximum swept path was entirely dictated by motions of the semitrailer. Although 2.9 m is on the upper limit for Level 1 road access, the Austrailan heavy vehicle fleet from which the limits were derived is limited to a maximum width of 2.5 m [20], whereas widths of up to 2.6 m are permitted in South Africa [1] (and the Flexiporter semitrailer is 2.6 m wide). As a result, TASP results can be expected to be up to 100 mm larger than an equivalent 2.5 m-wide Australian vehicle, resulting in the seemingly borderline result. Unlike the case of the baseline Maxiporter, the vehicle behaviour in the feed-out section is as expected. As in the case of rearward amplification, tracking ability on a straight path is not generally critical for tractor and semitrailer combinations [19].

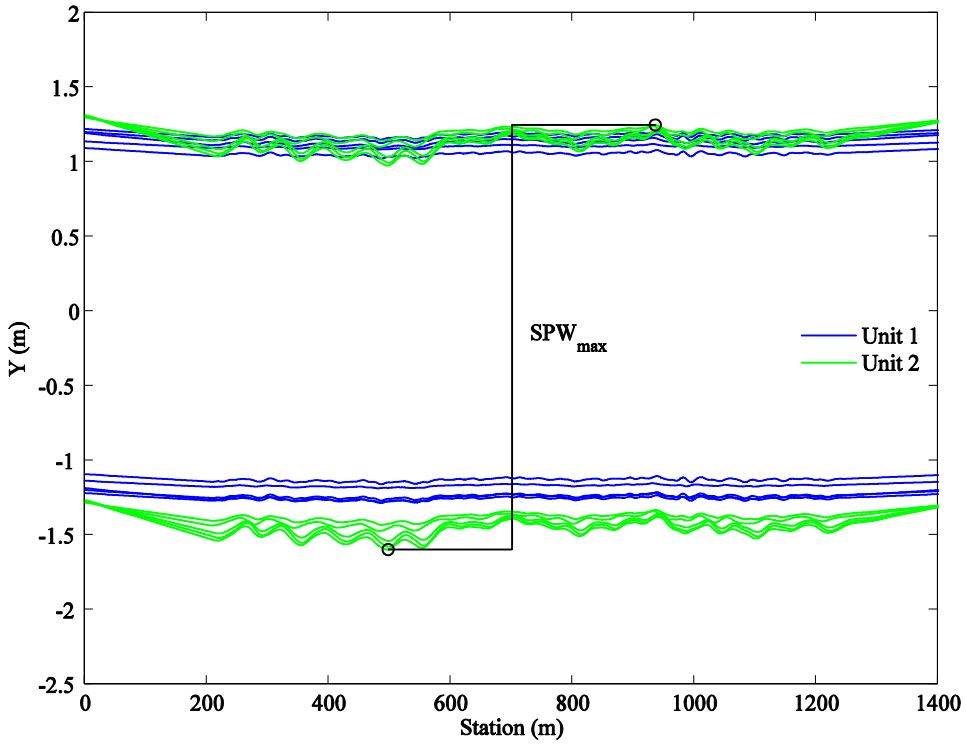


**Figure 3.30: Baseline Flexiporter, TASP, laden**

The assessment results of the baseline Flexiporter are summarised in Table 3.13 for all simulated loading scenarios. Results as rounded according to the requirements of the NTC for all worst-case loading scenarios are shown in Table 3.14. The vehicle combination failed to meet Level 1 road access criteria on three accounts: tail swing, difference of maxima and maximum of difference. As before, the TASP results in Table 3.13 represent the actual values observed but the value reported in Table 3.14 is based on the 99$^{th}$ percentile value (although these give the same result in this case).

**Table 3.13: Baseline Flexiporter results: not rounded, all loading scenarios**

| Standard | Unladen | Laden | Top laden |
|---|---|---|---|
| **LSSP** (m) | **6.539** | 6.531 | - |
| **TS** (m) | 0.372 | **0.377** | - |
| **FS** (m) | **0.337** | 0.333 | - |
| **DoM** (m) | 0.258 | **0.440** | - |
| **MoD** (m) | 0.529 | **0.644** | - |
| **STFD** (%) | **33** | 31 | - |
| **SRT** (*g*) | - | **0.422** | 0.439 |
| **RA** | - | 1.038 | **1.056** |
| **HSTO** (m) | - | **0.304** | 0.261 |
| **YDC** | - | 0.338 | **0.328** |
| **TASP** (m) | - | **2.846** | 2.822 |

**Table 3.14: Baseline Flexiporter results: rounded, worst-case loading scenario**

| Standard | Level 1 criterion | Result | PBS level achieved | Critical scenario |
|---|---|---|---|---|
| **LSSP** (m) | ≤ 7.4 | 6.6 | All | Unladen |
| **TS** (m) | ≤ 0.3 | 0.38 | **Level 4** | Laden |
| **FS** (m) | ≤ 0.7 | 0.4 | All | Unladen |
| **DoM** (m) | ≤ 0.2 | 0.44 | **None** | Laden |
| **MoD** (m) | ≤ 0.4 | 0.65 | **None** | Laden |
| **STFD** (%) | ≤ 80 | 33 | All | Unladen |
| **SRT** (*g*) | ≥ 0.35 | 0.42 | All | Laden |
| **RA** | ≤ 2.39 | 1.06 | All | Top laden |
| **HSTO** (m) | ≤ 0.6 | 0.4 | All | Laden |
| **YDC** | ≥ 0.15 | 0.32 | All | Top laden |
| **TASP** (m) | ≤ 2.9 | 2.9 | All | Laden |

### 3.5.4 Flexiporter observations and design considerations

Performance of the Flexiporter was shown to be sound for the dynamic performance standards due to factors such as roll-coupling and air suspension. However, the unsatisfactory performance in three of the manoeuvrability standards needs addressing.

Due to the 1 m front load projection, the frontal swing-out of the semitrailer exceeded that of the prime mover in two manners of interpretation: DoM and MoD. Not only does the semitrailer frontal swing-out influence DoM and MoD, but also the frontal swing-out of the prime mover itself. For a given semitrailer swing-out, a smaller prime mover swing-out increases the difference between the two and hence increases DoM and MoD.

The frontal swing of the Midlum was identified as being relatively low. Therefore, one approach to address the issues of DoM and MoD with minimal design modifications was to increase the frontal swing of the prime mover through the addition of a "nudge-bar".

A parametric study of the size and location of the nudge-bar was conducted to find an optimal solution which would meet MoD and DoM requirements whilst remaining within the frontal swing limit and within practical limits. A near-optimal solution was found which satisfied DoM, frontal swing and practical constraints, but could not fully satisfy the MoD constraint. Therefore, the semitrailer front load projection was reduced until MoD fell within the acceptable limit. A projection of 890 mm (2 375 mm ahead of the kingpin) was found to be suitable. The dimensions of the nudge-bar and allowable load projection are shown in Figure 3.31.

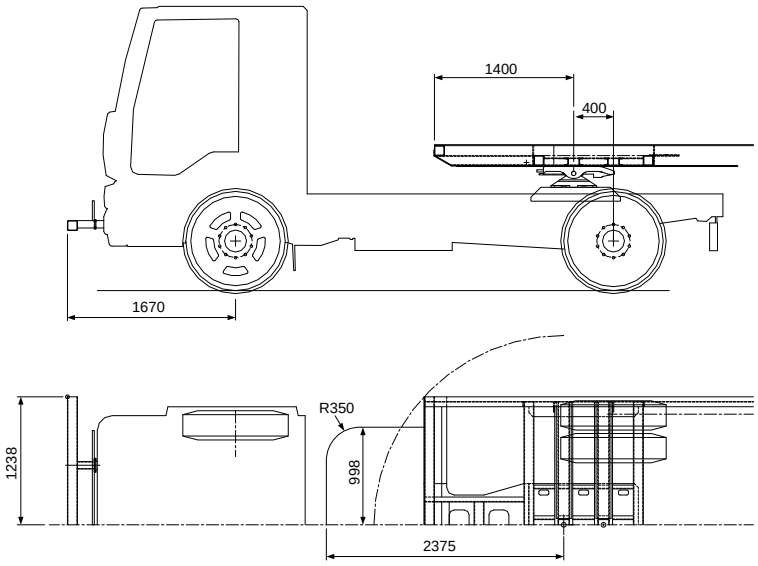


**Figure 3.31: Flexiporter modifications: nudge-bar and semitrailer load projection restriction (vehicle drawing courtesy of Unipower)**

In a practical sense, the nudge-bar provides the driver with a visible vehicle extremity which can be used to gauge obstacle clearance during low-speed turning. The swing-out behaviour of this extremity is representative of the swing-out behaviour of the semitrailer (within the acceptable tolerances prescribed by the NTC) such that there is a reduced chance of the semitrailer colliding with an obstacle that the driver has avoided through manoeuvring the prime mover. It provides the driver with increased surety regarding semitrailer swing-out and reduces the risk of unexpected semitrailer swing-out collisions.

The nudge-bar addressed two of the three standards of concern for the Flexiporter. An option for addressing the remaining tail swing concern was to taper the rear corner of the semitrailer in a manner similar to the Maxiporter. The tapered dimensions which would

satisfy the Level 1 tail swing criteria are shown in Figure 3.32. During the course of the assessment process, the lower platform was revised resulting in a 100 mm reduction in width – this lowered the tail swing of the lower platform to an acceptable limit. This tapering would therefore only apply to the upper loading platform.

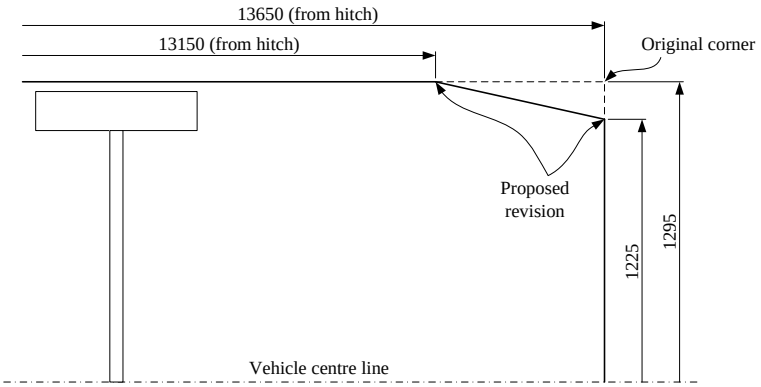


**Figure 3.32: Flexiporter semitrailer rear corner tapering dimensions to satisfy Level 1 tail swing criterion**

The proposed tapering could not be practically implemented on the Flexiporter because of the sliding linkage of the platform collapsing mechanism shown in Figure 3.33. During collapsing, the upright must slide rearward along a track that runs along the lateral extremity of the upper platform. When fully collapsed, the top corner of the upright is located at the rearmost point of the upper platform. The proposed tapering of the platform would obstruct the required motion of the upright and is hence not feasible without modification of the mechanism.

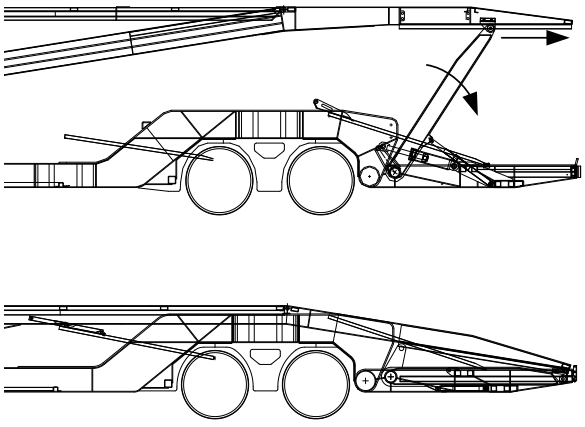

**Figure 3.33: Flexiporter semitrailer collapsing mechanism**

The other possible modification considered was to increase the wheelbase of the trailer but this was also not possible due to the collapsing mechanism. A large portion of the

Flexiporter's tail swing was shown to be due to the lateral overhang concept mentioned in the preceding section. This concept is expanded in the following section.

### 3.5.5 Tail swing reinterpretation

Tail swing was a concern for both vehicles; though the Flexiporter in particular highlighted an important point concerning the manner in which tail swing is measured. The wording of the NTC's vehicle assessment rules is, in some cases, unclear. A point in question is the definition of "entry tangent" relative to which tail swing is measured, and whether or not this definition refers to the tangent of the *prescribed path* or the tangent of the *trajectory of the reference point* being tracked. The ambiguity is perhaps exacerbated by the diagram provided for the purposes of illustration (reproduced in Figure 3.34). The problem lies in the fact that, in the example illustrated, the entry tangents of both the prescribed path and the reference point trajectory (outside rear corner) are collinear and so it is unclear to which of the paths the "Entry Path Tangent" label refers.

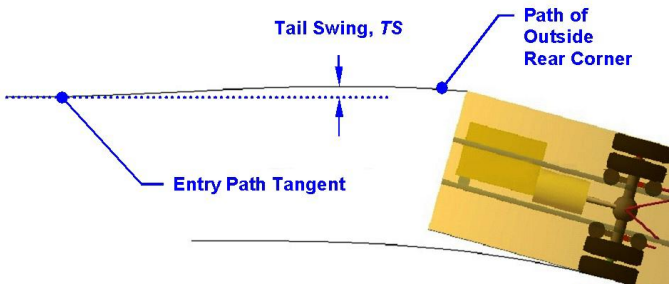


**Figure 3.34: Illustration of tail swing as provided by the NTC** [4]

Considering all sections of the document pertaining to the low-speed manoeuvrability standards relative to one another suggests that "entry tangent" and "exit tangent" refer to the tangents of the prescribed path itself – i.e. the path which the outer steer-tyre is made to follow. Hence, when the document prescribes that, "on the entry side of the turn, tail swing is the length of the longest line segment perpendicular to the low-speed turn entry tangent intersecting it and the path trajectory," it suggests that the datum from which tail swing is measured is in fact the entry tangent of the prescribed path. This is the interpretation that was utilised in this work.

A similar question can be raised for the case of frontal swing. However, in this instance the document leaves no room for misinterpretation. The NTC requires that frontal swing, "must be determined from the path trajectories of: (a) the outermost path scribed in the ground plane by the vertical projection of the furthest forward or outside point, or points, on the vehicle on the outside of the turn; and (b) the path scribed in the

ground plane of the outer most point on the outer tyre sidewall nearest to the ground, on the forward most outside steered-wheel." This clearer definition gives support to the interpretation utilised for tail swing.

Having established that tail swing is measured relative to the tangent of the prescribed path, an important implication of this definition can be deduced. The illustration in Figure 3.34 suggests that the width of the outside rear corner of the illustrated vehicle is equal to the width between extreme tyre walls on the steer axle. This is a likely scenario for large Australian trucks, especially the kind to be operated within a PBS scheme. In this case, the entry tangents of the prescribed path and of the motion path of the reference point are collinear as shown.

A problem arises when the steer-tyre track width is *not* the same as the maximum vehicle width, an example being maximum width trailers (i.e. 2.6 m in South Africa) being towed by narrow, light-duty prime movers. The Flexiporter is one such vehicle combination: the maximum width of the trailer is 2.600 m and the width between extreme steer-tyre walls is 2.277 m – a difference of 323 mm. This equates to 162 mm either side of the vehicle – the "lateral overhang". Applying the Australian definition of tail swing, the vehicle has a tail swing of 162 mm *before the prescribed manoeuvre has begun*. Due to its narrow steer axle track width, the vehicle has incurred a tail swing penalty of 162 mm and the effective PBS tail swing limit for the vehicle is 300 – 162 = 138 mm.

A narrower steer axle in no way increases the risk posed by the swing-out of the rear corner of a vehicle and it is only in the defined measurement of the standard that this predicament arises. Given a fixed maximum width limit (i.e. 2.6 m), the actual safety risk posed by this vehicle characteristic is how much the rear of the vehicle deviates *from its original path*. In fact, the NTC describes tail swing as being, "the maximum outward lateral displacement of the outer rearmost point on a vehicle unit," [4]. The term "displacement" suggests it should be a measure of the lateral movement of the corner from its original trajectory, not relative to the prescribed path.

Consider the two vehicles in Figure 3.35. Vehicles A and B are identical in every way, except that Vehicle A has a steer-tyre track width narrower than the maximum vehicle width, and Vehicle B has a steer-tyre track width equal to the maximum vehicle width. The vehicles are made to follow the *same* prescribed path of identical radius with respect to the outer steer-tyre wall. Vehicle A will give a higher tail swing measurement than Vehicle B due to the initial "penalty" as shown in the figure. The amount by which the tail has swung outward of its original path is the same in both cases (neglecting the effects due to small changes in path curvature for all tyres except the path-following tyre)

and yet the values for tail swing are different. The proposed tail swing measurement is indicated on the figure and is equal for both vehicles. This is a logical consequence as the vehicles are identical in every respect except steer axle dimensions. With such a revised tail swing interpretation, steer-tyre track width sensitivity is removed from the measurement of tail swing.

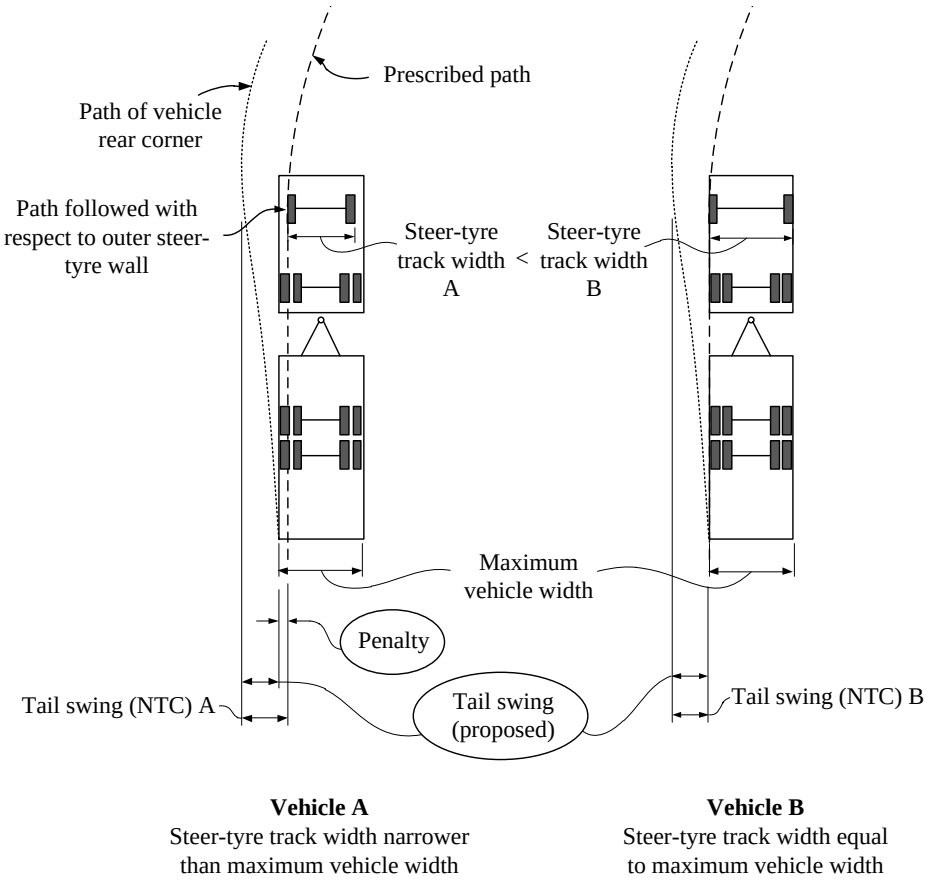


**Figure 3.35: Tail swing penalty incurred by vehicles with a narrow steer axle track width**

It was observed that affected industry members were willing to take drastic steps to gain compliance of their vehicles in the tail swing standard. Examples of proposed steps were: to fit spacers to each end of the steer axle (with associated negative impacts on bearing loads); to replace side-dish rims with centre-dish rims on the steer axle to increase track width (also with associated bearing load increases); to fit larger tyres to the vehicle than is standard (presenting clearance issues with the bodywork during steering); and to replace the truck or prime mover altogether with a larger, heavier-duty truck simply for the gain in track width.

The above measures are drastic (especially the fourth measure) and are not aligned with the ethos of the PBS initiative in South Africa. A vehicle with one or more of the above modifications could comply with the PBS criteria but would be less safe (due to

increased risk of bearing failure) or less efficient (due to a prime mover with specifications far in excess of the demand of the freight task).

Considering the above discussion, it was proposed that, in assessing South African vehicles for PBS approval, tail swing should be measured relative to the maximum width of the vehicle rather than relative to the prescribed path. The proposed method would more accurately reflect the safety risk posed and would mitigate the need for drastic measures being taken by industry to gain compliance. This proposal was accepted by the South African Smart Truck Review Panel, and the Flexiporter tail swing result could therefore be reduced by 162 mm. The vehicle hence meets the Level 1 tail swing requirement without modification to the trailer or its collapsing mechanism. Because the tapering of the Maxiporter trailer was implemented on manufactured vehicles before this decision was made, the tapering was retained. In any case, the lateral overhang adjustment for the Maxiporter would be insufficient to fully negate the need for tapering.

## 3.6 Revised Vehicle Assessments

In the preceding sections, various design modifications to the two vehicles were suggested. The modifications addressed all the relevant shortcomings and produced PBS Level 1-compliant vehicles. In this section, the PBS assessment results of the revised vehicles are presented. In summary, the modifications are:

- an increase in the Maxiporter trailer wheelbase from 9 m to 10 m,
- modification to the Maxiporter trailer rear corner geometry in accordance with Figure 3.20,
- the addition of a nudge-bar to the Flexiporter in accordance with Figure 3.31,
- a front load projection restriction of 890 mm (2 375 mm ahead of the kingpin) for the Flexiporter semitrailer, and
- the reinterpretation of the tail swing standard in accordance with the decision taken by the Smart Truck Review Panel.

### 3.6.1 Maxiporter

This section presents the PBS assessment results for the revised Maxiporter design with a 10 m trailer wheelbase and refined trailer rear corner geometry as per Figure 3.20. The final design of the vehicle is given in Appendix F.

Figure 3.36 shows the low-speed swept path of the revised vehicle which has increased from 6.7 m to 7.2 m (rounded from 7.187 m). The result is within the 7.4 m Level 1 limit. Tail swing (using the original interpretation of its measurement) is shown in Figure 3.37. The tail swing result is 0.30 m (rounded from 0.295 m). Frontal swing is shown in Figure 3.38, calculated to be 0.7 m (rounded from 0.629 m). The frontal swing decreased slightly over the original vehicle due to the change in axle load distributions. In all of the above cases, the laden scenario produced the worst-case results. Figure 3.39 shows STFD, calculated to be only slightly higher than before at 33.5% over the original 33.3%. This increase was due to the increased pitching moment of the prime mover as a result of increased hitch load. The rounded result is identical at 34%. The unladen condition gave rise to this worst-case result.

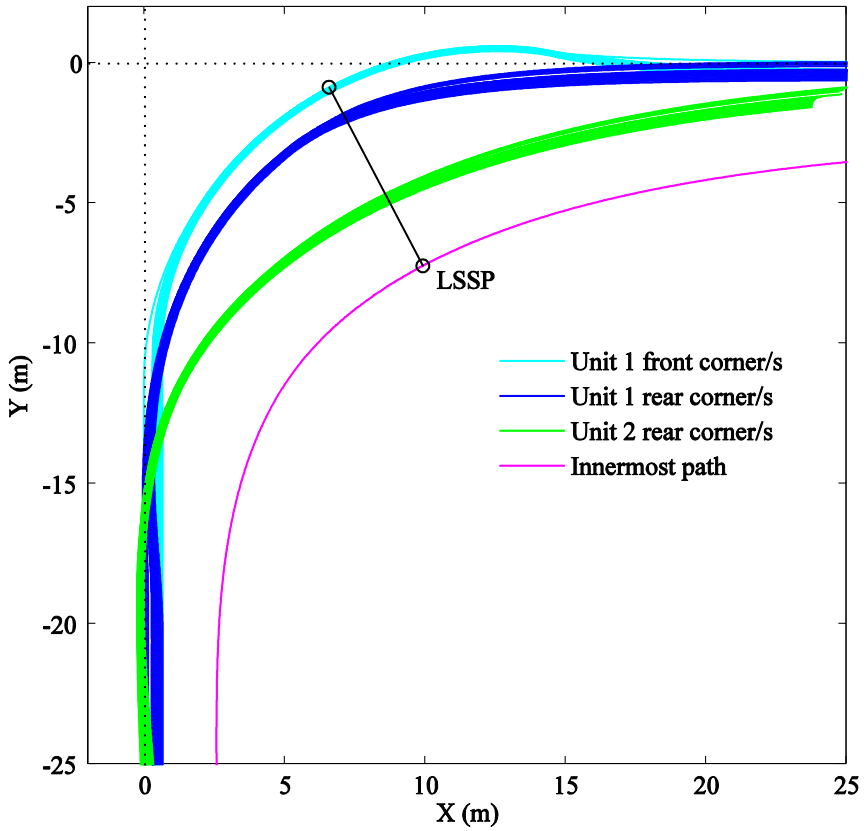


**Figure 3.36: Revised Maxiporter, LSSP, laden**

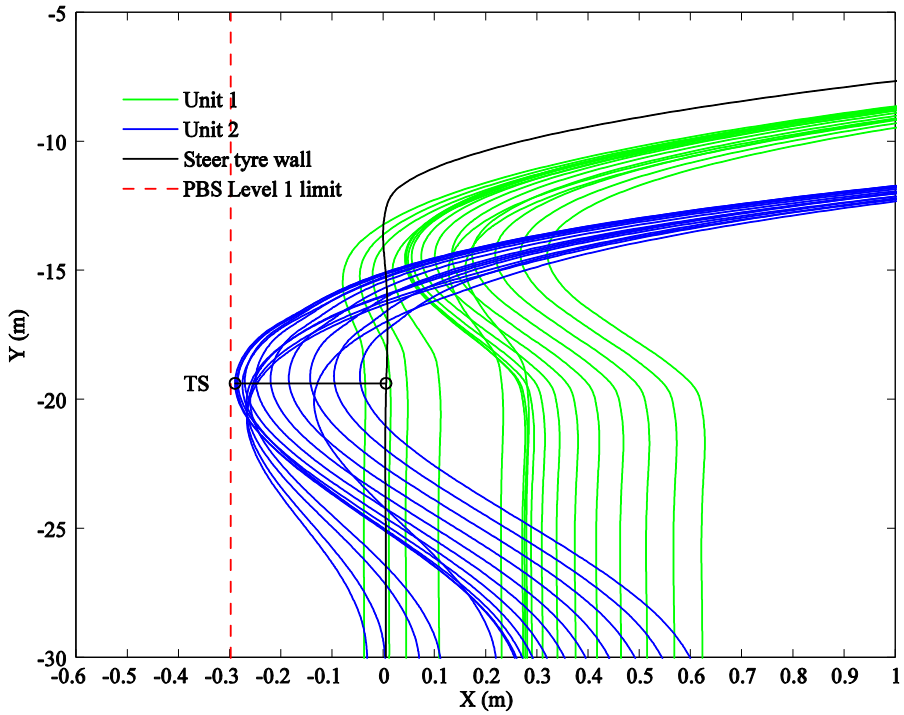


**Figure 3.37: Revised Maxiporter, TS, laden**

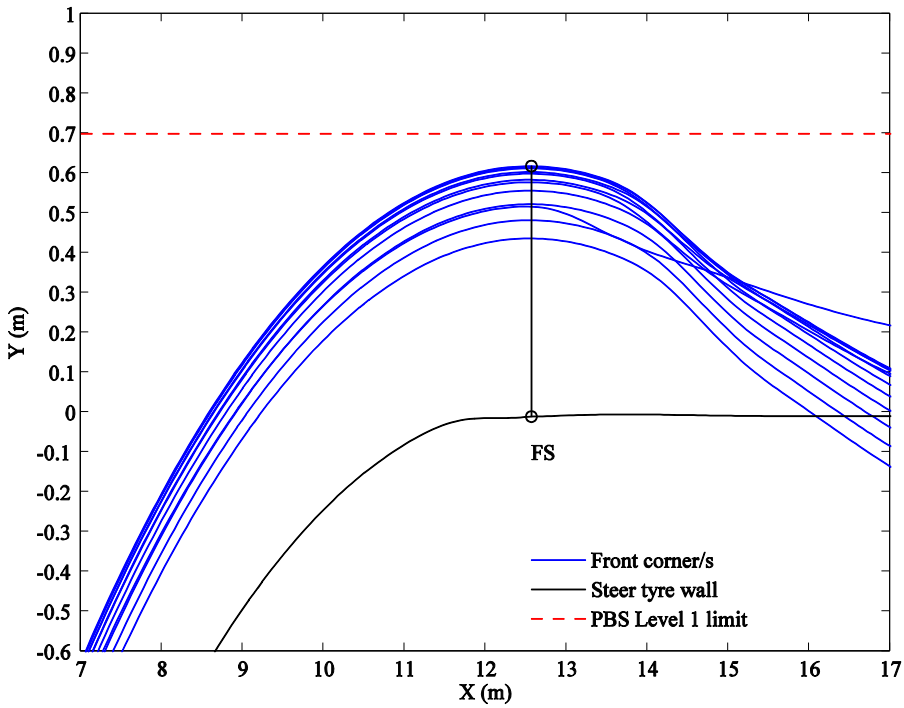


**Figure 3.38: Revised Maxiporter, FS, laden**

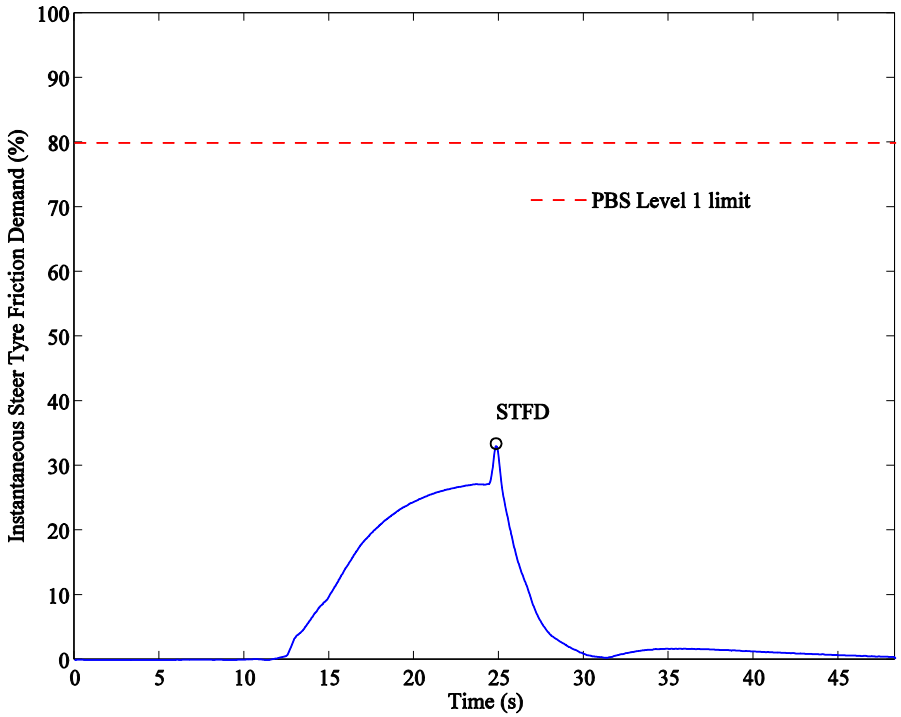


**Figure 3.39: Revised Maxiporter, STFD, unladen**

The results of the rollover simulation are shown in Figure 3.40. The static rollover threshold increased from 0.35·*g* to 0.38·*g* (rounded from 0.389·*g*) due to the increased hitch load as discussed in Section 3.5.2. Lash in the truck's suspension occurs at around 40 seconds or 0.30·*g* (slightly delayed compared to the baseline vehicle due to the increased axle loads). Due to the delayed truck rollover, the trailer in this case was able to enter into its suspension lash region at around 49 seconds or 0.35·*g*. Although not very clear in the figure, these effects are evident in the TruckSim® animations. The least favourable load condition was the fully laden scenario. This was different from the baseline vehicle for which the "top laden" scenario proved least favourable. The increased hitch load (due to the increased trailer wheelbase and the fact that the trailer is fully laden) has not only affected the overall SRT, but has had an effect on the critical load scenario of the truck as well. This suggests that there exists some critical combination of hitch load, sprung mass and sprung mass centre of gravity height for a given vehicle either side of which one load scenario is least favourable and another not. A quantitative parametric study of this assertion would highlight interesting aspects of this concept and is suggested for further work.

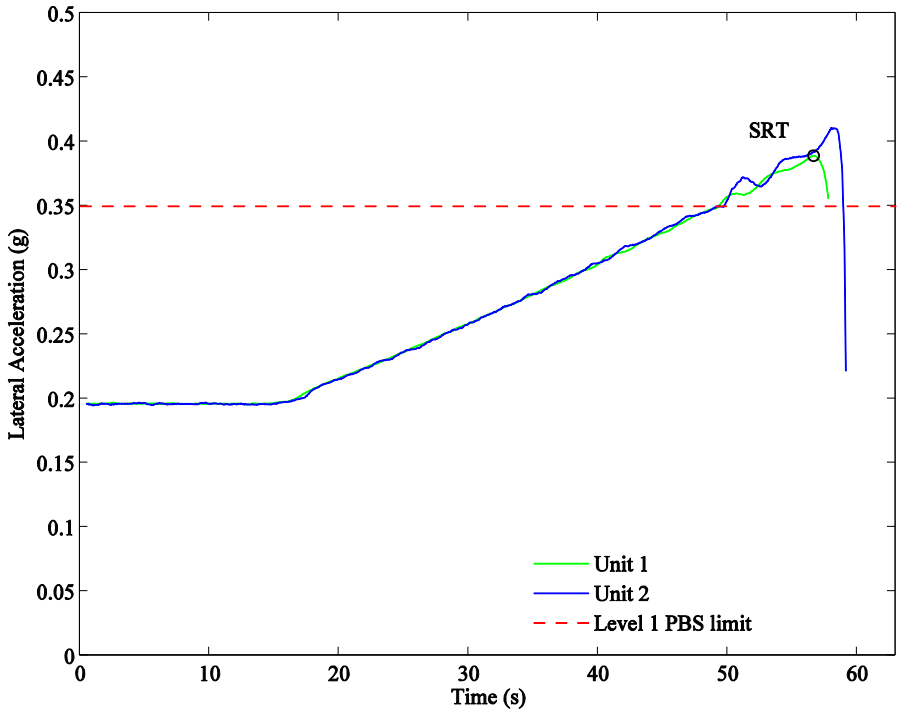


**Figure 3.40: Revised Maxiporter, SRT, laden**

Results for the single lane-change are given in Figure 3.41 and Figure 3.42. Rearward amplification has improved from 1.82 to 1.24 and high-speed transient offtracking improved from a non-compliant value of 0.7 m to a compliant value of 0.6 m (rounded from 0.529 m). These improvements were a direct result of the increased trailer wheelbase. Unlike the original design where the worst case scenario for both these standards was a fully laden trailer, the worst-case scenarios were "trailer top laden" and fully laden for rearward amplification and high-speed transient offtracking respectively.

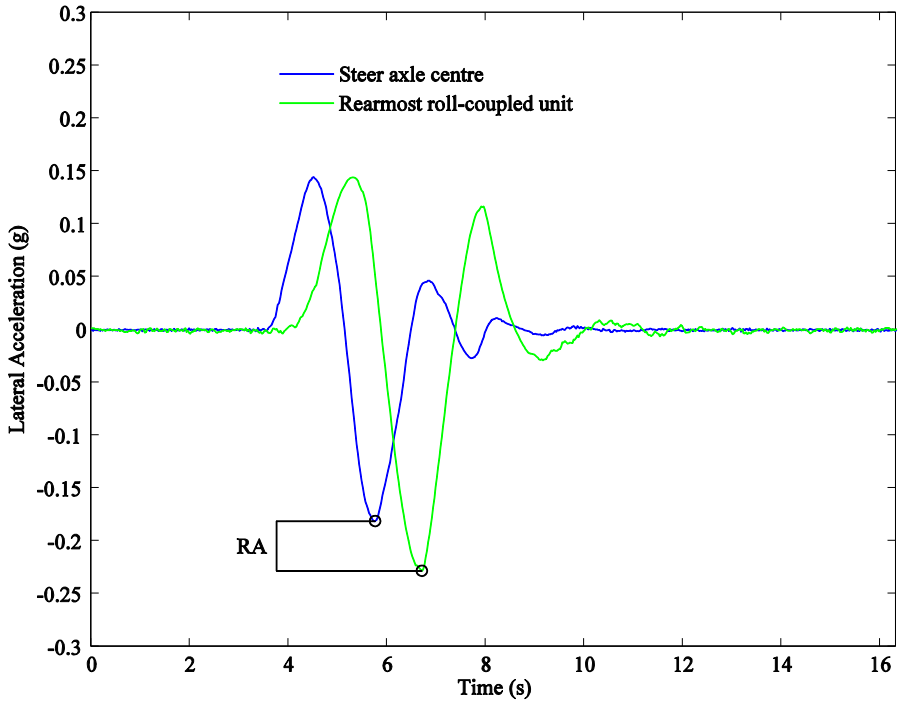


**Figure 3.41: Revised Maxiporter, RA, trailer top laden**

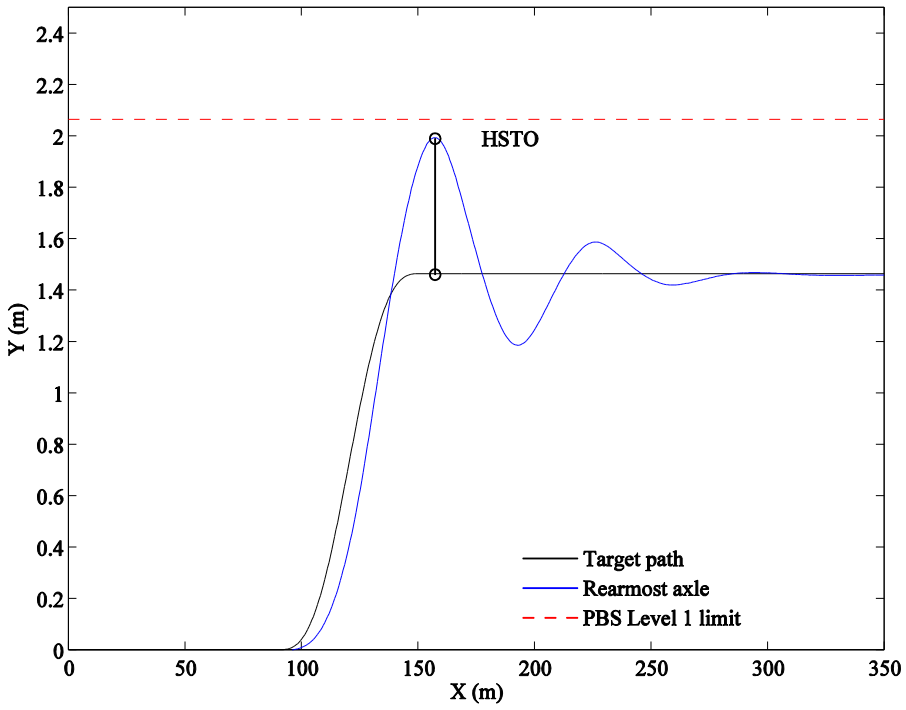


**Figure 3.42: Revised Maxiporter, HSTO, laden**

Yaw damping results are given in Figure 3.43. The result obtained was 0.29 (rounded from 0.299) for the "truck laden" condition. A significant improvement in yaw response of the vehicle is clear as a direct result of the increased trailer wheelbase.

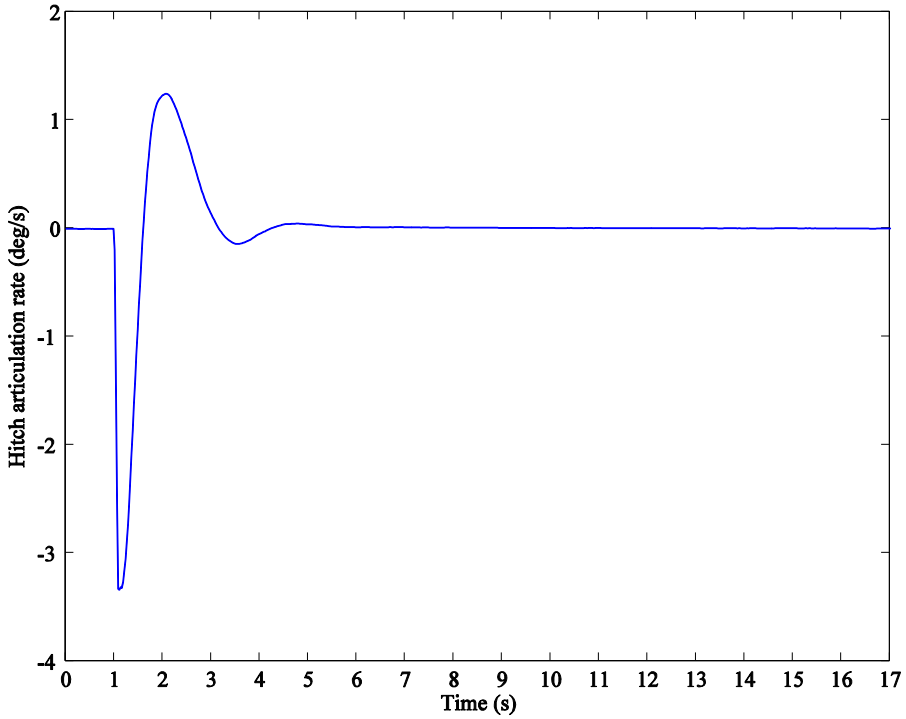


**Figure 3.43: Revised Maxiporter, YDC, truck laden**

The reason the "truck laden" scenario as opposed to the "top laden" scenario yielded the lowest yaw damping result was purely a consequence of calculation formalities. In the calculation of the amplitude ratio $\overline{A}, A_n$ must be at least 5% of the magnitude of $A_1$ (see Equation (3.5)). If this limit is reached before the sixth amplitude, only amplitudes up to and excluding the amplitude at which this criterion is first met must be considered. In the "truck laden" case, the amplitudes were 3.337, 1.247, and 0.142 °/s, where the third amplitude was less than 5% of the first. Therefore, only the first two amplitudes were used in the calculation. The load scenario that yielded the next lowest value of yaw damping was the "top laden" scenario with amplitudes 3.336, 1.447 and 0.290 °/s. These amplitudes clearly decayed at a slower rate than for the "truck laden" scenario suggesting poorer yaw damping response. Yet, because the third value was not within the 5% cut-off limit, it was included in the calculation giving a yaw damping coefficient of 0.381 which suggests improved yaw damping response. If only the first two magnitudes were used in this case, a yaw damping ratio of 0.25 (rounded from 0.257) would have been calculated – a poorer result than the "truck laden" scenario as should be the case. The calculation

method required for yaw damping is flawed in this respect and can lead to misleading results. Further investigation is suggested for future work.

Tracking ability on a straight path results are shown in Figure 3.44. The calculated result was 2.9 m (fully laden). The unrounded result was 2.873 m and the 99$^{th}$ percentile result was calculated to be 2.861 m, both of which were rounded to 2.9 m. This improvement over the original vehicle's TASP is due to the overall improvement in the stability of the vehicle as discussed in Section 3.5.2, and which is evident in the improved behaviour of the vehicle in the 200 m feed-out section of the manoeuvre.

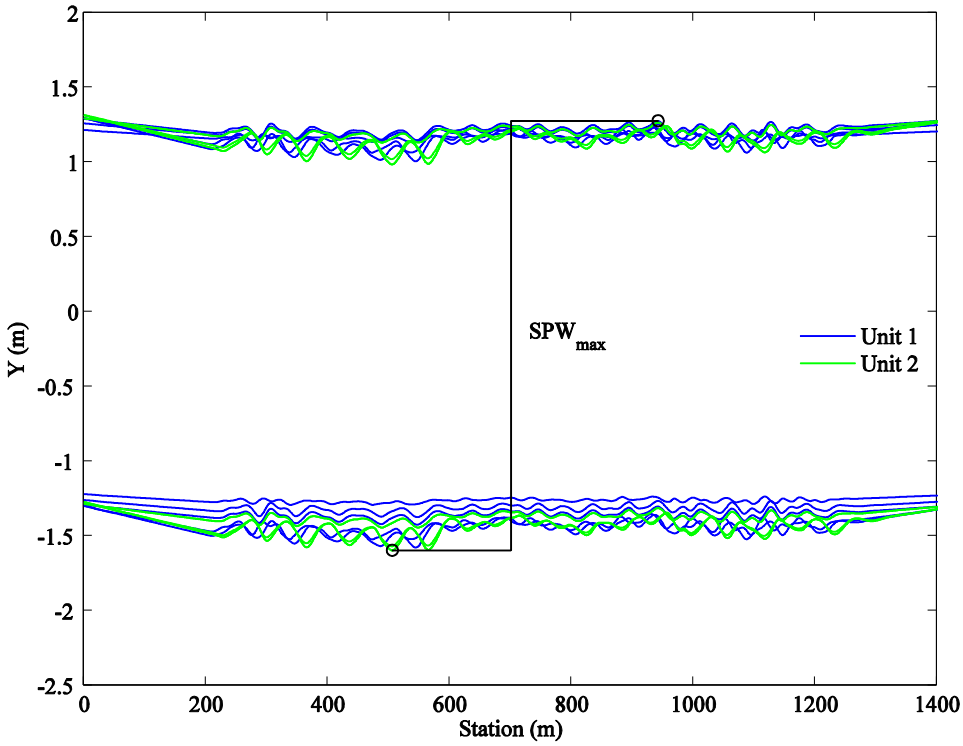


**Figure 3.44: Revised Maxiporter, TASP, laden**

A summary of the results of the PBS assessment for the revised Maxiporter design is given in Table 3.15. The vehicle was shown to meet all the safety criteria for Level 1 PBS approval. Performance was improved over the baseline vehicle in six of the nine standards at the expense of only low-speed swept path. The performance standards in which the vehicle exhibited the most significant improvements were tail swing, rearward amplification and yaw damping.

**Table 3.15: Revised Maxiporter results**

| Standard | Level 1 criterion | Baseline vehicle | Revised vehicle | PBS level achieved | Critical load scenario |
|---|---|---|---|---|---|
| **LSSP** (m) | ≤ 7.4 | 6.7 | 7.2 | All | Laden |
| **TS** (m) | ≤ 0.30 | **0.66** | 0.30 | All | Laden |
| **FS** (m) | ≤ 0.7 | 0.7 | 0.7 | All | Laden |
| **STFD** (%) | ≤ 80 | 34 | 34 | All | Unladen |
| **SRT** (*g*) | ≥ 0.35 | 0.35 | 0.38 | All | Laden |
| **RA** | ≤ 5.7·$SRT_{rrcu}$ | 1.82 | 1.27 | All | Trailer top laden |
| **HSTO** (m) | ≤ 0.6 | **0.7** | 0.6 | All | Laden |
| **YDC** | ≥ 0.15 | **0.09** | 0.29 | All | Truck laden |
| **TASP** (m) | ≤ 2.9 | **3.0** | 2.9 | All | Laden |

At the time of publication, a number of units of the revised Maxiporter had been built and commissioned, and are to be operated by Vehicle Delivery Services. A photograph of one such unit is shown in Figure 3.45, with the design modifications as per the findings and recommendations of this work.

**Figure 3.45: A Vehicle Delivery Services Volvo FM400+Maxiporter PBS car-carrier combination (10 m wheelbase trailer)**

## 3.6.2 Flexiporter

This section presents the PBS assessment results for the revised Flexiporter design with the addition of a nudge-bar to the truck-tractor, a reduction in the semitrailer front load projection, and incorporating the revised tail swing interpretation. The final design of the vehicle is given in Appendix F. As no significant changes to the inertial properties of the vehicle were incurred with the addition of a nudge-bar, there was no change to the dynamic performance of the vehicle. The modifications were assumed to be purely geometric and so the only performance standards affected were those pertaining to low-speed turning (excluding steer-tyre friction demand).

Figure 3.46 depicts the low-speed swept path which increased from 6.6 m to 6.9 m (rounded from 6.894 m). This increase was due to the increased prime mover frontal swing-out as a direct result of the nudge-bar. The unladen scenario yielded the least favourable results as a result of reduced axle loads.

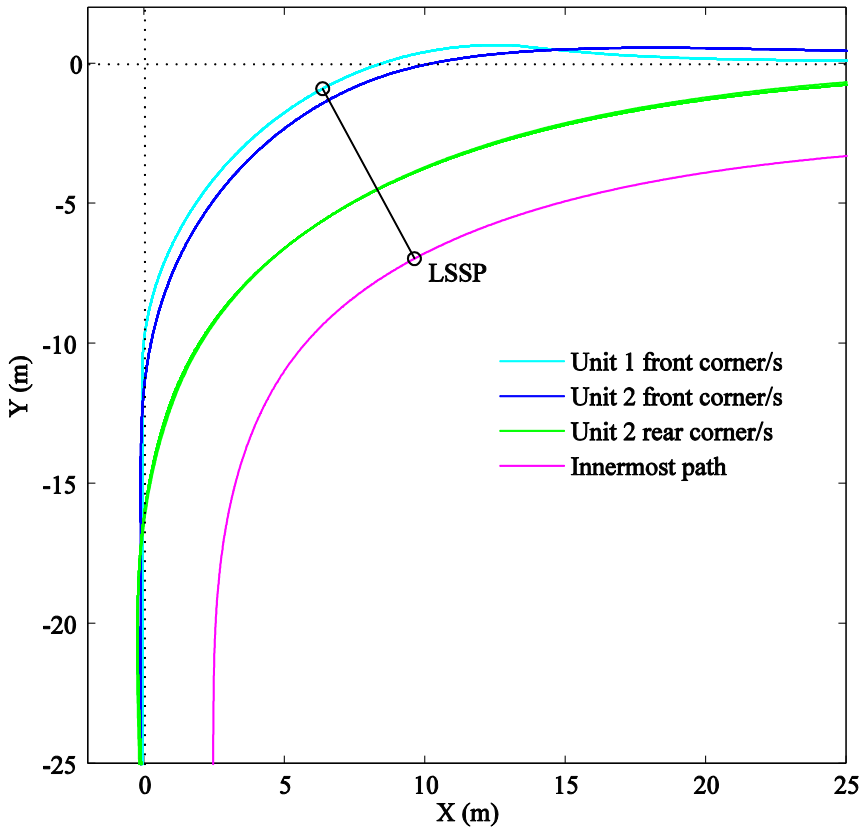


**Figure 3.46: Revised Flexiporter, LSSP, unladen**

Using the revised interpretation of tail swing, an adjustment of 0.162 m (the lateral overhang) was made to the Flexiporter's tail swing result, giving 0.377 m – 0.162 m = 0.215 m (the actual trajectories are unchanged). The least favourable loading scenario for tail swing was laden due to increased axle loads and the fact that the semitrailer and not the projecting load was the limiting case.

Frontal swing performance is depicted in Figure 3.47 for the worst-case unladen load condition. Frontal swing was optimised to the allowable limit to address the difference of maxima and maximum of difference results. The resulting value was calculated to be 0.7 m (rounded from 0.700 m). The unladen scenario was again least favourable due to axle load effects described previously. When the vehicle was laden, MoD and DoM were calculated to be 0.40 m and 0.02 m respectively (see Figure 3.48). MoD was optimised by limiting the front load projection to 890 mm.

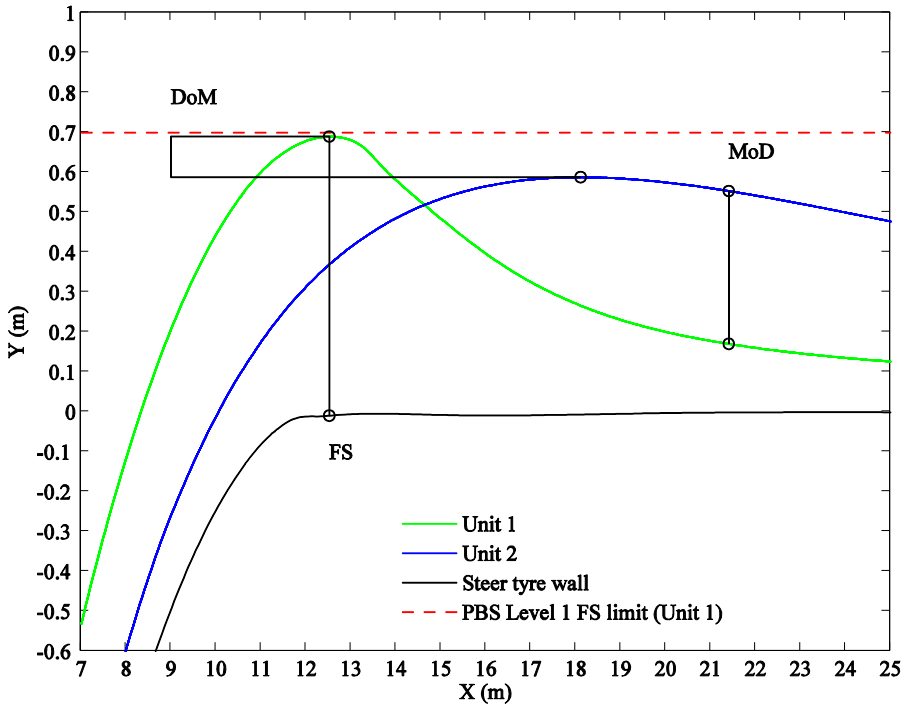


**Figure 3.47: Revised Flexiporter, FS, unladen**

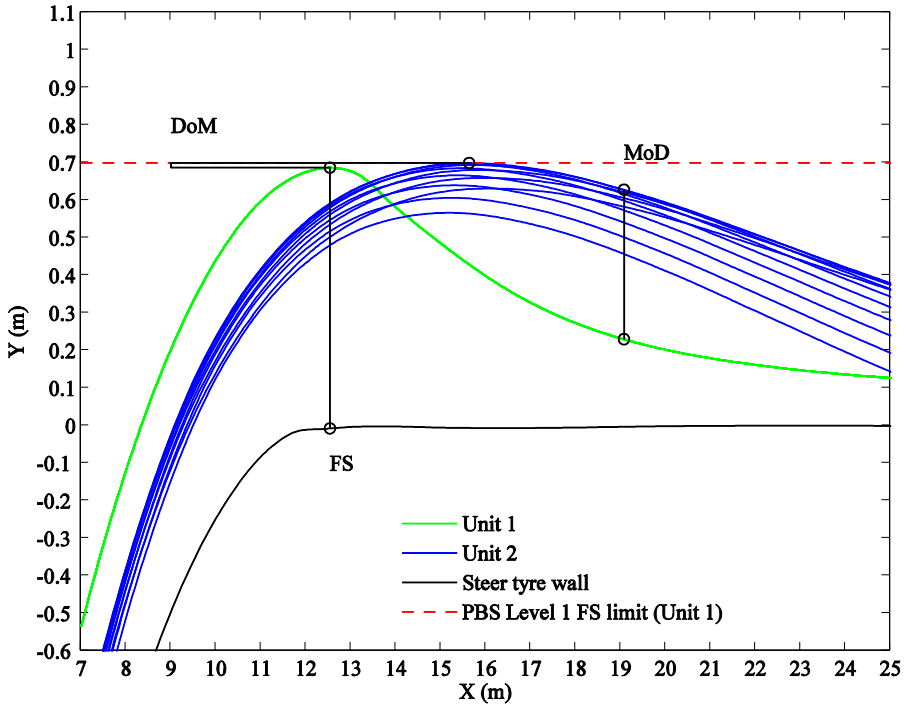


**Figure 3.48: Revised Flexiporter, DoM and MoD, laden**

A summary of the results of the revised Flexiporter assessment is given in Table 3.15. The vehicle passed all the safety criteria for Level 1 PBS approval with performance improvements in three of the nine standards at the expense of increases in low-speed swept path and frontal swing.

**Table 3.16: Revised Flexiporter results**

| Standard | Level 1 criterion | Baseline vehicle | Revised vehicle | PBS level achieved | Critical load scenario |
|---|---|---|---|---|---|
| **LSSP** (m) | ≤ 7.4 | 6.6 | 6.9 | All | Unladen |
| **TS** (m) | ≤ 0.3 | **0.38** | 0.22 | All | Laden |
| **FS** (m) | ≤ 0.7 | 0.4 | 0.7 | All | Unladen |
| **DoM** (m) | ≤ 0.2 | **0.45** | 0.02 | All | Laden |
| **MoD** (m) | ≤ 0.4 | **0.65** | 0.40 | All | Laden |
| **STFD** (%) | ≤ 80 | 33 | 33 | All | Unladen |
| **SRT** (*g*) | ≥ 0.35 | 0.42 | 0.42 | All | Laden |
| **RA** | $\leq 5.7 \cdot SRT_{rrcu}$ | 1.06 | 1.06 | All | Top laden |
| **HSTO** (m) | ≤ 0.6 | 0.4 | 0.4 | All | Laden |
| **YDC** | ≥ 0.15 | 0.32 | 0.32 | All | Top laden |
| **TASP** (m) | ≤ 2.9 | 2.9 | 2.9 | All | Laden |

## 3.7 Chapter Summary and Conclusions

The results of the detailed assessment of two Level 1 PBS car-carrier proposals were presented and discussed. The baseline vehicles were assessed and shown not to comply with certain performance standards. Specific aspects of each vehicle design were identified to be the primary causes of these non-compliances, and the vehicle designs were modified accordingly. The modified designs were assessed and shown to meet all the requirements for Level 1 road access.

The baseline Maxiporter truck and tag-trailer combination proposal exhibited very poor performance in the yaw damping and tail swing standards and also failed to meet the Level 1 requirements for tracking ability on a straight path and high-speed transient offtracking. The poor results in these standards were shown to be a direct result of the centre-axle configuration of the trailer. Increasing the trailer wheelbase from 9 m to 10 m yielded greatly improved performance in all these standards and resulted in Level 1 compliance in all standards except tail swing. The remaining excess tail swing was addressed by appropriately tapering the rear corners of the trailer.

The Flexiporter tractor and semitrailer combination proposal showed good performance in all the dynamic standards but failed to meet Level 1 criteria for the tail

swing, maximum of difference and difference of maxima standards. The poor performance in the MoD and DoM standards was shown to be a result of large semitrailer front overhang and load projection relative to the narrow dimensions of the truck-tractor. These shortcomings were addressed with the addition of a nudge-bar to the truck-tractor, a reduction in semitrailer front load projection, and a revised interpretation of tail swing measurement (now incorporated by the Smart Truck Review Panel).

Through the assessments, it was highlighted that the manner in which tail swing is determined according to the requirements of the NTC [4] is not representative of the safety risk being managed by the standard. Furthermore, the definition does not cater well for vehicle combinations with wide trailers and narrow prime movers. Such vehicles suffer a significant penalty in this regard that is not representative of any increased safety risk posed by these vehicles. It was proposed that the interpretation of the standard for the South African context address the above issue and hence close the gap between the definition and the actual safety risk being managed. This proposal was accepted by the Smart Truck Review Panel and tail swing is now measured relative to the maximum width of the vehicle and not relative to the prescribed path.

These PBS assessments are the first of their kind for car-carriers to be published and have highlighted a number of unique aspects of the vehicles. Payload variability was shown to have a significant effect on performance and identifying the least favourable load condition formed a critical aspect of the assessments. There is significant scope for further work on this topic in analytically predicting critical load scenarios for a given set of vehicle parameters. The assessments have shown how car-carrier safety may be improved through informed design decisions, whilst increasing productivity at the same time.

# Chapter 4

# Discussion and Conclusions

The structure of this dissertation is such that chapter-specific discussions and conclusions have, to a large extent, been included in the respective chapters. This chapter summarises these discussion points and discusses the all-encompassing observations and conclusions. The chapter is structured as follows:

1. Discussions pertaining specifically to the two main sections of this work – the low-speed turning model and the PBS assessments – are presented.
2. A discussion concerning the shortcomings of the Australian standards and factors specific to the South African context is presented.
3. The overall conclusions of this work are stated.
4. Recommendations for further work are suggested.

## 4.1 Discussion

### 4.1.1 Low-speed turning model

The low-speed turning model developed in Chapter 2 proved to be an accurate means of assessing the low-speed manoeuvrability of a range of vehicle combinations given only basic dimensions. The model is computationally very efficient and can determine the low-speed swept path, tail swing, frontal swing, difference of maxima and maximum of difference for a typical vehicle combination within a few seconds. The model is useful for preliminary proof-of-concept analyses for prospective PBS design proposals, and parametric studies of the low-speed manoeuvrability of a large sample of vehicle combinations (see for example Section 2.4). The model builds upon the work of others,

selecting and combining the advantages and remedying the disadvantages of previous work. The model was validated against more complex TruckSim® simulations and the results compared favourably with acceptable levels of error.

Through the development of the model, computational methods were developed to maximise the computational efficiency in calculating low-speed swept path and maximum of difference. These methods were shown to be effective without compromising accuracy and may prove useful for future studies. The "offset-adjustment" method for achieving steer-tyre path-following was shown to be effective, but there is room for improvement. Ideally, the model equations should be derived such that any reference point on the vehicle may be selected, relative to which the vehicle can follow the prescribed path.

The model could benefit from a number of additional improvements. Firstly, the formulation of the model equations is such that any prescribed path may be specified, no matter how complex. This is a very useful characteristic of the model. For this work, where only one particular prescribed path was required, the path was defined within the Matlab® m-file itself. For future work, the generification of the model such that any external input file (i.e. .txt or .xls) of suitably defined path coordinates may be selected and used in the model would prove useful.

The assumption that contributions of lateral hitch forces to low-speed turning behaviour are negligible is subject to further investigation. Morrison stated that the contributions observed in his work were small (up to a maximum of around 2%). Although overall errors for the Flexiporter were favourable (mostly within 1% for LSSP, FS and TS), those for the Maxiporter were slightly less favourable with the most notable being an absolute error of 156 mm for one case of LSSP. This equates to 2.6% and it is possible that a large portion of this error can be attributed to lateral hitch force effects. Including such effects in the model would require a more detailed method of incorporating tyre scrub effects (as opposed to the simple and computationally efficient "equivalent wheelbase" principle) and the addition of tyre properties to the required input data. For the anticipated application of the model, it was deemed suitable to forego some accuracy for the benefit of simplicity and computational efficiency.

The user-friendliness of inputting vehicle data could be improved, potentially benefitting from the capability of reading an external file with predefined vehicle data. Potentially, the model could be provided with the geometric constraints of a road intersection (along with the steering constraints of the prime-mover) and output a feasible

path for the driver to follow and determine whether the turn is possible or not (similar to the work of McGovern [29]).

Through the application of the model, the tail swing of the South African car-carrier fleet was identified as a significant concern, shown to be a result of the ineffectiveness of the National Road Traffic Regulations in limiting vehicle rear overhang. By comparison, the Australian rear overhang requirements are very strict and are the reason the NTC's tail swing criteria are seemingly so restrictive. The Australian tail swing limit of 0.30 m was shown to be a direct result of the 3.7 m rear overhang limit imposed by ADR 43/04 – a limit to which the South African fleet has not been constrained.

The model is under constant development within the CSIR and is being used in conjunction with TruckSim® as a preliminary PBS assessment tool. The afore-mentioned improvements may, in time, be incorporated into the model, enlarging its scope such that it may be applied to a variety of future research topics. In future, an assessment using the model may, along with bridge-loading and road wear analyses, form part of the encouraged application documentation for preliminary approval of South African PBS vehicles. It could also be combined with Dessein *et al.*'s optimisation model [16] to address the excluded standards of tail swing, frontal swing, difference of maxima and maximum of difference.

### 4.1.2 PBS assessments

The detailed PBS assessments of the Maxiporter and Flexiporter car-carrier vehicles are pivotal to this work and to the recently introduced car-carrier regulatory framework in South Africa. The motivation for these assessments was the decision made by the Abnormal Loads Technical Committee to discontinue the issuing of abnormal load permits to car-carriers due to concerns of rollover stability and over the definition of "indivisible load". Car-carriers operators are now required to gain RTMS and PBS approval before they are permitted to operate vehicles in excess of the height and length constraints of the National Road Traffic Regulations. Should they not gain approval, they will be restricted to operate within the full constraints of the NRTR and incur the subsequent productivity losses.

Due to uncertainty around the implications of the ALTC's decision and the associated time-frames, vehicle transport companies were initially reluctant to pursue the costly and time-consuming exercise of full PBS assessments required for approval. Also, the first organisation to participate in such an exercise would take on the risk of incurring the inevitable teething problems. Fortunately, Unipower (Natal), together with associated

transport operators, was willing to take on this risk and proposed the first two vehicle combinations for local PBS assessment. Fortunately again, the two proposed vehicle combinations consisted of two of the most typical car-carrier configurations in operation on South African roads today. Therefore, results of the assessments of these two vehicles gave a good indication of the general characteristics to be expected from similar proposals in future. Most notably, it is anticipated that longer trailer wheelbases will be required for car-carriers if the PBS criteria are to be met.

The most time-consuming aspect of the modelling process was obtaining vehicle and vehicle component data from relevant OEMs and suppliers. As this type of assessment is not common in South Africa, the necessary data were often not immediately available through local channels. Where data were unavailable, either generic data were sourced from the literature, appropriate calculations made, or the specific vehicle property excluded from the model. The use of generic data for certain vehicle parameters will always be necessary to some degree due to time constraints on important projects.

In some cases, where established empirical methods exist to determine certain vehicle properties, it is advisable to use such methods while taking note of their limitations. However in other cases, where no established methods exist, and one has to rely on first principles to derive a certain vehicle property, it may be best to ignore the contribution of that property altogether or to assume a generic or worst-case conservative value for it. Non-established methods may inaccurately model a vehicle property which could yield inaccurate results. Depending on the property in question and the methods used to estimate it, whether or not the estimate yields improved or diminished performance over the actual vehicle is uncertain. This uncertainty is to be avoided in such assessments and instead a conservative estimate should be used (even though it may be less accurate).

In the case of anti-roll bars, first principle methods *were* used to calculate roll stiffness and some OEM data were made available against which the method could be corroborated. In this case, the corroboration showed the method to be sound and it was hence deemed suitable for use (see Section C.2.3, Appendix C).

Conversely, first-principle methods were attempted for tandem load-sharing properties such as load transfer due to brake (or drive) torque and dynamic load transfer. These properties are not readily available and are typically obtainable only through experiment. Although first principles were able to derive seemingly acceptable predictions, these were subject to significant uncertainties and assumptions, and the use of generic properties was deemed preferable. In addition, varying values of load transfer due to brake torque resulted in unwanted effects on the SRT simulation of the Maxiporter. As the drive torque

increased on the drive axle at the higher speed region of the manoeuvre, significant load transfer was observed between the drive and tag axles having unpredictable effects on the SRT observed. In reality, vehicles can attain rollover speed without any drive torque (i.e. due to gravity), and so this effect should not be a deciding factor in the SRT result. In this instance, a tilt-table test would more accurately model rollover behaviour as it is in no way affected by load transfer due to brake torque. In this particular case, it was deemed more suitable to ignore the effect of load transfer due to brake torque rather than use unverified methods to estimate it. Similarly for dynamic load transfer, it was deemed more suitable to assume "perfect load-sharing" than to attempt to estimate the property via first principles. Deviation from the ideal "perfect load-sharing" is generally minimal [37] with subsequent minor effects on the respective PBS manoeuvres.

This raises the point of the accuracy of the data provided by OEMs. In some cases it may be that data provided are subject to a number of assumptions and estimations which are not necessarily made clear in the issuing of the data. The source of the data may be far removed from the point from which it is ultimately obtained, and it is hence difficult to establish the estimates used or assumptions made. At this stage of the South African PBS initiative, it can only be assumed that the data provided are correct, and conservative judgement must be applied in the interpretation of results. The NTC requires that where the values of vehicle properties are uncertain, a sensitivity analysis should be conducted, establishing the relative effects of varying the parameter in question on the overall vehicle performance. If done accurately, such an exercise would require an immense effort. In some cases it may be justifiable, but at this stage of the PBS demonstration project it was deemed unnecessary. Conservative judgement was used throughout.

TruckSim® proved to be a powerful and relatively simple heavy vehicle simulation tool. The fact that TruckSim® is a tailored heavy vehicle dynamics software package removes many of the lower-level modelling requirements typical of a generic multibody simulation package. From a PBS point-of-view however, a significant drawback of the software is its path-following behaviour, both in its lack of accuracy and stability at low-speed and its inability to follow a prescribed path with respect to a point other than a set datum point on the prime mover. Addressing this would be of significant benefit to future PBS work. Also, lateral acceleration of the steer axle should be included as an available variable for the accurate calculation of rearward amplification.

Turning attention to the particular PBS assessments conducted for this work, a number of informative observations were made. One of the initial concerns pertaining to car-carriers was their rollover stability as a result of their 4.6 m allowable laden height. Through this work it was shown that static rollover threshold performance of these

vehicles, although borderline in one case, is of less significance than other safety-related performance areas. The short trailer wheelbase of the truck and tag-trailer configuration was shown to be far more of a concern, resulting in poor performance in standards such as yaw damping, tracking ability on a straight path and tail swing. Increasing the trailer wheelbase improved performance in these standards at the expense of some additional road usage during low-speed turning. It is likely that future PBS car-carrier designs will have to incur similar modifications in order to meet the required PBS criteria.

It is interesting that a feasibility study of increased-capacity car-carriers in North America (conducted by UMTRI [46]) recommended that wheelbases should be made as small as possible. The study considered only low-speed offtracking performance. Full PBS considerations reveal short wheelbase trailers to yield poor dynamic performance, and so in a PBS context this recommendation would be subject to limitations. This highlights how a PBS framework can lead to better-informed design decisions.

An important aspect of this work observed in the context of car-carriers, but possibly of consequence to other vehicles, is that of payload variability. For most of the performance standards assessed, the NTC requires that the "least favourable load condition" be considered. For vehicles with a highly variable payload, identifying this condition is not a trivial matter. For most of the standards, both a high payload mass and a high payload centre of gravity have detrimental effects on vehicle performance. However, the combined effect of these properties is subject to other vehicle parameters and the distribution of the payload. Therefore, it cannot easily be ascertained whether a higher mass payload with lower centre of gravity is less favourable than a lower mass payload with a higher centre of gravity. A limited number of representative worst-case loading scenarios were considered in this work, though these scenarios were not exhaustive.

The concept of payload variability can have indirect implications such as was observed in the case of the Maxiporter. In the case of truck and tag-trailer combinations where a portion of the trailer load is supported by the truck, a payload variation on the trailer will yield a variation in axle loads on the preceding vehicle unit. Such axle load variations can result in variations in the rollover threshold of that vehicle unit, and possibly in other performance areas as well. This highlights an aspect of vehicles such as car-carriers that must be given consideration in PBS-type assessments: the "least favourable load condition" for the truck in a truck and tag-trailer combination could be the result of a particular trailer payload scenario. There is extensive scope for further study in this area either through parametric or analytical investigations.

The payload was in all cases assumed rigid, with a centre of gravity location fixed relative to the sprung mass of the unladen vehicle. However, due to the manner in which passenger vehicles are typically fastened to car-carriers – by securing the vehicles by the wheels (see for example the South African National Standard: Load Securement on Vehicles, Part 7 Abnormal Loads [47]) – the vehicles are free to roll on their suspension. The effect of this would be similar to the effect of liquid slosh in tankers though perhaps not as significant, and certainly in a different frequency domain. Significant work has been conducted on the effects of liquid slosh on heavy vehicle performance (see for example [48–51]) and similar (though less extensive) work has been conducted on the shifting load problem of hanging meat and livestock (see [50], [52], [53]). However, no published research exists for similar work on car-carriers.

The effect of passenger vehicle roll-compliance is two-fold. Firstly, the lateral displacement of the centre of gravity due to steady lateral acceleration would have an adverse effect on rollover-sensitive manoeuvres (for example, static rollover threshold and rearward amplification). Secondly, the frequency response of the passenger vehicles could have dynamic implications for dynamic manoeuvres such as rearward amplification and yaw damping. The frequency domain in which typical passenger vehicles can be excited would need to be determined and compared with the typical exciting frequencies of the PBS manoeuvres as has been done for studies of liquid slosh. If these frequencies are similar, resonance effects could be observed. There is extensive scope for these effects to be analysed. Initially, roll-plane models incorporating the roll motion and compliance of passenger vehicles could be developed to predict whether or not these effects would be of concern to car-carriers. At a later stage, the effects of vehicle roll-compliance could be modelled in TruckSim® (with the use of Simulink®) for a number of realistic scenarios and the results compared with analytical predictions.

The inherent variability of car-carriers presents a difficulty in applying a PBS framework to the regulation of these vehicles. One of the benefits of a prescriptive approach to heavy vehicle regulation is that it is simple and universally applicable to an extensive heavy vehicle fleet. The current situation in which the car-carrier industry has found itself is unique, and presents a unique problem: regulating a fleet of hundreds of highly variable vehicles through a framework designed for specialist-application vehicle fleets of a few dozen vehicles at most. Ideally therefore, the long-reaching goals of the PBS initiative for car-carriers in South Africa should be to establish, through an accumulation of PBS assessment results for a number of vehicle designs, a prescriptive framework within which car-carriers must operate. A set of special prescriptive constraints, founded on thorough PBS assessment data, could apply to South African car-

carriers in a manner similar to the practice in South Australia [22]. For example, for a given configuration – consider the case of a truck and tag-trailer combination – there could be a minimum trailer wheelbase imposed to address dynamic performance concerns. Similarly, there may be rear overhang limits enforced to address tail swing concerns. In fact, limiting rear overhang (to 3.7 m for example) will indirectly result in longer-wheelbase trailers. The establishment of such a prescriptive framework would require the collection of sufficient representative data and is suggested for future work.

### 4.1.3 Shortcomings of incorporating the Australian standards directly into a South African context

For the purposes of the PBS demonstration project in South Africa, the Australian PBS framework was adopted almost in its entirety. The methods of assessment and the cut-off criteria were incorporated without modification. The reasons for adopting the NTC's PBS framework are justified – it is arguably the most established framework of its kind in the world and based on a vast expanse of expertise. However, through the course of this work some aspects of the Australian standards – as applied within a South African context – were shown to exhibit certain undesirable attributes.

A point in question was discussed in depth in Chapter 3: the datum relative to which tail swing is measured. The NTC's rules require that tail swing is measured relative to the entry tangent of the prescribed path. Because the prescribed path is followed with respect to the outer steer-tyre wall, this definition introduces a sensitivity of tail swing to the steer axle track width and steer-tyre width. A variation in either of these two parameters is not representative of a variation in the safety risk posed by the swing-out behaviour of the vehicle. A revised interpretation of the measurement was proposed in which the datum is moved to the maximum vehicle width. The standard would hence govern the displacement of the vehicle rear corner beyond its original trajectory – with no sensitivity to steer axle dimensions or steer-tyre size. The proposal was accepted by the Smart Truck Review Panel the revised interpretation has been henceforth adopted for future PBS assessments in South Africa. This is a positive step towards fine-tuning the Australian standards to develop a robust South African PBS scheme.

Another point on which contentions may arise is the inherent differences in country-specific legislation. Tail swing, frontal swing, low-speed swept path and tracking ability on a straight path are all sensitive to vehicle width. The legal maximum vehicle width for Australian vehicles is 2.5 m and the criteria for these standards are based on vehicles of such width. In South Africa, where vehicle widths of up to 2.6 m are permitted, the

existing criteria are more constraining than they would be for Australian vehicles of similar configuration. The difference in rear overhang legislation and the implications for tail swing are another case in question, and this has been discussed in depth. For the sustainability of the South African PBS scheme, the criteria should be tailored to South African conditions while maintaining sound judgement in respect of safety risk and differences in road design standards.

The tracking ability on a straight path standard presents a point of contention in relation to vehicle length. The Level 1 Australian criterion is based upon a maximum vehicle length of 20 m. In South Africa, Level 1 PBS vehicles are permitted to have unladen lengths of up to 22 m (the maximum length allowed by the NRTR). So again the Australian standard is more constraining on South African vehicles than on Australian vehicles. Tracking ability on a straight path is hence effected by differences in both vehicle length and vehicle width between Australia and South Africa, and may as a result prove to be a particularly constrictive standard for South African PBS vehicles in future.

The 20 m overall length constraint presents a similar case for the low-speed swept path standard. A case in question is the B-double or "interlink" configuration. Of the vehicle types that could be classified under Level 1 road access, B-doubles have the poorest low-speed swept path behaviour [19]. It is unlikely therefore that a 22 m B-double (which would be considered for Level 1 road access in South Africa by virtue of its length) would meet the Australian Level 1 LSSP criteria. However, 22 m B-doubles are commonplace in South Africa and are allowed within normal South African legislation. One of the purposes of PBS is to increase productivity over that of legal vehicles, not to further constrain it. This is hence an area warranting further attention.

Returning to the subject of tracking ability on a straight path, two more shortcomings of the Australian standards were identified through this work: ambiguity concerning the definition of the road profile, and inconsistencies pertaining to the choice of reference points. The NTC provides assessors with a defined road profile in the form of left and right wheel path elevation profiles. This gives no indication of the road profile within or without these paths – road area that will certainly be covered by the wheels of offtracking trailing units. Individual assessors make varying assumptions regarding this road area which could lead to inconsistent results. A more suitable description for numerical modelling purposes therefore would be a three-dimensional description of the surface in a manner that is reproducible in all modern vehicle simulation software packages.

The choice of reference point is critical to the tracking ability result recorded for a vehicle. The higher the reference point above ground, the larger the lateral displacement

of the reference point due to roll motion, and the higher the subsequent tracking ability on a straight path. The NTC requires that where there is a choice of more than one point along a given vertical plane, the lowest point is to be selected. In the case of the car-carriers assessed in this work, their side profiles were such that the selected reference points are low relative to the ground and hence significant roll effects were excluded. An identical vehicle with identical roll motion and tracking behaviour but a side profile such that the top of the vehicle represents its widest point, would incur a large lateral displacement due to roll motion and could yield exaggerated results relative to the first vehicle. The choice of reference point should be made more consistent to avoid such discrepancies between similar vehicles.

The single lane-change test also presents some matters for consideration. Firstly, it is required that the test be conducted at 88 km/h whereas South African PBS vehicles are restricted to 80 km/h. It could be worth studying the effect of this difference but for now at least, it is conservative to use the higher speed. Secondly, the purpose of the high-speed transient offtracking standard is to address the lateral displacement of vehicles/trailers into adjacent lanes during an evasive manoeuvre. However, the variable of concern to the measurement is the lateral displacement of the rearmost axle, which is not necessarily representative of actual vehicle deviation. One vehicle, identical to another but with a longer rear overhang, would deviate further into an adjacent lane than the other during the manoeuvre depending on the yaw angle of the vehicle at the point of maximum deviation. The lateral deviation recorded at the rearmost axle however, would be identical. It is therefore suggested that vehicle reference points be used in this standard similar to those required for the low-speed turning standards or tracking ability on a straight path (subject to the amendments discussed above).

Lastly, the equations for determining yaw damping ratio were shown to exhibit certain undesirable properties due to the 5% cut-off requirement. The inclusion or exclusion of additional terms in the calculation of amplitude ratio will have an effect on the subsequent yaw damping ratio calculated. Such a difference can be misleading in favouring one vehicle's response over another.

Addressing all of the above points would lead to a more robust, less-restrictive South African PBS scheme that is more attractive to potential participants. Although the Australian scheme is founded on sound knowledge and many years of experience, it is inevitable that its direct application in a country with significantly different existing heavy vehicle legislation would result in complications. More participants in the South African scheme will yield more PBS assessment results and increased local expertise,

making a stronger case for the above recommendations and ensuring the overall sustainability and success of the PBS scheme in South Africa.

## 4.2 Conclusions

1. A geometric low-speed turning model for articulated and combination vehicles was developed. The model is loosely based upon the tractrix concept and utilises a discretised geometric solution method. The model was implemented in the form of a Matlab® m-file and exhibits the following characteristics:

    a. The model was verified against equivalent TruckSim® models for two common car-carrier configurations and a number of variations of each (fourteen in total). An average relative error of 2.0% was obtained. Some of the error was attributable to inherent inaccuracies in the TruckSim® simulations. The model is theoretically compatible with any vehicle combination consisting of any number of vehicle units.

    b. The model is able to calculate low-speed swept path, tail swing, frontal swing, difference of maxima and maximum of difference.

    c. The model is compatible with the steer-tyre path-following requirement of the NTC through the use of a suitable "offset-adjustment" technique. The model uses the NTC ninety-degree turn manoeuvre by default but is compatible with any arbitrarily complex motion path.

    d. The tyre scrub effect of non-steering tandem and tridem axle groups was incorporated through the application of Winkler *et al.*'s equivalent wheelbase principle. The model can theoretically incorporate the effects of non-steering axle groups of any number of axles.

2. The model was successfully used to benchmark the tail swing performance of the existing South African car-carrier fleet. Compliance with the Level 1 criterion of 0.30 m was shown to be about 20% due to the large rear overhangs of the vehicles. Such rear overhangs are allowable within the confines of the South African National Road Traffic Regulations, which were shown to theoretically permit rear overhangs of up to 7 m and tail swing of up to 1.25 m. In comparison, Australian regulations impose a strict 3.7 m constraint on vehicle rear overhang, which was shown to effectively constrain tail swing of Australian vehicles to 0.30 m.

3. Two proposed PBS Level 1 car-carrier combinations – one truck and tag-trailer and one tractor and semitrailer combination – were assessed in accordance with the Australian PBS scheme. The vehicles were found to exhibit a number of shortcomings in respect of PBS compliance: the truck and tag-trailer combination exhibited non-compliant performance in the tail swing, high-speed transient offtracking, tracking ability on a straight path and yaw damping standards; and the tractor and semitrailer combination in the tail swing, difference of maxima and maximum of difference standards.
4. The shortcomings of the proposed vehicles were addressed through a number of design modifications. An increase of one metre to the trailer wheelbase of the truck and tag-trailer combination along with a minor refinement of the trailer rear corner geometry addressed all the relevant shortcomings. The addition of a "nudge-bar" to the prime mover, a reduction in semitrailer front load projection, and a revision to the interpretation of the tail swing standard addressed the shortcomings of the tractor and semitrailer combination. The revised tail swing interpretation better reflects the safety risk concerned with the standard and has been formally adopted by the Smart Truck Review Panel.

## 4.3 Recommendations for Further Work

1. A number of improvements to the geometric low-speed turning model are suggested, including:
    a. an option to expand the equivalent wheelbase principle to include dual tyre effects and lateral hitch forces (though this would require tyre data),
    b. deriving the principle equations of the model such that the vehicle can follow a prescribed path with respect to any reference point, and
    c. developing a utility for incorporating actively steered axles or axle groups.
2. The implications of an additional 100 mm in permissible maximum vehicle width (2.6 m in South Africa compared to 2.5 m in Australia) on low-speed swept path, frontal swing, tail swing and tracking ability on a straight path should be quantified. The findings should be used to justify revisions to these standards for the South African PBS scheme. A similar study should evaluate the implications of the Level 1 maximum length difference (22 m in South Africa and 20 m in Australia) on the affected performance standards. The geometric low-speed turning model would be a useful in respect of the low-speed standards.

3. The high-speed transient offtracking standard should be revised to assess the actual lateral deviation of the vehicle into adjacent lanes and not only the lateral deviation of the rearmost axle. The use of vehicle reference points similar to those used for tracking ability on a straight path or tail swing is recommended.
4. The effect of an 8 km/h speed reduction on rearward amplification and high-speed transient offtracking should be investigated to assess the implications of South Africa's 80 km/h speed limit for PBS vehicles.
5. The yaw damping ratio calculations should be revised to remove unrepresentative sensitivities to the number of amplitudes used in the calculation.
6. The requirements for reference point selection in the tracking ability on a straight path should be reconsidered such that roll motion contributions are consistently included or excluded for all vehicles.
7. An in-depth analysis of each of the Australian performance standards should be conducted to identify any additional shortcomings, especially in applying them in a South African context. The shortcomings should be addressed through appropriate modification of definitions, descriptions, interpretations, compliance criteria or through the removal or addition of complete standards.
8. The steady-state and dynamic effects of the roll-compliance of passenger vehicles (constituting the payload of car-carriers) should be investigated through suitable analytical/parametric studies.
9. An extensive study of the effects of payload variations on the performance of car-carriers (and perhaps other vehicles) should be conducted to identify the relationships that determine the least favourable load condition for a given vehicle or vehicle combination.
10. An extensive PBS-based parametric study of various car-carrier configurations should be conducted to establish a prescriptive framework within which future car-carriers could be operated.
11. Limitations concerning the loading of vehicles on the upper platform of a car-carrier when the lower platform is empty should be enforced, giving cognisance to the practical implications of such a restriction. Requirement 12.1.1 of South Australia's "Code of Practice for Car Carriers" is as a good example of this [22].
12. If possible, and with the support of participating manufacturers and operators, full scale tests of one or both of the car-carriers should be conducted to give additional insight into their behaviour and the modelling process.

# References


[1] DoT, *National Road Traffic Act No. 93 of 1996 (as updated up to the National Road Traffic Amendment Act, No. 20 of 2003 and Government Gazzette 25541, 2003)*. National Department of Transport, Republic of South Africa, 2003.

[2] *TRH11: Draft guidelines for granting of exemption permits for the conveyance of abnormal loads and for other events on public roads*, 7th ed. Committee of State Road Authorities, Republic of South Africa, 2000.

[3] *TRH11: Dimensional and mass limitations and other requirements for abnormal load vehicles*, 8th ed. Department of Transport, Republic of South Africa, 2010.

[4] NTC, "Performance based standards scheme – The standards and vehicle assessment rules," National Transport Commission, Melbourne, 2008.

[5] J. Bosman, "Traffic loading characteristics of South African heavy vehicles," in *8th International Symposium on Heavy Vehicle Weights and Dimensions*, 2004.

[6] P. Perkins, J. Fedderke, and J. Luiz, "An analysis of economic infrastructure investment in South Africa," *South African Journal of Economics*, vol. 73, no. 2, pp. 211–228, 2005.

[7] P. A. Nordengen, "A new era of overloading control in South Africa," in *5th International Symposium on Heavy Vehicle Weights and Dimensions*, 1998, pp. 34–50.

[8] P. A. Nordengen, J. M. Schnell, and M. C. Hellens, "An overload control strategy for the province of Kwazulu-Natal, South Africa," in *6th International Symposium on Heavy Vehicle Weights and Dimensions*, 2000, pp. 435–446.

[9] P. A. Nordengen, H. Prem, and L. Mai, "An initiative to introduce a performance-based standards (PBS) approach for heavy vehicle design and operations in South

Africa," in *10th International Symposium on Heavy Vehicle Transport Technologies*, 2008, pp. 61–70.

[10] D. Rolland, R. A. Pearson, and J. P. Edgar, "Performance-based standards – Recent developments in Australia," in *9th International Symposium on Heavy Vehicle Weights and Dimensions*, 2006.

[11] P. A. Nordengen, H. Prem, and P. Lyne, "Performance-based standards (PBS) vehicles for transport in the agricultural sector," in *Proceedings of the South African Sugar Technologists' Association*, 2008, pp. 445 – 453.

[12] NTC, "Performance based standards scheme: Network classification guidelines," National Transport Commission, Melbourne, 2007.

[13] W. vdM Steyn, P. A. Nordengen, M. Roux, I. Sallie, and S. Kekwick, "National overload control strategy (CR-2002/67): National Department of Transport Republic of South Africa," CSIR Transportek, Pretoria, 2004.

[14] P. A. Nordengen and F. Oberholtzer, "A self regulation initiative in heavy vehicle transport to address road safety, accelerated road deterioration and transport productivity in South Africa," in *9th International Symposium on Heavy Vehicle Weights and Dimensions*, 2006.

[15] CSIR, "Smart truck programme: Rules for the development and operation of smart trucks as part of the performance-based standards research," National Department of Transport, Republic of South Africa, Pretoria, 2010.

[16] T. Dessein, F. Kienhöfer, and P. A. Nordengen, "A South African performance based standards (PBS) vehicle to transport steel pipes," in *11th International Symposium on Heavy Vehicle Transport Technologies*, 2010.

[17] T. Dessein and F. Kienhöfer, "PBS analysis: RBM side-tipping BAB-quad road train," University of the Witwatersrand, Johannesburg, 2011.

[18] R. L. Thorogood, "Performance based analysis of current South African semi trailer and B-double trailer designs," University of Kwazulu-Natal, 2009.

[19] NRTC, "Performance characteristics of the Australian heavy vehicle fleet," National Road Transport Commission, Melbourne, 2002.

[20] DoIT, *Australian Design Rule 43/04: Vehicle configuration and dimensions*, 3rd ed. Department of Infrastructure and Transport, Australia, 2007.

[21] G. Y. Agbegha, R. H. Ballou, and K. Mathur, "Optimising auto-carrier loading," *Transportation Science*, vol. 32, no. 2, pp. 174–188, 1998.

[22] DoTEI, "MR 379 06/11: Code of practice for car carriers." Department for Transport, Energy and Infrastructure, Government of South Australia, 2011.

[23] RTA, "Vehicle standards information sheet No. 5: Vehicle dimension limits," Roads and Traffic Authority of New South Wales, 1998.

[24] DoLP, "V13 Vehicle dimensional limits (Including Load)." Department of Lands and Planning, Northern Territory Government, Australia, 2011.

[25] NRTC, "Performance-based standards, Phase A – Standards and measures, Regulatory impact statement," National Road Transport Commission, Melbourne, 2003.

[26] N. Tarameroa and J. J. de Pont, "Characterising pavement surface damage caused by tyre scuffing forces," TERNZ Ltd., Auckland, New Zealand, 2008.

[27] Y. Wang and J. A. Linnett, "Vehicle kinematics and its application to highway design," *Journal of Transportation Engineering*, vol. 121, no. 1, 1995.

[28] T. W. Erkert, J. Sessions, and R. D. Layton, "A method for determining offtracking of multiple unit vehicle combinations," *Journal of Forest Engineering*, vol. 1, no. 1, pp. 9–16, 1989.

[29] J. McGovern, "Turning an articulated truck on a spreadsheet," *Level 3, Dublin Institute of Technology*, no. 1, 2003.

[30] W. R. B. Morrison, "A swept path model which includes tyre mechanics," in *Proceedings of the 6th Conference of the Australian Road Research Board*, 1972, pp. 149–182.

[31] C. B. Winkler and J. Aurell, "Analysis and testing of the steady-state turning of multiaxle trucks," in *5th International Symposium on Heavy Vehicle Weights and Dimensions*, 1998, pp. 135–161.

[32] T. D. Gillespie, *Fundamentals of Vehicle Dynamics*, 1st ed. Society of Automotive Engineers, 1992.

[33] A. Colepeper, "(Personal communication)," 23 August, 2011.

[34] P. S. Fancher, R. D. Ervin, C. B. Winkler, and T. D. Gillespie, "A factbook of the mechanical properties of the components for single-unit and articulated heavy trucks (UMTRI-86-12)," University of Michigan Transportation Research Institute, Ann Arbor, Michigan, UMTRI-86-12, 1986.

[35] C. B. Winkler, S. Bogard, and S. Karamihas, "Parameter measurement of a highway tractor and semitrailer (UMTRI-95-47)," University of Michigan Transportation Research Institute, Ann Arbor, Michigan, 1995.

[36] C. B. Winkler, "Inertial properties of commercial vehicles: Descriptive parameters used in analyzing the braking and handling of heavy trucks (UMTRI-83-17)," University of Michigan Transportation Research Institute, Ann Arbor, Michigan, 1983.

[37] C. B. Winkler and T. D. Gillespie, "The mechanics of heavy duty trucks and truck combinations – Course notes." University of Michigan Transportation Research Institute, Ann Arbor, Michigan, 2011.

[38] T. T. Fu and D. Cebon, "Analysis of a truck suspension database," *International Journal of Heavy Vehicle Systems*, vol. 9, no. 4, pp. 281–297, 2002.

[39] P. S. Fancher, "Measurements of the longitudinal and lateral traction properties of truck tires (UM-HSRI-81-19-3)," University of Michigan Transportation Research Institute, Ann Arbor, Michigan, 1981.

[40] NRTC, "Comparison of modelling systems for performance-based assessments of heavy vehicles," National Road Transport Commission, Melbourne, 2001.

[41] G. J. Heydinger, R. A. Bixel, W. R. Garrott, M. Pyne, J. G. Howe, and D. A. Guenther, "Measured vehicle inertial parameters – NHTSA's data through November 1998," *SAE Progress in Technology*, vol. 101, pp. 531–554, 2004.

[42] “1998 Ford Expedition SUV.” [Online]. Available: http://carblueprints.info/eng/view/ford/ford-expedition-1998. [Accessed: 07-Dec-2011].

[43] “1998 Ford Expedition specifications.” [Online]. Available: http://beta.vehix.com/research-cars/1998/ford/expedition/xlt/119-wb-xlt/specifications. [Accessed: 07-Dec-2011].

[44] J. J. de Pont, “The development of pro-forma over-dimension vehicle parameters,” TERNZ Ltd., Auckland, New Zealand, 2010.

[45] *ISO14791: Road vehicles - Heavy commercial vehicle combinations and articulated buses – Lateral stability test methods*. Geneva: International Organization for Standardization, 2000.

[46] Z. Bareket and P. S. Fancher, “Increased capacity automobile transporter – Feasibility study and road-handling analysis (UMTRI-2000-32),” University of Michigan Transportation Research Institute, Ann Arbor, Michigan, 2000.

[47] *SANS10187-7:2006: Load securement on vehicles. Part 7: Abnormal loads*. Standards South Africa, 2006.

[48] C. B. Winkler and R. D. Ervin, “Rollover of heavy commercial vehicles (UMTRI-99-19),” University of Michigan Transportation Research Institute, Ann Arbor, Michigan, 1999.

[49] R. D. Ervin, M. Barnes, and A. Wolfe, “Liquid cargo shifting and the stability of cargo tank trucks,” University of Michigan Transportation Research Institute, Ann Arbor, Michigan, 1985.

[50] J. J. de Pont, “Stability effects of sloshing liquids and hanging meat,” TERNZ Ltd., 2004.

[51] S. Sankar, S. Rakheja, R. Ranganathan, and R. N. Sabounghi, “On the stability of heavy articulated liquid tank vehicles,” in *2nd International Symposium on Heavy Vehicle Weights and Dimensions*, 1989.

[52] C. B. Winkler, “Rollover of heavy commercial vehicles,” *UMTRI Research Review*, vol. 31, no. 4, 2000.

[53] D. A. Fittanto, R. L. Ruhl, and M. G. Strauss, “Dynamics and roll stability of a loaded Class 8 tractor-livestock semi-trailer: An EDVDS application (HVE-WP-2010-1),” Engineering Dynamics Corporation, 2000.

[54] NASA, “Man-systems integration standards (NASA-STD-3000),” National Aeronautics and Space Administration, Washington, DC, 1995.

[55] E. Alptekin and M. Canakci, “Determination of the density and the viscosities of biodiesel-diesel fuel blends,” *Renewable Energy*, vol. 33, no. 12, pp. 2623–2630, Dec. 2008.

[56] R. C. Juvinall and K. M. Marshek, *Fundamentals of Machine Component Design*, 4th ed. John Wiley & Sons, 2006.

[57] R. C. Hibbeler, *Mechanics of Materials*, 6th ed. Prentice Hall, 2005.

[58] *Michelin Truck Tire Data Book*, 13th ed. Michelin North America, 2011.

[59] O. Franzese, H. Knee, and N. Wood, “U02: Heavy truck rollover characterization (Phase A) Final report,” National Transportation Research Center, Inc., Knoxville, Tennessee, 2008.

[60] O. Franzese, H. Knee, and T. LaClair, “U19: Heavy truck rollover characterization (Phase B) Final report,” National Transportation Research Center, Inc., Knoxville, Tennessee, 2009.

[61] T. LaClair, H. Knee, and O. Franzese, “U24: Heavy truck rollover characterization (Phase C),” National Transportation Research Center, Inc., Knoxville, Tennessee, 2010.

[62] D. J. M. Sampson, “Active roll control of articulated heavy vehicles,” University of Cambridge, 2000.

[63] E. Dahlberg, “Parameter sensitivity of the dynamic roll over threshold,” in *7th International Symposium on Heavy Vehicle Weights and Dimensions*, 2002, pp. 51–62.

[64] S. Surial, “Development of a knowledge-based system for heavy vehicle legality and stability,” Concordia University, 1992.

[65] M. O. Arant, “Assessing the effect of chassis torsional stiffness on the accuracy of heavy vehicle understeer and rollover modelling,” Clemson University, 2010.

[66] C. B. Winkler, “Experimental determination of the rollover threshold of four tractor-semitrailer combination vehicles (UMTRI-87-31),” University of Michigan Transportation Research Institute, Ann Arbor, Michigan, 1987.

# Appendix A

# Supplementary Data

## A.1 Low-Speed Turning Model: Validation

The results of the low-speed turning model validation (Section 2.3) are given in Table A.1 and Table A.2 for Vehicles 1 and 2 respectively.

**Table A.1: Vehicle 1 validation results**

| | | Original | Dual tyres | WB + 1 m | WB – 1 m | Unladen | | |
|---|---|---|---|---|---|---|---|---|
| | | | | | | 3 axles | 2 axles | 1 axle |
| **Scenario:** | | **1** | **2** | **3** | **4** | **5** | **6** | **7** |
| **Geom. Model (m)** | **LSSP** | 6.659 | 6.659 | 7.179 | 6.161 | 6.659 | 6.615 | 6.589 |
| | **TS (truck)** | 0.221 | 0.221 | 0.221 | 0.221 | 0.221 | 0.221 | 0.221 |
| | **TS (trailer)** | 0.586 | 0.586 | 0.338 | 0.931 | 0.586 | 0.612 | 0.628 |
| | **FS** | 0.545 | 0.545 | 0.545 | 0.545 | 0.545 | 0.545 | 0.545 |
| **TruckSim (m)** | **LSSP** | 6.569 | 6.531 | 7.111 | 6.006 | 6.613 | 6.593 | 6.594 |
| | **TS (truck)** | 0.213 | 0.214 | 0.212 | 0.216 | 0.211 | 0.210 | 0.209 |
| | **TS (trailer)** | 0.573 | 0.575 | 0.332 | 0.906 | 0.579 | 0.608 | 0.624 |
| | **FS** | 0.542 | 0.537 | 0.537 | 0.540 | 0.553 | 0.557 | 0.561 |
| TruckSim max. offset (m): | | 0.014 | –0.012 | 0.011 | 0.018 | 0.024 | 0.029 | 0.032 |

**Table A.2: Vehicle 2 validation results**

| | | Original | Dual tyres | WB + 1 m | WB – 1 m | Unladen | | |
|---|---|---|---|---|---|---|---|---|
| | | | | | | 2 axles | 1 axle | 3 axles |
| **Scenario:** | | **1** | **2** | **3** | **4** | **5** | **6** | **7** |
| **Geom. Model (m)** | **LSSP** | 6.702 | 6.702 | 7.236 | 6.187 | 6.702 | 6.677 | 6.744 |
| | **TS** | 0.372 | 0.372 | 0.242 | 0.593 | 0.372 | 0.380 | 0.359 |
| | **FS** | 0.475 | 0.475 | 0.475 | 0.475 | 0.475 | 0.475 | 0.475 |
| | **DoM** | 0.226 | 0.226 | 0.266 | 0.179 | 0.226 | 0.224 | 0.229 |
| | **MoD** | 0.539 | 0.539 | 0.588 | 0.484 | 0.539 | 0.537 | 0.543 |
| **TruckSim (m)** | **LSSP** | 6.680 | 6.683 | 7.217 | 6.160 | 6.689 | 6.669 | 6.718 |
| | **TS** | 0.378 | 0.374 | 0.248 | 0.597 | 0.373 | 0.384 | 0.359 |
| | **FS** | 0.475 | 0.474 | 0.474 | 0.474 | 0.479 | 0.481 | 0.476 |
| | **DoM** | 0.239 | 0.245 | 0.279 | 0.194 | 0.232 | 0.220 | 0.250 |
| | **MoD** | 0.554 | 0.560 | 0.602 | 0.501 | 0.552 | 0.539 | 0.572 |
| TruckSim offset (m): | | 0.008 | –0.009 | –0.009 | 0.010 | 0.010 | 0.012 | –0.011 |

## A.2 Low-Speed Turning Model: Application

The dimensions of the car-carriers used in the tail swing assessment of the existing South African fleet (Section 2.4.1) are given in Table A.3 and Table A.4 for the tractor and semitrailer, and truck and trailer combinations respectively. Front overhang is measured forward of the steer axle or kingpin (whichever is applicable), rear overhang is measured rearward of the geometric centre of the rearmost axle group, and load projections are measured in excess of these overhangs. Dimensions taken as constant for all vehicles were: a steer-tyre track width (between extreme tyre walls) of 2.480 m, a vehicle width of 2.6 m and a load projection width of 1.8 m.

The vehicle dimensions used for the study of tail swing within the National Road Traffic Regulations (Section 2.4.2) are given in Table A.5.

**Table A.3: South African car-carrier dimensions, tractor-semitrailer configurations**

| Vehicle: | "A" | "B" | "C" |
|---|---|---|---|
| Prime mover | | | |
| Front overhang (m) | 1.440 | 1.440 | 1.440 |
| Wheelbase (m) | 4.650 | 3.900 | 3.600 |
| Number of rear axles (m) | 1 | 1 | 1 |
| Hitch location (m) | 3.650 | 3.300 | 2.700 |
| Semitrailer | | | |
| Front overhang (m) | 1.911 | 1.400 | 1.050 |
| Front load projections (m) | 0.430 | 0.500 | 0.955 |
| Wheelbase (m) | 9.000 | 9.600 | 9.750 |
| Number of axles (m) | 1 | 2 | 2 |
| Axle spacing (m) | N/A | 1.350 | 1.300 |
| Rear overhang (m) | 4.400 | 4.160 | 4.555 |
| Rear load projection (m) | 0.500 | 0.500 | 0 |

**Table A.4: South African car-carrier dimensions, truck-trailer configurations**

| Vehicle: | "X" | "Y" | "Z" |
|---|---|---|---|
| Truck | | | |
| Front overhang (m) | 1.440 | 1.440 | 1.360 |
| Front load projection (m) | 0.500 | 0 | 0.800 |
| Wheelbase (m) | 5.775 | 6.075 | 4.080 |
| Number of rear axles (m) | 2 | 2 | 2 |
| Axle spacing (m) | 1.350 | 1.350 | 1.365 |
| Rear overhang (m) | 4.137 | 4.005 | 2.697 |
| Rear load projection (m) | 0.241 | 0.350 | 0.077 |
| Hitch location (m) | 7.405 | 7.600 | 5.742 |
| Trailer | | | |
| Wheelbase (m) | 9.200 | 7.440 | 9.000 |
| Number of axles (m) | 2 | 2 | 3 |
| Axle spacing (m) | 1.360 | 1.310 | 1.360 |
| Rear overhang (m) | 3.940 | 4.820 | 5.900 |
| Rear load projection (m) | 1.000 | 0.690 | 0.500 |

**Table A.5: Legal vehicle assessment, vehicle parameters**

| Vehicle type | Vehicle Parameters | |
|---|---|---|
| **Rigid truck** | Drive axles: | Three, 1.35 m axle spacing |
| | Wheelbase: | Varied from 3.5 to 6 m (maximum of 8.5 m permitted) |
| | Rear overhang: | 60%·Wheelbase (varies accordingly with wheelbase) |
| | Notes: | Maximum length of 12.5 m not exceeded |
| **Truck-trailer** | Truck: | Drive axles: one |
| | | Wheelbase: varied from 3.5 to 6 m |
| | | Hitch location: 1 m behind drive axle (fixed) |
| | Axles: | Three, 1.35 m axle spacing |
| | Drawbar length: | Varied from 0 to 2 m |
| | Length: | 11.3 m (maximum permitted) (fixed) |
| | Rear overhang: | 5.65 m (maximum permitted) (fixed) |
| | Wheelbase: | 11.3 - 5.65 - 1.35 + drawbar length = 4.3 to 6.3 m |
| | Notes: | Maximum total combination length of 22 m not exceeded |
| **Tractor-semitrailer** | Tractor: | Drive axles: one |
| | | Wheelbase: varied from 3.5 to 4.5 m (typical values) |
| | | Hitch location: 1 m forward of drive axle (fixed) |
| | Axles: | Three, 1.35 m axle spacing |
| | Wheelbase: | Varied between 4 and 8 m (up to 10 m permitted) |
| | Rear overhang: | 60%·wheelbase (varies accordingly with wheelbase) |
| | Notes: | Maximum articulated vehicle length of 18.5 m not exceeded |

# Appendix B

# Implementing the Low-Speed Turning Model in Matlab®

Matlab® is well-suited to the manipulation of large matrices of numbers and is hence well-suited for the implementation of the geometric model. A brief overview of some aspects of the Matlab® model such as input data structure and input data manipulation are discussed in this section.

The model was implemented in the form of an m-file. To initiate the model, the m-file must be in the current working directory and the function must be called by entering the following into the command window:

```
[SPW_max,TS,FS_1,DoM,MoD] = GeoLSSP()
```

The m-file will execute and the first dialog box will appear requesting input data. The first set of information requested is *T*, the steer-tyre track width, *N*, the number of vehicle units in the vehicle combination, the incremental step size, and whether or not results should be plotted. The default step size is 5 mm.

For each vehicle unit in the vehicle combination being assessed, a total of eleven additional parameters need to be specified. Most of these parameters have been introduced in one form or another, but for clarity all required input variables are listed and described in Table B.1. Figure B.1 gives an example of a truck and drawbar-trailer combination to illustrate these parameters. In cases where the parameter is irrelevant such as $FC_{long}$ for a dolly or *H* for the rearmost trailer, the parameter may simply be set to zero and will not interfere with the results of the model. The binary identifier, $Dolly_j$, is

required in order for the model to determine which vehicles to use in the calculation of MoD and DoM as well as aiding in the presentation of result plots.

**Table B.1: Input parameters required for each vehicle unit in the Matlab® geometric model**

| Parameter | Description |
|---|---|
| $WB_i$ | Geometric wheelbase (m) |
| $FC_{longq,i}$ | Longitudinal position of front corner (positive forward of the steer axle/hitch) (m) |
| $FC_{wid,j}$ | Vehicle width at front corner (= $FC_{lat}$·2) (m) |
| $RC_{longq,i}$ | Longitudinal position of rear corner (positive rearward of the steer axle/hitch) (m) |
| $RC_{wid,i}$ | Vehicle width at rear corner (= $RC_{lat}$·2) (m) |
| $n_i$ | Number of non-steering rear axles |
| $d_i$ | Axle spacing between non-steering rear axles (m) |
| $IE_{wid,i}$ | Vehicle width at inner edge (= $IE_{lat}$·2) (m) |
| $H_j$ | Hitch point location (positive rearward of the steer axle/hitch) (m) |
| $\theta_j(1)$ | Initial yaw angle (positive from the positive X axis to the positive Y axis) (rad) |
| $Dolly_i$ | Binary identifier denoting the vehicle unit to be a dolly (= 1) or not (= 0) |

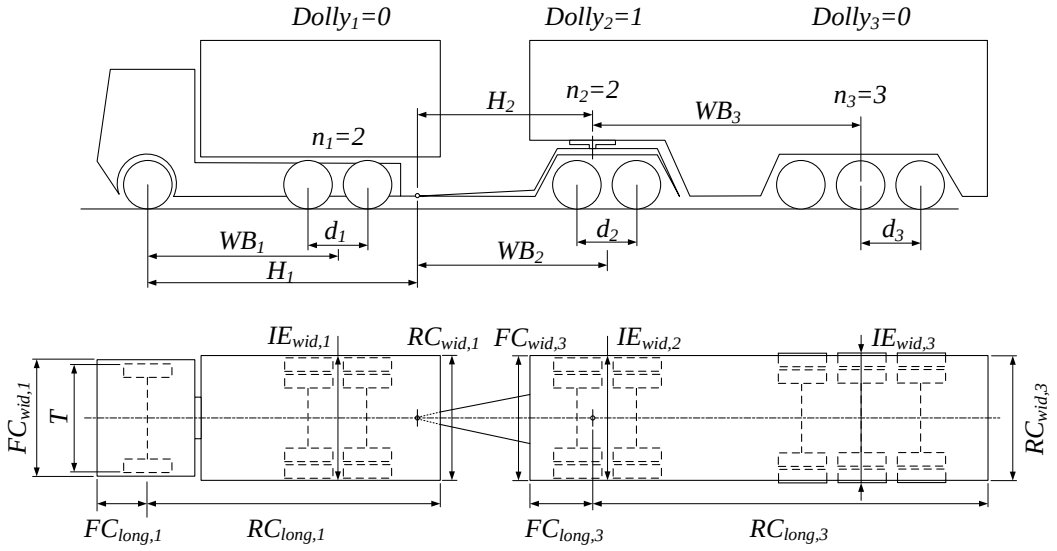


**Figure B.1: Illustration of input data required for the geometric model**

There are two methods of providing the model with these data. One is to input the values individually upon being requested to do so via the input dialog box pop-ups at the beginning of each run. The other is to set the data as default within the m-file itself. In the input dialog boxes, default values from the m-file are presented and the user can change all values as applicable. However, if the vehicle or vehicle combination being analysed is to undergo a parametric study or an optimisation process, and most of the values used in subsequent runs of the model will be the same, it is useful for the user to simply set the default values to those of the scenario in question. This way, only the parameters to be

parameterised or optimised require editing before running the model. Specifying default input data is the recommended method even where this is not the case. An example of user-specified default data for a vehicle combination such as the one in Figure B.1 is:

```
%           WB FClong FCwid RClong RCwid  n     d IEwid     H th(1) Dolly

Data(:,1)=[5.2;  1.26;  2.2;   6.9; 2.59; 2; 1.40;  2.6; 7.16; pi/2;    0];
Data(:,2)=[4.2;  0   ;    0;     0;    0; 2; 1.36;  2.6; 4.23; pi/2;    1];
Data(:,3)=[9.0;  2.47;  2.3;  12.5; 2.59; 3; 1.36;    0;    0: pi/2;    0];
```

Examples of the input dialog boxes presented to the user are shown in Figure B.2. Figure B.2 (a) shows the first input dialog box requesting fundamental model parameters such as steer-tyre track width and the incremental step size. Figure B.2 (b) shows an example of the dialog boxes requesting all the required dimensions of each vehicle unit. This dialog box will appear *N* times – once for each vehicle in the combination.

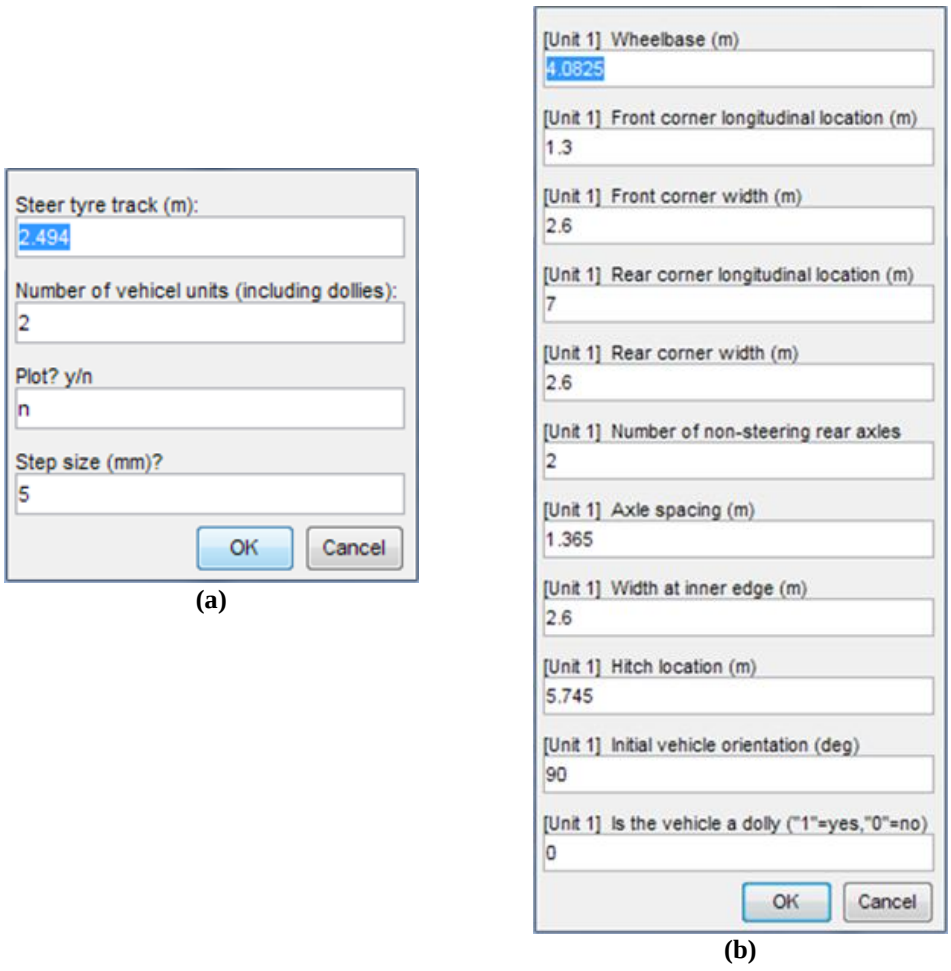


**(a)** **(b)**

**Figure B.2: Model input: (a) basic parameters and, (b) vehicle data.**

Once the input data have been provided by the user, the main body of the m-file will execute. Once complete, results are displayed in the command window as singular values in the case of LSSP and FS, as a vector of length *N* in the case of TS and as vectors of length *N*–1 in the cases of DoM and MoD. If "y" was selected for the "Plot?" request, plots of LSSP, TS and FS, as well as DoM and MoD if applicable, will be displayed and saved as .emf files in the active working directory. Example result plots for a truck and drawbar-trailer combination (similar to the example shown in Figure B.1) are shown in Figure B.3 to Figure B.5.

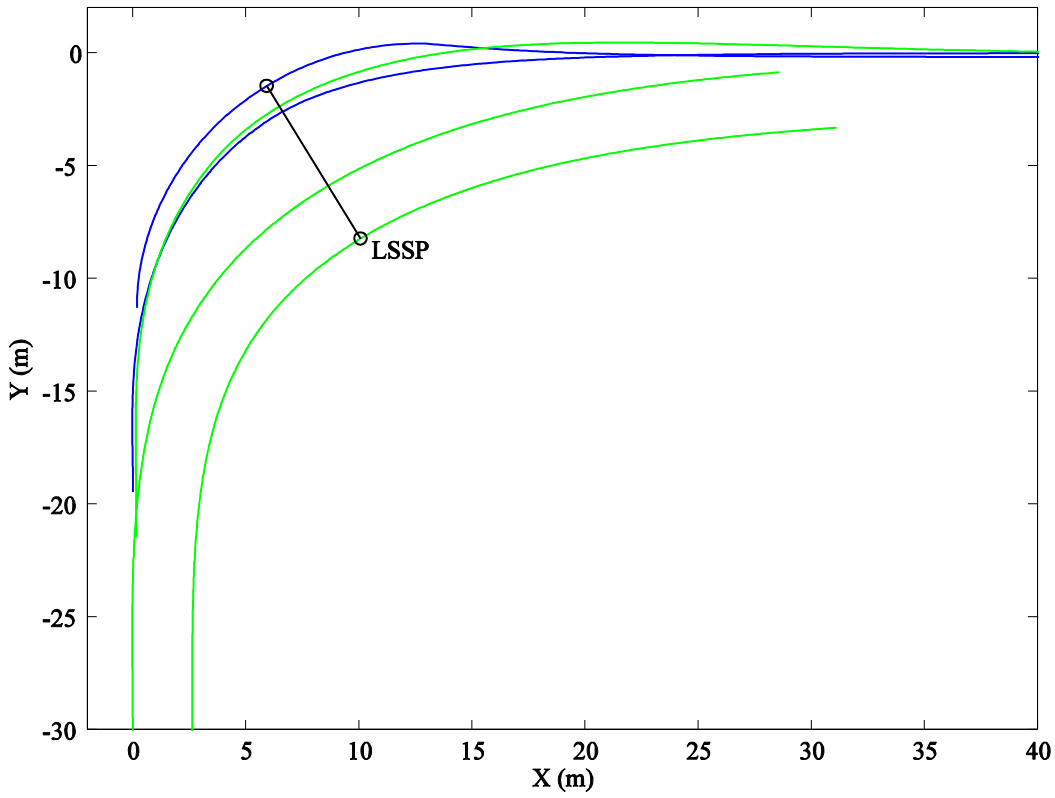


**Figure B.3: Example plot output from geometric model, LSSP**

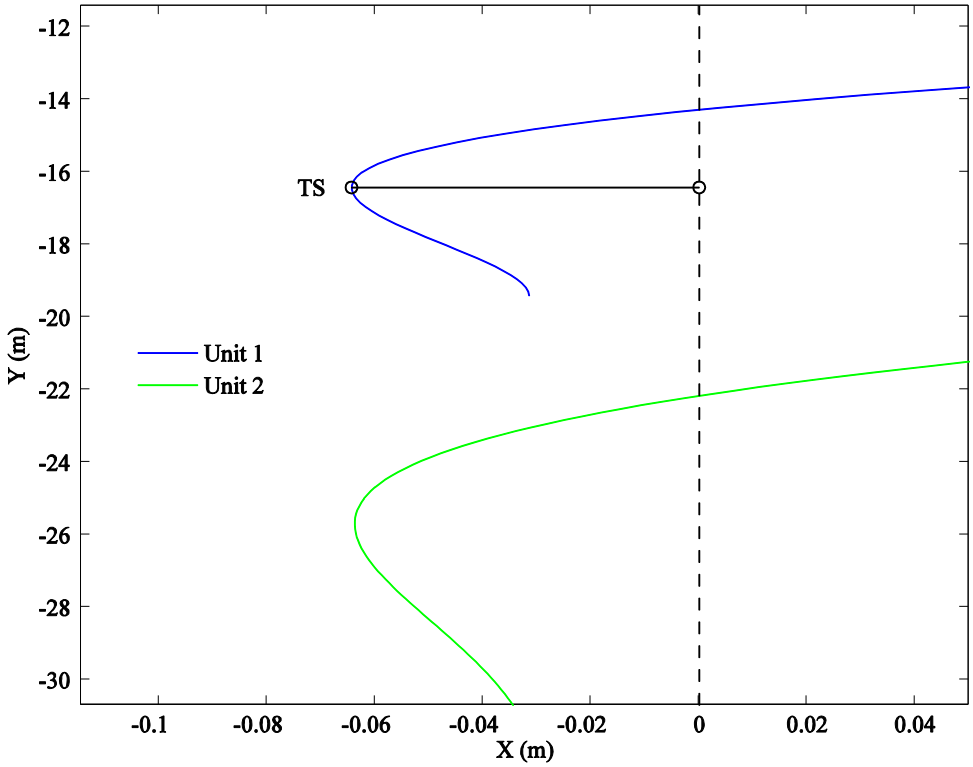


**Figure B.4: Example plot output from geometric model, TS**

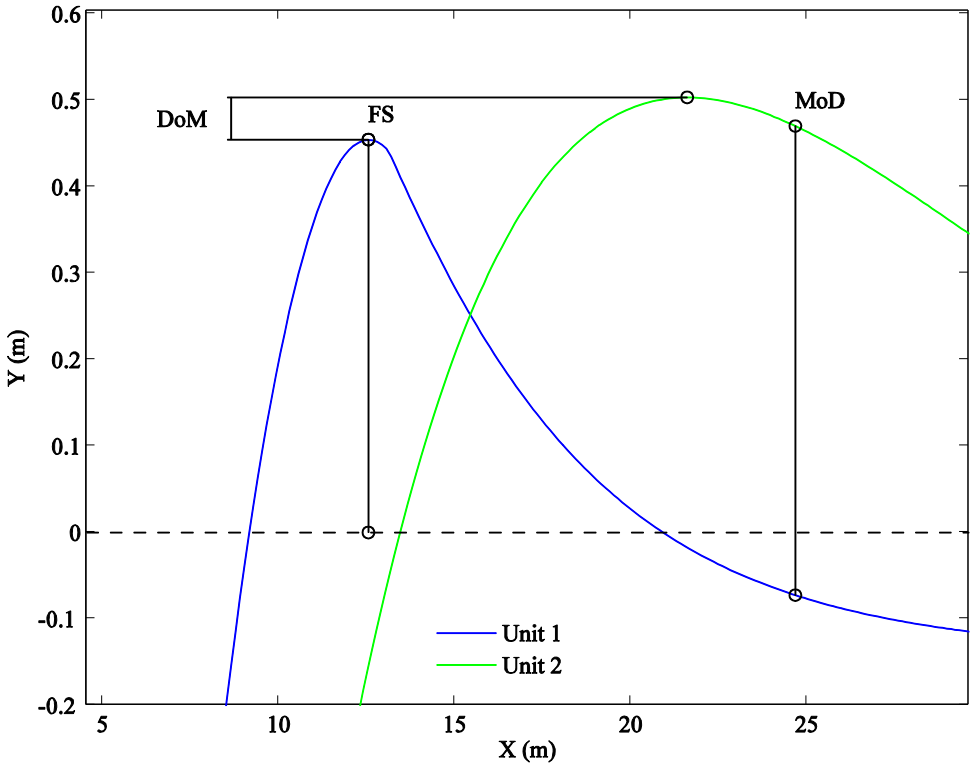


**Figure B.5: Example plot output from geometric model, FS, DoM, MoD**

# Appendix C

# Vehicle Modelling

In this section, the general methods, calculations and sources from which relevant vehicle data have been obtained are described. The vehicle-specific data for each of the two vehicles assessed are given in Appendix D and Appendix E.

## C.1 Inertial Properties

### C.1.1 Sprung mass

For the Volvo and Renault prime movers, inertial data were provided in the form of total mass, total centre of gravity height and axle loads. In some instances, unsprung masses were also supplied. Sprung mass, sprung mass centre of gravity height and longitudinal location, moments of inertia, and unknown unsprung masses were either calculated or estimated.

Taking the unsprung masses and unsprung mass centre of gravity locations to be known (see Section C.1.2), and assuming the vehicle centre of gravity to have no lateral offset, the sprung mass and sprung mass centre of gravity location were calculated using (refer to Figure C.1 for illustration)

$$m_s = m_{tot} - \sum m_{us}\,, \tag{C.1}$$

$$\bar{x}_{tot} = \frac{\sum \bar{x}_{us} M}{m_{tot}}, \tag{C.2}$$

$$\bar{x}_s = \frac{\bar{x}_{tot} m_{tot} - \sum \bar{x}_{us} m_{us}}{m_s}, \tag{C.3}$$

$$\bar{z}_s = \frac{\bar{z}_{tot} m_{tot} - \sum \bar{z}_{us} m_{us}}{m_s}, \tag{C.4}$$

where $m$ is mass in kg; $M$ is axle load in kg; $\bar{x}$ and $\bar{z}$ are the longitudinal and vertical locations of the centre of gravity in m; and the subscripts *s*, *us* and *tot* refer to the sprung, unsprung and total masses respectively.

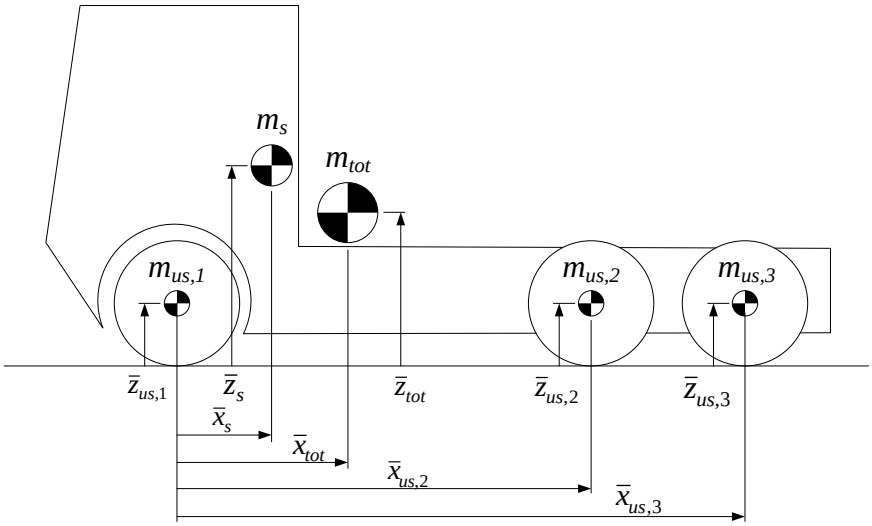


**Figure C.1: Determining the mass and centre of gravity of the sprung mass**

Roll, pitch and yaw moments of inertia of the sprung mass were estimated using the techniques suggested by UMTRI [34] which may be summarised as

$$I_{xx} = m_s \rho^2, \tag{C.5}$$

$$m_f = m_s \frac{(WB - x_s)}{WB}, \tag{C.6}$$

$$m_r = m_s \frac{(x_s)}{WB}, \tag{C.7}$$

$$I_{zz} = I_{yy} = (m_f + 0.4 m_r) \cdot x_s^{\,2} + 0.6 m_r \cdot (WB - x_s)^2, \tag{C.8}$$

where $I_{xx}$, $I_{yy}$ and $I_{zz}$ are the roll, pitch and yaw mass moments of inertia respectively in kg·m$^2$; and $\rho$ is the radius of gyration in m (assumed to be a constant value of 29" = 0.737 m).

In the case of the Volvo FM400, the total mass and centre of gravity height data provided did not include driver or fuel. In the case of the Renault Midlum, the quoted data included a driver and the fifth wheel but it was not clear whether fuel was included (it was hence assumed to have been excluded). Where not included, these additional

components were modelled separately and added as additional payloads on the vehicle. Driver inertial data were sourced from [54] and scaled for a typical 75 kg adult. Fuel was modelled according to the size and location of fuel tanks (derived from the supplied drawings), assuming maximum volumetric capacity and a diesel specific gravity of 0.84 [55].

The inertial properties of the truck superstructure and trailer of the Maxiporter, as well as the semitrailer of the Flexiporter, were derived from detailed three-dimensional CAD models of the assemblies as provided by Unipower. These data were corroborated against known mass data where this was available, and scaled if necessary, to take into account additional load contributions of spare wheels, tools *etc*.

The principles of modelling the actual payload consisting of a number of 1998 Ford Expeditions were discussed in sufficient detail in Section 3.3 and need not be repeated here. It should be clarified however that certain data from Heydinger *et al.*'s database were excluded from consideration. Data that was not considered included the following:

- Vehicles tested with more than one occupant. If a vehicle had only one occupant, the mass was removed from the overall mass and the effects on the centre of gravity location and moments of inertia were assumed small. An occupant mass of 75 kg was assumed where required.
- Any vehicles with missing mass or centre of gravity location data.
- Vehicles with ballasts to simulate load and/or additional occupants.
- Vehicles with any additional loads such as measuring equipment or outriggers.
- Any vehicle models dating from before 1990.

Lastly, TruckSim® requires vehicle inertial data to be specified for vehicles in their *unladen* condition. As payload is added, the sprung mass will lower according to spring and tyre stiffness properties (or just tyre stiffness properties in the case of air suspension). Therefore, where it was known that data were provided for the vehicle in its *laden* condition, full-load spring and tyre deflections were added to respective centres of gravity heights to give the appropriate unladen values.

### C.1.2 Unsprung Mass

Data for unsprung mass were provided by BPW for the trailer and semitrailer axles, provided to a certain extent for the Volvo FM400 (rear bogie mass was given as a total, not for individual axles) and not available for the Renault Midlum. The mass of the rear

bogie of the FM400 was given to be 2 200 kg and it was assumed that the drive axle accounted for 1 200 kg of this and the tag axle the remaining 1 000 kg. Renault Midlum unsprung masses were estimated from UMTRI data [34] and scaled according to axle load rating. This method was corroborated using the Volvo axles – where the unsprung masses were known – and shown to be suitably accurate.

The centres of gravity of respective unsprung masses were assumed to be located at the height of the wheel centre. This is reasonably accurate for most cases though least accurate for steer axles where the wheel centres are typically above the axle centre. Unsprung mass yaw/roll moments of inertia were estimated by scaling UMTRI data [36] according to unsprung mass. The effects of these small inaccuracies on overall vehicle performance were deemed negligible.

The spin inertias of rotating components of the axle assemblies (i.e. brake discs, brake drums, half shafts *etc.*) were estimated from UMTRI data [35] to be 2 $kg \cdot m^2$ where applicable. Similarly, wheel and tyre assembly spin moment of inertia data were derived from UMTRI work [35], [36]. Two values were derived: 10 $kg \cdot m^2$ for 19.5” wheels (based on data for 20” wheels [35]) and 12 $kg \cdot m^2$ for 22.5” wheels (based on 22.5” wheels [36]).

Where unsprung mass values were derived via indirect means for a prime mover (i.e. the Renault Midlum) these values directly affect the derived sprung mass of the vehicle according to Equations (C.1) to (C.4). If the unsprung mass is over-estimated, it will result in an underestimated sprung mass. However, the estimation methods used to derive unsprung masses yielded acceptable predictions compared with other known data and so the subsequent sprung mass estimation is deemed suitable as well.

## C.2 Suspension

### C.2.1 Spring kinematics

For all axle and suspension assemblies, detailed drawings were provided by the relevant OEMs. From these drawings, the track width, wheel centre height and lateral spring spacing could be deduced. Roll centre heights were provided by BPW for the trailer axles but required estimation for the FM400 and Midlum. UMTRI estimation methods were used for this purpose [37]. An example of this is illustrated in Figure C.2 (a) depicting a typical front suspension with a shackle connection at the rear. Lines connecting the front eye of the leaf spring to both eyes of the shackle are projected and the roll centre is taken

to be midway between these lines where these lines cross the axle plane. Where no shackle is present, the same method is used except that only one line is projected between the front leaf spring eye and the point of slipper contact at the rear. A similar method was used for the air suspension depending on the configuration and the inclination of the trailing arms.

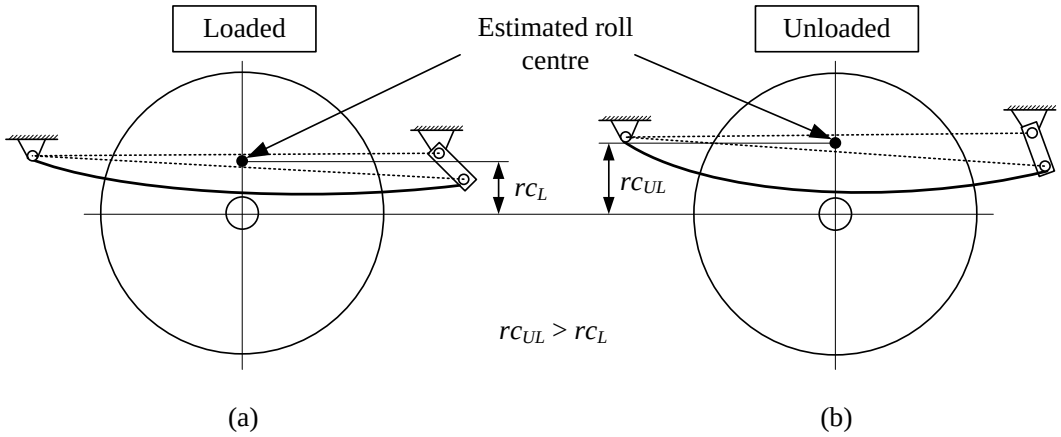


**Figure C.2: Roll centre height estimation using UMTRI methods and the effect of axle load on roll centre height relative to axle centre**

The roll-steer characteristics of the axle are derived from the angle of the line joining the front eye (or pivot point) and the roll centre. This line is taken to represent an equivalent "axle locating link" (see [40]). Three-dimensional geometric considerations can be shown to yield

$$\delta = -\arctan\left[\tan(\omega)\cdot\sin(\lambda)\right], \tag{C.9}$$

where $\delta$ is the roll-induced steer angle in ° (positive steer to the left), $\omega$ is the sprung mass roll angle relative to the unsprung mass in ° (positive clockwise when viewed from the rear), and $\lambda$ is the inclination of an equivalent axle locating link in ° (positive angled down at the rear).

As with the height of the sprung mass, the roll centre height (and to a lesser extent, the equivalent axle locating link inclination) are dependent on whether the measurement is taken with the vehicle laden or unladen. This effect is illustrated in Figure C.2 (a) and (b). Where applicable, the lower (conservative), laden roll centre height was used (making suspension deflection adjustments as necessary).

Other lateral constraints on an axle will affect the location of the roll centre. One example is a "track bar" connecting the top of the axle or differential to the chassis to provide additional (and dominant) lateral constraint [37]. In this case the location of this track bar would determine the location of the roll centre, but none of the axles considered

here had such mechanisms. In a similar manner however, the presence of an anti-roll bar could influence the location of the roll centre if both the axle and chassis connections of the bar were laterally constrained. It was assumed that this was not the case and that the presence of an anti-roll bar had no effect on the location of the roll centre.

The effects of other kinematic properties of the axles such as lateral, longitudinal and dive motions as a function of axle jounce were assumed negligible relative to the effect of roll centre height.

The location of bump and rebound stops were deduced from suspension drawings provided and/or damper extension/compression limits. Where such data were not available, the allowable wheel travel was overestimated. Bump and rebound stop stiffness was assumed to be 7 000 N/mm as per the default TruckSim® value.

### C.2.2 Spring compliance

Spring compliance properties were made available by the relevant OEMs. Spring data for the FM400 were provided in the form of loading curves of total vehicle deflection versus applied load at the steer axle and rear bogie respectively. The contribution of tyre deflection was removed from these data to deduce the individual spring stiffnesses. It was assumed that the total spring stiffness of the bogie was shared equally between the two axles with each possessing one half of the total spring stiffness. The drive axle suspension of the Midlum consists of two-stage leaf springs with a higher stiffness at higher axle load.

For the Flexiporter semitrailer airbags, BPW made detailed airbag loading curves available (for the BPW 30K airbag). The plot data were reprocessed to account for the trailing-arm lever ratio between airbag and axle.

An important factor in heavy vehicle suspensions is lash [37]. This refers to the gap between the spring leaf and the retaining pin below it. The effect of this lash on vehicle performance is that during roll motion, when the spring load on one side of the axle is reduced to zero, the sprung mass will roll a finite angle through the lash region with no additional increase in lateral acceleration. The results in a plateau in a plot of lateral acceleration versus roll angle. Depending on when the vehicle enters into this lash region before rollover (a function of static axle loads, sprung mass inertial properties and suspension stiffness), it may result in significant enough load transfer to roll the vehicle, or it may simply result in a higher roll angle in post-lash lateral acceleration.

The degree of lash was determined directly from suspension drawings. The actual lash experienced at the axle however was scaled according to the ratio of distances from the pivot point (i.e. the front eye of the leaf spring) to the axle and to the point of lash respectively. For the rear bogie of the FM400, it was assumed that the lash would be taken up in equal portions by each axle. The different "lash lever arm ratio" of each axle was used to infer the actual lash experienced at each axle. In all applicable cases, lash was incorporated by introducing a plateau region of each spring curve at zero load. Figure C.3 illustrates some of the spring compliance and kinematic concepts discussed. The example shown is for the rear suspension of the Volvo FM400 which has a unique load apportioning configuration.

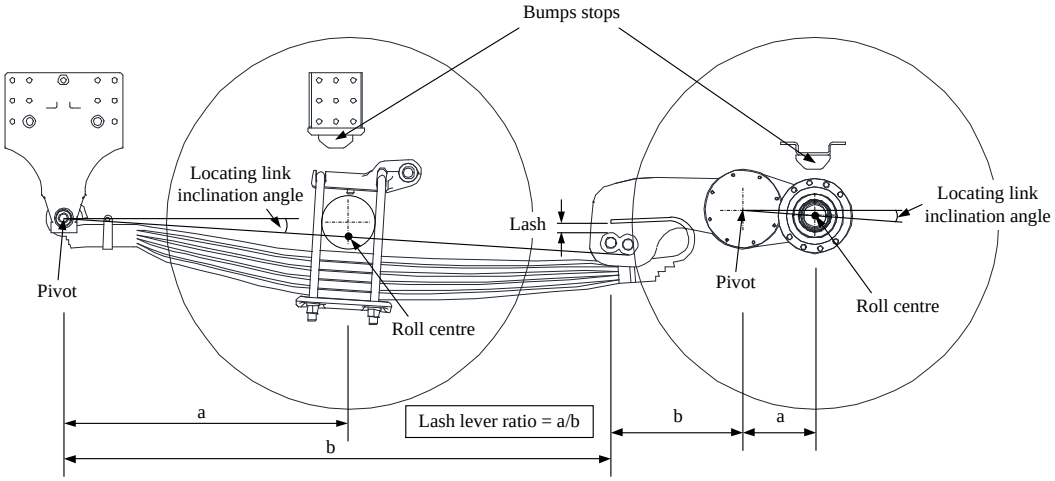


**Figure C.3: Volvo RADT-AR rear bogie, illustration of spring concepts (a simplified version of a drawing provided courtesy of Volvo Trucks SA)**

Another important feature of heavy vehicle suspensions is hysteresis. For leaf spring suspensions, the difference in force between the loading and unloading curves is equal to twice the amount of Coulomb friction present in the spring assembly. Where applicable, this was incorporated into the spring deflection curves as a vertical offset between loading and unloading curves. In TruckSim®, the rate of transition between loading and unloading curves is characterised by the parameter $\beta$, the "characteristic deflection". For lack of available data, the default TruckSim® $\beta$ value of 2 mm was used.

Typical values for Coulomb friction were sourced from UMTRI data [34] according to axle type and suspension configuration. An annotated example of a two-stage spring model is shown in Figure C.4 (Renault drive axle spring shown).

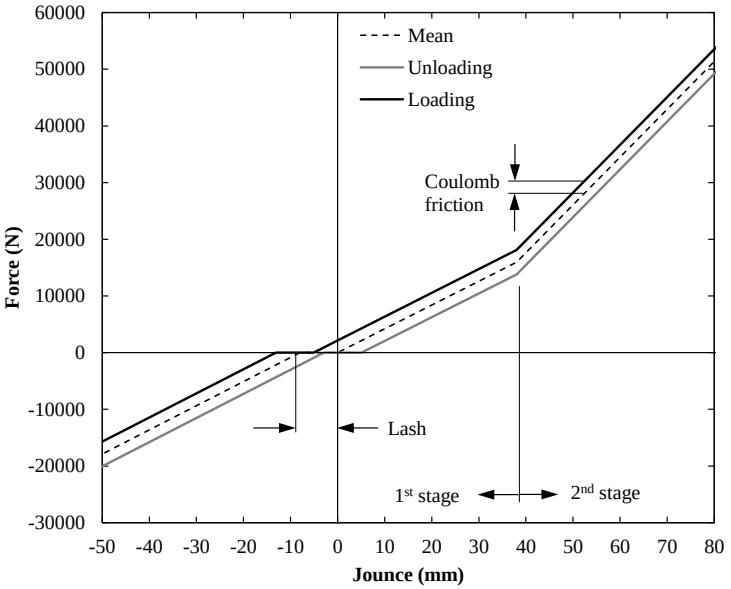


**Figure C.4: Example of a spring model used in TruckSim® (Renault drive axle spring shown)**

All suspension components besides the springs were assumed rigid and therefore all "compliance effects" were set to zero.

## C.2.3 Auxiliary roll stiffness

For all cases of leaf-spring suspension, auxiliary roll stiffness was assumed to be limited to the anti-roll bar. Where no such bar was present, zero auxiliary roll stiffness was assumed. Where applicable, detailed dimensions of the anti-roll bar were obtained from OEM drawings and the roll stiffness calculated from first principles. In calculating the roll stiffness of the bar, one end was assumed fixed in the vertical direction and a vertical force, *F*, was applied to the other. Pin joint constraints were applied to the chassis/axle mounts as applicable. The overall deflection of the one end relative to the other was calculated as a superposition of a number of individual beam deflections within respective regions of the bar.

Consider Figure C.5. The bar is divided into five regions, **A**, **B**, **C**, **D** and **E** as depicted. The individual deflections of the free end of the bar per kN of applied force are denoted "*s*" with subscripts "*b*" or "*t*" to denote whether the deflection is a result of beam bending or beam torsion respectively, and a second subscript is used to denote the region of the bar in which this respective bending or torsion occurs. $\tau$ denotes an angular deflection due to torsion. The individual components of the deflection are:

- $s_{b,D}$, the deflection of the cantilevered beam segment **D** in the transverse plane in mm,

- $\tau_{t,BCD}$ , the angular deflection in beam segment **BCD** in radians about the transverse axis as a result of force *F* applied at a moment arm equal to the length of **E**,
- $s_{t,BCD}$, the deflection at the point of force application as a result of $\tau_{t,BCD}$ in mm,
- $\tau_{b,A}$ , the angular deflection of beam segment **A** in radians about the transverse axis as a result of the moment applied at the effective pin joint joining **A** and **B** due to moment arm of length **E**,
- $s_{b,A}$, the deflection at the point of force application as a result of $\tau_{b,A}$ in mm, and
- $s_{b,E}$, the deflection of cantilevered beam segment **E** in the longitudinal plane in mm.

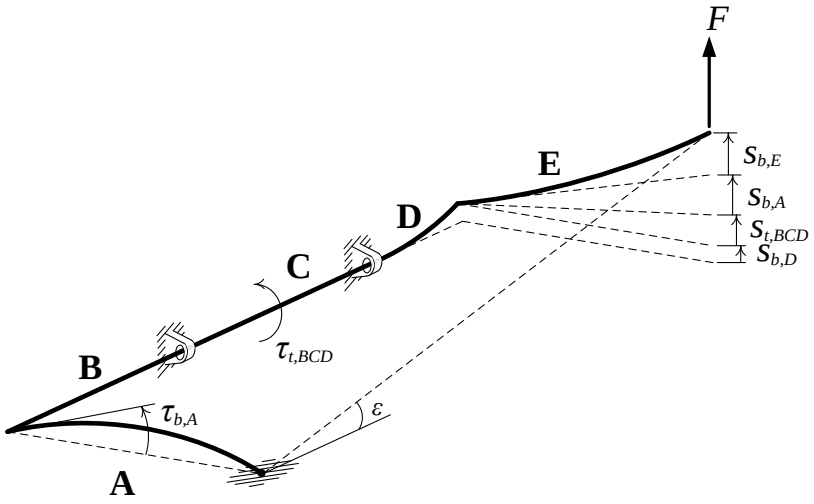


**Figure C.5: Anti-roll bar roll stiffness derivation**

Using simple beam deflection equations for each of the loading scenarios listed above, and assuming a constant cross section, the roll stiffness of the anti-roll bar was calculated. A Young's Modulus, *E*, of 207 GPa and a shear modulus, *G*, of 79 GPa were used (mild steel) [56].

Polar and bending moments of area, *J* and *I* respectively (in $mm^4$), were calculated using

$$J = \frac{\pi}{2}\left(r_o{}^4 - r_i{}^4\right), \tag{C.10}$$

$$I = \frac{\pi}{4}\left(r_o{}^4 - r_i{}^4\right), \tag{C.11}$$

where $r_i$ and $r_o$ are the inner and outer radii of the anti-roll bar cross-section respectively in mm. The individual beam deflections per kN applied force were calculated using [57]:

$$s_{b,D} = \frac{{l_D}^3}{3EI}, \tag{C.12}$$

$$\tau_{t,BCD} = \frac{l_A l_{BCD}}{JG}, \tag{C.13}$$

$$s_{t,BCD} = \tau_{t,BCD} l_A, \tag{C.14}$$

$$s_{b,E} = \frac{{l_A}^3}{3EI}, \tag{C.15}$$

$$\tau_{b,A} = \frac{{l_A}^2}{3EI}, \tag{C.16}$$

$$s_{b,A} = \tau_{b,A} l_A, \tag{C.17}$$

where $l$ is the length of the respective beam segments in mm. Finally, the overall roll stiffness of the anti-roll bar, $K_r$ (in Nm/rad), was calculated using

$$K_r = \frac{1000 \cdot F l_{BCD}}{\left(s_{b,D} + s_{t,BCD} + s_{b,E} + s_{b,A}\right)\frac{F}{l_{BCD}}} = \frac{1000 \cdot {l_{BCD}}^2}{s_{b,D} + s_{t,BCD} + s_{b,E} + s_{b,A}}. \tag{C.18}$$

The stiffness of some anti-roll bars was available against which the above method was verified. Renault quoted the drive axle anti-roll bar to have a roll stiffness of 2 548 Nm/°. The above method yielded a value of 2 718 Nm/° – an error of 7%. However, the stiffness of the bushings of the bar was known to be 20 N/m. Including the effect of the bushings yielded a roll stiffness of 2 677 Nm/° – an error of 5%.

In addition, another car-carrier manufacturer made available the results of some finite element analyses of selected anti-roll bars. In the one instance, the finite element analysis yielded 6 588 Nm/° and the above method yielded 6 720 Nm/° – an error of 2%. In the other instance, the finite element analysis yielded a roll stiffness of 14 835 Nm/° and the above method predicted 14 719 Nm/° – an error of less than 1%. The method described in this section was hence deemed accurate for use.

For the air suspension, auxiliary roll stiffness was estimated using the data of Fu and Cebon [38]. The auxiliary roll stiffness for a typical underslung air suspension was selected (6 080 Nm/°).

## C.2.4 Dampers

Force versus compression rate data for the dampers were sourced from the respective OEMs. The lateral spacing between dampers and the inclination of the dampers with respect to the horizontal (i.e. 90° represents vertical) were deduced from suspension assembly drawings. Where damper inclination was less than 90°, the velocity was scaled up and the force scaled down by the sine of the angle relative to the horizontal. This implies a lower damper rate effectively scaled down by the square of the sine of the inclination angle. In all cases the dampers were located at or near the axle and so no lever arm effects were included. A typical damper curve is shown in Figure C.6.

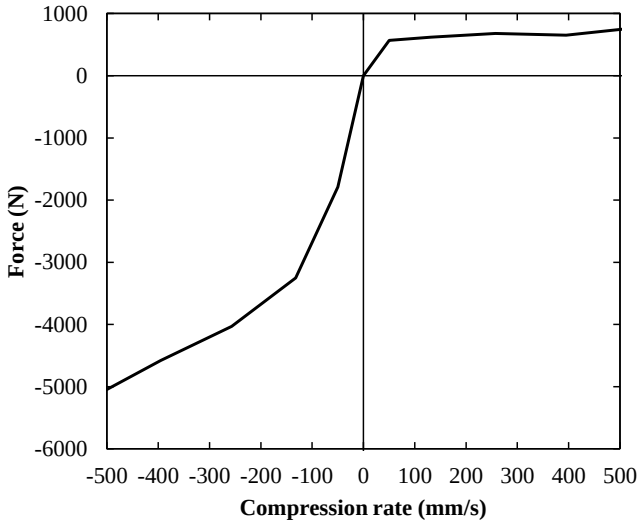


**Figure C.6: Example damper behaviour (Maxiporter steer axle shown)**

For leaf spring suspensions without dampers, damping is present in the form of Coulomb damping as opposed to the viscous damping of a traditional damper. Whereas viscous damping is a function of compression rate, Coulomb damping has a constant magnitude. In TruckSim®, specifying Coulomb friction within the spring model only has the effect of introducing hysteresis to the spring behaviour. It does not model Coulomb damping effects. This must be modelled separately as what may be termed a "Coulomb damper". Where applicable, this was achieved by specifying a damper with behaviour as illustrated in Figure C.7. The example shown has 1140 N of Coulomb friction and is defined so as to always oppose motion. The magnitude of Coulomb friction is equal to the value sourced for spring hysteresis.

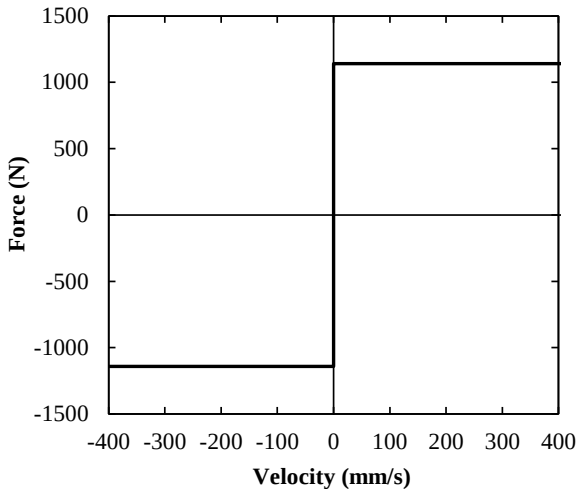


**Figure C.7: Example "Coulomb damper" behaviour (Maxiporter drive/tag axle shown)**

### C.2.5 Inter-axle load transfer

The distribution of static load between adjacent axles was either provided by the relevant OEM or assumed to be equal (i.e. a ratio of 0.5). Dynamic load transfer was taken to be 0.5 in all cases (i.e. perfect load-sharing). This is a reasonable assumption for most shared-spring and 4- and 6-spring cases [37]. For the air springs of the Flexiporter, the airbags are longitudinally inter-connected and so perfect load-sharing is closely approximated.

Load transfer due to brake torque was assumed zero in all cases. This is an accurate assertion for the air suspension though such effects could be significant in the FM400 bogie and the Maxiporter trailer axles. As none of the manoeuvres involve braking or significant acceleration, the effects of this assumption are deemed negligible (notwithstanding the indirect effect on SRT discussed on Section 4.1.2).

## C.3 Tyres

For each tyre size of the Maxiporter and Flexiporter, rated load, vertical stiffness, effective rolling radius and unloaded radius data were obtained from the 2011 "Michelin® Truck Tire Data Book" [58]. Where data for more than one model of tyre were available for the same tyre size, data were selected for the model that best fit the description of application.

Data for lateral stiffness, the most critical of tyre properties in dynamic manoeuvres, were sourced from extensive work conducted by UMTRI in the 1980s [39]. It was

assumed that because the tyres assessed in the study represent out-dated technology, the properties will be conservative for all possible makes and model of tyre (for a given size) that could be fitted to the car-carriers today. This is in line with the NTC's requirement that, "If generic, non-descript tyres were used in the analysis these should have cornering characteristics that are consistent with worst-case performing tyres of the same size to ensure that any tyre of the same size can be used."

Although lateral stiffness data were only available for slip angles up to 15°, preliminary assessments showed that none of the manoeuvres approached this limit. For the four tyre sizes used in this work, the lateral stiffness properties are provided in Table C.1 to Table C.4. The data have been converted from imperial units.

**Table C.1: Tyre lateral stiffness properties (385/65 R22.5) as per Uniroyal 15-22.5H** [39]

| **Vertical load (N) →** | 11 121 | 22 241 | 33 362 | 44 482 |
|---|---|---|---|---|
| **Slip angle (°)** | **Lateral force (N)** | | | |
| 0 | 0 | 0 | 0 | 0 |
| 1 | 1 729 | 3 270 | 4 739 | 5 720 |
| 2 | 2 858 | 5 577 | 8 020 | 9 911 |
| 4 | 4 752 | 9 221 | 13 430 | 16 933 |
| 8 | 7 256 | 14 160 | 20 561 | 26 055 |
| 12 | 8 497 | 16 670 | 23 272 | 29 500 |
| 16 | 8 482 | 16 789 | 24 298 | 30 906 |

**Table C.2: Tyre lateral stiffness properties (315/80 R22.5) as per Uniroyal 12.5-22.5G** [39]

| **Vertical load (N) →** | 8 896 | 17 793 | 26 689 | 35 586 |
|---|---|---|---|---|
| **Slip angle (°)** | **Lateral force (N)** | | | |
| 0 | 0 | 0 | 0 | 0 |
| 1 | 1 353 | 2 266 | 2 924 | 3 307 |
| 2 | 2 227 | 3 947 | 5 158 | 5 919 |
| 4 | 3 761 | 6 888 | 9 135 | 10 591 |
| 8 | 5 865 | 10 754 | 14 487 | 17 117 |
| 12 | 6 594 | 12 522 | 17 192 | 20 916 |
| 16 | 7 114 | 13 311 | 18 474 | 22 741 |

**Table C.3: Tyre lateral stiffness properties (295/80 R22.5) as per Michelin 12x22.5** [39]

| **Vertical load (N) →** | 8 896 | 17 793 | 26 689 | 35 586 |
|---|---|---|---|---|
| **Slip angle (°)** | **Lateral force (N)** | | | |
| 0 | 0 | 0 | 0 | 0 |
| 1 | 1 388 | 2 563 | 3 332 | 3 692 |
| 2 | 2 547 | 4 831 | 6 501 | 7 425 |
| 4 | 4 397 | 8 618 | 11 751 | 13 747 |
| 8 | 7 083 | 12 978 | 17 772 | 21 332 |
| 12 | 7 976 | 14 781 | 20 044 | 24 043 |
| 16 | 8 229 | 14 888 | 20 306 | 24 180 |

**Table C.4: Tyre lateral stiffness properties (285/70 R19.5) as per Michelin 11.0R20H** [39]

| **Vertical load (N) →** | 8 896 | 17 793 | 26 689 | 35 586 |
|---|---|---|---|---|
| **Slip angle (°)** | **Lateral force (N)** | | | |
| 0 | 0 | 0 | 0 | 0 |
| 1 | 1 432 | 2 588 | 3 306 | 3 664 |
| 2 | 2 532 | 4 821 | 6 475 | 7 513 |
| 4 | 4 397 | 8 511 | 11 699 | 13 851 |
| 8 | 6 851 | 12 813 | 17 575 | 20 871 |
| 12 | 7 868 | 14 763 | 19 906 | 24 016 |
| 16 | 8 501 | 15 715 | 20 973 | 25 212 |

Although the UMTRI study did also feature longitudinal stiffness and aligning moment data, such data were not available for all required tyre sizes. Therefore, and because these properties do not have a significant effect on the manoeuvres assessed in this work, default TruckSim® data were used. TruckSim® has default data available for tyre load ratings of 2 000 kg, 3 000 kg and 3 500 kg. Using Michelin® load ratings [58], TruckSim® data for the nearest load rating were selected for each tyre. TruckSim® longitudinal stiffness and aligning moment properties for the three load ratings are given in Table C.5 to Table C.10.

Due to a lack of data, and the relative insensitivity of the simulations to the data, relaxation lengths were calculated as recommended by TruckSim®. The relaxation length for longitudinal force generation was calculated as 10% of the unloaded radius and the relaxation length for lateral force and aligning moment generation was calculated as twice the unloaded radius. Where the tyre was fitted to a steer axle, a relaxation length of 100 mm was specified to avoid the instabilities described in Section 3.4.1.

Tyre rolling resistance data, wheel toe and camber, and camber thrust properties were set to zero.

**Table C.5: Tyre longitudinal stiffness properties, TruckSim® 2 000 kg rated tyre**

| **Vertical load (N) →** | 4 905 | 9 810 | 19 620 | 29 430 | 39 240 |
|---|---|---|---|---|---|
| **Slip ratio** | **Longitudinal force (N)** | | | | |
| 0.025 | 1 518 | 2 927 | 5 421 | 7 480 | 9 215 |
| 0.050 | 2 718 | 5 241 | 9 706 | 13 395 | 16 501 |
| 0.075 | 3 509 | 6 767 | 12 532 | 17 295 | 21 305 |
| 0.100 | 3 973 | 7 662 | 14 189 | 19 581 | 24 121 |
| 0.125 | 4 223 | 8 144 | 15 082 | 20 813 | 25 639 |
| 0.150 | 4 344 | 8 378 | 15 515 | 21 411 | 26 376 |
| 0.175 | 4 390 | 8 466 | 15 679 | 21 637 | 26 654 |
| 0.200 | 4 391 | 8 469 | 15 683 | 21 643 | 26 662 |
| 0.225 | 4 366 | 8 421 | 15 594 | 21 519 | 26 509 |
| 0.250 | 4 325 | 8 342 | 15 448 | 21 318 | 26 261 |
| 0.300 | 4 220 | 8 138 | 15 070 | 20 797 | 25 619 |
| 0.350 | 4 102 | 7 910 | 14 649 | 20 215 | 24 903 |
| 0.400 | 3 983 | 7 681 | 14 224 | 19 630 | 24 181 |
| 0.450 | 3 868 | 7 459 | 13 814 | 19 063 | 23 483 |
| 0.500 | 3 759 | 7 249 | 13 424 | 18 525 | 22 820 |
| 0.550 | 3 656 | 7 051 | 13 057 | 18 019 | 22 197 |
| 0.600 | 3 560 | 6 866 | 12 714 | 17 546 | 21 614 |
| 0.650 | 3 470 | 6 693 | 12 394 | 17 104 | 21 071 |
| 0.700 | 3 387 | 6 532 | 12 096 | 16 693 | 20 563 |
| 0.750 | 3 309 | 6 382 | 11 818 | 16 309 | 20 090 |
| 0.800 | 3 236 | 6 241 | 11 558 | 15 950 | 19 649 |
| 0.850 | 3 168 | 6 110 | 11 316 | 15 615 | 19 236 |
| 0.900 | 3 105 | 5 988 | 11 089 | 15 302 | 18 851 |
| 0.950 | 3 045 | 5 873 | 10 876 | 15 009 | 18 489 |
| 1.000 | 3 045 | 5 873 | 10 876 | 15 009 | 18 489 |

**Table C.6: Tyre longitudinal stiffness properties, TruckSim® 3 000 kg rated tyre**

| **Vertical load (N) →** | 7 358 | 14 715 | 29 430 | 44 145 | 58 860 |
|---|---|---|---|---|---|
| **Slip ratio** | **Longitudinal force (N)** | | | | |
| 0.025 | 2 277 | 4 391 | 8 131 | 11 221 | 13 822 |
| 0.050 | 4 077 | 7 862 | 14 559 | 20 092 | 24 751 |
| 0.075 | 5 264 | 10 151 | 18 798 | 25 942 | 31 957 |
| 0.100 | 5 959 | 11 493 | 21 283 | 29 371 | 36 181 |
| 0.125 | 6 334 | 12 216 | 22 622 | 31 219 | 38 458 |
| 0.150 | 6 516 | 12 567 | 23 273 | 32 116 | 39 563 |
| 0.175 | 6 585 | 12 700 | 23 518 | 32 455 | 39 980 |
| 0.200 | 6 587 | 12 704 | 23 525 | 32 464 | 39 992 |
| 0.225 | 6 549 | 12 631 | 23 391 | 32 279 | 39 764 |
| 0.250 | 6 488 | 12 513 | 23 172 | 31 977 | 39 392 |
| 0.300 | 6 329 | 12 207 | 22 605 | 31 195 | 38 429 |
| 0.350 | 6 153 | 11 866 | 21 973 | 30 323 | 37 355 |
| 0.400 | 5 974 | 11 522 | 21 336 | 29 444 | 36 272 |
| 0.450 | 5 802 | 11 189 | 20 720 | 28 594 | 35 224 |
| 0.500 | 5 638 | 10 873 | 20 135 | 27 787 | 34 230 |
| 0.550 | 5 484 | 10 576 | 19 586 | 27 028 | 33 296 |
| 0.600 | 5 340 | 10 299 | 19 072 | 26 319 | 32 422 |
| 0.650 | 5 206 | 10 040 | 18 592 | 25 657 | 31 606 |
| 0.700 | 5 080 | 9 798 | 18 144 | 25 039 | 30 845 |
| 0.750 | 4 964 | 9 572 | 17 727 | 24 463 | 30 136 |
| 0.800 | 4 854 | 9 362 | 17 337 | 23 925 | 29 473 |
| 0.850 | 4 753 | 9 166 | 16 973 | 23 423 | 28 855 |
| 0.900 | 4 657 | 8 982 | 16 633 | 22 953 | 28 276 |
| 0.950 | 4 568 | 8 810 | 16 314 | 22 513 | 27 734 |
| 1.000 | 4 568 | 8 810 | 16 314 | 22 513 | 27 734 |

**Table C.7: Tyre longitudinal stiffness properties, TruckSim® 3 500 kg rated tyre**

| **Vertical load (N) →** | 8 584 | 17 168 | 34 335 | 51 503 | 68 670 |
|---|---|---|---|---|---|
| **Slip ratio** | **Longitudinal force (N)** | | | | |
| 0.025 | 2 656 | 5 122 | 9 486 | 13 091 | 16 126 |
| 0.050 | 4 756 | 9 172 | 16 986 | 23 441 | 28 876 |
| 0.075 | 6 141 | 11 843 | 21 932 | 30 265 | 37 284 |
| 0.100 | 6 953 | 13 408 | 24 830 | 34 266 | 42 212 |
| 0.125 | 7 390 | 14 252 | 26 393 | 36 422 | 44 867 |
| 0.150 | 7 602 | 14 662 | 27 151 | 37 469 | 46 157 |
| 0.175 | 7 683 | 14 816 | 27 438 | 37 864 | 46 644 |
| 0.200 | 7 685 | 14 821 | 27 446 | 37 875 | 46 658 |
| 0.225 | 7 641 | 14 736 | 27 289 | 37 659 | 46 391 |
| 0.250 | 7 569 | 14 598 | 27 033 | 37 306 | 45 957 |
| 0.300 | 7 384 | 14 241 | 26 373 | 36 394 | 44 833 |
| 0.350 | 7 178 | 13 843 | 25 635 | 35 377 | 43 580 |
| 0.400 | 6 970 | 13 442 | 24 893 | 34 352 | 42 317 |
| 0.450 | 6 769 | 13 054 | 24 174 | 33 360 | 41 095 |
| 0.500 | 6 578 | 12 685 | 23 491 | 32 418 | 39 935 |
| 0.550 | 6 398 | 12 339 | 22 850 | 31 533 | 38 845 |
| 0.600 | 6 230 | 12 015 | 22 250 | 30 705 | 37 825 |
| 0.650 | 6 073 | 11 713 | 21 690 | 29 933 | 36 873 |
| 0.700 | 5 927 | 11 431 | 21 168 | 29 212 | 35 986 |
| 0.750 | 5 791 | 11 168 | 20 681 | 28 540 | 35 158 |
| 0.800 | 5 664 | 10 922 | 20 227 | 27 913 | 34 386 |
| 0.850 | 5 545 | 10 693 | 19 802 | 27 327 | 33 664 |
| 0.900 | 5 433 | 10 479 | 19 405 | 26 779 | 32 989 |
| 0.950 | 5 329 | 10 278 | 19 033 | 26 266 | 32 356 |
| 1.000 | 5 329 | 10 278 | 19 033 | 26 266 | 32 356 |

**Table C.8: Tyre aligning moment stiffness properties, TruckSim® 2 000 kg rated tyre**

| **Vertical load (N) →** | 4 905 | 9 810 | 19 620 | 29 430 | 39 240 |
|---|---|---|---|---|---|
| **Slip angle (°)** | **Aligning moment (Nm)** | | | | |
| 1 | 38.2 | 148.4 | 512.7 | 975.0 | 1 733.3 |
| 2 | 50.5 | 202.1 | 766.7 | 1 384.2 | 2 460.8 |
| 3 | 45.0 | 188.8 | 808.4 | 1 818.9 | 3 233.5 |
| 4 | 29.9 | 133.9 | 706.6 | 1 721.0 | 3 059.5 |
| 6 | –5.0 | –19.9 | 315.1 | 1 078.4 | 1 917.1 |
| 8 | –24.9 | –138.1 | –68.1 | 336.1 | 597.5 |
| 10 | –26.1 | –164.7 | –284.5 | –186.4 | –331.4 |
| 12 | –18.3 | –104.9 | –325.3 | –432.1 | –745.8 |
| 14 | –11.1 | –26.5 | –267.9 | –443.9 | –789.2 |
| 16 | –7.2 | –2.4 | –191.1 | –375.2 | –667.1 |
| 18 | –4.4 | –8.5 | –130.9 | –290.3 | –516.1 |
| 20 | –3.4 | –8.5 | –90.8 | –218.6 | –388.7 |
| 25 | –1.6 | 0.0 | –42.2 | –111.3 | –197.9 |
| 30 | –1.1 | 0.0 | –23.6 | –62.8 | –111.6 |
| 35 | –0.6 | 0.0 | –14.8 | –39.5 | –70.3 |
| 40 | 0.0 | 0.0 | –10.0 | –26.6 | –47.3 |
| 45 | 0.0 | 0.0 | 0.0 | 0.0 | 0.0 |

**Table C.9: Tyre aligning moment stiffness properties, TruckSim® 3 000 kg rated tyre**

| **Vertical load (N) →** | 7 358 | 14 715 | 29 430 | 44 145 | 58 860 |
|---|---|---|---|---|---|
| **Slip angle (°)** | **Aligning moment (Nm)** | | | | |
| 1 | 86.0 | 333.9 | 1 153.5 | 2 193.7 | 3 899.9 |
| 2 | 113.7 | 454.7 | 1 725.2 | 3 114.4 | 5 536.7 |
| 3 | 101.1 | 424.9 | 1 818.9 | 4 092.4 | 7 275.4 |
| 4 | 67.4 | 301.3 | 1 589.8 | 3 872.2 | 6 884.0 |
| 6 | –11.3 | –44.7 | 709.0 | 2 426.4 | 4 313.6 |
| 8 | –56.1 | –310.8 | –153.2 | 756.2 | 1 344.3 |
| 10 | –58.7 | –370.5 | –640.1 | –419.5 | –745.7 |
| 12 | –41.2 | –236.1 | –731.9 | –972.2 | –1 678.2 |
| 14 | –24.9 | –59.6 | –602.8 | –998.8 | –1 775.7 |
| 16 | –16.2 | –5.4 | –429.9 | –844.2 | –1 500.9 |
| 18 | –10.0 | –19.0 | –294.5 | –653.1 | –1 161.1 |
| 20 | –7.6 | –19.0 | –204.3 | –491.9 | –874.5 |
| 25 | –3.7 | 0.0 | –95.0 | –250.4 | –445.2 |
| 30 | –2.6 | 0.0 | –53.1 | –141.3 | –251.1 |
| 35 | –1.3 | 0.0 | –33.3 | –88.9 | –158.1 |
| 40 | 0.0 | 0.0 | –22.6 | –59.8 | –106.4 |
| 45 | 0.0 | 0.0 | 0.0 | 0.0 | 0.0 |

**Table C.10: Tyre aligning moment stiffness properties, TruckSim® 3500 kg rated tyre**

| **Vertical load (N) →** | 8 584 | 17 168 | 34 335 | 51 503 | 68 670 |
|---|---|---|---|---|---|
| **Slip angle (°)** | **Aligning moment (Nm)** | | | | |
| 1 | 117.1 | 454.5 | 1 570.1 | 2 985.9 | 5 308.2 |
| 2 | 154.7 | 618.9 | 2 348.1 | 4 239.1 | 7 536.1 |
| 3 | 137.7 | 578.3 | 2 475.7 | 5 570.3 | 9 902.7 |
| 4 | 91.7 | 410.1 | 2 163.9 | 5 270.5 | 9 369.9 |
| 6 | –15.3 | –60.9 | 965.1 | 3 302.6 | 5 871.2 |
| 8 | –76.4 | –423.0 | –208.5 | 1 029.2 | 1 829.7 |
| 10 | –79.9 | –504.3 | –871.3 | –570.9 | –1 015.0 |
| 12 | –56.0 | –321.4 | –996.3 | –1 323.3 | –2 284.2 |
| 14 | –33.9 | –81.1 | –820.5 | –1 359.5 | –2 416.9 |
| 16 | –22.1 | –7.4 | –585.2 | –1 149.1 | –2 042.9 |
| 18 | –13.6 | –25.9 | –400.9 | –889.0 | –1 580.4 |
| 20 | –10.3 | –25.9 | –278.0 | –669.6 | –1 190.3 |
| 25 | –5.0 | 0.0 | –129.3 | –340.9 | –606.0 |
| 30 | –3.5 | 0.0 | –72.3 | –192.3 | –341.8 |
| 35 | –1.7 | 0.0 | –45.3 | –121.0 | –215.1 |
| 40 | 0.0 | 0.0 | –30.7 | –81.4 | –144.8 |
| 45 | 0.0 | 0.0 | 0.0 | 0.0 | 0.0 |

## C.4 Couplings

The hitches were assumed to perfectly constrain translational motion in all three principle directions. Roll, pitch and yaw constraints were assumed zero in the case of the Maxiporter, and zero pitch and yaw constraint was assumed for the Flexiporter.

Fifth wheel roll stiffness was taken to be 56 500 Nm/°. This value was sourced from the NTC [40] after obtaining a number of representative values from previous work [40], [59–65]. Due to the large variation between values, the most conservative lowest value as offered by the NTC's report was chosen. Much of the work cited took into account lash in the fifth wheel assembly. The effects of this are reasonably well documented (see for example [48], [65], [66]) but representative values used in previous work varied immensely. A number of representative values were used in preliminary simulations resulting in a negligible effect on the PBS results but a significant effect on the volatility of resultant data. As a result, a decision was taken to exclude lash from the fifth wheel and to use only a conservative linear roll stiffness of 56 500 Nm/°.

Chassis compliance effects have not been included in this work due to a lack of data and a lack of the modelling capabilities required to model these effects. This assumption is reasonable for the Maxiporter truck and trailer and the Flexiporter semitrailer where the car-carrying superstructures may contribute some stiffness to the vehicles (relative to a flatbed trailer for example).

## C.5 Steering

All steering compliances and kinematic effects were assumed negligible. The premise for this is that the simulations in question are to assess vehicle performance as the vehicle is made to follow certain paths, and should not be dependent on the steering behaviour required to do so. The only steering property that was defined was the steering wheel to road wheel gear ratio which was taken to be 25-to-1.

# Appendix D

# Maxiporter Input Data

## D.1 Inertial properties

### D.1.1 Sprung mass

**Table D.1: Sprung mass properties, Maxiporter**

| Vehicle Parameter | Units | Truck | Trailer |
|---|---|---|---|
| Sprung mass | kg | 5 430 | 7 355 |
| CoG height above ground | mm | 1 124 | 1 311 |
| CoG distance behind steer axle/hitch | mm | 936 | 8 133 |
| CoG lateral coordinate (positive left) | mm | 0 | 0 |
| Roll moment of inertia | $kg \cdot m^2$ | 2 946 | 14 722 |
| Pitch moment of inertia | $kg \cdot m^2$ | 11 492 | 121 808 |
| Yaw moment of inertia | $kg \cdot m^2$ | 11 492 | 120 019 |

**Table D.2: Additional sprung mass properties, Maxiporter**

| Vehicle Parameter | Units | Truck superstructure | Fuel and driver |
|---|---|---|---|
| Sprung mass | kg | 3 452 | 831 |
| CoG height above ground | mm | 2 058 | 813 |
| CoG distance behind steer axle/hitch | mm | 3 254 | 1 525 |
| CoG lateral coordinate (positive left) | mm | 0 | –474 |
| Roll moment of inertia | $kg \cdot m^2$ | 6 372 | 561 |
| Pitch moment of inertia | $kg \cdot m^2$ | 16 692 | 555 |
| Yaw moment of inertia | $kg \cdot m^2$ | 16 989 | 852 |

**Table D.3: Sprung mass properties of payloads, Maxiporter**

| Vehicle Parameter | Units | Truck | | Trailer | |
|---|---|---|---|---|---|
| | | Full | Top only | Full | Top only |
| Number of passenger vehicles | - | 3 | 2 | 6 | 3 |
| Sprung mass | kg | 7 686 | 5 124 | 15 372 | 7 686 |
| CoG height above ground | mm | 2 948 | 3 503 | 2 384 | 3 355 |
| CoG distance behind steer axle/hitch | mm | 2 633 | 2 254 | 8 807 | 9 165 |
| CoG lateral coordinate (positive left) | mm | 0 | 0 | 0 | 0 |
| Roll moment of inertia | $kg \cdot m^2$ | 9 783 | 5 426 | 26 532 | 13 775 |
| Pitch moment of inertia | $kg \cdot m^2$ | 55 322 | 45 298 | 260 030 | 117 197 |
| Yaw moment of inertia | $kg \cdot m^2$ | 51 541 | 44 424 | 247 281 | 110 879 |

### D.1.2 Unsprung mass

**Table D.4: Unsprung mass properties per axle, Maxiporter**

| Vehicle Parameter | Units | Steer | Drive | Tag | Trailer |
|---|---|---|---|---|---|
| Unsprung mass | kg | 750 | 1 200† | 1 000† | 650 |
| CoG height above ground | mm | 513 | 535 | 536 | 432 |
| Axle assembly roll/yaw moment of inertia | $kg \cdot m^2$ | 526 | 572 | 477 | 525 |
| Axle components spin moment of inertia (per side) | $kg \cdot m^2$ | 2 | 2 | 2 | 2 |
| Wheel assembly spin moment of inertia (per wheel) | $kg \cdot m^2$ | 12 | 12 | 12 | 10 |

† Total bogie mass given as 2200 kg. Individual unsprung masses weighted towards drive axle

## D.2 Suspension

### D.2.1 Springs

**Table D.5: Suspension geometry, Maxiporter**

| Vehicle Parameter | Units | Steer | Drive | Tag | Trailer |
|---|---|---|---|---|---|
| Track width | mm | 2 109 | 1 854 | 1 854 | 2 310 |
| Wheel centre height | mm | 513 | 535 | 536 | 432 |
| Roll centre height above axle CoG | mm | 85 | –38 | 0 | –80 |
| Roll steer locating link angle | ° | –2.8 | 2.6 | 5.2 | 2.7 |
| Axle lateral movement vs. jounce | mm/mm | 0 | 0 | 0 | 0 |
| Axle longitudinal movement vs. jounce | mm/mm | 0 | 0 | 0 | 0 |
| Axle dive vs. jounce | °/mm | 0 | 0 | 0 | 0 |

**Table D.6: Spring compliance, Maxiporter**

| Vehicle Parameter | Units | Steer | Drive | Tag | Trailer |
|---|---|---|---|---|---|
| Spring stiffness | N/mm | 311 | 746 | 746 | 650 |
| Spring track | mm | 825 | 988 | 988 | 1 600 |
| Lash at spring connection | mm | 0 | 20 | 20 | 44 |
| Lash lever arm ratio | | N/A | 0.51 | 0.61 | 0.51 |
| Lash at wheel | mm | N/A | 10.1 | 12.4 | 22.4 |
| Coulomb friction | N | 887 | 1 140 | 1 140 | 1 752 |
| $\beta$ | mm | 2 | 2 | 2 | 2 |
| Compliance effects | (various) | 0 | 0 | 0 | 0 |
| Auxiliary roll moment | Nm/° | 6 299 | 0 | 0 | 0 |
| Wheel-to-spring jounce ratio | - | 1:1 | 1:1 | 1:1 | 1:1 |

**Table D.7: Tandem suspension properties, Maxiporter**

| Vehicle Parameter | Units | Drive/Tag | Trailer |
|---|---|---|---|
| Static load ratio supported by rear axle of each two-axle pair | - | 0.44 | 0.5 |
| Dynamic load transfer coefficient | - | 0.5 | 0.5 |
| Load transfer due to brake torque | 1/m | 0 | 0 |

## D.2.2 Dampers

**Table D.8: Damper properties, Maxiporter**

| Vehicle Parameter | Units | Steer | Drive | Tag | Trailer |
|---|---|---|---|---|---|
| Damper model | - | Sachs 20769819 | - | - | - |
| Damper angle relative to horizontal | ° | 90 | - | - | - |
| Damper track | mm | 1 130 | - | - | - |
| Damper rate (including inclination effect) | N/(mm/s) | Table D.9 | - | - | - |
| Auxiliary roll damping | Nm-s/° | 0 | 0 | 0 | 0 |

**Table D.9: Damper behaviour, Maxiporter steer axle**

| Velocity (mm/s) | Force (N) | |
|---|---|---|
| | Jounce | Rebound |
| 0 | 0 | 0 |
| 50 | 570 | 1 790 |
| 132 | 620 | 3 250 |
| 257 | 680 | 4 030 |
| 395 | 650 | 4 580 |
| 508 | 750 | 5 080 |

## D.3 Couplings

**Table D.10: Coupling properties, Maxiporter**

| Vehicle Parameter | Units | Hitch |
|---|---|---|
| Distance behind steer axle | mm | 5 745 |
| Height above ground | mm | 595 |
| Lateral offset | mm | 0 |
| Roll stiffness | Nm/° | 0 |
| Pitch stiffness | Nm/° | 0 |
| Yaw stiffness | Nm/° | 0 |

## D.4 Tyres

**Table D.11: Tyre properties, Maxiporter**

| Vehicle Parameter | Units | Steer | Drive/Tag | Trailer |
|---|---|---|---|---|
| Size | - | 385/65 R22.5 | 315/80 R22.5 | 285/70 R19.5 |
| Single/Dual | - | Single | Dual | Single |
| UMTRI tyre used for lateral stiffness data [39] | - | Uniroyal 15.0-22.5H | Uniroyal 12.5-22.5G | Michelin 11.0R20H |
| Michelin tyre used for rated load, vertical stiffness, effective rolling radius, unloaded radius data [58] | - | XFE Widebase | XZA2 Energy | XZE2+ |
| Rated load | kg | 4 500 | 4 125 | 2 900 |
| Effective rolling radius | mm | 521 | 521 | 433 |
| Unloaded radius | mm | 536 | 537 | 448 |
| Vertical stiffness | N/mm | 1 193 | 987 | 801 |
| Dual tyre spacing | mm | N/A | 352 | N/A |
| Rolling resistance | % | 0 | 0 | 0 |
| Relaxation length for $F_y$ and $M_z$ | mm | 100[†] | 1 074 | 896 |
| Relaxation length for $F_x$ | mm | 54 | 54 | 45 |
| Load rating for TruckSim® longitudinal and aligning moment stiffness properties | kg | 3 500 | 3 500 | 3 000 |
| Wheel toe | ° | 0 | 0 | 0 |
| Wheel camber | ° | 0 | 0 | 0 |

[†] Value chosen for steer-tyres to avoid erratic steering motion whilst maintaining acceptable path-following behaviour

## D.5 Steering

**Table D.12: Steering system properties, Maxiporter**

| Vehicle Parameter | Units | Value |
|---|---|---|
| Steering wheel to road wheel gear ratio | °/° | 25-to-1 |
| Parking torque (each side) | Nm | 0 |
| Axle wrap compliance | °/Nm | 0 |
| Steer-to-wrap ratio | °/° | 0 |
| Wheel steer vs. axle jounce | °/mm | 0 |
| Steering assembly compliances | (various) | 0 |
| Kingpin offset | mm | 0 |
| Lateral inclination | ° | 0 |
| Caster angle | ° | 0 |
| Kingpin centre ahead of wheel centre | mm | 0 |

# Appendix E

# Flexiporter Input Data

## E.1 Inertial properties

### E.1.1 Sprung mass

**Table E.1: Sprung mass properties, Flexiporter**

| Vehicle Parameter | Units | Tractor | Semitrailer |
|---|---|---|---|
| Sprung mass | kg | 3 743[†] | 7 367 |
| CoG height above ground | mm | 1 067 | 1 334 |
| CoG distance behind steer axle/hitch | mm | 863 | 6 512 |
| CoG lateral coordinate (positive left) | mm | 0 | 0 |
| Roll moment of inertia | $kg \cdot m^2$ | 2 031 | 12 421 |
| Pitch moment of inertia | $kg \cdot m^2$ | 6 808 | 157 231 |
| Yaw moment of inertia | $kg \cdot m^2$ | 6 808 | 157 733 |

[†] Includes driver and fifth wheel

**Table E.2: Sprung mass properties of payloads, Flexiporter**

| Vehicle Parameter | Units | Semitrailer | |
|---|---|---|---|
| | | Full | Top only |
| Number of passenger vehicles | - | 6 | 3 |
| Sprung mass | kg | 15 372 | 7 686 |
| CoG height above ground | mm | 2 618 | 3 519 |
| CoG distance behind steer axle/hitch | mm | 6 453 | 6 252 |
| CoG lateral coordinate (positive left) | mm | 0 | 0 |
| Roll moment of inertia | $kg \cdot m^2$ | 23 401 | 11 145 |
| Pitch moment of inertia | $kg \cdot m^2$ | 353 648 | 210 064 |
| Yaw moment of inertia | $kg \cdot m^2$ | 341 643 | 204 629 |

### E.1.2 Unsprung mass

**Table E.3: Unsprung mass properties per axle, Flexiporter**

| Vehicle Parameter | Units | Steer | Drive | Trailer |
|---|---|---|---|---|
| Unsprung mass | kg | 710 | 1 210 | 750 |
| CoG height above ground | mm | 505 | 519 | 429 |
| Axle assembly roll/yaw moment of inertia | $kg \cdot m^2$ | 498 | 577 | 606 |
| Axle components spin moment of inertia (per side) | $kg \cdot m^2$ | 2 | 2 | 2 |
| Wheel assembly spin moment of inertia (per wheel) | $kg \cdot m^2$ | 12 | 12 | 10 |

## E.2 Suspension

### E.2.1 Springs

**Table E.4: Suspension geometry, Flexiporter**

| Vehicle Parameter | Units | Steer | Drive | Trailer |
|---|---|---|---|---|
| Track width | mm | 1 982 | 1 834 | 2 310 |
| Wheel centre height | mm | 505 | 519 | 429 |
| Roll centre height above axle CoG | mm | 118 | 244 | –99 |
| Roll steer locating link angle | ° | –1.6 | 0 | 4.2 |
| Axle lateral movement vs. jounce | mm/mm | 0 | 0 | 0 |
| Axle longitudinal movement vs. jounce | mm/mm | 0 | 0 | 0 |
| Axle dive vs. jounce | °/mm | 0 | 0 | 0 |

**Table E.5: Spring compliance, Flexiporter**

| Vehicle Parameter | Units | Steer | Drive | Trailer |
|---|---|---|---|---|
| Spring stiffness | N/mm | 227 | 426/840 | Figure E.1 |
| Spring track | mm | 820 | 1 000 | 1 500 |
| Lash at spring connection | mm | 0 | 16 | 0 |
| Lash lever arm ratio | - | N/A | 0.5 | N/A |
| Lash at wheel | mm | N/A | 8 | N/A |
| Coulomb friction | N | 887 | 2 169 | N/A |
| $\beta$ | mm | 2 | 2 | 2 |
| Compliance effects | (various) | 0 | 0 | 0 |
| Auxiliary roll moment | Nm/° | 6 326 | 2 677 | 6 080 |
| Wheel-to-spring jounce ratio | - | 1:1 | 1:1 | 1.76:1 |

**Table E.6: Tandem suspension properties, Flexiporter**

| Vehicle Parameter | Units | Trailer |
|---|---|---|
| Static load ratio supported by rear axle of each two-axle pair | - | 0.5 |
| Dynamic load transfer coefficient | - | 0.5 |
| Load transfer due to brake torque | 1/m | 0 |

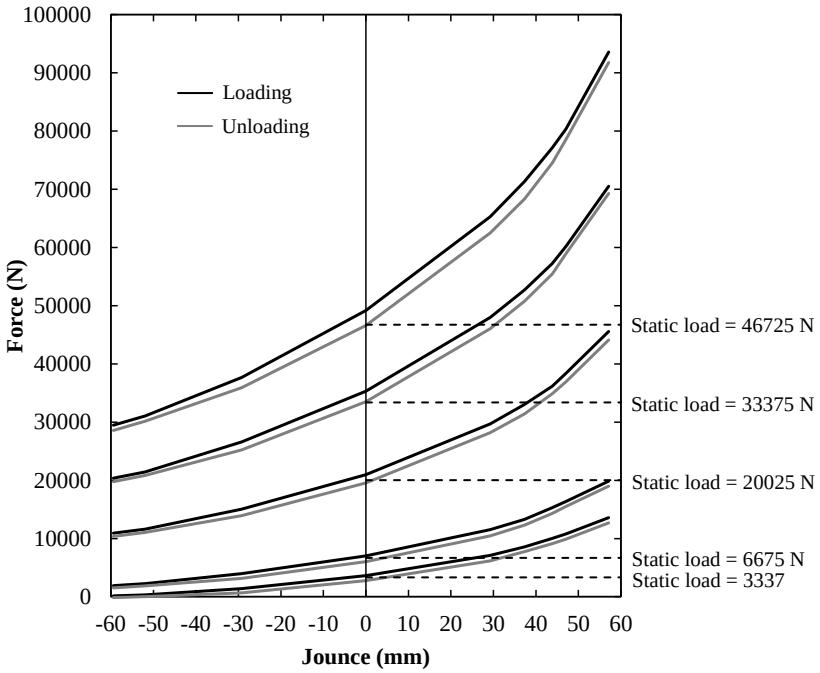


**Figure E.1: Spring plot, Flexiporter semitrailer axle (BPW 30K airbag)**

## E.2.2 Dampers

**Table E.7: Damper properties, Flexiporter**

| Vehicle Parameter | Units | Steer | Drive | Trailer |
|---|---|---|---|---|
| Damper model | - | Monroe E530240A | Tenneco E5304601 | BPW 02.3722.83.00 |
| Damper angle relative to horizontal | ° | 90 | 60 | 56 |
| Damper track | mm | 1 013 | 780 | 1 258 |
| Damper rate (including inclination effect) | N/(mm/s) | Table E.8 | Table E.9 | Table E.10 |
| Auxiliary roll damping | Nm-s/° | 0 | 0 | 0 |

**Table E.8: Damper behaviour, Flexiporter steer axle**

| Velocity (mm/s) | Force (N) | |
|---|---|---|
| | Jounce | Rebound |
| 0 | 0 | 0 |
| 50 | 370 | 3 020 |
| 130 | 830 | 4 230 |
| 260 | 1 010 | 4 310 |
| 390 | 1 110 | 4 420 |
| 520 | 1 190 | 4 520 |
| 1 040 | 1 480 | 4 810 |
| 1 560 | 1 730 | 5 210 |

**Table E.9: Damper behaviour, Flexiporter drive axle**

| Actual damper properties | | | Equivalent vertical damper | | |
|---|---|---|---|---|---|
| Velocity (mm/s) | Force (N) | | Velocity (mm/s) | Force (N) | |
| | Jounce | Rebound | | Jounce | Rebound |
| 0 | 0 | 0 | 0 | 0 | 0 |
| 10 | 270 | 540 | 12 | 234 | 468 |
| 26 | 350 | 1 950 | 30 | 303 | 1 689 |
| 52 | 580 | 5 350 | 60 | 502 | 4 633 |
| 130 | 1 300 | 6 500 | 150 | 1 126 | 5 629 |
| 260 | 1 450 | 6 800 | 300 | 1 256 | 5 889 |
| 390 | 1 550 | 7 000 | 450 | 1 342 | 6 062 |
| 520 | 1 650 | 7 150 | 600 | 1 429 | 6 192 |
| 1 040 | 1 900 | 7 700 | 1 201 | 1 645 | 6 668 |
| 1 560 | 2 200 | 8 350 | 1 801 | 1 905 | 7 231 |
| 3 000 | 2 550 | 10 550 | 3 464 | 2 208 | 9 137 |

**Table E.10: Damper behaviour, Flexiporter semitrailer axle**

| Actual damper properties | | | Equivalent vertical damper | | |
|---|---|---|---|---|---|
| Velocity (mm/s) | Force (N) | | Velocity (mm/s) | Force (N) | |
| | Jounce | Rebound | | Jounce | Rebound |
| 0 | 0 | 0 | 0 | 0 | 0 |
| 52 | 1 800 | 8 600 | 63 | 1 492 | 7 130 |
| 130 | 2 800 | 13 100 | 157 | 2 321 | 10 860 |
| 260 | 3 800 | 14 200 | 314 | 3 150 | 11 772 |
| 390 | 4 400 | 14 700 | 470 | 3 648 | 12 187 |
| 520 | 5 000 | 15 200 | 627 | 4 145 | 12 601 |
| 650 | 5 600 | 15 600 | 784 | 4 643 | 12 933 |
| 780 | 6 200 | 16 100 | 941 | 5 140 | 13 348 |
| 910 | 6 800 | 16 600 | 1 098 | 5 637 | 13 762 |
| 1 040 | 7 400 | 17 100 | 1 254 | 6 135 | 14 177 |

# E.3 Couplings

**Table E.11: Coupling properties, Flexiporter**

| Vehicle Parameter | Units | Fifth wheel |
|---|---|---|
| Distance behind steer axle | mm | 3 400 |
| Height above ground | mm | 1 221 |
| Lateral offset | mm | 0 |
| Roll stiffness | Nm/° | 56 500 |
| Pitch stiffness | Nm/° | 0 |
| Yaw stiffness | Nm/° | 0 |

## E.4 Tyres

**Table E.12: Tyre properties, Flexiporter**

| Vehicle Parameter | Units | Steer | Drive | Trailer |
|---|---|---|---|---|
| Size | | 295/80 R22.5 | 295/80 R22.5 | 285/70 R19.5 |
| Single/Dual | | Single | Dual | Single |
| UMTRI tyre used for lateral stiffness data [39] | | Michelin 12x22.5 | Michelin 12x22.5 | Michelin 11.0R20H |
| Michelin tyre used for rated load, vertical stiffness, effective rolling radius, unloaded radius data [58] | | XZA2 Energy | XZA2 Energy | XZE2+ |
| Rated load | kg | 3 550 | 3 550 | 2 725 |
| Dual tyre spacing | mm | N/A | 352 | N/A |
| Rolling resistance | | 0 | 0 | 0 |
| Effective rolling radius | mm | 509 | 509 | 433 |
| Unloaded radius | mm | 524 | 524 | 448 |
| Vertical spring rate | N/mm | 916 | 916 | 801 |
| Relaxation length for $F_y$ and $M_z$ | mm | 100[†] | 1 048 | 896 |
| Relaxation length for $F_x$ | mm | 52 | 52 | 45 |
| Load rating for TruckSim® longitudinal and aligning moment stiffness properties | kg | 3 500 | 3 500 | 3 000 |
| Wheel toe | ° | 0 | 0 | 0 |
| Wheel camber | ° | 0 | 0 | 0 |

[†] Value chosen for steer-tyres to avoid erratic steering motion whilst maintaining acceptable path-following behaviour

## E.5 Steering

(See Table D.12.)

# Appendix F

# Vehicle Drawings

The drawings that appear on the following pages were created by – and appear here courtesy of – Mr. Andrew Colepeper and Unipower (Natal).

| **Drawing No.** | **Description** |
|---|---|
| 409-600-PBS001 | Maxiporter (final design): Dimensions |
| 409-600-PBS002 | Maxiporter (final design): Example maximum payloads |
| 407-100-PBS001 | Flexiporter (final design): Dimensions |
| 407-100-PBS002 | Flexiporter (final design): Example maximum payload |

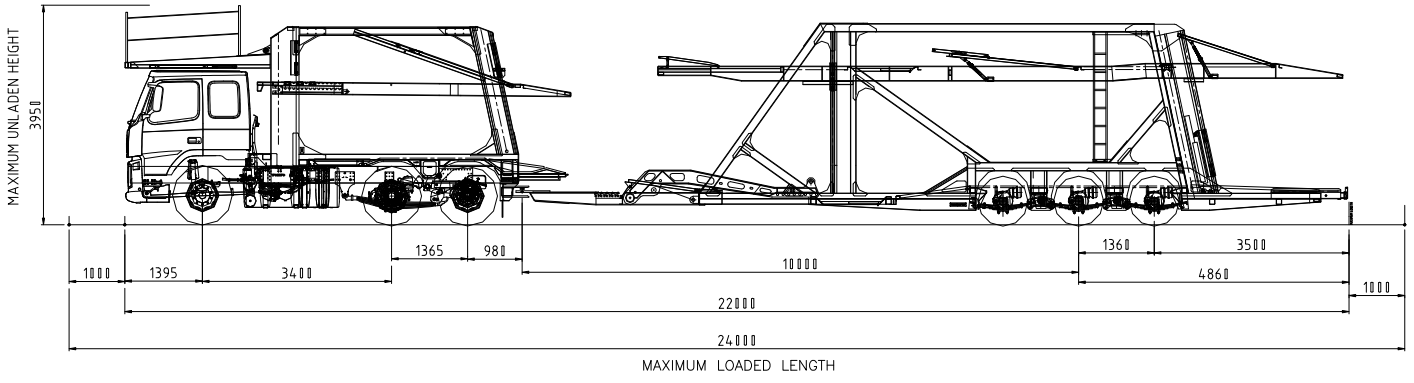


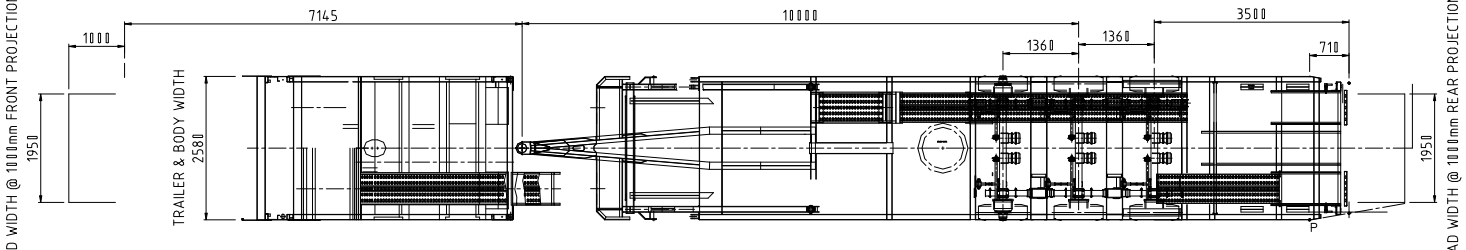


| STEER | | DRIVE | | TRAILER | |
|---|---|---|---|---|---|
| | 7 700 KG | A | 18 000 KG | A | 25 000 KG |
| TARE* | 6 075 KG | TARE* | 6 755 KG | TARE* | 9 180 KG |
| PAYLOAD | 1 625 KG | PAYLOAD | 11 245 KG | PAYLOAD | 15 820 KG |

*all TARE masses are with unit uncoupled

TRUCK CHASSIS : VOLVO FM400 6x2

MIN Bhp : 400

VOLVO

BPW MECHANICAL SUSPENSION ON TRAILER

TRAILER WHEELS : 285/70 R19.5 SINGLE FITMENT

TOTAL GCM 45 000 KG

VEHICLE COMPLIES WITH RTA WHEN UNLADEN

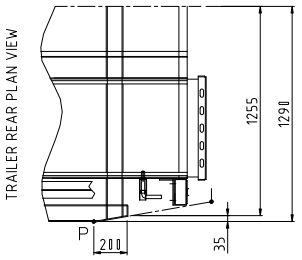


A4

DO NOT SCALE

maxiporter MK3



| DRAWN/DESIGN | SERIES | DATE ORIGINATED | LAST UPDATE |
|---|---|---|---|
| AJ COLEPEPER | UNIPORTER | 13/03/2012 | 13/03/2012 |

CONTRANSMATIC CC T\A UNIPOWER

TITLE: PBS DIMS : MAXIPORTER MK3

DRAWING No. 409-600-PBS001

EDITION 01

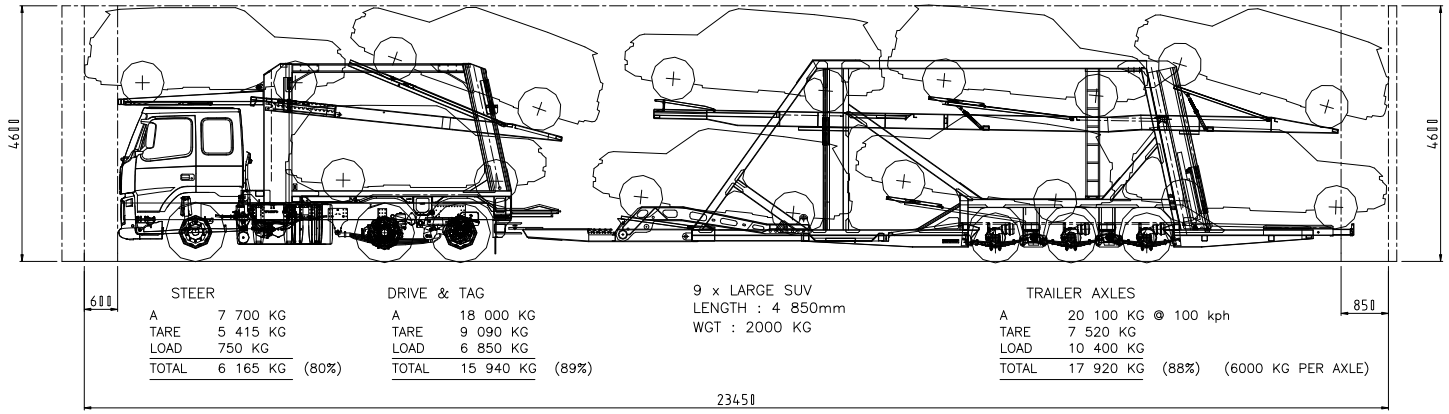


| STEER | | | DRIVE & TAG | | | 9 x LARGE SUV | TRAILER AXLES | | |
|---|---|---|---|---|---|---|---|---|---|
| A | 7 700 KG | | A | 18 000 KG | | LENGTH : 4 850mm | A | 20 100 KG @ 100 kph | |
| TARE | 5 415 KG | | TARE | 9 090 KG | | WGT : 2000 KG | TARE | 7 520 KG | |
| LOAD | 750 KG | | LOAD | 6 850 KG | | | LOAD | 10 400 KG | |
| TOTAL | 6 165 KG | (80%) | TOTAL | 15 940 KG | (89%) | | TOTAL | 17 920 KG | (88%) (6000 KG PER AXLE) |

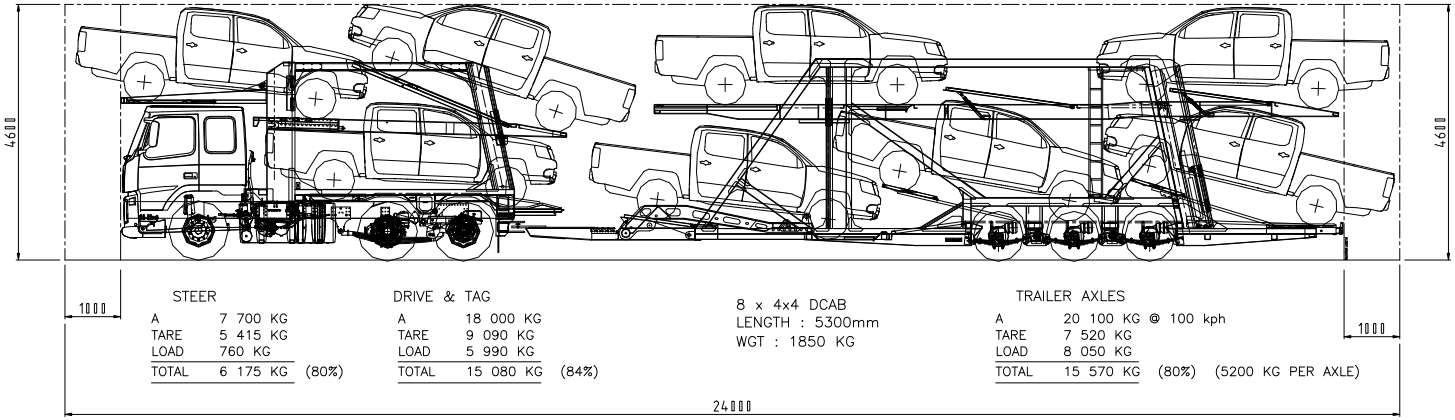


| STEER | | | DRIVE & TAG | | | 8 x 4x4 DCAB | TRAILER AXLES | | |
|---|---|---|---|---|---|---|---|---|---|
| A | 7 700 KG | | A | 18 000 KG | | LENGTH : 5300mm | A | 20 100 KG @ 100 kph | |
| TARE | 5 415 KG | | TARE | 9 090 KG | | WGT : 1850 KG | TARE | 7 520 KG | |
| LOAD | 760 KG | | LOAD | 5 990 KG | | | LOAD | 8 050 KG | |
| TOTAL | 6 175 KG | (80%) | TOTAL | 15 080 KG | (84%) | | TOTAL | 15 570 KG | (80%) (5200 KG PER AXLE) |

TRUCK CHASSIS : VOLVO FM400 6x2

MIN Bhp : 400

VOLVO

A4 DO NOT SCALE

maxiporter™ MK3



| DRAWN/DESIGN | SERIES | DATE ORIGINATED | LAST UPDATE |
|---|---|---|---|
| AJ COLEPEPER | UNIPORTER | 13/03/2012 | 13/03/2012 |

CONTRANSMATIC CC T\A UNIPOWER

TITLE: PBS LOAD EXAMPLES : MAXIPORTER MK3

DRAWING No. 409-600-PBS002 EDITION 01

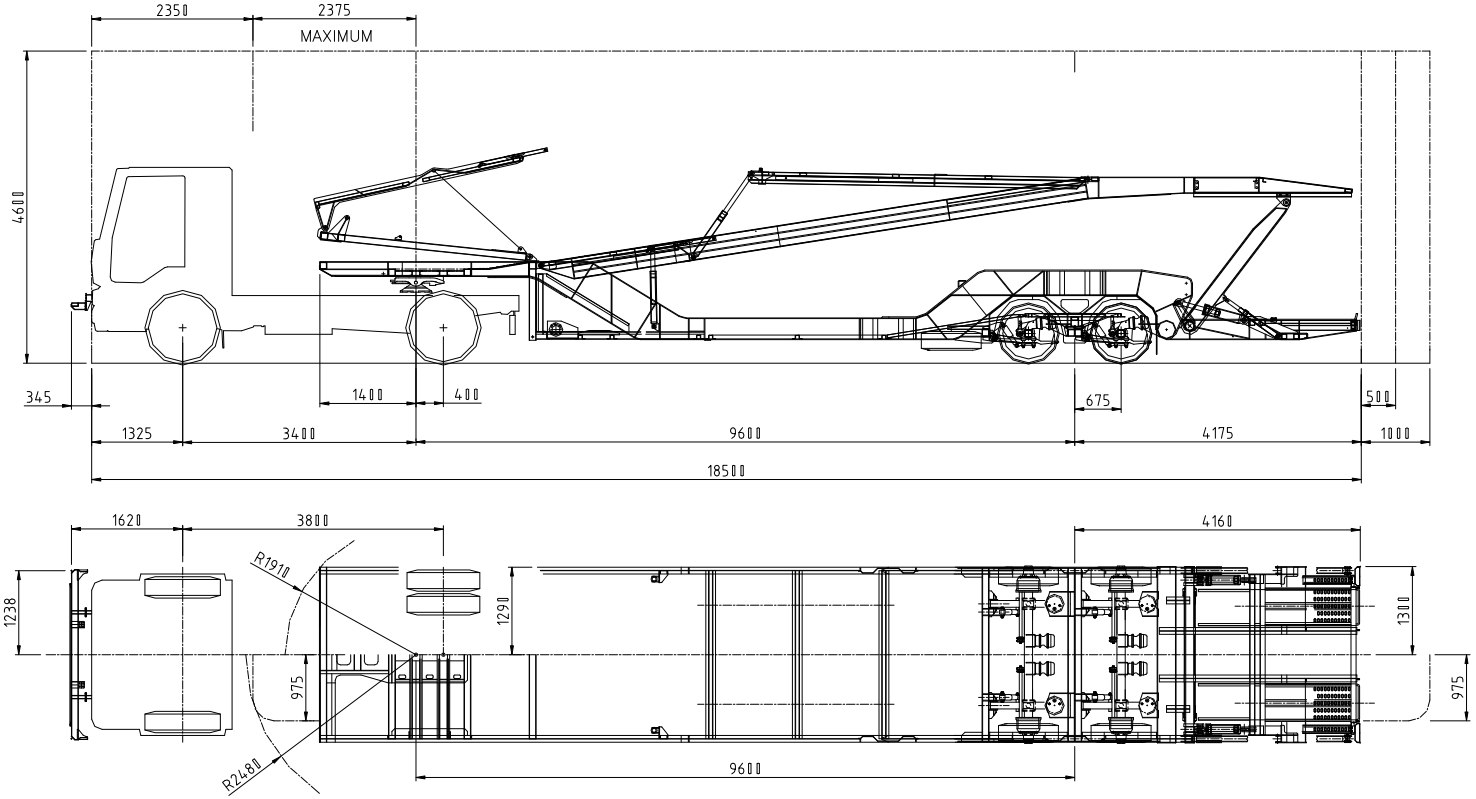


| | | | |
|---|---|---|---|
| STEER 7100 Kg | KINGPIN | DRIVE | 9000 Kg |
| TARE 300 Kg | TARE TRAILER 2980 Kg | TARE | 2680 Kg |
| TARE 2800 Kg | TARE TRUCK CHASSIS | TARE | 2100 Kg |
| IMPOSED LOAD 500 Kg | MAX PAYLOAD 4 700 Kg | PAYLOAD | 4220 Kg |

MAX GCM 30 000 Kg

BPW AIR SUSPENSION ON TRAILER

TRAILER WHEELS : 285/70 R19.5 SINGLE FITMENT

TRAILER AXLES 14000 Kg @ 80 Kph

TARE 5700 Kg

PAYLOAD 8300 Kg

TRUCK CHASSIS : RENAULT MIDLUM 280.18

Flexiporter™

A4

DO NOT SCALE



| DRAWN/DESIGN | SERIES | DATE ORIGINATED | LAST UPDATE |
|---|---|---|---|
| AJ COLEPEPER | UNIPORTER : FLEXIPORTER MK2 | 07/05/2012 | 07/05/2012 |

CONTRANSMATIC CC T\A UNIPOWER

TITLE: FLEXIPORTER MK2 PBS DIMENSIONS

| DRAWING No. | AUTHORISED | EDITION |
|---|---|---|
| 407-100-PBS001 | | 01 |

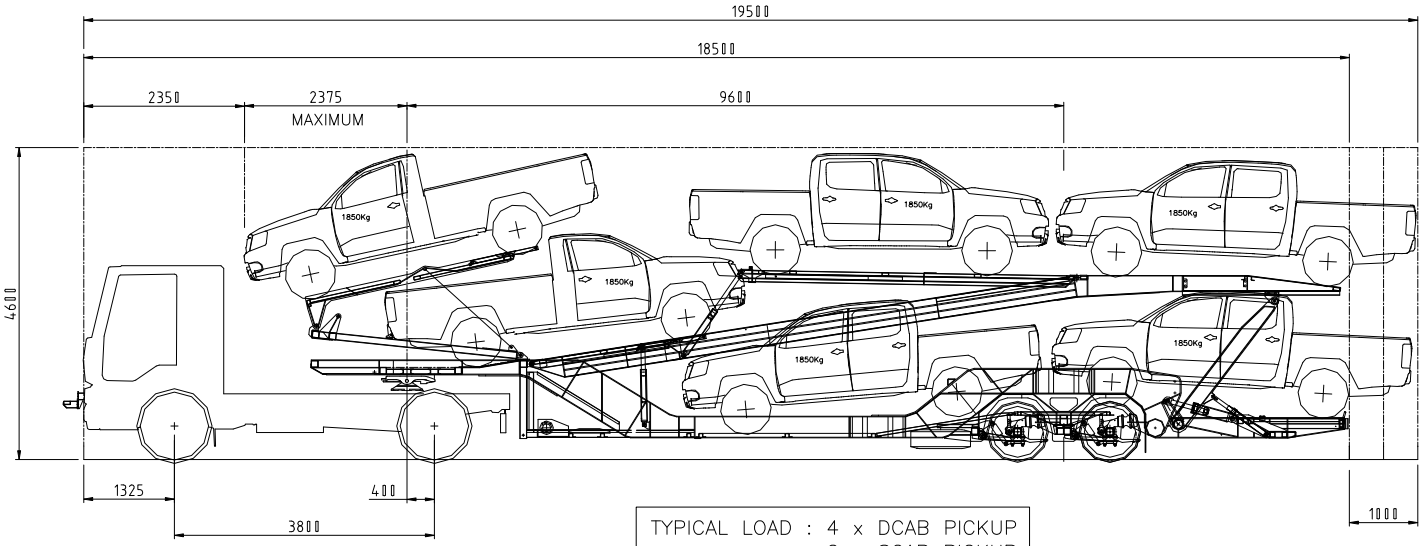


TRUCK CHASSIS : RENAULT MIDLUM 280.18

TYPICAL LOAD : 4 x DCAB PICKUP
2 x SCAB PICKUP
(ALL 4x4)

| | | |
|---|---|---|
| STEER | 7100 Kg | |
| TARE | 300 Kg | |
| TARE | 2800 Kg | |
| IMPOSED LOAD | 390 Kg | |
| AXLE LOAD | 3490 Kg | (50%) |

| | |
|---|---|
| KINGPIN | |
| TARE TRAILER | 2980 Kg |
| TARE TRUCK CHASSIS | |
| PAYLOAD IMPOSED | 3 590 Kg |

| | | |
|---|---|---|
| DRIVE | 9000 Kg | |
| TARE | 2680 Kg | |
| TARE | 2100 Kg | |
| PAYLOAD | 3 200 Kg | |
| AXLE LOAD | 7 980 Kg | (89%) |

| | | |
|---|---|---|
| TRAILER AXLES | 14000 Kg @ 80 Kph | |
| TARE | 5700 Kg | |
| PAYLOAD | 7580 Kg | |
| AXLE LOAD | 13 280 Kg | (95%) |

Flexiporter™

A4

DO NOT SCALE



| DRAWN/DESIGN | SERIES | DATE ORIGINATED | LAST UPDATE |
|---|---|---|---|
| AJ COLEPEPER | UNIPORTER : FLEXIPORTER MK2 | 07/05/2012 | 07/05/2012 |

CONTRANSMATIC CC T\A
UNIPOWER

TITLE: FLEXIPORTER MK2 PBS LOAD DISTRIBUTION

| DRAWING No. | AUTHORISED | EDITION |
|---|---|---|
| 407-100-PBS002 | | 01 |